UNIVERSITY OF NOVA GORICA
GRADUATE SCHOOL

MICROBIAL INTERACTIONS INSIDE THE OLIVE KNOT

DISSERTATION

Daniel Passos da Silva

Mentor: Vittorio Venturi

Nova Gorica, 2014

"The saddest aspect of life right now is that science gathers knowledge faster than society gathers wisdom."

Isaac Asimov

ABSTRACT

Although the great majority of bacteria found in nature are living in multispecies communities, microbiological studies have historically focused on single species or on simple competition and antagonism experiments between two different bacterial species. Future directions need to focus more on microbial communities in order to better understand what occurs in the wild. The olive knot disease of the olive plant (*Olea europea* L.) was used as model to study the role and interaction of multispecies bacterial communities in disease establishment/development. In the olive knot, non-pathogenic bacteria (e.g. *Erwinia toletana*) are coexisting with the pathogen (*Pseudomonas savastanoi* pv. *savastanoi*) and they were previously shown to cooperate by sharing quorum sensing signals. The outcome of this interaction is a more aggressive disease when co-inoculations are made compared to single ones. Studies performed in this thesis have shown that *in planta* these two species are co-localizing in the olive knot and this close proximity most probably facilitates exchange of quorum sensing signals and metabolites. The genome of *E. toletana* was sequenced here and *in silico* recreation of the metabolic pathways of *E. toletana* and *P. savastanoi* indicated possible complementing pathways implicating in the sharing of metabolites. This was further corroborated by phenotypic microarray experiments. Furthermore, microbiome studies of nine naturally occurring olive-knots have shown that in the olive-knot the pathogen co-habits with a set of bacterial species having great bacterial diversity, however the presence of a core of five genera (i.e. *Pseudomonas*, *Pantoea*, *Curtobacterium*, *Pectobacterium* and *Erwinia*) was found in all samples. Biofilm studies *in vitro* have also shown that these two species when co-inoculated can form a larger structure than when single inoculated and that the synthase mutant of quorum sensing signal generator of *E. toletana* produces more biofilm in single and co-inoculations when compared to the wild-type. Additionally, the discovery of second canonical *N*-acyl homoserine lactone system in *E. toletana* which could not be activated in

the studies presented here raises new questions on how *P. savastanoi* and *E. toletana* are interacting in the olive knot. This thesis initiated several lines of research and sets the olive knot as a model to study microbial interactions in a plant disease.

POVZETEK

Čeprav velika večina vseh bakterij, ki jih najdemo v naravnih okoljih, živi v mešanih združbah večih vrst, so se tradicionalne mikrobiološke študije predvsem posvečale posameznim vrstam ali preprostim eksperimentom kompeticije in antagonizma med dvema bakterijskima vrstama. Za razumevanje stanja v naravi se je v prihodnje tako potrebno osredotočiti na mikrobne združbe. Za študij vloge in interakcij večih vrst v mešanih bakterijskih združbah pri pojavu in razvoju bolezenskih stanj smo kot model uporabili bakterijsko oboljenje oljčni rak, ki napada oljke (*Olea europea* L.). Pri tem oboljenju nepatogene bakterije (npr. *Erwinia toletana*) sobivajo s patogenimi vrstami (*Pseudomonas savastanoi* pv. *savastanoi*). Predhodno je bilo pokazano, da njihovo sodelovanje poteka na nivoju medceličnega signaliziranja. Ob sočasni inokulaciji je rezultat te interakcije pojav agresivnejše bolezni kot ob posameznih inokulacijah. Z *in planta* študijami sem v doktorskem delu pokazal, da pri oljčnem raku omenjene bakterijske vrste sobivajo in da njihova tesna povezanost po vsej verjetnosti povzroča izmenjavo sporočil medceličnega signaliziranja in metabolitov. Določitev genomskega zaporedja *E. toletana* ter *in silico* analiza metaboličnih poti *E. toletana* in *P. savastanoi* so pokazali verjetno dopolnjevanje omenjenih poti preko skupnih metabolitov. To je bilo nadaljnje potrjeno z uporabo fenotipskih mikromrež. V nadaljevanju so mikrobiomske študije na primeru devetih naravno prisotnih oljčnih rakov pokazale, da patogen oljčnega raka sobiva s skupino raznolikih bakterijskih vrst, med katerimi je najbolj zastopanih pet rodov, ki so bili identificirani v vseh analiziranih vzorcih (i.e. *Pseudomonas*, *Pantoea*, *Curtobacterium*, *Pectobacterium* and *Erwinia*). *In vitro* študije biofilmov so prav tako pokazale, da omenjeni vrsti ob sočasni inokulaciji lahko tvorijo večje strukture v primerjavi s posameznimi inokulacijami. Spremenjeni organizmi medceličnega signaliziranja *E. toletana* so v primerjavi z divjim tipov tvorili večje biofilme, tako ob sočasni kot pri posameznih inokulacijah. Odkritje drugega N-acil homoserin laktonskega sistema v *E. toletana*, ki ne more biti aktiviran v

predstavljenih študijah odpira nova vprašanja o interakcijah *P. savastanoi* in *E. toletana* pri oljčnem raku. Doktorsko delo odpira več raziskovalnih vprašanj in predstavlja oljčni rak kot ustrezen model študij mikrobnih interakcij pri obolenjih rastlin.

PUBLICATIONS

This thesis is based on the following publications:

PASSOS DA SILVA, D., CASTANEDA-OJEDA, M. P., MORETTI, C., BUONAURIO, R., RAMOS, C. & VENTURI, V. Bacterial multispecies studies and microbiome analysis of a plant disease. Microbiology. 2014.

PASSOS DA SILVA, D., DEVESCOVI, G., PASZKIEWICZ, K., MORETTI, C., BUONAURIO, R., STUDHOLME, D. J. & VENTURI, V. Draft genome sequence of *Erwinia toletana*, a bacterium associated with olive knots caused by *Pseudomonas savastanoi* pv. *savastanoi*. Genome Announcements. 2013.

VENTURI, V. & **DA SILVA, D.P.** Incoming pathogens team up with harmless "resident" bacteria. Trends in Microbiology (Regular Ed.). , v.20, p.160 - 164, 2012.

Other publications:

BERTANI, I., **PASSOS DA SILVA, D.**, ABBRUSCATO, P., PIFFANELLI, P. & VENTURI, V. Draft genome sequence of the plant pathogen *Dickeya zeae* DZ2Q, isolated from rice in Italy. Genome Announcements. , v.1, p.e00905-13 - e00905-13, 2013.

COUTINHO, B. G., **PASSOS DA SILVA, D.**, PREVIATO, J. O., MENDONCA-PREVIATO, L. & VENTURI, V. Draft genome sequence of the rice endophyte *Burkholderia kururiensis* M130. Genome Announcements. , v.1, p.e00225-12 - e00225-12, 2013.

PATEL, H. K., **PASSOS DA SILVA, D.**, DEVESCOVI, G., MARAITE, H., PASZKIEWICZ, K., STUDHOLME, D. J. & VENTURI, V. Draft genome sequence of *Pseudomonas fuscovaginae*, a broad-host-range pathogen of plants. Journal of Bacteriology, v.194, p.2765 - 2766, 2012.

ACKNOWLEDGEMENTS

I would like to to thank ICGEB, Trieste for the opportunity to greatly develop my academic career.

I am extremely grateful for the opportunity to work with my PhD supervisor Vittorio Venturi which is a great professional and fantastic person. Thanks for everything you have taught me. It was a great pleasure and honour to work with you.

I want to thank all current and past members from the Bacteriology Lab. To Giulia Devescovi for her friendship and tireless will to explain, help and discuss scientific (and non-scientific) issues. To Iris Bertani for her availability in all moments of need and methodological panic. To Giuliano Degrassi for his technical guidance and personal advices.

I am very grateful to have had the opportunity to spend 2 months in Prof. Cayo Ramos' Lab. Thanks for the shared enthusiasm and all contributions to our collaboration. Thanks to Roberto Buonario and Chiaraluce Moretti for the contribution in the 9 olive knots project. Thanks to David Studholme and Konrad Paszkiewicz for the *Erwinia toletana* genome sequencing. Thanks to Stefano Mocali and Marco Galardini for the exciting collaboration on the phenotypic microarray analysis.

Thanks to my grandparents Nerias Leandro da Silva e Heminia Teixeira da Silva for raising me like a son and being crucial in my development. You will always be with me. Thanks to my parents Neise dos Santos Passos and Paulo Cesar Teixeira da Silva for the lessons, discipline, friendship and love. You are my creators and my pride. Thanks to my parents-in-law Suzana Barros Gonçalves and Paulo Luiz de Andrade Coutinho, for being much more than I could have ever asked. Thanks for everything you have done for me but more importantly for being great examples to be followed.

Finally thanks to my partner, wife and friend Bruna Gonçalves Coutinho. Without you surely this journey would not be as fantastic as it is. Thanks for the shared dreams and thoughts. Let's keep pushing! I love you!

CONTENTS

LIST OF FIGURES

LIST OF TABLES

KEYWORDS

Biofilm

Erwinia toletana

Genome sequencing

Interspecies interactions

Metabolic sharing

Metagenomics

Microbiome

Multispecies communities

Olive knot

Pantoea agglomerans

Pathway Tools

Pseudomonas savastanoi pv. *savastanoi*

Quorum sensing

ABBREVIATIONS

ACP acyl carrier protein

AHLs *N*-acyl-homoserine lactones

Amp Ampicilin

CFU Colony forming units

CLASI Combinatorial labeling and spectral imaging

CLSM Confocal laser scanning microscopy

Cm Chloramphenicol

d.p.i Days post inoculation

DF Butyrolactone

DMF *N*,*N*-dimethylformamide

DSF *cis*-11-methyl-2-dodecenoic acid

ET *Erwinia toletana*

FISH Fluorescence *in situ* hybridization

Gm Gentamicin

HR Hypersentive response

HSL Homoserine lactone

IAA Indole acetic acid

IAA-lys Indole-3-acetyl-ε-L-lysine

IAM Indoleacetamide

Km Kanamycin

LPS Lipopolysaccharide

Nif Nitrofurantoin

OTU Operational taxonomic units

PAG *Pantoea agglomerans*

PFA Paraformaldehyde

PNA Peptide nucleic acids

PSV *Pseudomonas savastanoi* pv. *savastanoi*

QS Quorum sensing

RP-HPLC Reverse phase High performance liquid chromatography

SAM S-adenosylmethionine

SIMS Secondary ion mass spectrometry

T3SS Type III secretion system

Tc Tetracyclin

VFDB Virulence Factors Database

X-Gal 5-bromo-4-chloro-3-indolyl-β-D-galactopyranoside

1 INTRODUCTION

Scientific research has intensively focused on the interactions between pathogenic microbes and hosts such as humans, plants, animals and insects due to their importance in health and food security. These studies have shown that diseases are a result of complex interactions between the pathogen and host. Most bacterial research in plant pathology thus far, with the exception of crown gall caused by *Agrobacterium tumefaciens*, has focused on herbaceous plant diseases rather than woody plant diseases (Mansfield *et al.* 2012). In recent years, the olive pathogen *Pseudomonas savastanoi* pv. *savastanoi* (PSV) has been recognized as a suitable model for understanding woody plant diseases (Rodriguez-Moreno *et al.* 2008; Rodriguez-Moreno *et al.* 2009; Rodriguez-Palenzuela *et al.* 2010). Olive trees (*Olea europaea* L.) infected by PSV develop overgrowths, referred to as galls, knots or tumors mainly on the aerial parts of the plants, with their incidence being rare on leaves and fruits. The productivity of olive trees infected with PSV is reduced and no effective treatment is yet in place (Schroth *et al.* 1973; Young 2004; Quesada *et al.* 2010; Matas *et al.* 2012; Ramos *et al.* 2012). Invading pathogens are thought to encounter a large number of different harmless and beneficial bacterial species, which colonize and reside in different hosts. Surprisingly, very few studies have focused on possible interactions between incoming pathogens and the resident bacterial community. These few studies have revealed that resident bacteria can assist different types of incoming pathogens via a wide variety of mechanisms including cell–cell signaling, metabolic interactions, evasion of the immune response and a resident-to-pathogen switch. Interestingly, several bacterial species isolated from olive knots are harmless or nonpathogenic to the plant (Rojas *et al.* 2004; Ouzari *et al.* 2008; Moretti *et al.* 2011). The possible roles of some of these PSV co-residents in the olive knot has recently been identified; isolates of *Pantoea agglomerans* (PAG) and *Erwinia toletana* (ET) have been detected in multispecies communities associated with PSV. The focus of this thesis is on the multispecies interactions occurring in the olive knot disease. It is believed that this will be a good model system to study multispecies interaction between a pathogen and resident bacteria.

1.1 Multispecies communities

Considering that bacteria form the largest domain with a predicted 10^{30} species (Curtis *et al.* 2002), microbiologists are aware that in most cases species live alongside many other different species forming interspecies communities. In some cases the diversity of microorganisms in a very small niche can be up to hundreds of species as found in the human oral cavity (Cantarel *et al.* 2011) or even thousands as in soil samples (Gans *et al.* 2005; Roesch *et al.* 2007). Regardless of the increasing knowledge of multispecies composition in many niches in the wild, experimental studies remain to be at large focused on pure cultures. Although we are aware of the omnipresence and importance of microbial communities, the information that we now possess about microbial-microbial interactions is very limited.

Scientists have unraveled only some of the mechanisms that modulate bacterial interactions and little knowledge is available regarding the importance of cooperation and competition in these associations. There is an urge to better understand the potential of cooperation among bacteria as this information can be used to design antimicrobial therapy of multispecies infections or to engineer bacterial consortia to perform biological tasks with higher efficiency. It is believed that interactions between microbial species can lead to many different social phenotypes. These phenotypes not only can control growth rate (Kreft 2004), but also the ability to secrete compounds that promote or inhibit neighboring cell growth (Kerr *et al.* 2002; Griffin *et al.* 2004; Mitri *et al.* 2011). Co-inoculation experiments reveal the importance of the fitness costs and benefits for multispecies interactions, with the potential of cooperation to be stabilized by either constraints on competitive traits (Foster *et al.* 2004; Harrison *et al.* 2008), or by strategies that make cooperation carry little or no cost (Ramsey *et al.* 2011; Xavier *et al.* 2011).

Another important property of bacteria in the wild is that majority exist in microbial communities that grow as a sessile biofilm. Routine laboratory experiments involve bacterial growth under shaking conditions which is known to limit their spatial structure (Griffin *et al.* 2004; Harrison *et al.* 2008). The biofilm structure increases the potential for social interactions, since there is less movement and more time for each bacterial cell to interact with its neighbors (O'Toole and Kolter 1998; Hall-Stoodley *et al.* 2004; Monds and O'Toole 2009). Biofilm communities are defined by their secreted polymers that helps to glue the cells together (Miller and Bassler 2001). They exhibit several properties that require molecular communication and cooperation among the participant species, including differentiation among the cells to produce highly resilient biofilm structure, stratification to optimize productivity, and formation of channels to maximize nutrient and oxygen flow (Stoodley *et al.* 2002). In a similar way, studies with quorum sensing have showed how bacterial communities regulate group phenotypes (Miller and Bassler 2001). Detection and response to signals allows bacteria to perform tasks that are mainly beneficial to large populations of cells. One example is the production and secretion of plant-cell-degrading compounds by bacterial phytopathogens in response to QS signals (Barnard *et al.* 2007). It is thought that quorum sensing allows pathogenic bacteria to express traits only when host defenses can be overwhelmed (Miller and Bassler 2001). Interestingly, quorum sensing regulated traits can be modulated differently at the different regions of the biofilm. For instance, in a region of the biofilm where the diffusible signal molecules tends to be more concentrated as a consequence of the channel formation, the phenotypes expressed by the cells would be different from the cells on the edge of the biofilm, where the diffusion of these molecules are much greater. The biofilm model associated with epifluorescence microscopy is most often used to study the interaction between two species (Monier and Lindow 2005; Dalton *et al.* 2011).

1.1.1 Methods/approaches to study multispecies communities

New methods for visualizing multispecies communities are being developed. These include two methods based on fluorescence *in situ* hybridization (FISH) which are very sensitive. In one method, oligonucleotide probes are designed to bind to species-specific 16s rRNA and the 5' of these probes are covalently modified by different fluorophores. . This technique is called Combinatorial Labeling and Spectral Imaging (CLASI-FISH) (Valm *et al.* 2011). Another approach uses the enhanced properties of peptide nucleic acids (PNA) on binding DNA sequences and different fluorophores conjugated to these probes; since this is also a variation of a FISH method it is known as PNA FISH (Almeida *et al.* 2011). Other methods to approach the study of interspecies interactions, especially for uncultivable microorganisms, include using single-cell-based technologies such as Raman microspectroscopy (Huang *et al.* 2004; Huang *et al.* 2010) or nano secondary ion mass spectrometry (nanoSIMS) (Kuypers and Jorgensen 2007; Oehler *et al.* 2010). Raman microspectroscopy is a non-invasive technique that acquires chemical signals from a small volume of sample. Usually the data coming from a Raman analysis is rich in information, including data from nucleic acid, proteins, carbohydrates and lipids. This information can provide insights into the molecular composition, structure, and physiological state which enables the differentiation of cell types, nutrient conditions and phenotypic changes (Huang *et al.* 2004; Huang *et al.* 2010). The technique can also be combined with optical tweezers and epifluorescence, generating the Raman tweezers (Xie *et al.* 2005), or with FISH techniques (Huang *et al.* 2009). NanoSIMS is a technique able to measure important elements such as carbon, nitrogen and sulfur (Oehler *et al.* 2010). It has a beam size of approximately 50 nm which is small enough to analyze single cells, or parts of cells. It is mildly destructive, since it removes one to three atomic layers of the sample (approximately 1 nm) to obtain vaporized sample for the analysis. NanoSIMS can also combine features like high resolution imaging, stable isotope probing, and microbial detection

methods that rely on molecular biomarkers. A combination of these techniques can help the study of complex uncultivable microorganism communities on diverse environments and reveal the nature of interactions between members of these communities as they occur (Kuypers and Jorgensen 2007).

Metagenomics is a technique to study the genomic potential or to identify bacterial species present in DNA samples. Once the DNA is isolated from the sample of interest, it can be processed in several ways (Thomas *et al.* 2012). The DNA extraction procedure can be a challenging step and it is crucial for the following steps of cloning, amplification and/or sequencing (Lundberg *et al.* 2012). Although researchers proposed methods to enrich bacterial DNA from environmental samples (Jiao *et al.* 2006; Burke *et al.* 2009) DNA extraction from host-associated bacteria can be more complex than from other environmental samples due to the high risk of eukaryotic DNA contamination.

Metagenomics approaches also include ways to functionally isolate DNA from a niche of interest. In this case, the DNA is cloned into a vector and transformed usually into a heterologous system and screened for the functions of interest (e.g. antibiotic production/resistance, nitrogen fixation, degradation of xenobiotics). In a sequence based analysis, the DNA can be randomly sequenced allowing the determination of the whole metabolic potential of the community from which it was isolated (Sessitsch *et al.* 2012). Another commonly used methodology is the amplification of housekeeping genes throughout bacterial species (e.g. rRNA 16S/18S) using degenerate primers which allows taxonomical classification of bacteria present in the environmental sample (Bowman *et al.* 2012).

The decreasing cost in the sequencing techniques have been an essential catalyst for the search of microbial diversity in several environments, such as ocean (Yooseph *et al.* 2007), stromatolites (Baumgartner *et al.* 2009) and hydrothermal vents (Sogin *et al.* 2006). Other "omics" approaches, like metaproteomics, metabolomics and metatranscriptomes have also been used to gain further insights into novel microbial communities (Wilmes and Bond 2006;

Gilbert *et al.* 2008) and improved bioinformatics resources were essential to allow the analysis of such large amount of data (Meyer *et al.* 2008; Sboner *et al.* 2011; Schloss *et al.* 2011). Post sequencing data storage, processing and analysis has now become relevant to the sequencing costs and are thought to increase in the future (Sboner *et al.* 2011).

1.1.2 Multispecies communities associated with humans

Considerable interest is now focused on studying the human microbiome (Turnbaugh *et al.* 2007). Metagenomics data from intestine, oral cavity and skin compose the great part of the information we now have about the human microbiome. The number of microorganisms associated with the human gut is estimated to be 10^{14} which is believed to be represented by more than 10^{3} different species (Tlaskalova-Hogenova *et al.* 2004). In the human oral microbiota hundreds of species are mainly organized in biofilm structures believed to contain 10^{10} of total bacterial cells. The respiratory tract is exposed to several microorganisms and parts like the oropharynx are colonized by staphylococci, streptococci and Gram-negative cocci. The gastrointestinal tract is one of the most bacterially colonized parts of the body composed mainly of anaerobes mostly attached to the mucus in the colon.

In humans, microbiota is first passed through the maternal hand-over at birth (Dominguez-Bello *et al.* 2010). Following colonization, the microbiota is shaped by complex interactions with the environment throughout life, which comprises diseases, drug usage, diet etc (Figure 1-1). The dynamism of the microbes also changes the metabolic phenotype of the host and has significant importance to disease susceptibility (Nicholson *et al.* 2012). The protective role of this microbiota has been thoroughly described and there are different mechanisms to conceive this role that varies from physical barrier against the

colonization of pathogens, competition for nutrients, confusing the signaling system of incoming pathogens and even shaping the immune system (Lee and Mazmanian 2010). The shaping of the immune system is a two-way road, since the immune system selects back the microbiota that will colonize the host. The cross-talk between host and microbiota during this process utilizes a wide number of signaling pathways that go far beyond just the immune system. These include chemical and metabolic interactions that connects several organs including gut, liver, muscle and brain. The resulting combinatorial metabolism from host-microbiota cross talk results in the production of essential compounds like choline, bile acids, and short-chain fatty acids (Nicholson *et al.* 2012).

Although the benefits provided by the microbiota in humans are evident and exhaustively described, recent papers have demonstrated that in some specific scenarios beneficial human-associated bacteria can aid the incoming pathogens. In two different studies, experiments demonstrated the possibility that the gut microbiota assist infection by viruses. In the first scenario the mouse mammalian tumor virus interacts with the epithelial bacteria to form viral particles covered with lipopolysaccharide (LPS). This hybrid particle then interacts with the white blood cells via Toll-like receptor 4 to induce the production of interleukin-10 so that viral suppression by the immune system is blocked (Kane *et al.* 2011). In another case, it was shown that transmission of poliovirus was enhanced in the presence of the gut microbiota, whereas in antibiotic-treated mice the virus had a diminished replication rate, therefore lowering mortality after poliovirus infection (Kuss *et al.* 2011). Besides viral assistance, it has also been reported that nematode egg hatching in the gut is a bacterial mediated process (Hayes *et al.* 2010).

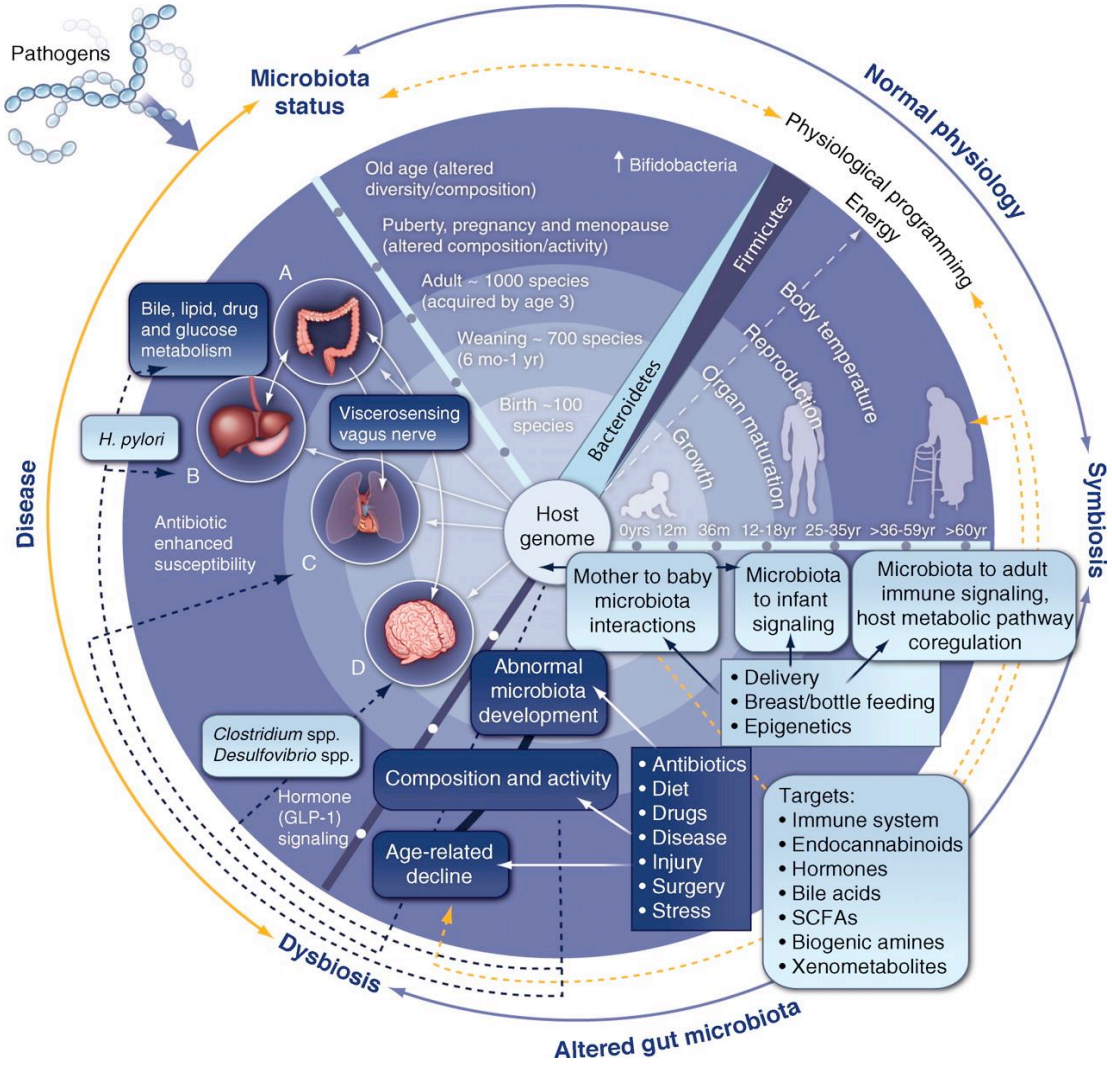

Figure 1-1. Schematic representation of human microbiota contribution during different periods of life (Nicholson *et al.* 2012).

The oral cavity is also a good model to study multispecies interactions in biofilms. A recent study showed a key interaction via metabolic exchange between an opportunistic pathogen *Aggregatibacter actinomycetemcomitans* and a common commensal bacteria *Streptococcus gordonii*. *S. gordonii* is more efficient in utilizing a superior carbon source like glucose and, degrades it to L-lactate, which is preferred by *A. actinomycetemcomitans*, allowing growth of both species without competition. This is an example of metabolic complementarity leading to the mutual benefit (Ramsey *et al.* 2011). Multispecies communities residing in humans are therefore important for health but can

however also aid the incoming pathogen via metabolic exchanges or interspecies signaling. It is most likely that other mechanisms may be in place for interactions between resident microbiota and other pathogens.

1.1.3 Multispecies communities associated with insects

Insects are important pathogens of animals and plants, and insect-associated microorganisms play an important role in their physiology (Steinhaus 1960). Although lower than in humans, insects are colonized by several bacterial species (Steinhaus 1963; Buchner 1965; Lysenko 1985). Insect microbiota is believed to have potential utilization in biotechnology, such as in the production of antiviral or antitumoral compounds (Chernysh *et al.* 2002). In addition, insect symbionts are believed to play a role in the control of incoming pathogens and this could lead the way of potential application in agriculture (Beard *et al.* 2002). Several studies have been made and more are underway in order to elucidate the presence and role of bacteria in insect biology (Brummel *et al.* 2004; Sharon *et al.* 2010; Storelli *et al.* 2011). The *Drosophila melanogaster* microbiota is well described (Corby-Harris *et al.* 2007; Cox and Gilmore 2007; Ryu *et al.* 2008; Wong *et al.* 2011), however most of the insects species we have no information regarding its indigenous microbial community. It is thought that some of the species composing the microbiota are derived from the environment, for example from the plant phylloplane or the animal host in which the insect feeds, but the degree of persistence of these microorganisms in insects is currently unknown. Recent studies on the microbiota of *D. melanogaster* have shown that the microbial diversity present in the insect gut is one to two orders of magnitude lower compared to mammals (Corby-Harris *et al.* 2007; Cox and Gilmore 2007; Ren *et al.* 2007; Ryu *et al.* 2008). These studies have suggested that the complexity of the digestive tract of the insect is directly related to its microbial diversity (Anderson *et al.* 1984; Tanada and Kaya 1993).

In some cases the presence of some bacterial species is dependent on others (Dillon and Charnley 2002). For example, the colonization of germ-free locust by *Pantoea agglomerans* (PAG) is favored by the presence of two other species, *Klebsiella pneumonia* subsp. *pneumoniae* and *Enterococcus casseliflavus*. In this multispecies community it was determined that the production of certain phenolic compounds occurs as a result of metabolic complementarity between members of the microbial community (Dillon and Charnley 1995). The presence of metabolic pathways in microorganisms that are absent in insect also helps the host to overcome some biochemical barriers to herbivory. For example, microorganisms are able to detoxify plant allelochemicals such as flavonoids, tannins and alkaloids (Bhat *et al.* 1998). It was demonstrated that the reintroduction of commensal microbiota into larvae that were grown in axenic conditions and raised in poor media accelerated their developmental timing (Storelli *et al*. 2011). Even mating behavior of *Drosophila* populations was demonstrated to be at least in part controlled by the microbiota (Sharon *et al.* 2010). Commensal insect-associated bacteria may also be involved in interactions that are not beneficial to insect health. A set of experiments concluded that the incoming bacterial *Bacillus thuringiensis*, was being aided by commensal flora of the host (Broderick *et al.* 2006; Broderick *et al.* 2009). Although the mechanism of this interaction is currently under debate (Johnston and Crickmore 2009; Raymond *et al.* 2009; Raymond *et al.* 2010; Mason *et al.* 2011) a possible way that has been proposed is the commensal-to-pathogen switch occurring as a result of *B. thuringiensis* produced pores in the epithelial gut allowing commensals to explore environments otherwise inaccessible.

1.1.4 Multispecies communities associated with plants

Bacteria live in close contact with plants and may be found (i) in the soil zone closest to the root as rhizospheric bacteria (ii) inside the plant in intercellular spaces as endophytes and (iii) living on outside aerial surfaces as epiphytes (Figure 1-2). The soil region closest to the roots directly influenced by plant secretions is called the rhizosphere, while the outside surfaces of the aerial plant parts is the phyllosphere and regions inside plants is called the endosphere (Lindow and Brandl 2003; Hardoim *et al.* 2008). Although plants are economically and ecologically very important for humans the knowledge about their microbiome is currently limited.

Compared to other plant habitats, the phyllosphere is the least studied. It is known that although bacteria are considered to be the dominant inhabitants, archaea, fungi and yeasts are also part of the complex community living in the aerial parts of plants (Figure 1-3) (Inacio *et al.* 2002; Arnold *et al.* 2003). The estimated plant surface area is thought to be 6.4×10^8 km^2 and the bacterial density per cm^2, is thought to be around 10^{26} cells (Lindow *et al.* 2002). A study in the Atlantic forest in Brazil has shown that the number of bacteria present on the leaf surface of this geographic region to be 2 – 13 million bacterial species (Lambais *et al.* 2006). These numbers are most probably underestimated, since the majority of the studies so far are based in culture-dependent methods (Wagner *et al.* 1993; Yang *et al.* 2001). α and γ proteobacteria are generally the major inhabitants of the phyllosphere community however bacteroidetes, β proteobacteria and firmicutes are also present in large numbers. Acidobacteria, cyanobacteria and actinobacteria are present in rare situations (Kadivar and Stapleton 2003; Idris *et al.* 2004; Lambais *et al.* 2006).

The rhizosphere is the most studied bacterial niche associated with plants. Microbial community present in the soil is the biggest bank of microorganism diversity known until now (Curtis *et al.* 2002; Torsvik *et al.* 2002; Buee *et al.* 2009).

It is thought that one gram of rhizosphere can contain up to 10^{11} microbial cells comprising over 30000 species (Egamberdieva *et al.* 2008; Mendes *et al.* 2011).

The microbiome of the soil is mostly starved, thus there is a considerable competition for the plant nutrients released through root exudates (Raaijmakers *et al.* 2009). It has been shown that bacterial communities in the rhizosphere are able to suppress incoming pathogens. Organic amendments can stimulate the activity of some microbial communities, enhancing the pathogen control effect (Hoitink and Boehm 1999). In some cases there are specific pathogen suppression mechanisms (Weller *et al.* 2002; Garbeva *et al.* 2004; Raaijmakers *et al.* 2009). One of the most studied and accepted plant-bacteria beneficial interactions in the rhizosphere is atmospheric N_2 fixation in nodules formed by bacteria belonging to the rhizobia group (Bais *et al.* 2006). Although specific microorganisms are able to protect directly or indirectly the plant, the rest of the microbial community present in the soil can greatly affect this plant beneficial community. Bacteria may interact synergistically; for example, non-antagonistic species can become antagonistic against a third species in the presence of other bacterial strains (De Boer *et al.* 2007). *Pseudomonas fluorescens* PF0-1 undergoes interspecies interactions by fine-tuning its transcriptional and metabolic responses in the presence of other bacteria (Garbeva *et al.* 2011). In the rhizosphere community, QS is thought to play an important role, since several bacterial species found in this niche use this signaling system (Elasri *et al.* 2001). Studies have also shown that bacteria are able to respond to signals produced by plants via a novel interkingdom signaling pathway (Teplitski *et al.* 2000; Gao *et al.* 2003; Teplitski *et al.* 2004; Ferluga and Venturi 2009).

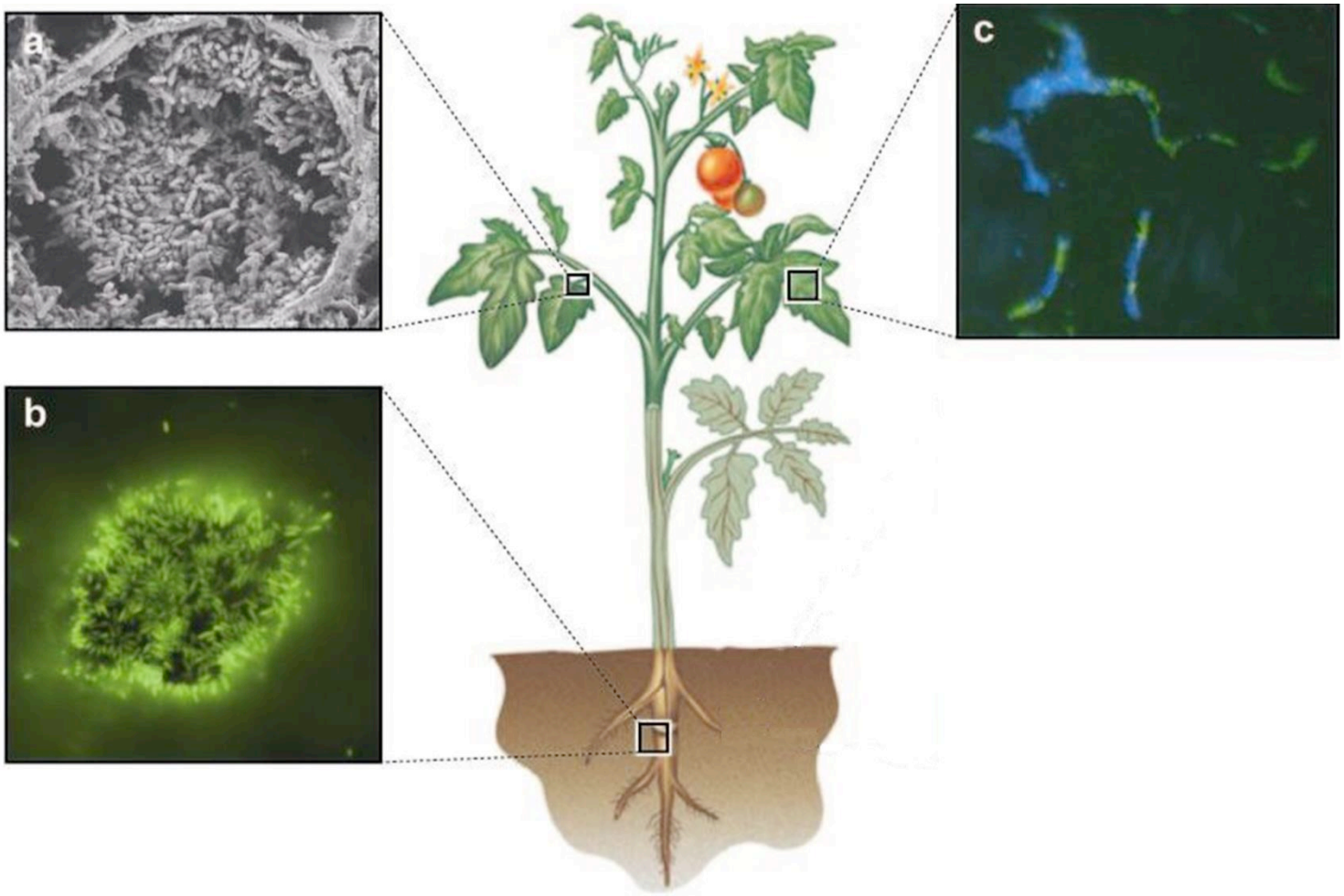

Figure 1-2. Localization of plant associated bacteria (a) endophytes, (b) rhizosphere bacteria or (c) epiphytes (Danhorn and Fuqua 2007).

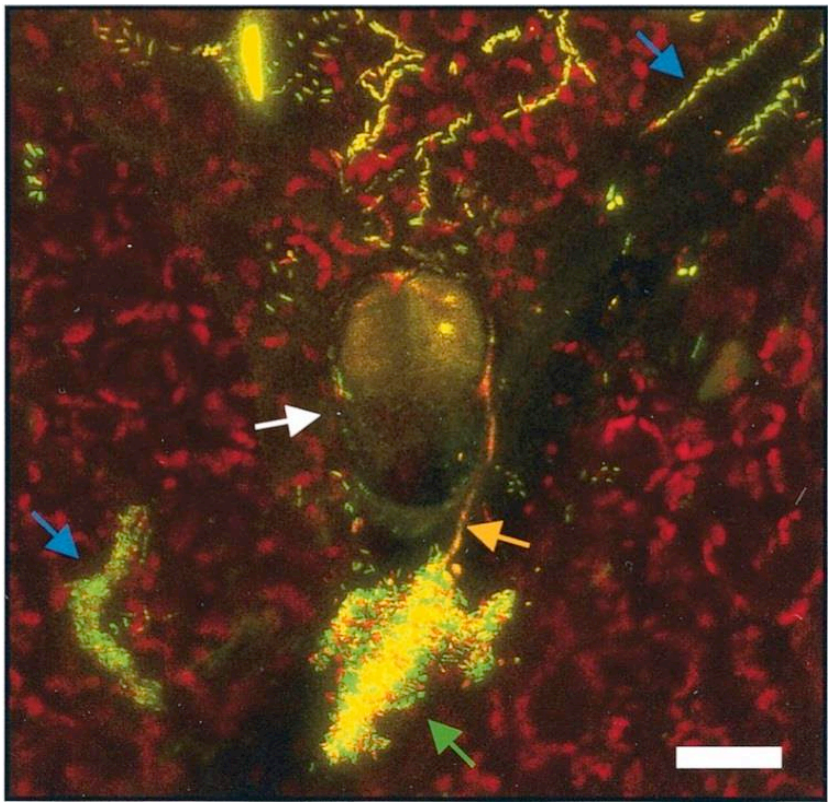

Figure 1-3. Fluorescence micrograph of the natural microbial flora colonizing the bean phyllosphere. A large mixed bacterial aggregate (green arrow), which also includes a fungal hypha (orange arrow), has formed at the base of a glandular trichome (white arrow). Bacteria are present also at plant cell junctions and on veins (blue arrows) Gram-positive bacteria are tagged in red and gram negative ones are tagged in green (Lindow and Brandl 2003).

Microorganisms living in the rhizosphere can also be presented the opportunity to enter the plant through the openings in the lateral roots (Elsas *et al.* 2007). Similarly, epiphytes enter inside plants via stomata or injuries in the aerial parts caused by climatic events, insects or by other ways (McCully 2001). Once inside the plant if microbes are able to colonize and persist they are considered endophytes (Rosenblueth and Martinez-Romero 2006). Endophytes most commonly colonize intercellular spaces and in some cases can also enter and grow in the vascular system (James *et al.* 2002; Chi *et al.* 2005; Compant *et al.* 2005; Lacava *et al.* 2007). Endophytic bacteria have been isolated from both

monocotyledonous and dicotyledonous plants. Protocols for isolating endophytes are currently based in culture dependent methods after sterilization of the plant surface material (Miche and Balandreau 2001). Molecular approaches for detecting endophytic bacteria currently used are mainly based on 16S rRNA amplification and sequencing. Among the inhabitants of pea (*Pisum sativum)*, maize (*Zea mays)*, sorghum (*Sorguhm bicolor*), soybean (*Glycine max*) and wheat (*Triticum spp.)* the predominant bacteria found through this method are *Clavibacter*, *Pseudomonas*, *Cellulomonas*, *Micobacterium* and *Curtobacterium* (Elvira-Recuenco and van Vuurde 2000; Zinniel *et al.* 2002)

Microbiome studies of different plant parts using metagenomics are increasing dramatically (Lundberg *et al.* 2012; Sessitsch *et al.* 2012; Peiffer *et al.* 2013). Recently, a microbiome study was performed on 600 samples via 16s rRNA amplification of soil, rhizosphere and the endophytic compartment of the model plant *Arabidopsis* providing interesting insight on bacterial diversity. This study has shown that in the soil and rhizosphere there is a predominance of Proteobacteria, whereas the endophytic compartment was enriched for Actinobacteria (Lundberg *et al.* 2012). A more recent study of maize rhizosphere corroborated with the results of Lundberg and colleagues, since the community was composed mainly of Proteobacteria (Peiffer *et al.* 2013). A functional metagenomics approach to characterize the endophytic community and its metabolic potential has been performed in rice (Sessitsch *et al.* 2012). In this study, it was reported that majority of bacterial cells belonged to Proteobacteria phylum, followed by Firmicutes. Predominant features of the rice endophytic bacteria were presence of genes coding for flagella, plant-polymer-degrading enzymes, protein secretion systems, iron acquisition and storage, quorum sensing, and detoxification of reactive oxygen species (Sessitsch *et al.* 2012). Understanding the bacterial community present in the different regions directly or indirectly in contact with plants and its metabolic potential is a crucial step if we envisage a more sustainable agriculture where the use of pesticides and fertilizers are reduced.

1.2 The olive knot

The olive plant (*Olea europaea* L.) is thought to be the most important fruit tree in the Mediterranean region. The cultivation and consumption of olives has been increasing in the last decade due to its beneficial effects for human health (Owen *et al.* 2000). As the areas of olive production increase, so do the economic losses due to diseases caused by diverse pathogens, such as insects, nematodes and bacteria. An important olive plant disease is the olive knot; this is an overgrowth of parts of the stem of the olive tree, caused by the bacterial pathogen *Pseudomonas savastanoi* pv. *savastanoi* (PSV). The first report of this disease dates all the way back to the 4th century B.C. by the Greek, Theosphrastus. The first report of the causative pathogen comes from the 19th century (Savastano 1886) and beginning of the 20th century (Smith and Rorer 1904).The pathogen PSV seems to have then spread throughout the world along with the plant (Bradbury 1986). The disease is now present in all olive plant growing areas of the world (Bradbury 1986).

The olive knot disease symptoms are characterized by the appearance of tumors (hyperplasia) on the aerial parts of the trees either as a single knot (Figure 1-4) or in multiple units close to each other. The most common place for tumor development is on twigs and young branches, but can also occur on the main trunk, damaged leaves, roots and fruit stems (Varvaro and Surico 1978). Fruit infection appears as circular brown spots with 0.5 - 2.5 mm of diameter, although rare, it can occur in particularly wet summers (Panagopoulos 1993). In the beginning of the knot-formation process small white/cream swellings rapidly grow into green spherical knots of 3 - 5 mm in diameter, increasing in size (up to 2.5 cm) and changing color to a dark brown with furrows (Iacobellis 2001).

Figure 1-4. Symptoms of the olive knot. Picture taken by Daniel Passos da Silva.

1.2.1 *Pseudomonas savastanoi* pv. *savastanoi*

As mentioned above, the causal agent of the olive knot disease was described for the first time in 1886 by Luigi Savastano. This report was then challenged since it was shown that Savastano's isolate was a mixed culture and the causal agent was a second species isolated along with Savastano's described isolate (Smith and Rorer 1904). After being assigned to the genus *Bacillus*, it was finally assigned to the genus *Pseudomonas*. Throughout the last century this bacteria would still change its taxonomical classification to *Pseudomonas syringae* pv. *savastanoi*, until it was classified as *Pseudomonas savastanoi* pv. *savastanoi* (Gardan *et al.* 1992). Despite significant advances in molecular phylogeny and taxonomy, the nomenclature and classification of PSV is still under dispute. This

bacterium is part of the *P. syringae* group that comprises over 60 species (Bull *et al.* 2010; Young 2010). DNA-DNA hybridization experiments separated the *P. syringae* group into 9 genomospecies (Gardan *et al.* 1999; Young 2010). PSV was included in genomospecies 2 along with 16 other *P. savastanoi-P. syringae* pathovars and other three new species, namely *P. amygdali*, *P. ficuserectae* and *P. meliae*. Multilocus sequence analysis points to a closer similarity between PSV and several other *P. syringae* pathovars. Although the nomenclature *P. savastanoi* is broadly used, a reclassification of this species name to *P. syringae* appears to be suitable along with all the other species from genomospecies 2 group (Sarkar and Guttman 2004; Parkinson *et al.* 2011). Besides olive trees, different pathovars of *P. savastanoi* are able to infect oleander (*Nerium oleander* L.), ash (*Fraxinus* spp.), jasmine (*Jasminum* spp.), privet (*Ligustrum* spp.), buckthorn (*Rhamnus alaternus* L.), myrtle (*Myrtus communis* L.), *Forsythia* spp. and *Philyrea* spp. (Saad and Hanna 2002). The symptoms presented in all plant species due to PSV infection are similar.

PSV does not survive in the soil but can be isolated from the phyllosphere of healthy olive trees as a resident epiphyte. The seasonal presence of PSV and the composition of the olive tree epiphytic community has been studied by isolation (Ercolani 1978; Ercolani 1991), molecular detection (Penyalver *et al.* 2000; Quesada *et al.* 2007) and scanning electron microscopy (Surico 1993). PSV can live epiphytically on the host, it multiples on the surface and can spread to neighboring plants through rain, wind, frost, insects, pruning, harvesting and etc. Damage to the plant, mainly occurring as a result of weather, allows PSV to access the inside of the plant to initiate its virulence program (Baratta and Di Marco 1981). Interestingly, there is a higher incidence of the disease during warm and wet months (Quesada *et al.* 2007). Recently the analysis of PSV infections *in planta* was made by confocal and scanning electron microscopy. Results have shown that the tumor is divided in two areas, one where the vascular cylinder is very similar to the one present in non-infected stems, with a pith parenchyma, xylem, cambium, phloem and epidermis. The second area is characterized by hypertrophied tissue with disorganized hyperplasic cells and displayed internal

cavities surrounded by plasmolysed cells and clusters of primary cell walls. Further magnification of the area showed the presence of xylem vessels coming out of the stem towards the tumoral area (Rodriguez-Moreno *et al.* 2009).

1.2.1.1 Virulence Factors

Several PSV virulence factors have thus far been shown to be involved in tumor development, these include production of phytohomones such as indole acetic acid (IAA) and cytokinins (Comai and Kosuge 1980; Comai and Kosuge 1982; Surico *et al.* 1985; Rodriguez-Moreno *et al.* 2008; Aragon *et al.* 2014), expression of a functional type III secretion system (T3SS) and its effectors (Sisto *et al.* 2004), quorum sensing system (Hosni *et al.* 2011). Recently a signature-tagged mutagenesis screening resulted in the identification of numerous other mechanisms associated with virulence of PSV (Matas *et al.* 2012).

Phytohormones are responsible for unregulated multiplication and size expansion of plant cells leading to galls and knot formation (Surico *et al.* 1985). The pathogenesis process is therefore directly influenced by bacterial phytohormone production (Iacobellis *et al.* 1994) which alters the physiological balance in the infected tissues and causes their uncontrolled proliferation. This process is characterized by cell enlargement and division and it also includes differentiation into xylem and phloem elements arranged in bundles or cyclic nodules (Surico and Iacobellis 1992). In PSV, the phytohormone IAA is synthetized in a two-step process. First the enzyme tryptophan 2-monooxygenase, encoded by the *iaaM* gene, catalyzes the conversion of tryptophan to indoleacetamide (IAM). In the second step IAM hydrolase, encoded by *iaaH,* catalyzes the conversion of IAM to IAA. Although PSV has two copies of *iaaL (*Matas *et al.* 2009), the gene that encodes a indole-3-acetyl-ε-L-lysine (IAA-lys) synthetase, IAA-lys has not been detected experimentally in PSV

cultures (Evidente *et al.* 1985; Glass and Kosuge 1988). In contrast to IAA production which is widespread in *P. savastanoi* pathovars, the production of cytokinins has been described only for olive and oleander pathovars (Powell and Morris 1986; Iacobellis *et al.* 1994). The *ptz* gene, encoding a isopentenyl transferase is located in a plasmid in *P. savastanoi* pv. *savastanoi* NCPPB 3335 (Rodriguez-Moreno *et al.* 2008).Plasmid curing experiments have shown the importance of this phytohormone, since in its absence knot volume was reduced in comparison to knots caused by the wild-type strain (Iacobellis *et al.* 1994; Rodriguez-Moreno *et al.* 2008; Bardaji *et al.* 2011).

Plant pathogens belonging to the genera *Erwinia*, *Pseudomonas*, *Ralstonia* and *Xanthomonas* share common features; they colonize the intercellular space of plants, are able to kill plant cells and possess the *hrp* genes, responsible for the assembly of the T3SS (Alfano and Collmer 1997). A great number of these pathogens are species-specific, and cause wide variety of symptoms in their respective hosts, while in non-host plants they usually induce a hypersensitive response (HR). This is a defense-associated process that consists of isolating the infected location by inducing cell death in surrounding area (Dangl *et al.* 1996). PSV pathogenicity has been associated with the presence of a functional T3SS (Sisto *et al.* 2004). Mutants of *hrp* genes failed to cause disease symptoms in olive trees and HR in non-host, but interestingly when inoculated in micropropagated olive plantlets they were able to generate a tumor, although it did not develop necrosis or the internal open cavities, which is characteristic of mature tumors (Rodriguez-Moreno *et al.* 2008; Perez-Martinez *et al.* 2010). Additionally, analysis of *P. savastanoi* pv. *savastanoi* NCPPB 3335 genome and plasmid sequence has shown the presence of at least 30 genes encoding type III effectors (Rodriguez-Palenzuela *et al.* 2010; Bardaji *et al.* 2011).

More recently the role of QS in PSV virulence was studied. It has been reported that PSV produces 3-oxo-C6 HSL and 3-oxo-C8 HSL signals through the expression of *pssI* which encodes an *N*-acyl homoserine lactone synthase. A transcriptional regulator, named PssR, which responds to the cognate AHLs is

also present. Pathogenicity tests using mutants for the synthase (PSVPSSI) and of the transcriptional regulator (PSVPSSR) indicated that QS is crucial for tumor development (Figure 1-5). Co-inoculations of the PSVPSSI mutant with a harmless bacterial species, called *Erwinia toletana* , commonly isolated from olive knots rescued the disease symptoms via cross feeding of the AHLs signal molecules to PSV PSSI (Hosni *et al.* 2011).

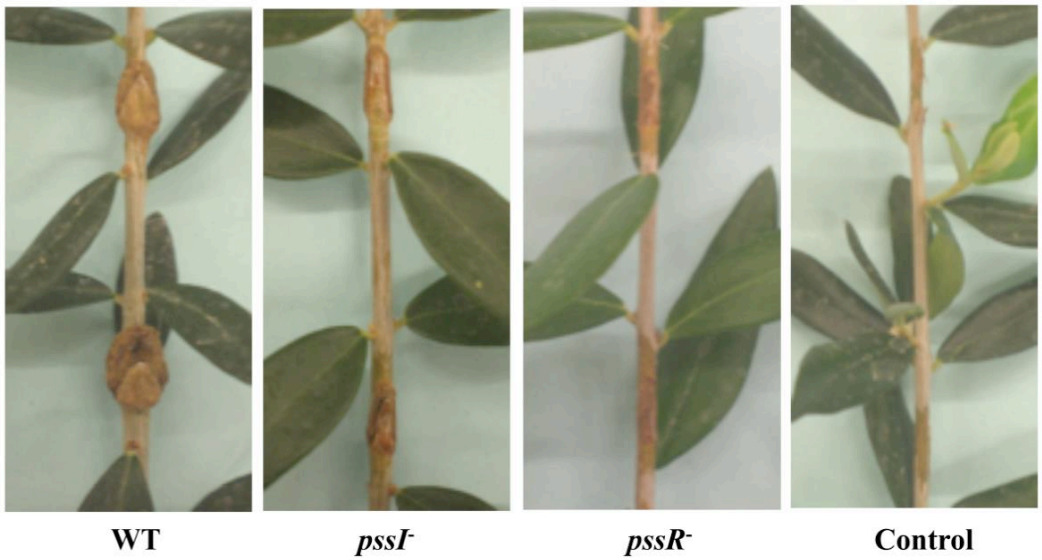

Figure 1-5. Role of the QS system in knot development. While the PSV wild type strain was able to cause tumors, mutants for the AHL synthase gene (*pssI*) and of the transcriptional regulator (*pssR*) resulted in much attenuated symptoms (Hosni *et al.* 2011).

1.2.2 *Erwinia toletana*

In 2004 a study that concentrated on isolating bacteria from olive knots in the region of Toledo, Spain, resulted in the first description of the new species designated as *Erwinia toletana* (ET). ET was isolated from several different knots along with the causal pathogen PSV. It is a gram-negative bacterium, catalase-positive, oxidase-negative, motile, fermenting glucose without gas formation

with an optimal growth temperature of 28°C, being able to grow on temperatures up to 36°C. Colonies grown in nutrient agar are circular, slightly convex, translucent and non-pigmented while in KB medium present the same characteristics including a mucoid phenotype (Rojas *et al.* 2004). Its contribution to the disease is still unknown, but recently its ability to cross feed AHLs to PSV was described. Furthermore, the same study provided evidence that more factors could be involved in the beneficial interaction of ET with the PSV (Hosni *et al.* 2011).

1.2.3 Community present on olive knots

Several different bacterial species have been isolated from the knot produced by PSV (Ercolani 1978; Rojas *et al.* 2004; Marchi *et al.* 2006; Ouzari *et al.* 2008; Moretti *et al.* 2011). Many of these species are known to be able to synthetize phytohormones; however the possible role in disease of this trait is currently unknown (Marchi *et al.* 2006; Ouzari *et al.* 2008). One of the most common bacteria isolated from knots is PAG and its growth is stimulated in the presence of PSV (Marchi *et al.* 2006; Quesada *et al.* 2007). PAG is commonly present as epiphyte in a diverse set of hosts (Lindow and Brandl 2003) and although it is not able to cause tumors on olive plants it carries a pathogenicity island that encodes a functional T3SS, pathway for IAA biosynthesis and production of cytokinins (Valinsky *et al.* 1998). The interaction between PSV and PAG is still unclear since there are reports of both PAG increasing and decreasing the number of PSV cells in the tumor (Marchi *et al.* 2006; Hosni *et al.* 2011). ET is also commonly found in tumors caused by PSV as already mentioned above (Rojas et al. 2004). ET and PSV interaction constitutes a stable dual species community and sharing of AHLs appears to have a role in this stability. It is likely that more interspecies interactions are taking place. *Erwinia oleae* has also been recently described as an endophyte associated with the olive knot and studies

shown that it can also promote a more aggressive disease due to its interactions with PSV (Moretti *et al.* 2011).

1.2.3.1 *Erwinia toletana* and *Pseudomonas savastanoi pv. savastanoi* interaction

Studies of bacterial diseases have been most commonly performed using a single species inoculum. While this minimalist strategy prioritizes the interaction between bacteria and host, it has become clear that interspecies interactions in disease are important not only among bacterial species (Duan *et al.* 2003; Sibley *et al.* 2008a; Sibley *et al.* 2008b) but also with fungi, nematodes, viruses etc and can play a crucial role in a disease model (Hayes *et al.* 2010; Kane *et al.* 2011; Kuss *et al.* 2011).

ET is able to interact in a beneficial way with PSV during knot development. This is evident not only in increased number of cells of PSV and ET but also in increased tumor volume during co-inoculations compared to single inoculations. The production of IAA by ET could be one of its contributions to the consortia. Curiously ET synthetizes, through the expression of *etoI*, the same AHLs (3-oxo-C6 HSL and 3-oxo-C8 HSL) as PSV and it was shown *in vivo* that there is a cross feeding of these molecules in the tumor tissue (Hosni *et al.* 2011). It is possible that ET might contribute to the increase in knot volume through additional factors like metabolic complementarity, improving the biofilm structure, cross feeding of siderophores etc (Figure 1-6). The understanding of specific molecules and processes that decide the stability of this interesting consortium could help the scientific community to learn the basic rules that govern a simple microbial community in plants. The olive knot could therefore be a model of multispecies disease in plants where one of the microorganisms is a resident bacterium. This is one of the aims of this thesis.

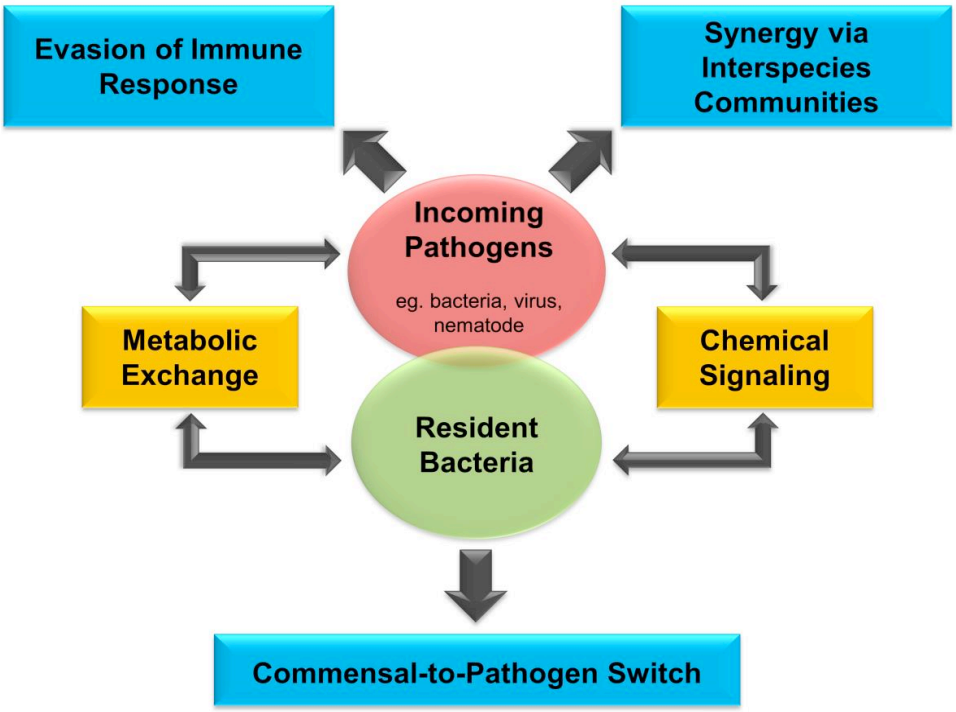

Figure 1-6. Schematic representation of possible mechanisms involved in the interaction between incoming pathogens (red) and resident bacteria (green). The interactions involving both residents and pathogens such as signaling or metabolic exchange are shown in yellow whereas changes of phenotypes or effects on the host are shown in blue (Venturi and da Silva 2012).

2 AIMS

A large number of different microorganisms live in different niches resulting in a multispecies microbial community. For example in the oral cavity of a human up to 10^3 species can be found and in the human gut many more; these interactions are now beginning to be intensively studied. Importantly, incoming pathogens will also therefore encounter and interact with the residential microbial community when attacking the host. The aim of this thesis is to use the olive know as model system to study bacterial multispecies interactions. The olive knot disease is caused by *Pseudomonas savastanoi* pv. *savastanoi* (PSV) and several other non-pathogenic bacteria, such as *Erwinia toletana* (ET), have been reported to be living in this niche.

The main objectives of this thesis are:

A. Genome sequence and analysis of the genome of the endophytic bacterium *Erwinia toletana* associated with the pathogen inside the olive knot;

B. Determine how closely PSV and ET localize during the knot formation process;

C. Determine possible mechanisms of interspecies interaction between PSV and ET which leads to mutual benefit for both species;

D. Identify the microbial community commonly present in the olive knot.

3 MATERIALS AND METHODS

3.1 Bacterial strains and growth conditions

PSV DAPP-PG 722 and ET DAPP-PG 735 and their derivatives were routinely grown at 28°C on King's B (KB) broth (Sambrook and Russell 2001). All media composition is described in Appendix 7.1. When required, antibiotics were added in the following concentrations: nitrofurantoin, 100 µg mL^{-1}, ampicillin, 100 µg mL^{-1}, tetracycline, 40 µg mL^{-1}, gentamicin, 40 µg mL^{-1}, chloramphenicol, 250 µg mL^{-1} and kanamycin, 100 µg mL^{-1}. *E. coli* strains were grown at 37°C on LB broth and when required appropriate antibiotics were added in the following concentrations: ampicillin, 100 µg mL^{-1}, tetracycline 10 µg mL^{-1}, gentamycin 10 µg mL^{-1}, chloramphenicol, 25 µg mL^{-1} and kanamycin, 50 µg mL^{-1} (Table 3.1).

Table 3-1. Bacterial strains used in this study.

Strains	Relevant characteristics	Source
***E. coli* DH5α ™**	Φ80*lacZ*ΔM15, Δ(*lacZYA-argF*) U169, *recA*1, *endA*1, *hsdR*17 (rK^-, mK^+), *phoA*, *supE*44, λ^-, *thi*-1, *gyrA*96, *relA*1	Invitrogen-LifeTechnologies™
***E. coli* DH5α ™ pRK2013**	Derivative of *E. coli* DH5α ™ containing pRK2013 (Km^R oriColE1 RK2-Mob^+ RK2-Tra^+)	(Figurski and Helinski 1979)
***Agrobacterium tumefaciens* NTL4 pZLR4**	Derivative of NT1, Δ*tetC*58, Tc^S containing pZLR4 (*traG*::*lacZ*, *traR*, Gm^+)	(Luo *et al.* 2003)
ET DAPP-PG 735	Amp^R, Nif^R	(Hosni *et al.* 2011)
ETETOI	*etoI*::Km^R of ET DAPP-PG735	(Hosni *et al.* 2011)
ETETOR	*etoR*::Km^R of ET DAPP-PG735	(Hosni *et al.* 2011)
ETG200_18815	*G200_18815::mTn5 Km^R of ET DAPP-PG735	This study
PSV DAPP-PG 722	Amp^R, Nif^R	(Hosni *et al.* 2011)
PSVPSSI	*pssI*::Km^R of PSV DAPP-PG722	(Hosni *et al.* 2011)
PSVPSSR	*pssR*::Km^R of PSV DAPP-PG722	(Hosni *et al.* 2011)

*Refers to NCBI code number for the putative intermembrane protein coding sequence.

3.2 Reagents and chemicals

All chemicals used for culture media preparation were purchased from Difco (Franklin Lakes, NJ, USA) and Sigma (St. Louis, MO, USA). Molecular biology reagents were acquired from New England Biolabs (Ipswich, MA, USA), Promega (Madison, WI, USA) and Ambion (Austin, TX, USA).

3.3 Recombinant DNA techniques

Recombinant DNA techniques, including digestion with restriction enzymes, agarose gel electrophoresis, purification of DNA fragments and ligations with T4 DNA ligase were performed as described (Sambrook and Russell 2001). The composition and preparation of solutions used are provided in Appendix 7-1.

3.3.1 Genomic DNA extraction

All DNA manipulations and transformation, were performed as described previously (Sambrook and Russell 2001). Genomic DNA from ET and PSV was isolated by Sarkosyl-pronase lysis method (Better *et al.* 1983).

3.3.2 DNA agarose gel electrophoresis

DNA samples were analyzed routinely on agarose gels (0.8-2.0% w/v) in TAE 1x (40 mM Tris base, 1 mM EDTA pH 8.0, 0.1% glacial acetic acid). To visualize DNA, SYBR Green I nucleic acid gel stain (Invitrogen, Carlsbad, CA, USA) was added 1:10000 into the gel solution prior to pouring the gel. Electrophoresis was performed in Biorad (Hercules, CA, USA) minisubTM cell chamber, at 5 V cm^{-1}, and TAE 1x was used as running buffer (Sambrook and Russell 2001).

3.3.3 Cloning of PCR products

Cloning and expression vectors used are listed in Table 3-2. For cloning purposes, DNA fragments were PCR amplified from approximately 50 ng of chromosomal DNA. For general PCR reactions, 0.6 U of GoTaq Flexi (Promega, Madison, WI, USA) were used, and the reaction mix was composed by 200 µM dNTPs, 1.5 mM $MgCl_2$, 0.1 µM of each primer. Restriction sites were added to the primers at the 5' ends when required. PCR reactions were performed in an Applied Biosystems PCR GeneAmp 2400 thermocycler. The DNA template was initially denatured at 94°C for 5 min, followed by 30 cycles of denaturation at 94°C, annealing at appropriate temperature depending on primer melting point for 30 seconds and extension at 72°C for 1-3 min, according to the length of the fragment to be amplified. A last extension cycle at 72°C during 5 min was used to ensure completion of strands.

In all cases, fragments were separated by electrophoresis and extracted from the gel by using the EuroGold gel extraction kit (EuroClone, Italy). Blunt ended fragments were cloned into pBlueScript II KS+ (Agilent Technologies, Wilmington, DE, USA) and protruding A- fragments were cloned into pGEM®-T

easy (Promega, Madison, WI, USA), according to the instructions of the manufacturer. Subsequently, each fragment was excised with restriction enzymes, ligated into the final vector, and sequenced (Macrogen Europe, Amsterdam, AZ, The Netherlands) to verify the identity and orientation of the insert.

Table 3-2. Cloning and expression vectors used in this study.

Plasmids	Relevant characteristics	Reference
pGEM®-T easy	Cloning vector, Amp^R	Promega
pBlueScript II KS+	Cloning vector, Amp^R	Stratagene
pMP220	Promoter probe vector, IncP, LacZ, Tc^R	(Spaink *et al.* 1987)
pMP77	Promoter probe vector, IncQ, Cm^r	(Spaink *et al.* 1987)
pBBR1MCS2	Broad-host-range vector, Km^R	(Kovach *et al.* 1995)
pBBR1MCS3	Broad-host-range vector, Tc^R	(Kovach *et al.* 1995)
pBBR1MCS5	Broad-host-range vector, Gm^R	(Kovach *et al.* 1995)
pCRS530	Contains mTn5-GNm, Km^R Amp^R	(Reeve *et al.* 1999)

New England Biolabs (Ipswich, MA, USA) restriction enzymes were used to cut genomic and plasmid DNA. Generally 0.5-1 µg of DNA were digested by using 10 U of enzyme in a final volume of 25 µL, with the addition of the buffer suggested by the provider. Reactions were incubated from 2 h to 10 h, and when required heat inactivation at 65-80°C was performed to stop the reaction. For ligation reactions, a 1:2.5 ratio of vector to insert was used, and 1 U of T4 DNA ligase (Promega, Madison, WI, USA) was added in a final volume of 20 µL. Ligation reactions were incubated for 12 h at room temperature.

3.3.4 Plasmid isolation

Plasmid DNA isolation from *E. coli* was performed by using EuroGold columns (EuroClone, Italy) according to the manufacturer's instructions. Briefly, overnight cultures were submitted to alkaline lysis and neutralization. After removal of the cellular debris the lysates were loaded in a silica column and eluted with previously heated (75°C) sterile water.

3.3.5 Bacterial transformation and conjugation

Preparation of *E. coli* competent cells was done by using the protocol described in Appendix 7.4 (Hanahan *et al.*, 1991). Transformation was performed by mixing 5 µL plasmidic DNA with 100 µL of competent cells. The mixture was incubated on ice for 30 min, and then heat shocked at 42°C for 90 secs. The heat shock was stopped by incubation on ice for two min, and 1 mL of pre-warmed LB was added. Cells were then grown 1-2 hours in agitation at 37°C, and transformants were selected on LB agar plates with the proper antibiotics.

Plasmids were mobilized from *E. coli* to PSV or ET by tri-parental matings using the helper strain *E. coli* (pRK2013) (Figurski and Helinski, 1979). Overnight cultures from donor, helper and acceptor were diluted 1 to 25 in fresh LB medium, and then grown during 6 hours. Each culture was then harvested and washed twice, and optical density was determined. Volumes equivalent to 5 $x10^8$ cells from donor and helper were mixed with the corresponding volume to 2 $x10^8$ cells from the acceptor. The mixture of cells was then centrifuged and resuspended in 100 µL of medium, and cells were spotted on top of a 0.45 µm nitrocellulose filter, previously placed on a LB agar plate. The conjugation mixture was incubated 12 h at 28°C. Thereafter, cells were then resuspended in 1

mL LB broth, serially diluted and plated on LB agar, with proper antibiotics. Mixtures of donor cells plus acceptor were used as negative control.

3.3.6 Southern hybridization

For Southern analysis, approx. 1 µg of genomic DNA was digested overnight with 10 U of restriction enzyme (s) (NewEngland Biolabs). Digested DNA was then electrophoresed in 0.8% agarose gels, visualized and photographed. Thereafter, the gel was depurinated by soaking it in a 125 mM HCl solution during 10 min, followed by denaturation during 30 min in denaturation solution (1.5 M NaCl, 0.5 M NaOH). The gel was then blotted to transfer the DNA to a nylon membrane (Hybond™-XL-Amersham, Biosciences), according to procedures described by the manufacturer. Subsequently, the membrane was dried and fixed by UV crosslinking. Solutions for hybridization are described in Appendix 7.1. Membranes were prehybridized in Denhardt's buffer at 65°C for at least 1 hour before addition of the radiolabeled probe. Probes were prepared by using a Random Primed DNA labeling kit (Roche), with 25 ng of DNA-template and 0.05 mCi [α-32P] dCTP, as stated in the provider's instruction handbook. For removal of unincorporated dNTPs, a G-25 sephadex column was used (Quick Spin Columns- Roche). Once purified, the probe was diluted to 20 mL with hybridization solution, and denatured by heating at 100°C for 10 min. At this stage the denatured probe was added to the membrane. Hybridizations were performed overnight at 65°C. After probe removal, the membrane was washed once with wash solution 1 (2x SSC, 0.1%SDS) at room temperature followed by two washes of solution 2 (1X SSC, 0.1% SDS) at 65°C. Finally, the membrane was washed twice with (0.1x SSC 0.1% SDS) at 65°C. To identify the DNA fragments hybridized to the probe used, KODAK Biomax MS Films were exposed on the membrane, enclosed in a cassette and incubated at -80°C, and developed after 6 hours.

3.4 Construction of plasmids pBBR2GFP, pBBR5GFP, pBBR2DsRedExpress and pBBR5DsRedExpress

Digestion of plasmids pBK-miniTn*7*-*gfp*1 (Koch *et al.* 2001) and miniTn*7*(Km, Sm) $P_{A1/04/03}$-DsRedExpress-a (Lambertsen *et al.* 2004) with NotI yielded fragments of 2 kb which were blunt ended by treatment with Quick Blunting Kit (New England Biolabs Ipswich, MA, USA). Fragments were cloned into pBBR1MCS5 digested with SmaI and dephosphorylated with TSAP (Promega, Madison, WI, USA) resulting in the constructs pBBR5GFP and pBBR5DsRedExpress. To generate pBBR2GFP and pBBR2DsRedExpress the cassette was then transferred to pBBR1MCS2 using ClaI/SpeI restriction enzymes (Table 3-3). The resulting plasmids were maintained in *E. coli* DH5α ™ and transferred to PSV or ET by triparental conjugation using the helper strain *E. coli* DH5α ™ (pRK2013).

3.5 Plant infection and isolation of bacteria from olive knots

Olive plants (*Olea europaea* L.) derived from seeds germinated *in vitro* (originally collected from a cv. Arbequina plant) were micropropagated and rooted, as previously described (Rodriguez-Moreno *et al.* 2008), in Driver Kuniyuki Walnut (DKW) medium (Driver and Kuniyuki 1984). Rooted explants were transferred to DKW medium without hormones and kept for at least 2 weeks in a growth chamber at 25°C with a 16-h photoperiod prior to infection. The olive plants used for *in vitro* studies were 60 to 80 mm long (stem diameter, 1 to 2 mm) and contained three to five internodal fragments.

Micropropagated olive plants were wounded by excision of an intermediate leaf and infected in the stem wound with a bacterial suspension

under sterile conditions. For this purpose, bacterial lawns were grown for 48 h on LB plates and resuspended in 10 mM $MgCl_2$. The concentration of the bacterial cells was adjusted to an optical density at 600 nm of 0.1 on single inoculations, corresponding to approximately 10^8 CFU mL^{-1}. For co-inoculations, a mixed bacterial suspension containing approximately 10^8 CFU mL^{-1} of each species was prepared. The plant wounds were infected with 2 µl of the resulting cell suspension. The plants were then incubated in a growth chamber at 25°C with a 16-h photoperiod and a light intensity of 35 µmol m^2s^{-1}. At different time points, PSV and ET cells were recovered from the infected explants and spotted onto LB plates as previously described (Maldonado-Gonzalez *et al.* 2013). Population densities were calculated from at least three replicates. The morphology of the olive plants infected with bacteria was visualized using a stereoscopic microscope (Leica MZ FLIII).

3.6 Real-time monitoring of bacterial infection by epifluorescence microscopy and confocal laser scanning microscopy (CLSM)

To visualize bacterial infection within tumors in real time, whole knots were directly examined with a stereoscopic fluorescence microscope with 3, 7, 21 and 28 days post inoculation (d.p.i.) (Leica MZ FLIII) equipped with a 100-W mercury lamp, a GFP2 filter (excitation, 480/40 nm; emission 510LP) and a RFP filter (excitation, 546/10; emission, 570LP). Images were captured using a high-resolution digital camera (Nikon DXM 1200).

To visualize bacterial infection within the tumors of the olive plants with CLSM, the knots were sampled 28 d.p.i., at 1 cm above and below the inoculation point. These samples were fixed and embedded in agarose as previously described (Rodriguez-Moreno *et al.* 2009). Samples were fixed overnight at 4°C in 2.5% paraformaldehyde (PFA) prepared in 0.1 M phosphate buffer, pH 7.4. The fixed

samples were then transferred into 2.5% PFA with an ascending gradient of 10, 20, and 30% sucrose for 10, 20, and 30 min, respectively. Finally, samples were embedded in 7% low-melting-point agarose and cooled to 4°C. Sections (40 and 60 µm thick) were cut from the knot samples using a vibrating microtome (Leica CM1325). Fluorescence of the bacterial cells within knot sections was visualized by epifluorescence microscopy using a Nikon Microphot FXA microscope.

For confocal microscopy, it was used an inverted CLSM (model TCS-NT; Leica, Germany) equipped with detectors and filters that simultaneously detect green and red fluorescence. Images of green fluorescence were acquired at an excitation wavelength of 488 nm and an emission wavelength of 500 to 550 nm while red fluorescence emission was recorded in the interval between 575 and 625 nm. The images were acquired by sequential scan analysis and processed using Leica LAS AF Lite software.

3.7 *Erwinia toletana* genome sequencing

The genome sequence was determined using a 36-bp paired-end library with the Illumina GA sequencing system as described previously (Studholme *et al.* 2009). We performed *de novo* assembly using Velvet 1.1.03 (Zerbino and Birney 2008), generating 94 contigs which were further joined into 23 scaffolds with a mean length of 226 kbp. Automated annotation of the ET draft genome sequence using RAST (Aziz *et al.* 2008) assigned a total of 4766 candidate protein-coding genes. This Whole Genome Shotgun project has been deposited at DDBJ/EMBL/GenBank under the accession number AOCZ01000000.

Table 3-3. Plasmid constructs generated in this study.

Plasmids	Description	Primer	Primer sequence	Amplicon/insert size (bp)
pBBR3TOLI	pBBR1MCS3 containing *tolI* gene from ET	TolIexpressionFw TolIexpressionRv	GTCTCGAGCAAATCTGCTGATGCCGC GGACTAGTGCCTGGCTGCTGATTACTTT	692
pTOLI220	pMP220 containing the promoter region of *tolI* gene from ET	TolIpromFw TolIpromRv	GGTACCGAGATCTTCAGCTTGCCTGTTATGC GGGCCCTGAATTCATAATCTTCATCACTGTCCCC	156
pTOLI77	pMP77 containing the promoter region of *tolI* gene from ET	TolIpromFw TolIpromRv	GGTACCGAGATCTTCAGCTTGCCTGTTATGC GGGCCCTGAATTCATAATCTTCATCACTGTCCCC	156
pTOLR220	pMP220 containing the promoter region of *tolR* gene from ET	TolRpromFw TolRpromRv	CGAATTCGCGACAACTAATGCCGTT ACTGCAGATACGCAGTGTCATTCGC	226
pBBR5G200_18815	pBBR1MCS5 containing G200_18815 gene from ET	18815expressFw 18815expressRv	CGGATTATAACGCCGCTCAT CGGACACGACAACAGGAATAG	775
pBBR5TOLR	pBBR1MCS5 containing *tolR* gene from ET	TolRexpressFw TolRexpressRv	CTCGAGACTCCGGCATTTACCAGC ACTAGTTTAAATTAGGCCTGTGGCG	789
pBBR5GFP	pBBR1MCS5 containing GFP extracted from pBK-miniTn7-*gfp*1 digested with NotI			≅ 2000
pBBR2GFP	pBBR1MCS2 containing GFP extracted from pBBR5GFP digested and cloned using ClaI/SpeI			≅ 2000
pBBR5DsRedExpress	pBBR1MCS5 containing DsRedExpress extracted from miniTn7 $P_{A1/04/03}$DsRedExpress-a and cloned with NotI			≅ 2000
pBBR2DsRedExpress	pBBR1MCS2 containing DsRedExpress extracted from pBBR5DsRedExpress-a and cloned using ClaI/SpeI			≅ 2000

3.8 Whole genome analysis of ET

Analysis of ET genome sequence was performed in Unix environment using Perl scripts and MUMmer (Kurtz *et al.* 2004). Categorization of putative coding protein sequences was done in RAST. The genome of ET was aligned against the *Erwinia billingiae* Eb661 using the software Mauve 2.3.1 build 173 (Darling *et al.* 2010) to generate an image of the whole genome alignment. Identification of putative virulence factors was done using the Virulence Factors Database (VFDB) (Chen *et al.* 2012) as guide and found by Blast feature against ET genome in RAST webserver.

3.9 Pathway Tools: SavCyc, TolCyc and SavtolCyc creation and availability

Metabolic pathways were recreated using the software Pathway Tools (Karp *et al.* 2010). The PathoLogic input file was prepared according to the instructions in the Pathway Tools (version 16.5) user's guide by feeding the software with the latest annotated files of PSV (Rodriguez-Palenzuela *et al.* 2010) or ET (Passos da Silva *et al.* 2013) draft genomes and merged files of PSV and ET draft genomes. An initial build of PSV, ET and the joined PSV and ET metabolic pathways were named SavCyc, TolCyc and SavtolCyc, respectively, using the default reference database, MetaCyc (Caspi *et al.* 2012). No manual curation was performed on the created databases. Created databases are available via Pathway tools software and at ftp://ftp.icgeb.org/pub/tmp/Passos.

3.10 Phenotypic microarray of ET and PSV using Biolog

The Biolog Phenotype Microarray (PM) technology comprise a total of 1920 tests and uses tetrazolium violet irreversible reduction to formazan as a reporter of active metabolism (Bochner *et al.* 2001). Twenty 96-well microarray plates were used (PM 1-20) for each of the three inocula: 1) ET, 2) PSV, 3) PSV + ET, for a total of 60 plates processed.

The twenty microarray plates comprehend different metabolic and toxic compound conditions, including 192 assays of C-source metabolism (PM 1-2), 384 assays of N-source metabolism (PM 3, 6-8), 96 assays of P-source and S-source metabolism (PM 4), 96 assays of biosynthetic pathways (PM 5), 96 assays of ion effects and osmolarity (PM 9), 96 assays of pH effects (PM 10), and sensitivity to 240 chemicals (PM 11-20). The reduction of the dye causes the formation of a purple color that is recorded by a charge coupled-device camera every 15 min and provides quantitative and kinetic information about the response of the cells in PM plates. All procedures were performed as indicated by the manufacturer as described in the Appendix 7.2.

3.11 Biodegradation of aromatic compounds

PSV and ET were tested for growth on minimal M9 medium (Sambrook and Russell 2001) with sole carbon sources. Co-inoculations of ET and PSV were performed on M9 minimal medium containing a sole carbon source as follows: ET and PSV were grown overnight in rich medium and cells were then pelleted and washed twice in M9 medium without carbon source. ET and PSV were then resuspended in M9 medium and these cultures were used as inoculum into M9 medium with a unique carbon source. Amounts of PSV and ET that were

inoculated resulted in a 0.05 OD_{600} for each isolate meaning that the mixed culture had an OD_{600} of 0.1. Bacterial growth was monitored constantly by measuring OD_{600} and by plating culture dilutions on rich medium.

The biodegradation of aromatic acids by ET and PSV was analyzed by reverse-phase HPLC, using a Varian 9010 solvent delivery system equipped with a Varian 9050 UV/vis detector. ET and PSV were grown in M9 minimal medium supplemented with 0·1% of the aromatic acid. Samples were withdrawn from cultures after 24h of growth and were centrifuged at 12000 g. The supernatant was diluted 100-fold into methanol and filtered through 0·2 µm filters; 10 µL sample was loaded on a 5 µm spherical C18 reverse-phase column (Supelcosil LC18 150×4·6 mm; Supelco) and eluted with 35% methanol and 65% water with 0·1% acetic acid at a flow rate of 0·8 mL min^{-1}. The eluted metabolites were detected at 280 nm.

3.12 Sample collection and processing for metagenomics

Young knots were collected from diseased olive trees of cultivars Frantoio, Cima di Mola and Oliva Rossa, grown in Umbria (Central Italy) and Apulia (South Italy). Genomic DNA was isolated from 1 g of fresh-weight knots using the plant DNA extraction mediprep with cetyltrimethylammonium bromide CTBA protocol. Briefly, knots were ground to a fine powder in liquid nitrogen within a cooled mortar. The ground tissue was mixed with 6 mL of ice cold extraction buffer (100 mM Tris–HCl, pH 8.0; 500 mM NaCl; 50 mM EDTA; 10 mM ß-mercaptoethanol) and transferred to a 15 mL Falcon tube. After addition of 0.8 mL of 10% SDS and incubation at 65°C for 30 min, 2 mL of ice cold 5/3 KAc solution (5 M CH_3CO_2K; CH_3COOH) were added. The suspension was centrifuged for 10 min at 5000 *g* at 4°C and supernatant was filtered through a paper filter (S&S 595). After isopropanol precipitation and centrifugation for 10 min at 10000 *g* at

room-temperature, pellet was dissolved in 400 µL TE (10 mM Tris–HCl pH 8.0, 1mM EDTA) and RNase (20 mg mL^{-1}) treatment was performed for 20 min at room-temperature. After incubation for 15 min at 65°C with CTAB buffer [0.2 M Tris-HCl, pH 7.5; 2 M NaCl; 0.05 M EDTA; 2% (w/v) (CTBA)], two chloroform/isoamylic alcohol (24:1) extractions were performed. Nucleic acid was precipitated from the aqueous layer by the addition of an equal volume of ethanol (96%). After centrifugation, the pellet was washed with 70% (v/v) ethanol, air-dried, and resuspended in 110 µl nuclease free water.

3.13 Bacterial 16S rRNA PCR amplification and pyrosequencing

The PCR strategy was carried out by GATC Biotech (Konstanz, D) as follows: first 16S-rRNA PCR for the V1/V3 region using primers 27F and 534R was performed. The PCR conditions used were: denaturation step at 98°C for 30s, followed by 25 cycles of 98°C 10s, 56°C 30s, 72°C 10s and a final extension of 72°C for 1 min. Next, PCR products were column purified and a second PCR was performed to add the sequencing adaptors and multiplex identifiers. The PCR conditions for the second PCR were the same as above, except only 5 amplification cycles were performed. The library was sequenced on the Roche GS FLX following standard protocols from Roche.

3.14 Metagenomics data analysis

Unassembled reads were uploaded to the open access Metagenome Rapid Annotation using Subsystem Technology (MG-RAST) server (http://metagenomics.anl.gov/) (Meyer *et al.* 2008). Analyses were performed using the MG-RAST pipeline applying the RDP dataset. Results were imported

into an excel spreadsheet manually curated for graphical presentation and table creation on Microsoft Excel. α-diversity was estimated using MG-RAST metagenomics analysis server using the same sequencing reads for classification. Results are based on RDP using a maximum e-value of 1e-2, a minimum identity of 80%, and a minimum alignment length of 50 bp applying Bray-Curtis distance and ward clustering. Data were normalized based on MG-RAST version 3.0. Sequences obtained during this study were deposited for public access in MG-RAST server under the accession numbers: 4516653.3, 4516654.3, 4516655.3, 4516656.3, 4516657.3, 4516658.3, 4516659.3, 4516660.3, 4516661.3.

3.15 Biofilm quantification and visualization under static conditions

Biofilm quantification in polystyrene microtiter plates (BD, Franklin Lakes, NJ) was assayed as described previously (O'Toole and Kolter 1998; Huber *et al.* 2001). Biofilms were cultured in KB medium and incubated at 28°C for 120 h. To visualize biofilm formation under static conditions, strains were tagged with GFP or DsRedExpress using plasmids pBBR2GFP, pBBR5GFP, pBBR2DsRedExpress and pBBR5DsRedExpress and the steps were followed as described previously (O'Toole *et al.* 1999). KB medium (15 mL) was placed on a 50 mL Falcon tube and bacterial cells inoculated to a final OD_{600} of 0.1. A sterile borosilicate microscopic slide was inserted in the Falcon tube and the culture incubated at 28°C for 120 h. After this period the surface of the borosilicate microscopic slide was checked for biofilm presence. A coverslip was introduced on top of the biofilm and sealed with nail polish to eliminate desiccation and shifting of the coverslip during the analysis. Images were acquired using Leica DMIRE2 inverted fluorescence microscope equipped with Coolsnap K4 CCD and Metamorph Premiere control software. Images were processed using ImageJ software (Schneider *et al.* 2012).

3.16 Promoter activity measurements

To measure transcriptional activity of promoters of interest two constructs were created using a promoterless vector pMP220. Promoter regions from the genes *tolR* (pTOLR220) and *tolI* (pTOLI220) of ET were amplified using primers listed on Table 3-3 and cloned upstream the gene encoding for the β-galactosidase protein. Quantification of promoter activity was done as described in Appendix 7.3.

3.17 Detection of AHL signaling molecules produced by TolI

For the detection of signaling molecules produced by the synthase protein encoded by *tolI*, this gene was amplified using PFU polymerase Promega (Madison, WI, USA) and cloned into the vector pBBR1MCS3 for expression in heterologous system (*E. coli* DH5α^{TM}) and in a homologous system mutated in the synthase gene *etoI* (ETETOI) (Table 3-3). Bacterial strains were grown in KB medium and cell free supernatant extracted with ethyl acetate and separated on C_{18} reverse-phase TLC plates using methanol:water (70:30) as mobile phase. Bioassay for the detection was performed by overlaying the TLC plate with a thin layer of LB top agar containing bacterial sensor strain *Chromobacterium violaceum* CVO26 or with AB top agar supplemented with 100 μg mL^{-1} of 5-bromo-4-chloro-3-indolyl-β-D-galactopyranoside (X-Gal) inoculated with the sensor strain *Agrobacterium tumefaciens* NTL4/pZLR4, as described before (Shaw *et al.* 1997).

3.18 MiniTn5 mutant bank construction and screening

For the generation of a miniTn5 mutant bank of ET, the plasmid pCRS530 (Table 3-2) was mobilized into this strain by triparental conjugation as described in section 3.3.5. Subsequent selection on KB plates with appropriate antibiotics was performed as previously described (Nif 100 µg mL-1, Amp 100 µg mL-1 and Km 100 µg mL-1). A screening to select colonies of interest was performed using the report system pTOLI77 (Table 3-3) which possesses a *xylE* gene encoding a 2,3 - catechol dioxygenase. Mutants that presented a higher *tolI* promoter activity due to the miniTn5 insertion were selected upon spraying with a 0.1 M catechol solution.

3.19 Detection of miniTn5 site and orientation of insertion

Southern blot analyses using a probe for the upstream region of *tolR* was performed to verify the fidelity of all marker exchange events in the mutants. To detect the orientation of the miniTn5 insertion a PCR reaction was performed. Once all mutants were confirmed to be in the region upstream the *tolR* gene by Southern analysis a PCR reaction was performed using the pair of primers mTn5Downint (GCATCGCCTTCTATCGCCTTC) and TolRpromRv (ACTGCAGATACGCAGTGTCATTCGC) using the genomic DNA of all 35 mutants. The PCR conditions used were: denaturation step at 95°C for 5 min, followed by 25 cycles of 95°C 30s, 52°C 30s, 72°C 45s and a final extension of 72°C per 5 min.

4 RESULTS

4.1 PSV and ET cells co-localize in the olive knot

It was previously reported that the bacterial pathogen PSV and the bacterial resident ET share AHL QS signals in the olive knot and when co-inoculated lead to a more aggressive disease as seen in a larger knot-size and larger population sizes of both bacteria in the hyperplasic tissue (Hosni *et al.* 2011). In order to get insight into this *in planta* interspecies interaction between a pathogen and a harmless resident, PSV, ET, their synthase mutants (PSVPSSI and ETETOI, respectively) and their transcriptional regulator mutants (PSVPSSR and ETETOR, respectively) were inoculated separately and together into *in vitro* micropropagated olive plants. Bacterium localization in single and co-inoculation experiments was followed in real time throughout knot development by stereoscopic epifluorescence microscopy of fluorescently tagged bacteria. PSV and PSVPSSI were tagged with GFP while ET and ETETOI were tagged with DsRedExpress (Figures 4-1, 4-2, 4-3, 4-4, 4-5, 4-6 and 4-7).

In single inoculations both PSV and PSVPSSI could be detected as early as 3 d.p.i and an increase in tumor size was followed by the increase in fluorescence due to the higher number of tagged bacteria in the inoculation site (Figure 4-1 and 4-3). On the other hand ET or ETETOI were not detected (the red observed is mostly autofluorescence of the plant) (Figure 4-2) with the exception of Figure 4-2 E and F where a small number of ET cells was observed in the surface of the olive plant in the vicinity of the inoculation site. However, when both ET and ETETOI were co-inoculated with PSV or PSVPSSI, ET and ETETOI cells were more abundant and visible at the inoculation site (Figures 4-4, 4-5, 4-6 and 4-7). In addition, epifluorescence revealed that ET and ETETOI were distributed throughout the knot so that their localization coincided with of PSV and PSVPSSI cells present in the knot. Pathogen distribution as observed with epifluorescence did not show any significant alteration in the knot when inoculated alone compared to when co-inoculated with ET (Figures 4-4, 4-5, 4-6 and 4-7).

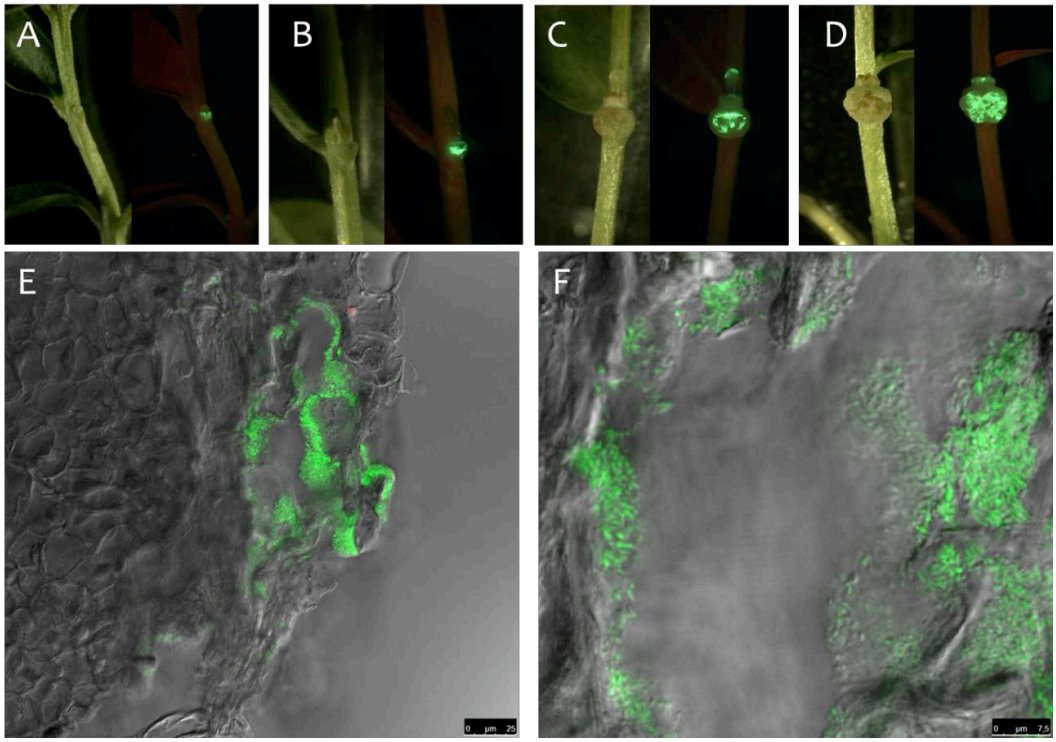

Figure 4-1. Stereoscopic epifluorescence microscopy and CSLM of *Olea europaea* inoculated with PSV-GFP. Images were acquired at (A) 3 d.p.i., (B) 7 d.p.i., (C) 21 d.p.i. and (D) 28 d.p.i. Transversal cuts of *Olea europaea* with PSV GFP at 28 d.p.i analyzed by CLSM with objective of (E) 63x and (F) 63x with zoom.

Interestingly, differently from what was observed by Hosni *et al.* 2011, single inoculation with PSVPSSI or co-inoculations of PSVPSSI with ET or ETETOI resulted in normal tumor development (Figures 4-3, 4-6 and 4-7). It is known that different cultivars of olive tree have different susceptibility to infection by PSV (Penyalver *et al.* 2006); so this phenotype could be due to different cultivars of *Olea europaea* used in this study (Arbequina) and in the study performed by Hosni *et al*. 2011 (Frantoio). Alternatively, tumor development might be affected by different modes of growth and growth stages of the plants used in these two studies.

To further study the localization and distribution of the two species expressing autofluorescent proteins in the knot, transversal sections via vibratome-sectioning of the knot were analyzed by CLSM (Figures 4-1, 4-2, 4-3, 4-4, 4-5, 4-6 and 4-7). This allowed visualization of inner localization and

distribution of PSV, PSVPSSI, ET and ETETOI within the knot without the necessity of further manipulation or staining of the samples. It was observed that ET were localized in the vicinity of PSV-GFP or PSVPSSI cells, suggesting that ET strictly requires the close presence of PSV for growth and persistence in the olive knot (Figures 4-4 and 4-6). ETETOI when co-inoculated with PSVPSSI could be found only in close association (Figure 4-7), however when ETETOI was in the presence of PSV its localization could not be determined by CLSM (Figure 4-5). These results suggest that not only QS is important for the interaction between these two bacteria, but other processes are most probably also involved. In both single (Figures 4-1 and 4-3) and co-inoculations (Figures 4-4, 4-5, 4-6 and 4-7), PSV and PSVPSSI were mainly present on the surface or in outer regions of the tumor as it was reported to be its common location by Maldonado-Gonzalez et al, 2013. This indicated that the presence of ET or ETETOI does not interfere with the preferred positioning within the knot of either PSV or PSVPSSI.

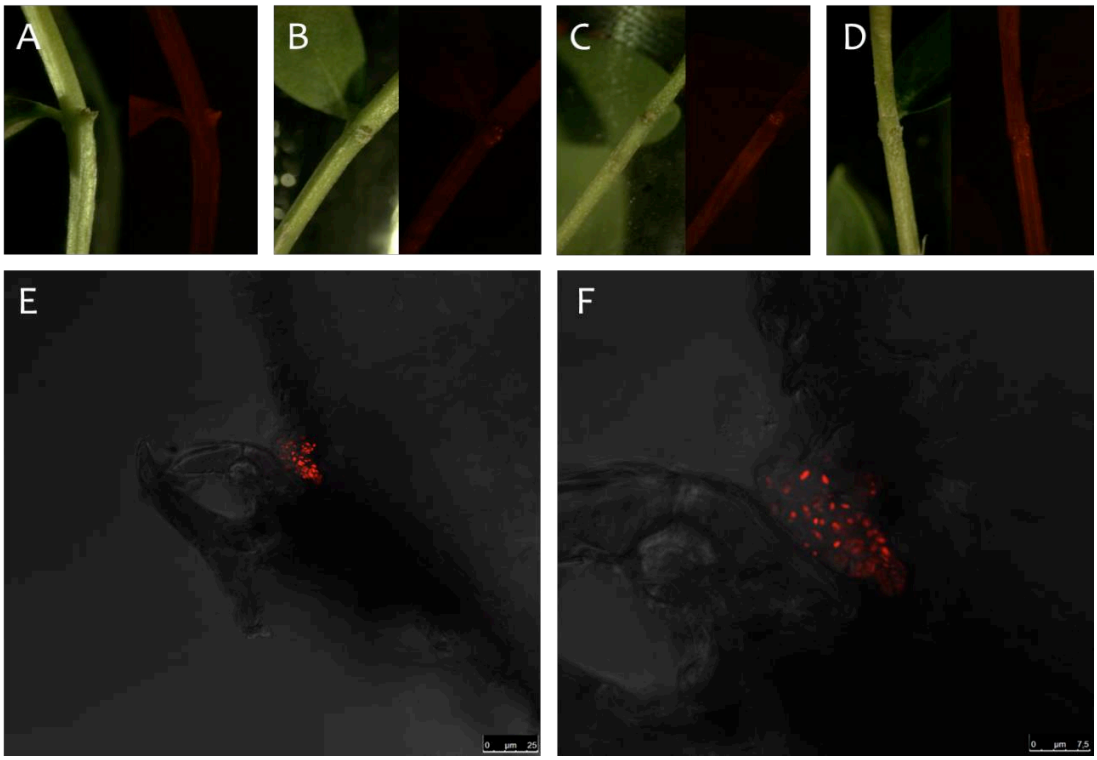

Figure 4-2. Stereoscopic epifluorescence microscopy and CSLM of *Olea europaea* inoculated with ET-DsRedExpress. Images were acquired at (A) 3 d.p.i., (B) 7 d.p.i., (C) 21 d.p.i. and (D) 28 d.p.i. Transversal cuts of *Olea europaea* with ET-DsRedExpress at 28 d.p.i analyzed by CLSM with objective of (E) 63x and (F) 63x with zoom.

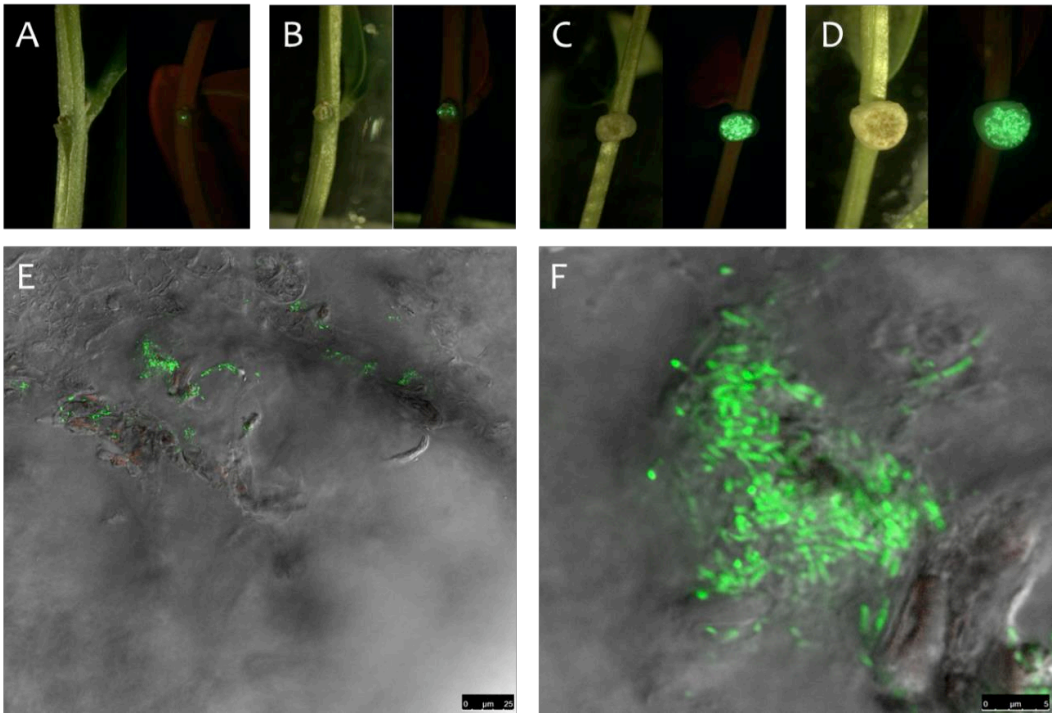

Figure 4-3. Stereoscopic epifluorescence microscopy and CSLM of *Olea europaea* inoculated with PSVPSSI-GFP. Images were acquired at (A) 3 d.p.i., (B) 7 d.p.i., (C) 21 d.p.i. and (D) 28 d.p.i. Transversal cuts of *Olea europaea* with PSVPSSI-GFP at 28 d.p.i analyzed by CLSM with objective of (E) 63x and (F) 63x with zoom.

In order to quantify the effects of interspecies interactions on the growth of each species during the knot development the numbers of colony forming units (CFU) in inoculated olive plants was measured at 0 and 28 d.p.i (Figure 4-8). Results show that in the presence of PSV, CFU numbers of ET increases dramatically compared to single inoculations. These observations partially corroborate the observations reported by Hosni et al. 2011 suggesting that experiments performed in micropropagated olive plants can correlate with what occurs in adult plants. In co-inoculations with ET or ETETOI, the number of cells of PSV or PSVPSSI increases during the course of the disease, but it does not grow more than in single inoculations as it was observed by Hosni et al. 2011 in one-year old plants.

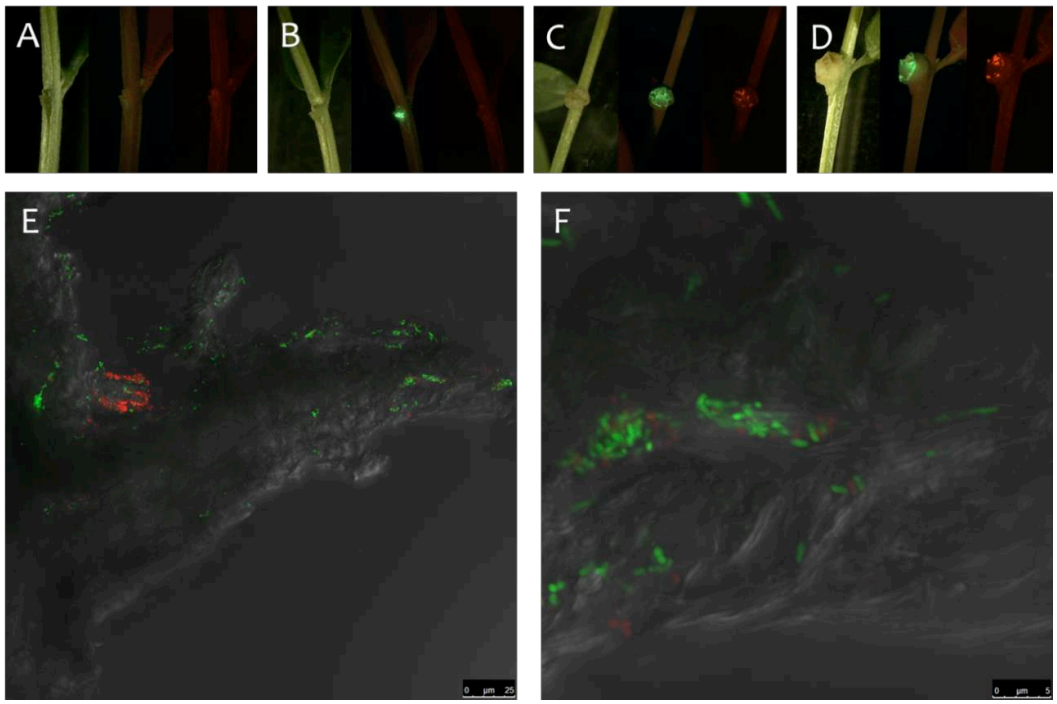

Figure 4-4. Stereoscopic epifluorescence microscopy and CSLM of *Olea europaea* inoculated with PSV-GFP and ET-DsRedExpress. Images were acquired at (A) 3 d.p.i., (B) 7 d.p.i., (C) 21 d.p.i. and (D) 28 d.p.i. Transversal cuts of *Olea europaea* with PSV-GFP and ET-DsRedExpress at 28 d.p.i analyzed by CLSM with objective of (E) 63x and (F) 63x with zoom.

Single inoculation of ETETOI resulted in no detectable colonies in the inoculation site at 28 d.p.i. This suggests that in micropropagated olive plants ET QS might play a role on dispersal. As it was observed by CLSM when ETETOI was co-inoculated with PSV its cell number were greatly diminished on the inoculation site. However when co-inoculated with PSVPSSI, cell counting of ETETOI increased during the course of the disease. These results suggest that ET QS is very important for *in planta* survival, since in single inoculations ETETOI could not be isolated from the inoculation site but when co-inoculated with PSV, ETETOI could persist in the inoculation site aided by PSV. This effect from PSV could be due to suppression of plant defense, to metabolic complementarity or via sharing of QS signals. Co-inoculations with PSVPSSI induced even higher CFU suggesting that PSV QS has some inhibitory effect of ET growth.

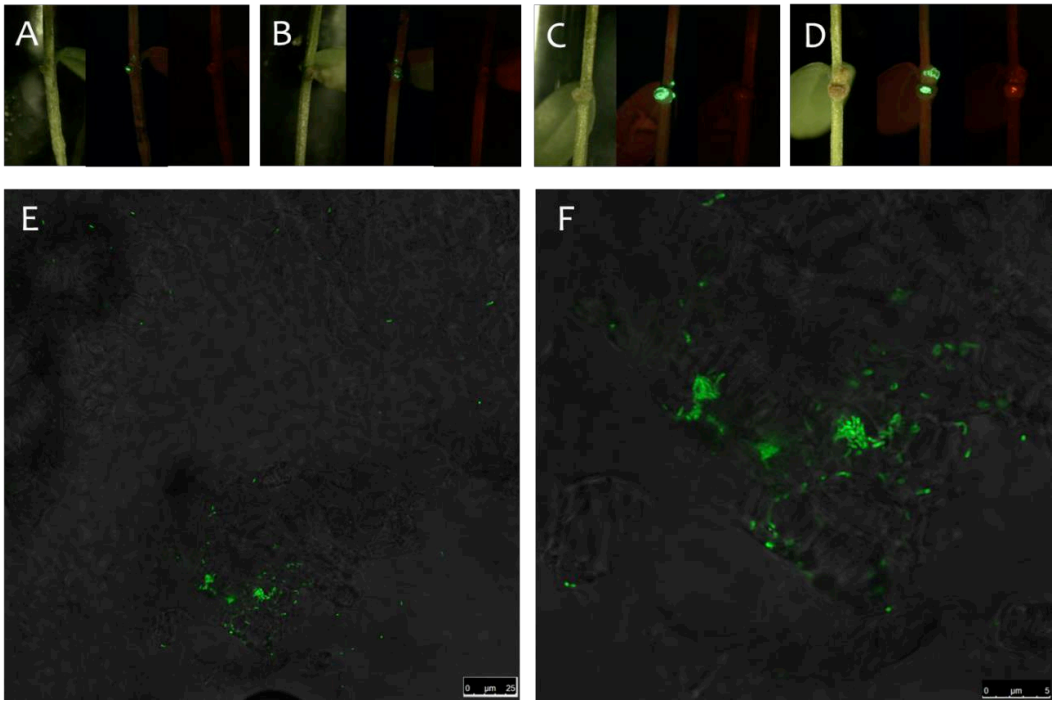

Figure 4-5. Stereoscopic epifluorescence microscopy and CSLM of *Olea europaea* inoculated with PSV-GFP and ETETOI-DsRedExpress. Images were acquired at (A) 3 d.p.i., (B) 7 d.p.i., (C) 21 d.p.i. and (D) 28 d.p.i. Transversal cuts of *Olea europaea* with PSV-GFP and ETETOI-DsRedExpress at 28 d.p.i analyzed by CLSM with objective of (E) 63x and (F) 63x with zoom.

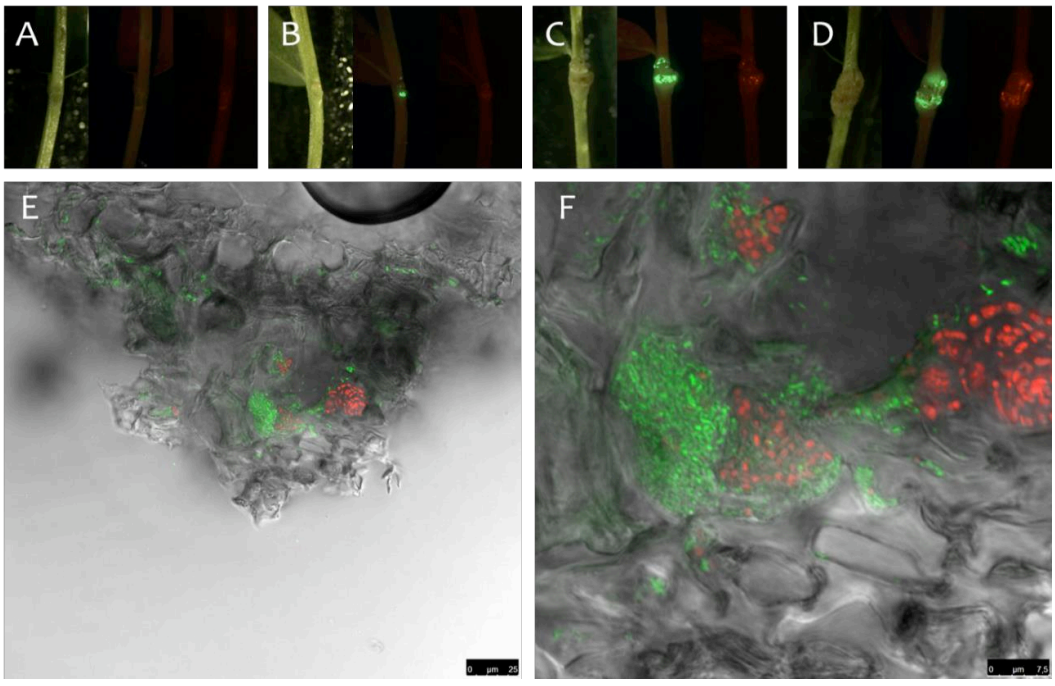

Figure 4-6. Stereoscopic epifluorescence microscopy and CSLM of *Olea europaea* inoculated with PSVPSSI-GFP and ET-DsRedExpress. Images were acquired at (A) 3

d.p.i., (B) 7 d.p.i., (C) 21 d.p.i. and (D) 28 d.p.i. Transversal cuts of *Olea europaea* with PSVPSSI-GFP and ET-DsRedExpress at 28 d.p.i analyzed by CLSM with objective of (E) 63x and (F) 63x with zoom.

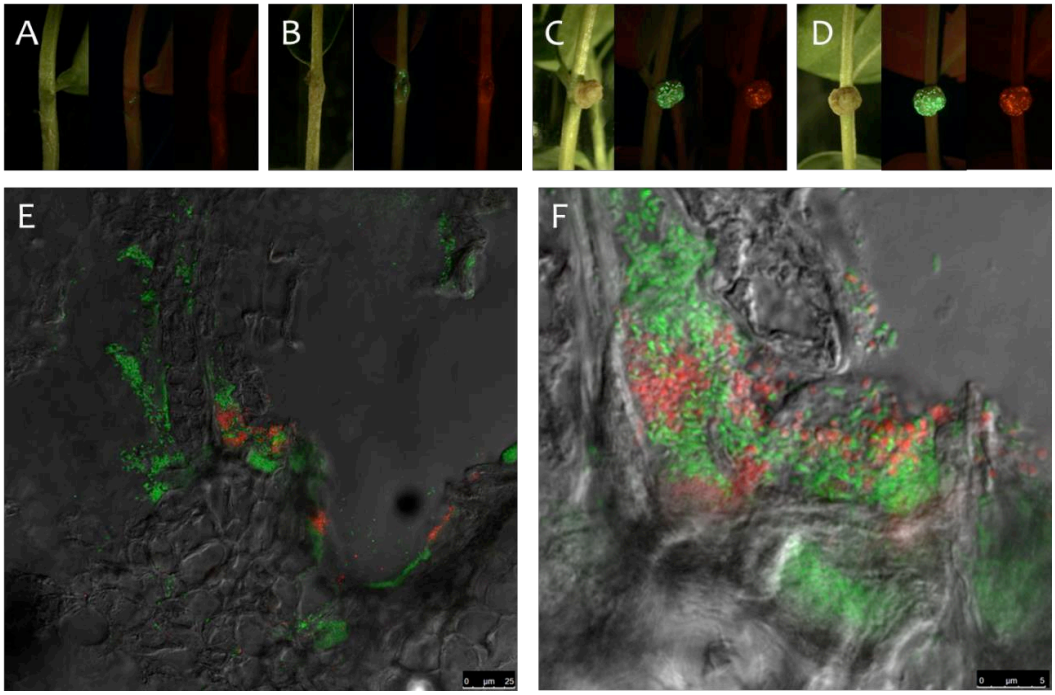

Figure 4-7. Stereoscopic epifluorescence microscopy and CSLM of *Olea europaea* inoculated with PSVPSSI-GFP and ETETOI-DsRedExpress. Images were acquired at (A) 3 d.p.i., (B) 7 d.p.i., (C) 21 d.p.i. and (D) 28 d.p.i. Transversal cuts of *Olea europaea* with PSVPSSI-GFP and ETETOI-DsRedExpress at 28 d.p.i analyzed by CLSM with objective of (E) 63x and (F) 63x with zoom.

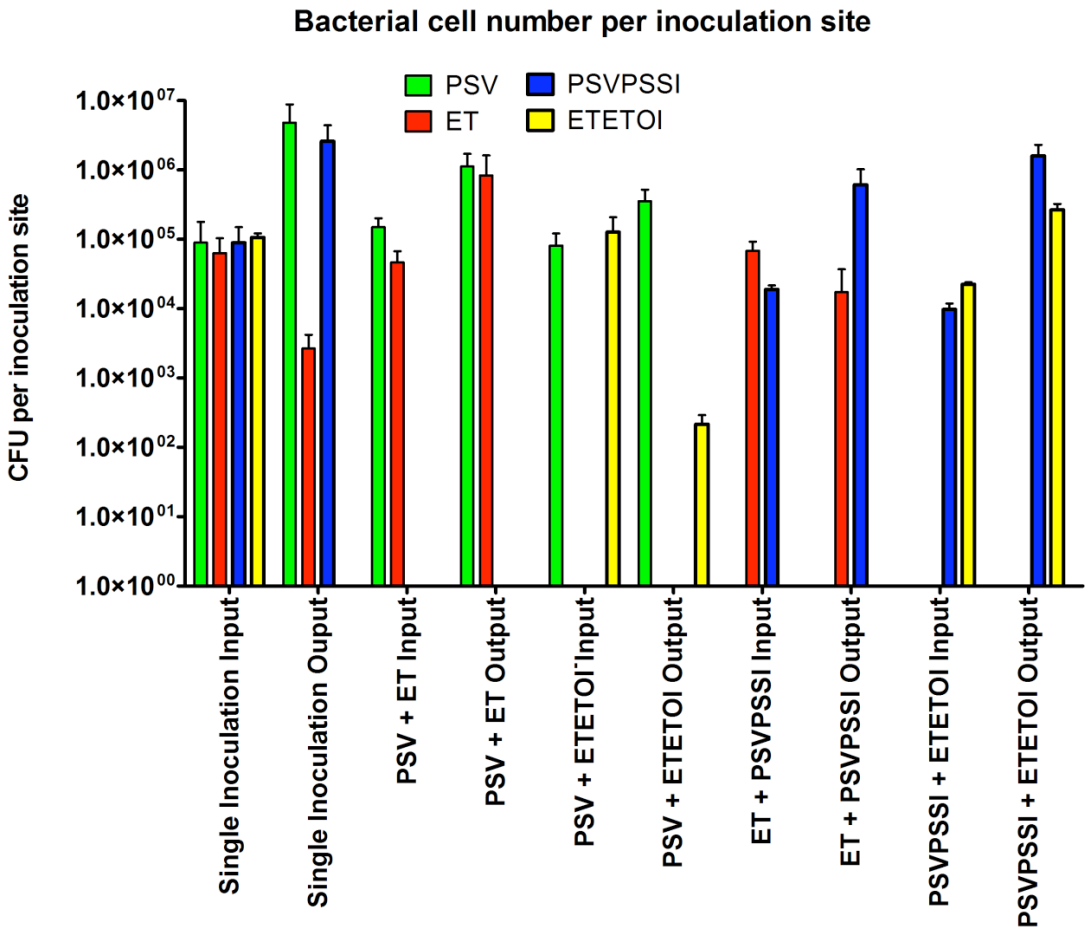

Figure 4-8. Counts (CFU) per inoculation site of PSV, PSVPSSI, ET and ETETOI in single and co-inoculations. Input represents the number of cells used for the inoculation while output stands for the number of cells retrieved from the inoculation site at 28 d.p.i.

4.2 Whole genome analysis of ET

As no ET genome was yet sequenced it was decided to sequence the genome of the ET DAPP-PG735 used in these olive plant infection experiments. The genome sequence of ET was obtained using 36 bp pair-end library with the Illumina GAII platform and assembly using Velvet 1.1.0.3 resulting in 23 scaffolds with a mean length of 226 kbp. The total length of the scaffold assembly was 5.2 Mbp, and the N50 length was 576 kbp, assuming a genome size of 5.2 Mbp. The longest scaffold obtained was 2.2 Mbp long. The G+C content was 53.6%, similar to that of other sequenced *Erwinia* genomes. Automated annotation of the ET draft genome sequence using RAST (Aziz *et al.* 2008) assigned a total of 4766 candidate protein-coding genes. Among all the predicted genes, a total of 1057 genes were annotated as encoding hypothetical proteins which represents around 1/4 of all predicted genes of ET genome. A total of 3 rRNA and 49 tRNA genes were also identified in the RAST annotation. Classification into subsystem was performed using RAST and resulted 27 different classes containing predicted coding sequences (Figure 4-9). The amount of assigned genes to the subsystems of carbohydrate and nitrogen metabolism (1102 genes) represented around 1/3 of the assigned features of ET genome (3528 genes). Genes related to cell wall, membrane and membrane transport (402) accounts for about 1/10 of the subsystems. Interestingly, although ET is not a pathogen, RAST putatively assigned 97 genes as virulence-associated or to disease and defense associated loci; this calls for a careful analysis of the genome and possible involvement of ET in the olive knot disease. Using a well-established bacterial virulence database (VFDB) as reference, 29 T3SS, 50 flagellar/chemotaxis, 26 iron uptake, 10 T4SS, 10 toxin/antitoxin and 6 QS and regulation related genes have been identified (Appendix Table 7-2). The presence of T3SS related genes might represent a possible way that ET uses to aid PSV in causing a more aggressive disease.

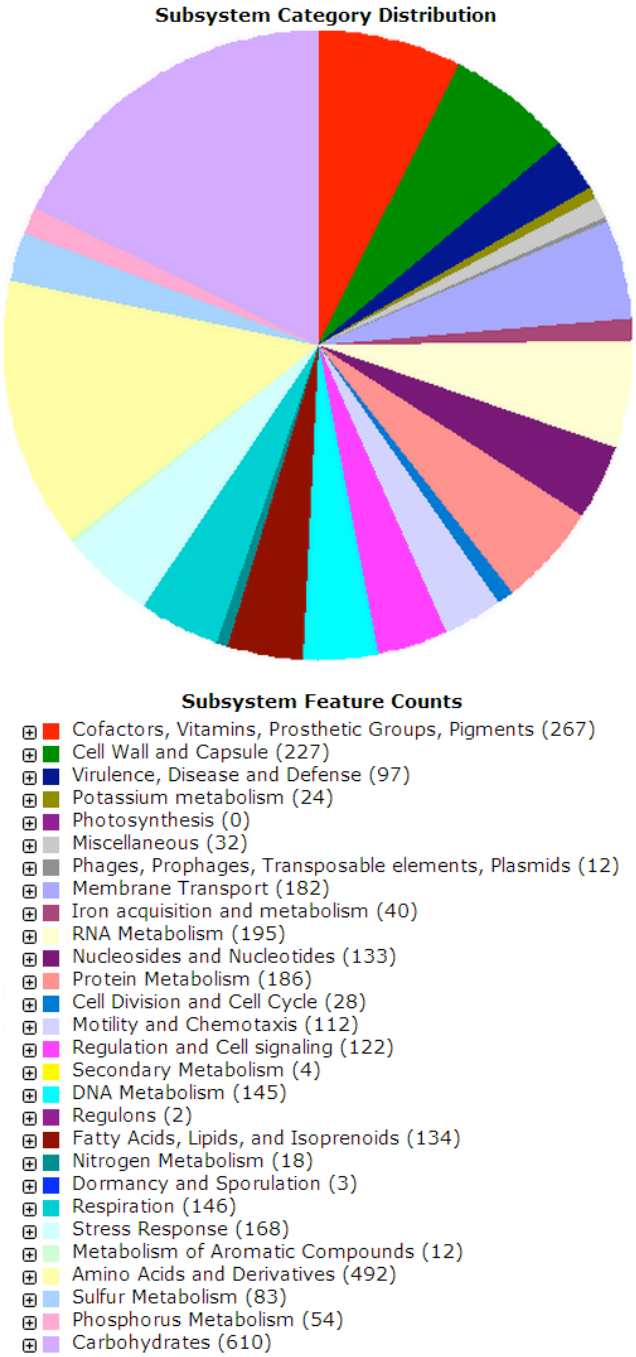

Figure 4-9. RAST subsystem features categorization. Total number of genes that were assigned to subsystems was 3528.

Whole genome alignment against the completely sequenced closest related species indicated that ET genome is not highly similar to other species of the *Erwinia* genus. Interestingly it displayed higher levels of similarity to genomes

of some species of the *Pantoea* genus (Table 4-1). The reason for low levels of shared features with other members of the *Erwinia* genus is currently unknown. It is possible that adaptation to a specific niche such as the olive knot might contribute to distinct features of ET DAPP-PG735 when compared to other *Erwinia* sp.; interestingly thus far ET has only been isolated from olive knots while other *Erwinia* species live in many diverse niches.

Table 4-1. Whole genome multiple genome alignment of ET DAPP-PG735 using MUMmer. Query stands for ET DAPP-PG735 genome sequence.

Reference Aligned	Reference sequence	Query Aligned	Sequence identity
23.83%	NC_014306 *Erwinia billingiae* Eb661	22.67%	83.78%
19.71%	NC_014837 *Pantoea* sp. At-9b	15.92%	83.57%
21.30%	NC_014562 *Pantoea vagans* C9-1	15.88%	83.65%
19.33%	NC_010694 *Erwinia tasmaniensis* Et1/99	13.76%	83.84%
18.20%	NC_012214 *Erwinia pyrifoliae* Ep1/96	13.43%	83.84%
17.98%	NC_013961 *Erwinia amylovora* CFBP1430	12.54%	83.93%
17.96%	NC_013971 *Erwinia amylovora* ATCC 49946	12.52%	83.86%
11.81%	NC_013956 *Pantoea ananatis* LMG 20103	10.18%	83.50%
5.31%	NC_012912 *Dickeya zeae* Ech1591	4.34%	83.61%
4.56%	NC_013592 *Dickeya dadantii* Ech586	3.65%	83.91%
4.64%	NC_012880 *Dickeya dadantii* Ech703	3.62%	83.84%

To generate a more comprehensive comparison between the closest complete sequenced species, an alignment using a different algorithm based on progressiveMauve was used. As observed in the results of MUMmer multiple alignment percentage of ET genome aligned against *E. billingiae* Eb661 was low, although aligned regions usually possessed a high identity (Figure 4-10). Another useful feature available in Mauve is the "Move Contigs", by using a reference genome which has been completely sequenced it is possible to determine the most probable contig organization of a bacterial draft genome. Unfortunately due to the low percentage of alignment between ET and *E. billingiae* Eb661, this feature did not provide results with reliable confidence levels (Figure 4-10).

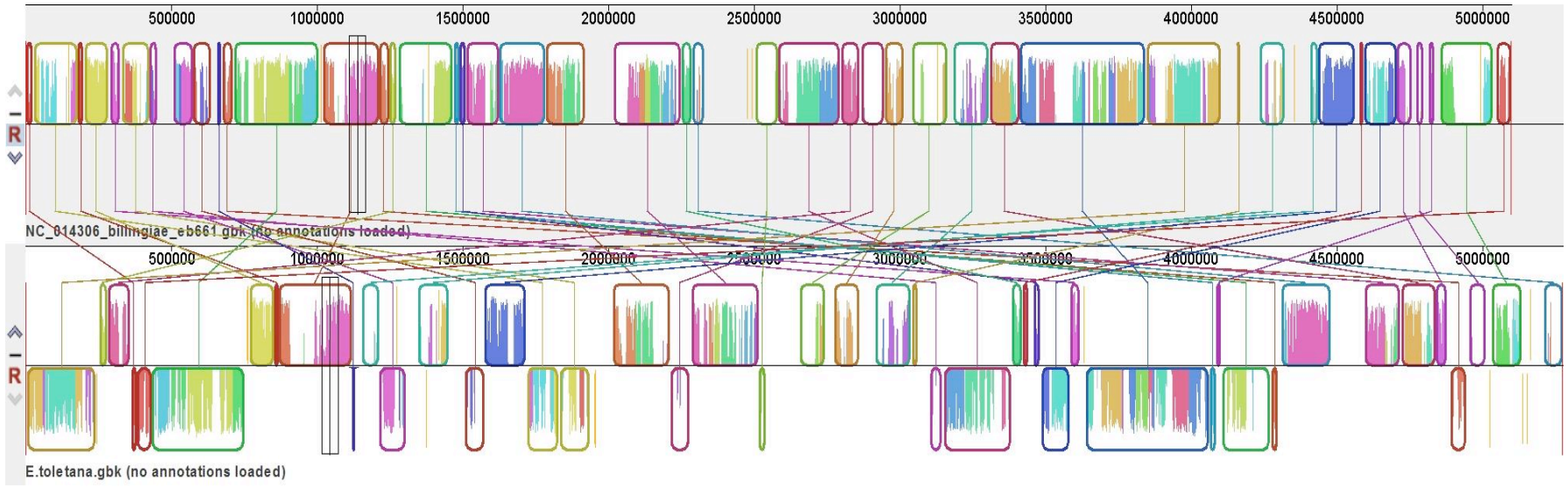

Figure 4-10. Whole genome alignment using progressiveMauve aligner. Color levels inside each block represent identity level of nucleotide sequences present in respective regions.

4.3 Possible metabolic complementarity/exchanges between ET and PSV

The previous report of AHL signal sharing and mutualistic behavior as well as results shown here on strict co-localization of PSV and ET prompted the analysis of the recently published genome of PSV and that of ET for possible metabolic complementarity and/or exchange. This is in view that both species grow more in the olive knot when present together indicating probable metabolic benefits. In 28-days kòoold olive knots of plantlets used for localization experiments, when co-inoculated however only ET had higher CFU counts compared to single inoculations. This is in contrast to what was observed in 60 days-old olive knots using one-year old olive plants where both ET and PSV had significantly higher CFU counts compared to single inoculations as reported by Hosni *et al*., 2011.

An analysis of the metabolic potential of the two genomes via the reconstruction of metabolic pathways was performed. This was achieved by feeding the annotated draft genome sequence of the two species (PSV and ET) separately and merged into PathoLogic (version 16.5) to predict their metabolic pathways. Reconstruction of predicted pathways from PSV (SavCyc), ET (TolCyc) and joined genomes of both species (SavtolCyc) was made by matching all fed annotated enzymes with a database of enzymes with known function in order to predict possible single reactions which can be assembled into pathways that were experimentally tested (Karp *et al.* 2010). After creating the predicted pathways, the merged SavtolCyc was used to highlight all the new pathways that could emerge by joining the enzymes present in the two separate genomes (Figure 4-11). By evidencing all the reactions not shared between SavtolCyc/SavCyc and SavtolCyc/TolCyc on the cellular overview panel, an interactive visual method to track all singular contributions given by the two single bacterial species to the pathways was possible. Interestingly, pathways involving several plant related compounds including shikimate, sucrose and

salicylate (Figure 4-12) were evidenced since their predicted degradation pathways were only complete when the genomes of the two species are combined.

The degradation benefits of these aromatic compounds by bacterial consortia could be relevant since these phenolics are commonly found on plants. The presence of both ET and PSV could allow this bacterial community to more efficiently metabolize and utilize these aromatic compounds as carbon sources or even to detoxify them since they could be toxic if found at high concentrations. In addition, salicylates and phenols are known to be involved in plant defense response in plant-pathogen interactions (Loake and Grant 2007). This has also been reported for olive-PSV interactions(Roussos *et al.* 2002). It is therefore a possibility that the increased tumor size generated by PSV and ET co-inoculation in olive plants (Hosni *et al.* 2011) is due to the collaborative bacterial degradation of these plant defense compounds.

In silico predictions have also indicated that sorbitol and β-D-glucose-6-phosphate could only be fully utilized when both species were present. For sorbitol degradation it was predicted that the first two metabolic conversions were only performed by PSV, the third step of fructose-6-phosphate conversion could only be catabolized by ET and then both species were able to perform the last steps. For β-D-glucose-6-phosphate what was predicted was that its degradation generates two intermediates (6-phospho-gluconate and fructose-6-phosphate). The degradation of 6-phospho-gluconate was only performed by PSV, while the degradation of fructose-6-phosphate only by ET (Figure 4-13).

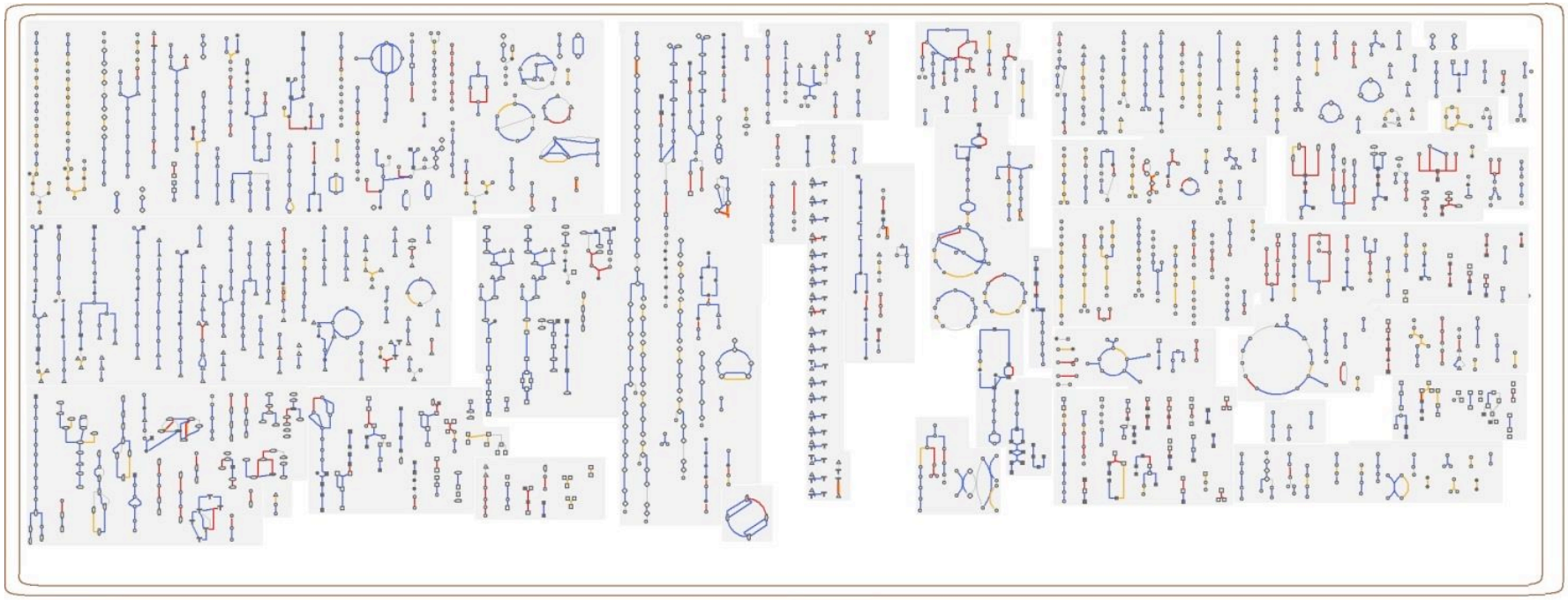

Figure 4-11. Cellular overview representing contributions of each species to the construction of metabolic pathways. Red, orange and blue lines represents enzymatic reactions catalyzed only by ET, PSV or both respectively. Gray lines are enzymatic reactions in which both organisms do not putatively possess enzymes to perform them.

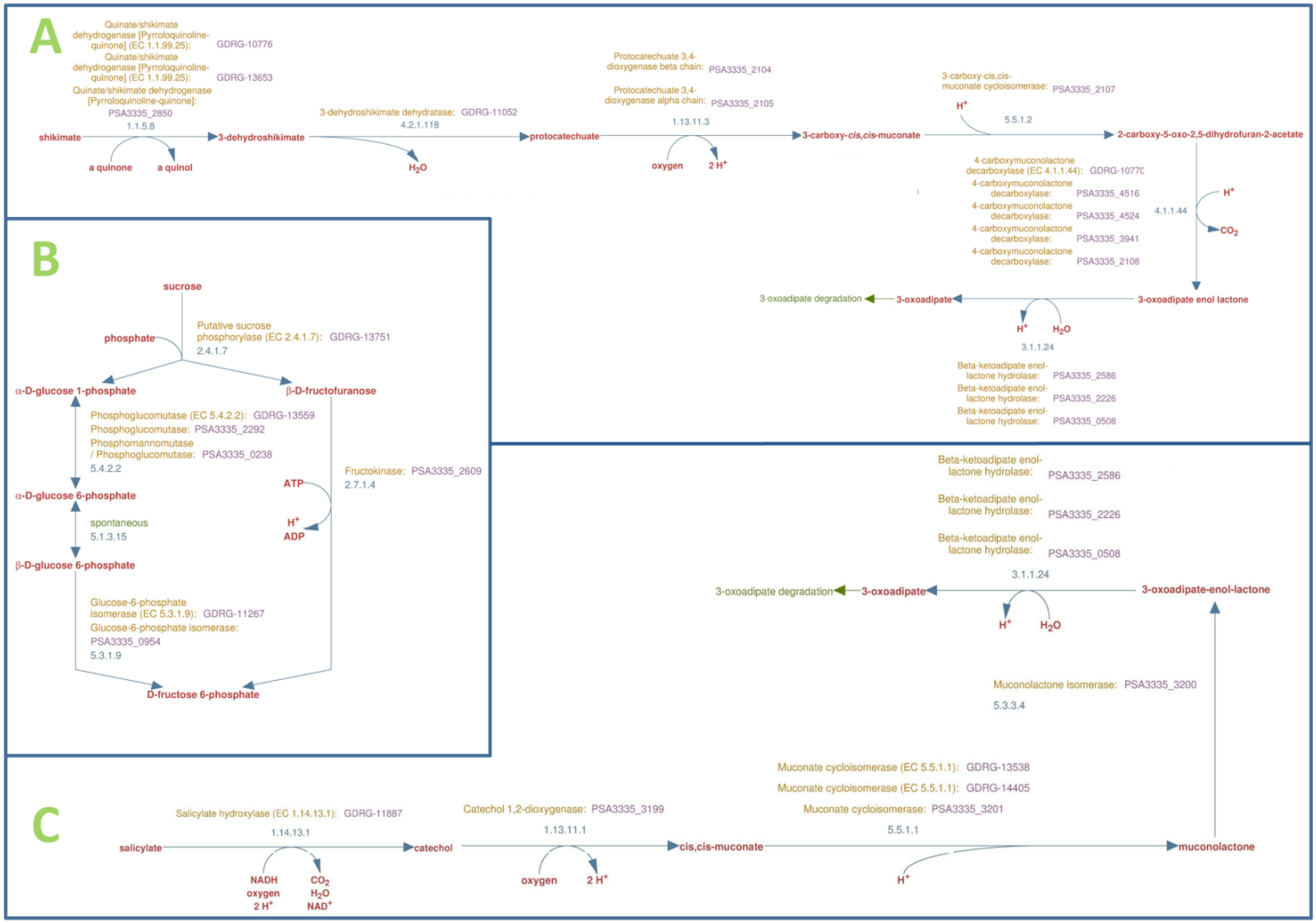
A
Quinate/shikimate dehydrogenase [Pyrroloquinoline-quinone] (EC 1.1.99.25): GDRG-10776
Quinate/shikimate dehydrogenase [Pyrroloquinoline-quinone] (EC 1.1.99.25): GDRG-13653
Quinate/shikimate dehydrogenase [Pyrroloquinoline-quinone]: PSA3335_2850
1.1.5.8
shikimate
a quinone
a quinol
3-dehydroshikimate
3-dehydroshikimate dehydratase: GDRG-11052
4.2.1.118
H2O
protocatechuate
Protocatechuate 3,4-dioxygenase beta chain: PSA3335_2104
Protocatechuate 3,4-dioxygenase alpha chain: PSA3335_2105
1.13.11.3
oxygen
2 H+
3-carboxy-cis,cis-muconate
3-carboxy-cis,cis-muconate cycloisomerase: PSA3335_2107
H+
5.5.1.2
2-carboxy-5-oxo-2,5-dihydrofuran-2-acetate
4-carboxymuconolactone decarboxylase (EC 4.1.1.44): GDRG-10770
4-carboxymuconolactone decarboxylase: PSA3335_4516
4-carboxymuconolactone decarboxylase: PSA3335_4524
4-carboxymuconolactone decarboxylase: PSA3335_3941
4-carboxymuconolactone decarboxylase: PSA3335_2108
4.1.1.44
H+
CO2
3-oxoadipate enol lactone
3-oxoadipate degradation
3-oxoadipate
H+
H2O
3.1.1.24
Beta-ketoadipate enol-lactone hydrolase: PSA3335_2586
Beta-ketoadipate enol-lactone hydrolase: PSA3335_2226
Beta-ketoadipate enol-lactone hydrolase: PSA3335_0508
B
sucrose
phosphate
Putative sucrose phosphorylase (EC 2.4.1.7): GDRG-13751
2.4.1.7
α-D-glucose 1-phosphate
β-D-fructofuranose
Phosphoglucomutase (EC 5.4.2.2): GDRG-13559
Phosphoglucomutase: PSA3335_2292
Phosphomannomutase / Phosphoglucomutase: PSA3335_0238
5.4.2.2
Fructokinase: PSA3335_2609
2.7.1.4
ATP
H+
ADP
α-D-glucose 6-phosphate
spontaneous
5.1.3.15
β-D-glucose 6-phosphate
Glucose-6-phosphate isomerase (EC 5.3.1.9): GDRG-11267
Glucose-6-phosphate isomerase: PSA3335_0954
5.3.1.9
D-fructose 6-phosphate
Beta-ketoadipate enol-lactone hydrolase: PSA3335_2586
Beta-ketoadipate enol-lactone hydrolase: PSA3335_2226
Beta-ketoadipate enol-lactone hydrolase: PSA3335_0508
3.1.1.24
3-oxoadipate degradation
3-oxoadipate
3-oxoadipate-enol-lactone
H+
H2O
Muconolactone isomerase: PSA3335_3200
5.3.3.4
C
Muconate cycloisomerase (EC 5.5.1.1): GDRG-13538
Muconate cycloisomerase (EC 5.5.1.1): GDRG-14405
Muconate cycloisomerase: PSA3335_3201
5.5.1.1
H+
muconolactone
Salicylate hydroxylase (EC 1.14.13.1): GDRG-11887
1.14.13.1
salicylate
NADH
oxygen
2 H+
CO2
H2O
NAD+
catechol
Catechol 1,2-dioxygenase: PSA3335_3199
1.13.11.1
oxygen
2 H+
cis,cis-muconate

Figure 4-12. Graphical representation of complementary metabolic pathways between PSV and ET. Gene codes encoded by PSV possess the prefix PSA, while when encoded by ET possesses the prefix GDRG. In these *in silico* pathways, the degradation of shikimate (a), sucrose (b) and salicylate (c) could only be catalyzed by one of the species. It is therefore possible that the absence of one of the two species would impair the complete mineralization of these compounds.

Phenotypic microarray analysis of single and co-inoculations of ET and PSV on Biolog plates PM1-20 were performed in order to get further insight into possible metabolic exchange. Metabolic activities for each test substrate in each well are summarized in Table 7-2 (columns G, H and I). The activity is indicated by values ranging from 0 (absence of metabolic activity) to 9 (maximum metabolic activity). Metabolic activities of ET are different from the activity profile of PSV. The activities of co-inoculations are more closely related to ET rather than to the activities of PSV. In Figure 4-14, the prevalence of green color in the ET activity ring, as well as in the activity ring of both bacterial species tested together, indicate a higher metabolic activity in these two tests than in PSV tested alone. This is especially true in the PM plates testing the metabolism of different chemical compounds, of osmolites and pH dependent growth, and also in PM tests for carbon metabolism (Table 7-2 and Figure 4-14). The analysis using the Ring graphs showed that the majority of the chemicals tested were metabolized better when ET was inoculated alone. However in some cases involving carbon, phosphate and sulphur metabolism, a change in the color gradient was observed indicating an improvement of metabolism of these compounds when the two species were co-inoculated. Global analysis of carbon metabolism demonstrated that while PSV metabolized reasonably well (yellow and green colors) approximately 12% of the chemicals, ET had higher metabolic activities, being able to metabolize equally well (yellow and green colors) approximately 33% of the compounds tested. However when PSV and ET were co-inoculated an augmentation of the metabolic activity (yellow and green colors) was observed to approximately 41% (Figure 4-15). Improvement was also observed for

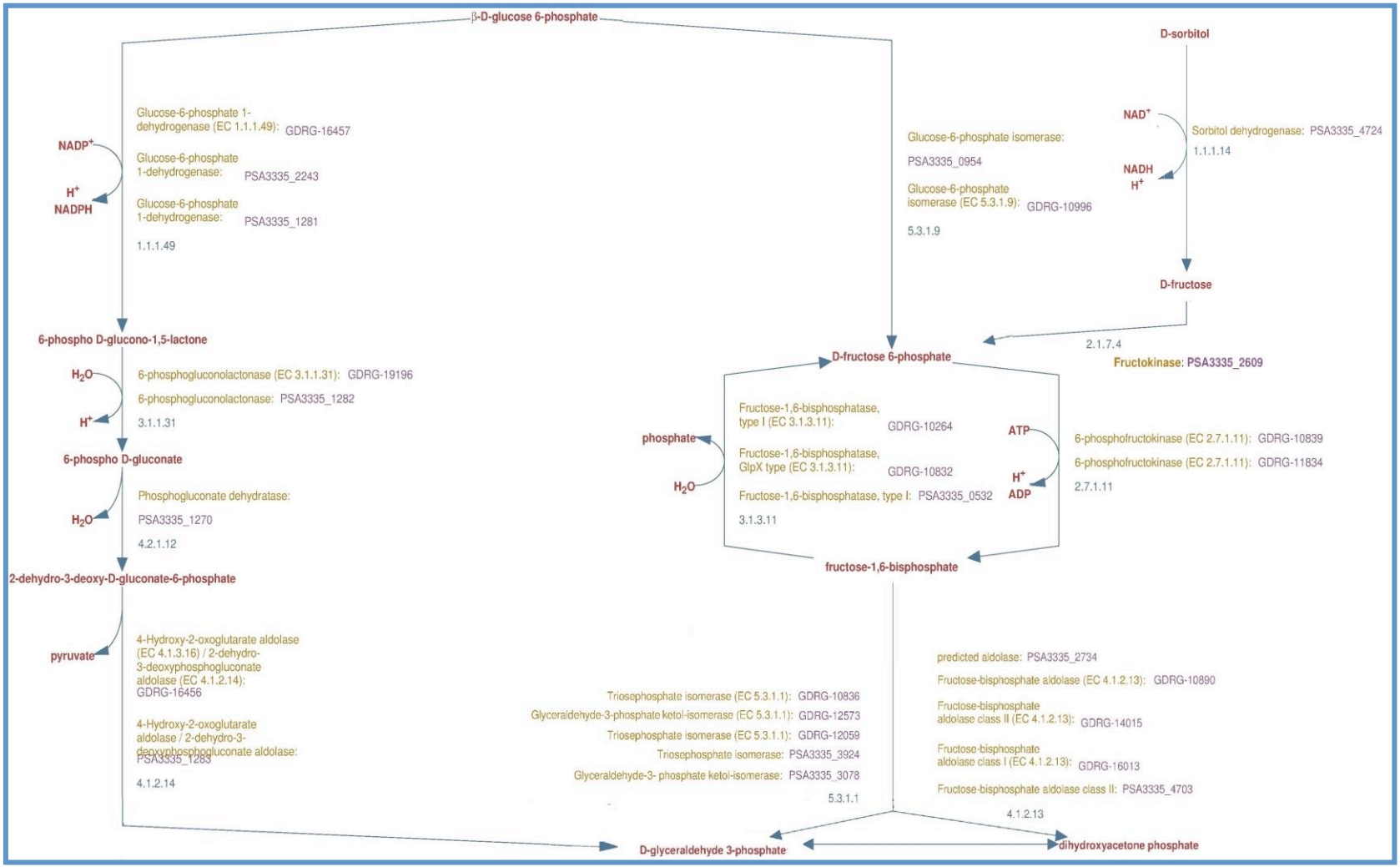
β-D-glucose 6-phosphate
D-sorbitol
NADP+
H+
NADPH
Glucose-6-phosphate 1-dehydrogenase (EC 1.1.1.49): GDRG-16457
Glucose-6-phosphate 1-dehydrogenase: PSA3335_2243
Glucose-6-phosphate 1-dehydrogenase: PSA3335_1281
1.1.1.49
Glucose-6-phosphate isomerase: PSA3335_0954
Glucose-6-phosphate isomerase (EC 5.3.1.9): GDRG-10996
5.3.1.9
NAD+
NADH
H+
Sorbitol dehydrogenase: PSA3335_4724
1.1.1.14
D-fructose
6-phospho D-glucono-1,5-lactone
H2O
H+
6-phosphogluconolactonase (EC 3.1.1.31): GDRG-19196
6-phosphogluconolactonase: PSA3335_1282
3.1.1.31
D-fructose 6-phosphate
2.1.7.4
Fructokinase: PSA3335_2609
6-phospho D-gluconate
H2O
Phosphogluconate dehydratase: PSA3335_1270
4.2.1.12
phosphate
H2O
Fructose-1,6-bisphosphatase, type I (EC 3.1.3.11): GDRG-10264
Fructose-1,6-bisphosphatase, GlpX type (EC 3.1.3.11): GDRG-10832
Fructose-1,6-bisphosphatase, type I: PSA3335_0532
3.1.3.11
ATP
H+
ADP
6-phosphofructokinase (EC 2.7.1.11): GDRG-10839
6-phosphofructokinase (EC 2.7.1.11): GDRG-11834
2.7.1.11
fructose-1,6-bisphosphate
2-dehydro-3-deoxy-D-gluconate-6-phosphate
pyruvate
4-Hydroxy-2-oxoglutarate aldolase (EC 4.1.3.16) / 2-dehydro-3-deoxyphosphogluconate aldolase (EC 4.1.2.14): GDRG-16456
4-Hydroxy-2-oxoglutarate aldolase / 2-dehydro-3-deoxyphosphogluconate aldolase: PSA3335_1283
4.1.2.14
Triosephosphate isomerase (EC 5.3.1.1): GDRG-10836
Glyceraldehyde-3-phosphate ketol-isomerase (EC 5.3.1.1): GDRG-12573
Triosephosphate isomerase (EC 5.3.1.1): GDRG-12059
Triosephosphate isomerase: PSA3335_3924
Glyceraldehyde-3- phosphate ketol-isomerase: PSA3335_3078
5.3.1.1
predicted aldolase: PSA3335_2734
Fructose-bisphosphate aldolase (EC 4.1.2.13): GDRG-10890
Fructose-bisphosphate aldolase class II (EC 4.1.2.13): GDRG-14015
Fructose-bisphosphate aldolase class I (EC 4.1.2.13): GDRG-16013
Fructose-bisphosphate aldolase class II: PSA3335_4703
4.1.2.13
D-glyceraldehyde 3-phosphate
dihydroxyacetone phosphate

Figure 4-13. Graphical representation of complementary metabolic pathways between PSV and ET. Gene codes encoded by PSV possess the prefix PSA, while when encoded by ET possesses the prefix GDRG.

phosphate and sulphur metabolism; metabolic activities (yellow and green colors) were 38%, 67% and 60% for ET, PSV and PSV + ET, respectively (Figure 4-15). Although comparison of PSV alone and PSV + ET revealed a decrease in thedegradation levels of these chemicals (yellow and green colors), it could be considered an improvement since PSV alone could not metabolize (Red color) 30% of sulphurs and phosphate substrates. However when co-inoculated all the substrates could be metabolized. For several compounds PSV had no activity (red color); in these cases when ET was co-inoculated PSV did not alter the activity of ET indicating no interference thus a probable 'friendly' co-existence under these conditions (Figure 4-15 and Appendix Table 7-3). For several other compounds, improvement of the metabolic activities was detected when the two species were co-inoculated (Appendix Table 7-3 rows highlighted in yellow).

With respect to sucrose and salicylic acid (used as antimicrobial compound and not as carbon source), improved metabolic activity was observed when PSV and ET were co-inoculated; this is in accordance with the *in silico* predictions as described above (Table 7-2 PM1 D11 and PM17 B04, respectively). Predictions of sorbitol and β-D-glucose-6-phosphate (Table 7-2 PM1 B02 and PM1 C01, respectively) were also in agreement with the *in silico* analysis, where the metabolic activity of co-inoculations on these substrates were improved when compared to its single inoculations. Growth in shikimic acid however did not result in improved metabolic activity when compared to single inoculations. Evidence from *in silico* analysis and phenotypic microarray indicated that utilization/transformation of sucrose and salicylic acid by PSV and ET could involve metabolic exchange. In laboratory growth experiments it was established that PSV could not grow on salicylic acid and sucrose as unique carbon sources, confirming the *in silico* data; however, this experimental data is in disagreement

with the phenotypic microarray analysis of PSV which showed some levels of metabolic activities towards these compounds. Similarly ET also could not grow under laboratory conditions in either sucrose or salicylic acid. According to the *in silico* metabolic profiles, ET was predicted to be able utilize sucrose as unique carbon source but not salicylic acid. Laboratory growth studies on mixed inoculums of ET and PSV with either sucrose or salicylic acid as sole energy source (as described in the Materials and Methods section).

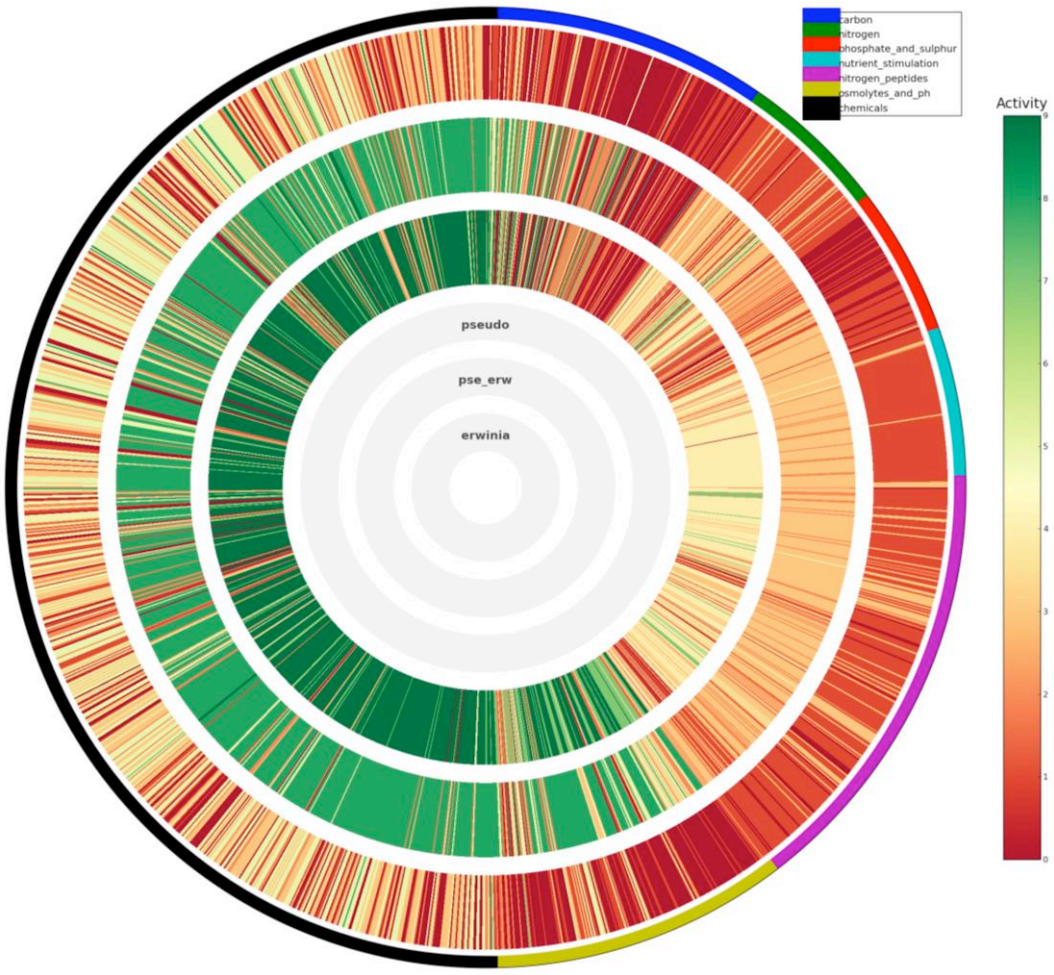

Figure 4-14. Ring graphs obtained from the dphenome module of the DuctApe software. Concentric rings represent metabolic activity in ET (inner circle), PSV (outer circle) and PSV + ET (middle circle). Inside the circles each line represents the metabolic activity towards a chemical which is color coded where red encodes for no activity and green maximum activity.

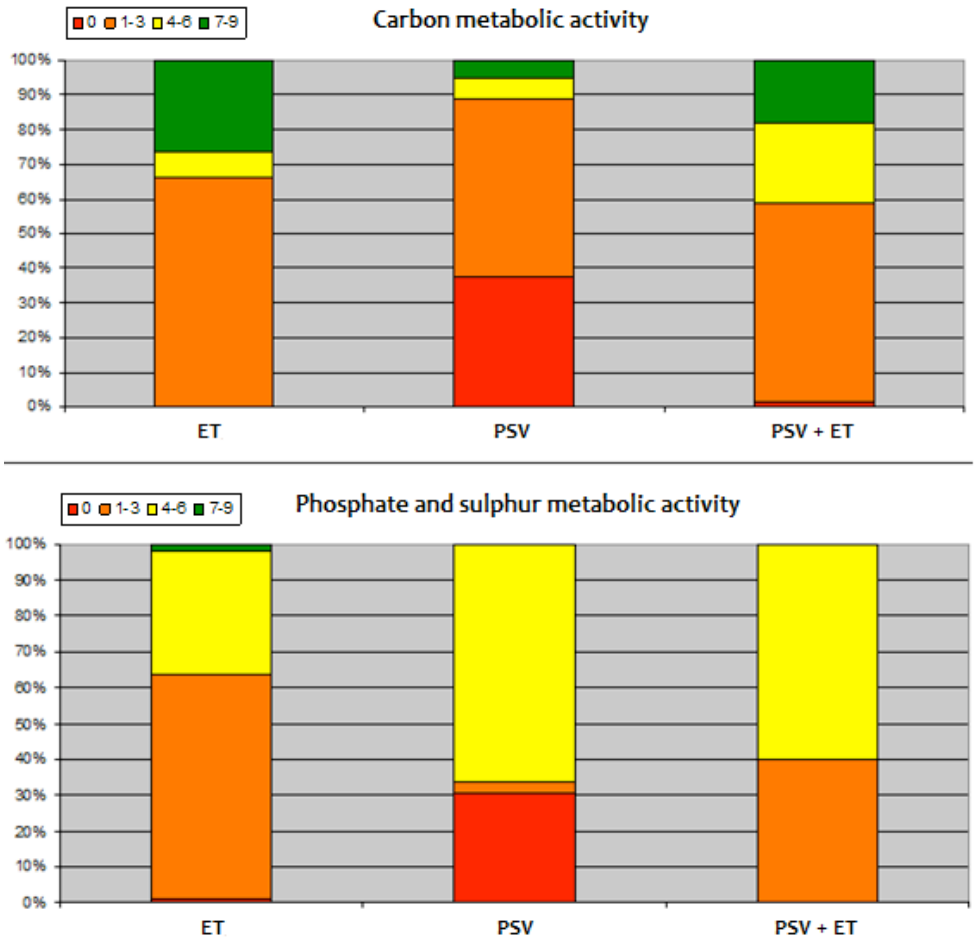

Figure 4-15. Metabolic activities for the different categories of metabolic tests. Colors represents different levels of metabolic activity going from 0 (Red), 1-3 (Orange), 4-6 (Yellow) and 7-9 (Green).

were also performed. When providing salicylic acid, no growth or transformation (as determined by RP-HPLC analysis of spent supernatants) of the aromatic acid was observed in a mixed inoculum of PSV and ET (Figure 4-16). In minimal growth medium with sucrose, similar results were obtained, i.e. no growth when using a mixed inoculum of ET and PSV. These initial binary growth tests do not evidence metabolic complementarity as it was indicated by the *in silico* analysis; the reason for this is currently unknown.

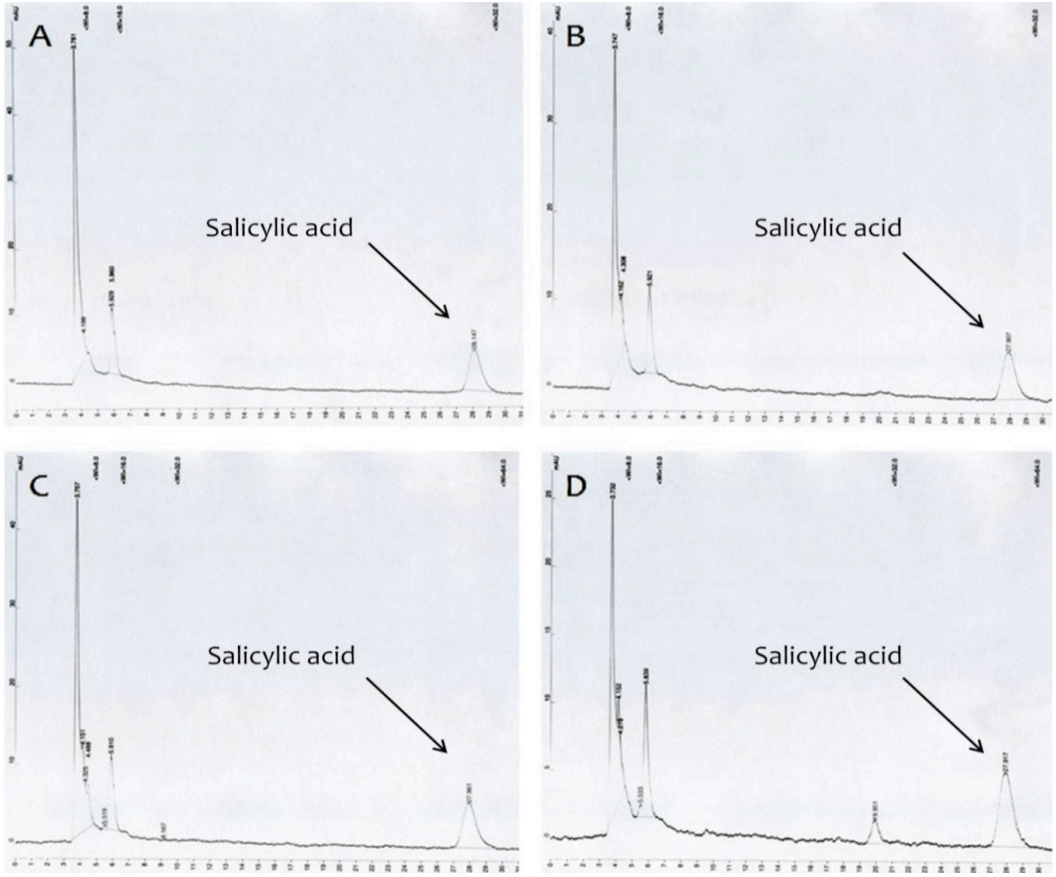

Figure 4-16. RP-HPLC analysis of M9 salicylic acid. Samples without inoculation (A) after 24h, inoculated with PSV (B), ET (C) and PSV + ET (D) after 24h. 10 µL samples were loaded on a 5 µm spherical C18 reverse-phase column (Supelcosil LC18 150×4·6 mm; Supelco) and eluted with 35% methanol and 65% water with 0·1% acetic acid at a flow rate of 0·8 mL min−1. The eluted metabolites were detected at 280nm.

4.4 Identification of olive knot bacterial communities via metagenomics

Several bacterial species have been isolated from olive knots using standard culturing methods possibly indicating the presence of a multispecies bacterial community within the olive knot (Rojas *et al.* 2004; Ouzari *et al.* 2008; Moretti *et al.* 2011); many of these isolates belong to the *Erwinia* and *Pantoea* genera. It was of interest here to carry out an exhaustive high throughput analysis of the bacterial population inside olive knots since to our knowledge it has never been performed. Nine olive knots belonging to three different varieties of olive trees were collected from five regions of Italy and a metagenomics approach based on the amplification and sequencing of the hypervariable 16s rRNA regions V1/V3 was used as described in section 3.13.

The data indicated rich and diverse bacterial life in this niche; it is worthwhile to note that the olive knot material was not sterilized prior to DNA purification as knots are porous and PSV is known to also colonize intercellular spaces very near the surface. It is therefore possible that some of the identified bacterial species could be living on the surface of the olive knot as epiphytes (it cannot be excluded however that some of these can then enter the olive knot). Among all bacterial 16s rRNA sequences retrieved, the Gammaproteobacteria class was by far the most represented, accounting for up to 90% of the total bacterial population (Table 4-1). Unsurprisingly, PSV makes up for almost 50% of the bacterial load; the other most abundant bacteria belong to the *Pantoea* genera (Figure 4-17) Interestingly, PAG has been known to be commonly associated with olive knots (Savastano 1886; Quesada *et al.* 2007; Ouzari *et al.* 2008; Hosni *et al.* 2011). The abundance of other genera showed some distinct features in every knot however among the different samples a common core of bacterial genera was evident composed of *Clavibacter, Curtobacterium, Enterobacter*, *Erwinia*, *Hymenobacter, Kineococcus, Pectobacterium* and *Sphingomonas* (Figure 4-17). Geographical position of extraction seems to have

little effect on the common core, but for bacterial genera that are underrepresented such as *Vibrio*, its abundance is greater in samples from south of Italy. The number of operational taxonomic units (OTU) that could not be assigned precisely to any bacterial genera was rather large possibly suggesting that this very specific niche might contain new bacterial species.

Data analysis regarding bacterial 16s rRNA abundance and α-diversity indicates that geographical location or cultivar could play a significant role on the abundance level and diversity of the bacterial community in olive knots (Table 4-2). Bacterial 16S rRNA abundance in general was higher in the samples from south Italy. Even among all samples from the same cultivar (e.g. Frantoio), the ones from southern Perugia (Frantoio 4, 5 and 6) had an average higher abundance and also α-diversity than the samples of more northern regions of Italy (Frantoio 1, 2 and 3). Comparisons between the other samples proved to be difficult, since it is harder to infer if differences are due to geographical and climatic factors or if it is due to the different cultivars used; however the samples from southern Italy (Clima di Mola, Oliva Rossa 1 and 2) had higher 16S rRNA abundance and α-diversity when compared to samples from Perugia (Frantoio 1, 2, 3, 4, 5 and 6).

Table 4-2. Relative 16S rRNA bacterial abundance. Results are expressed in percentage.

Phylum	Class	Order	CM	FR1	FR2	FR3	FR4	FR5	FR6	OR1	OR2
Proteobacteria			84	75	81	88	89	90	92	84	94
	Gammaproteobacteria		82	67	75	77	86	86	91	82	93
		Pseudomonales	69	52	55	68	76	74	64	79	70
		Enterobacteriales	11	6	16	8	0,7	10	18	1	23
	Betaproteobacteria		1	6	4	3	2	3	1	1	0.5
		Burkholderiales	1	6	4	3	2	3	1	1	0.5
	Alphaproteobacteria		0.5	3	1	0.5	0.5	2	0.3	0.6	0.2
		Rhizobiales	0.3	2	0.8	0.4	0.3	0.8	0.2	0.4	0.1
		Sphingomonadales		0.6	0.09	0.05	0.01	0.4	0.06	0.04	
		Rhodobacteriales		0.2			0.04	0.09	0.02	0.04	
		Caulobacteriales		0.1							
Firmicutes			0.1	5	2	2	2	2	2	2	0.7
	Bacilli		0.6	4	0.9	0.9	1	0.9	0.5	0.9	0.2
		Lactobacillales	0.5	3	0.9	0.9	1	0.9	0.5	0.9	0.2
		Bacillales	0.05	0.4							
	Clostridia		0.7	1	1	1	1	1.1	0.8	0.4	0.5
		Clostridiales	0.6	1	0.9	1	1	1	0.8	0.4	0.5

CM – Clima di Mola; FR – Frantoio; OR – Oliva Rossa.

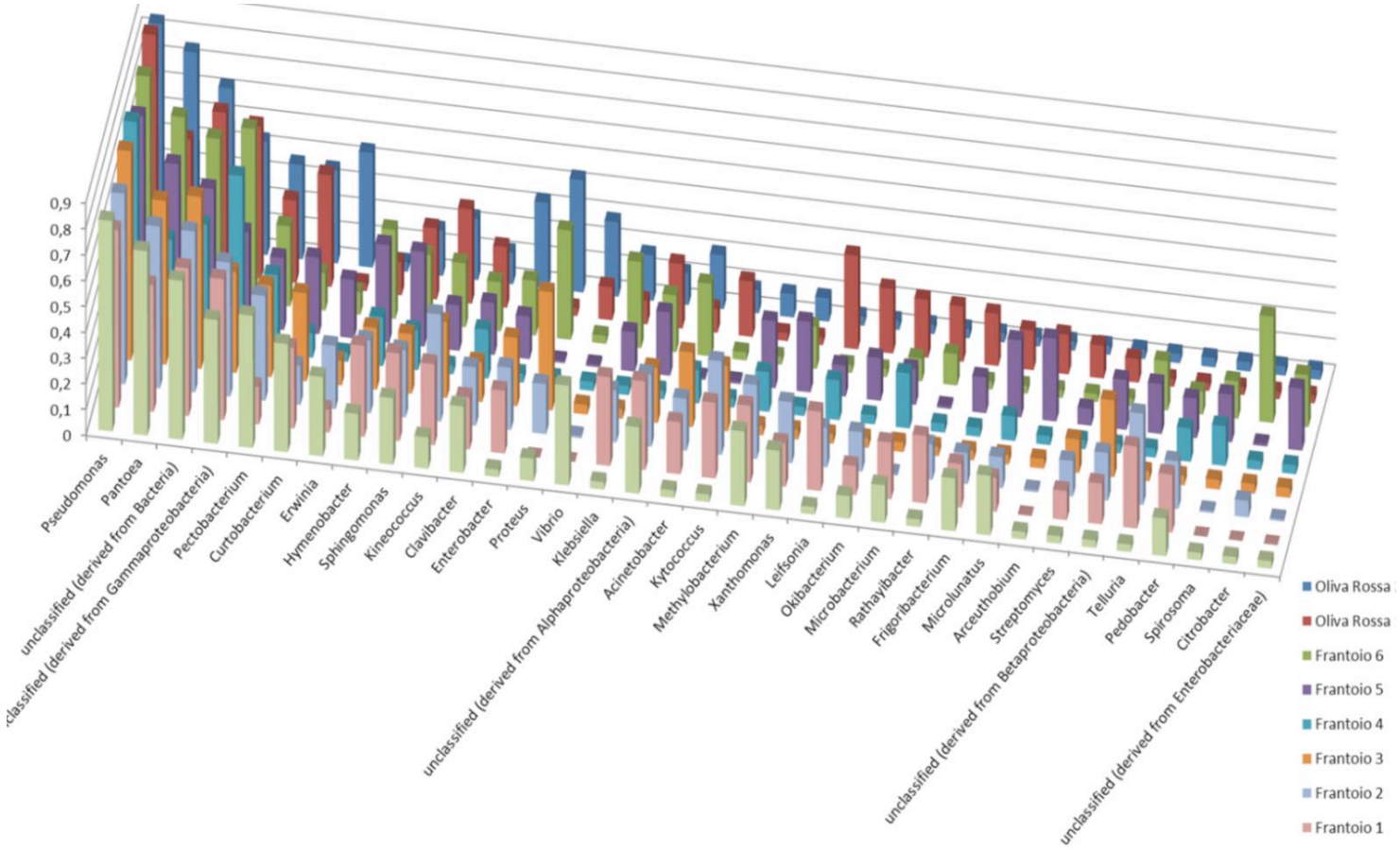

Figure 4-17. Graphical representation of bacterial abundance from the microbiome of 9 olive knots. Different colors are assigned to each one of the nine samples and the organization of the legend follows the same order as the samples on the graph (From bottom to top). Genera *Pseudomonas* and *Pantoea* are clearly the main constituents of these communities.

Table 4-3. Metadata from the 9 olive knots project.

Sample name	MG-RAST ID	Bacterial 16S rRNA abundance	Bacterial 16S rRNA α-diversity	Geographical location	Sequence Counts
Clima di Mola	4516653.3	98,043	7.653	41.04, 16.88	81,369
Frantoio 1	4516654.3	9,128	4.542	43.1, 12.34	115,319
Frantoio 2	4516655.3	15,940	6.929	43.1, 12.34	88,193
Frantoio 3	4516656.3	14,715	6.129	43.1, 12.34	105,082
Frantoio 4	4516657.3	17,655	5.97	42.96, 12.7	84,653
Frantoio 5	4516658.3	14,905	7.56	42.96, 12.7	89,754
Frantoio 6	4516659.3	25,638	6.958	42.96, 12.7	85,331
Oliva Rossa 1	4516660.3	25,130	6.787	40.7, 17.33	83,984
Oliva Rossa 2	4516661.3	45,212	11.013	40.75, 17.32	89,519

4.5 Biofilm formation in single and co-inoculations with PSV and ET

It was previously shown that QS plays a role in the interaction between PSV and ET and results presented here indicate that ET and PSV could possibly share metabolites improving the stability of this multispecies bacterial community. It was also established by bacterial localization experiments that in the olive knot, ET can be found only in close association with PSV in aggregates, most probably in multispecies biofilm structures. It was therefore of interest to assess if and how these two bacterial species organize themselves in single and dual species biofilms and the importance of QS for this process. Biofilm formation/quantification assays were performed using 96-well polystyrene plates

and for visualization of biofilms formed on microscopic slides epifluorescence microscopy was used. Results from these experiments, established that QS did not affect EPS or colony morphology of PSV and its QS mutants derivatives (PSVPSSI and PSVPSSR). In the case of ET however, ETETOI presented a rough colony morphology compared to smooth phenotype of the wild type probably due to lower EPS production and ETETOR showed a very mucoid aspect possibly due to very higher EPS production (Figure 4-18). Exogenously added OC6 and OC8 reverted ETETOI rough phenotype to apparent wild type levels.

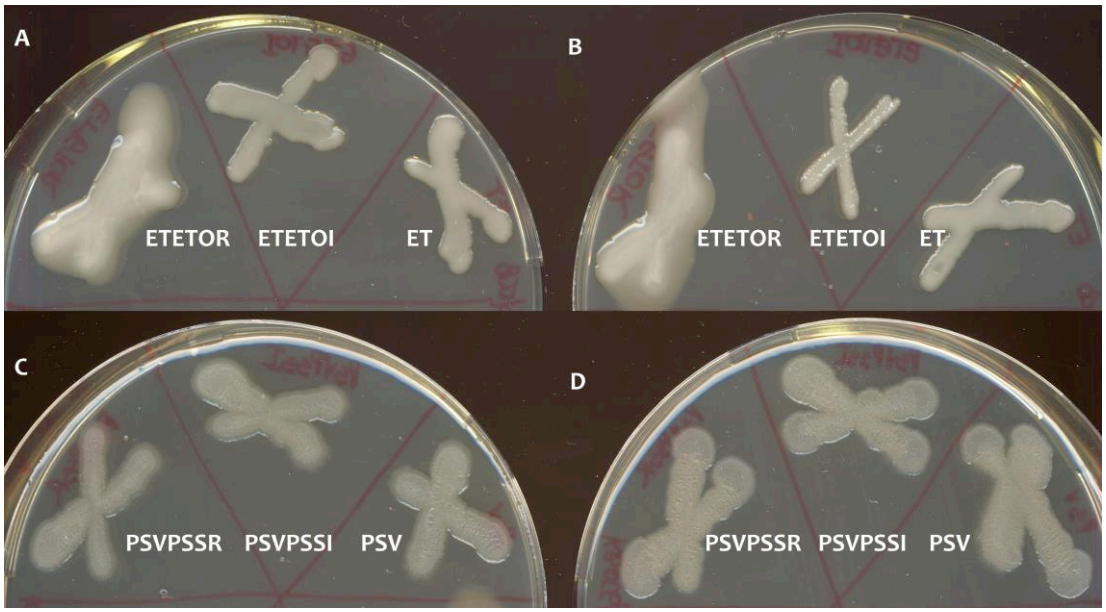

Figure 4-18. QS influence in the EPS phenotype of ET, PSV and their QS derivatives in KB. (A) and (C) are KB plates supplemented with 5µM of OC6 and OC8, while (B) and (D) are KB plates without AHLs supplementation. Bacterial cells were grown for 96h.

Biofilm quantification on 96-well microtiter plates showed that PSV and its QS derivative mutants were very poor in biofilm formation. ET and its QS derivative mutants on the other hand produced considerable biofilms (Figure 4-18). Interestingly, co-inoculations using PSV and ET resulted in improvement of biofilm formation when compared to single inoculations (Figure 4-19).

Importantly, the ETETOI mutant when co-inoculated with PSV, PSVPSSI or PSVPSSR also showed considerable improved biofilm formation when compared to single inoculations (Figure 4-19). This improvement in these mixed biofilms was reversed when 10 uM of AHLs (5uM OC6 + 5uM OC8) was exogenously provided at the start of the experiment and furthermore a reduction in biofilm formation in single ETETOI biofilms was also observed upon addition of AHLs. Mixed biofilm formation of PSV + ET was also affected by the exogenous addition of AHLs (Figure 4-19). These results clearly show that mixed cultures result in improved biofilm formation and that QS is important for ET in single or dual species biofilm formation.

To further address the importance of QS in mixed biofilm architecture fluorescently tagged ET and PSV were used to analyze biofilms grown on borosilicate slides placed on 50 mL Falcon tube by epifluorescence microscopy. Imaging showed that single and co-inoculations using fluorescently tagged PSV, PSVPSSI, PSVPSSR, ET, ETETOI and ETETOR presented differences in biofilm structure. In single inoculations, PSV and ET biofilms consisted of densely packed structures, however while PSV biofilms were more compact and fragile, ET biofilms were more spread and stable. In single inoculations PSVPSSI, PSVPSSR, ETETOI and ETETOR biofilms were less packed but consisted in probably microcolonies that are not in direct physical contact (Figures 4-20 and 4-21), while dual-species biofilms combinations possessed diverse spatial organization (Figures 4-22 and 4-23).

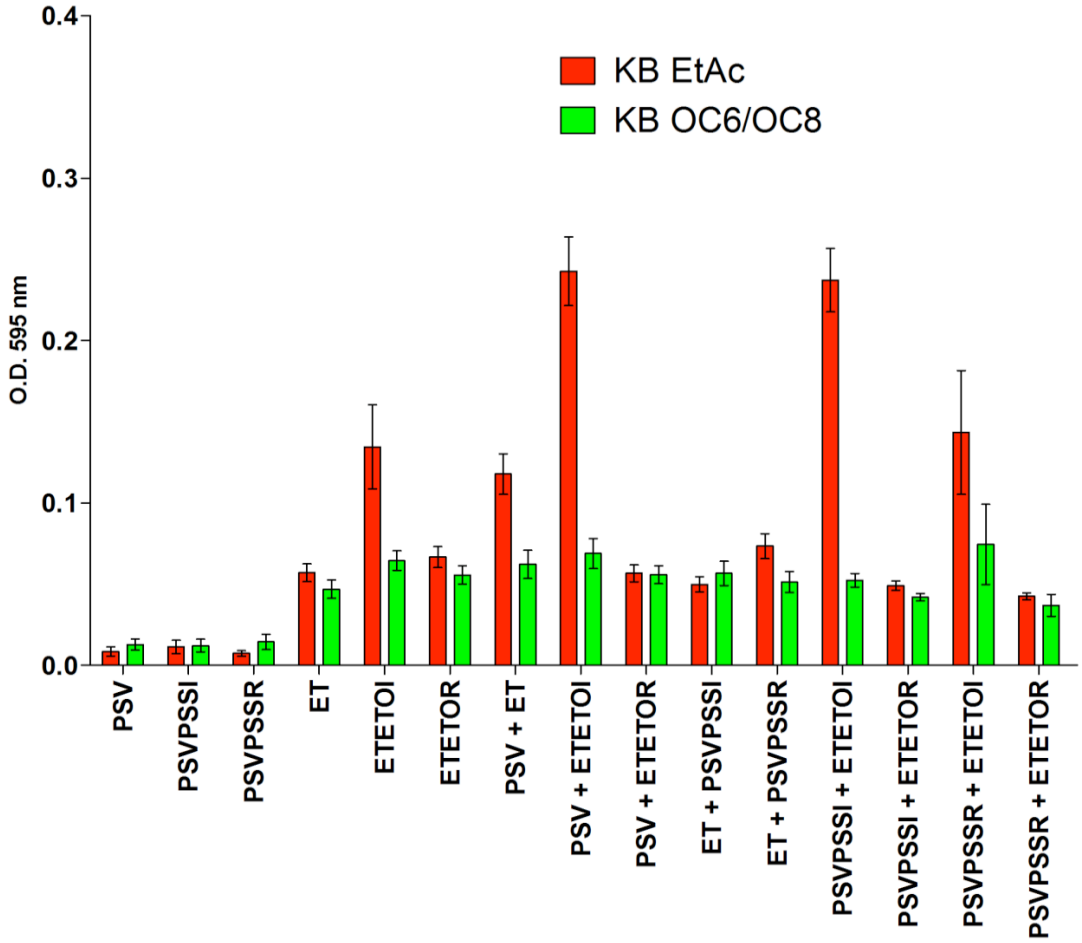

Figure 4-19. Biofilm quantification on 96-well polystyrene plates using KB as growth medium. Single inoculations were done using $O.D_{600}$ 0.1 and co-inoculations with each bacterium at $O.D_{600}$ 0.05. Biofilms were cultured at 28°C and quantified after 120h. Red bars indicate inoculations with ethyl acetate and green bars inoculations using a mix of 5 uM OC6 and 5 uM OC8 at the start of the experiment. Values shown are the means with SEM of three independent experiments.

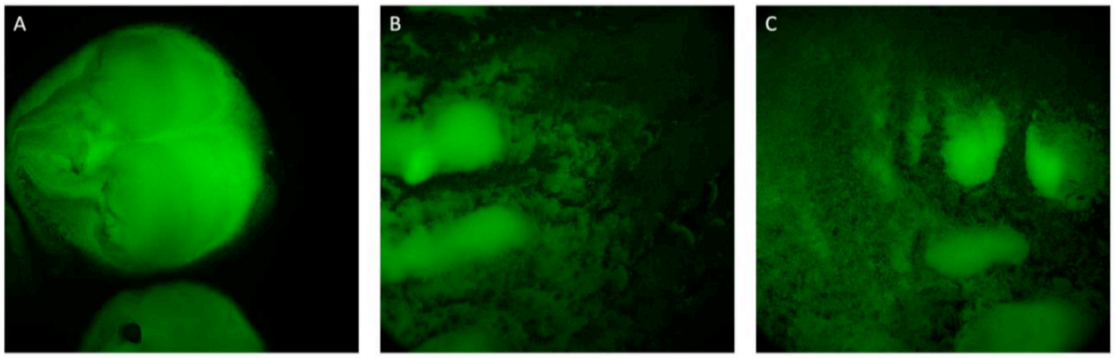

Figure 4-20. Epifluorescence microscopy of PSV (A), PSVPSSI (B) and PSVPSSR (C). Bacterial cells were tagged with GFP using objective of 10x. Biofilms were grown for 120h.

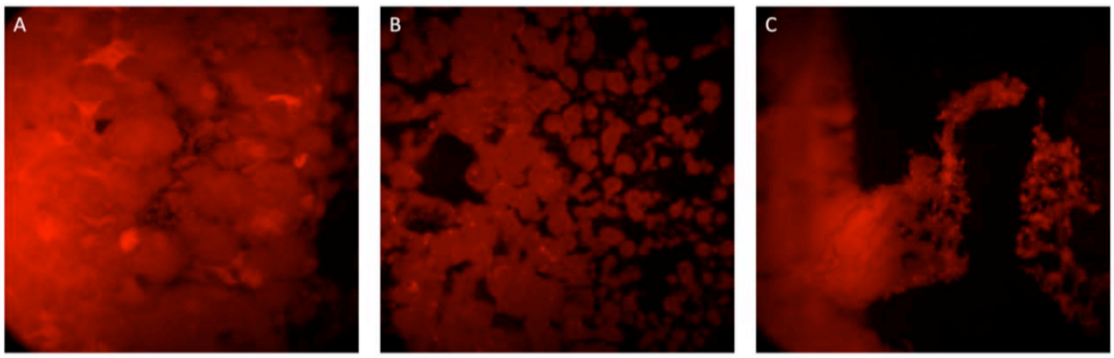

Figure 4-21. Epifluorescence microscopy of ET (A), ETETOI (B) and ETETOR (C). Bacterial cells were tagged with DsRedExpress using objective of 10x and biofilms were grown for 120h.

More precisely, when co-inoculations of PSV + ET were performed biofilms presented a well-mixed densely packed aggregate of both species (Figure 4-22A). On the other hand when PSV + ETETOI or PSVPSSI + ETETOI were co-inoculated a significantly reduced level of mixing in the biofilm between the two bacterial species was observed (Figure 4-22B and 4-22C, respectively). In PSV + ETETOI co-inoculation, PSV seems to have a biofilm growth advantage over ETETOI, while in PSVPSSI + ETETOI both appear to be equally grown. This could indicate that the active PSV QS have a detrimental effect on ETETOI biofilm

formation. Another interesting observation is that although PSV and PSVPSSI can be found in ETETOI biofilm, the opposite does not occur as no or little red fluorescence was observed in PSV and PSVPSSI biofilm. Interestingly when co-inoculations were performed using PSVPSSI + ETETOR (Figure 4-23A) the amount of ETETOR was severely decreased and it was mainly embedded into PSVPSSI biofilm (Figure 4-23A). Cross-feeding of AHLs from ETETOR to PSVPSSI could be activating the QS of PSVPSSI and thus repressing biofilm formation of ETETOR. Finally co-inoculation of PSVPSSR + ETETOR resulted in a biofilm which did not mix between PSVPSSR and ETETOR with the two species growing separately (Figure 4-23B).

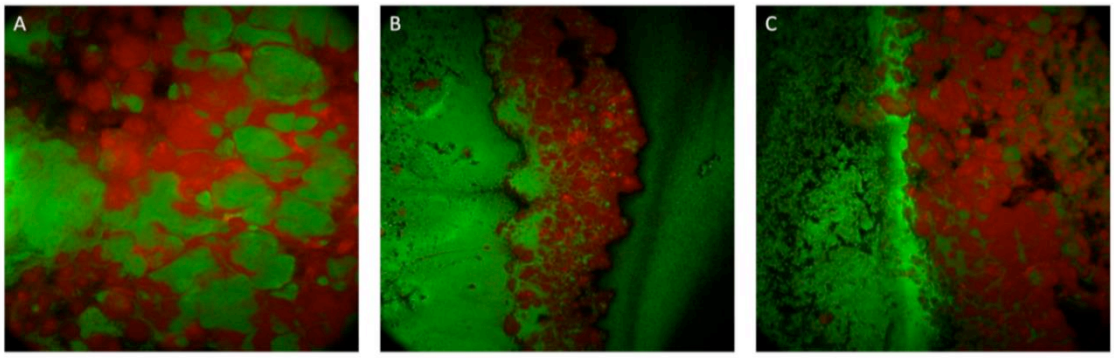

Figure 4-22. Epifluorescence microscopy of PSV-GFP + ET-DsRedExpress (A), PSV-GFP + ETETOI-DsRedExpress (B) and PSVPSSI-GFP + ETETOI-DsRedExpress (C). Objective of 10x was used and biofilms were grown for 120h.

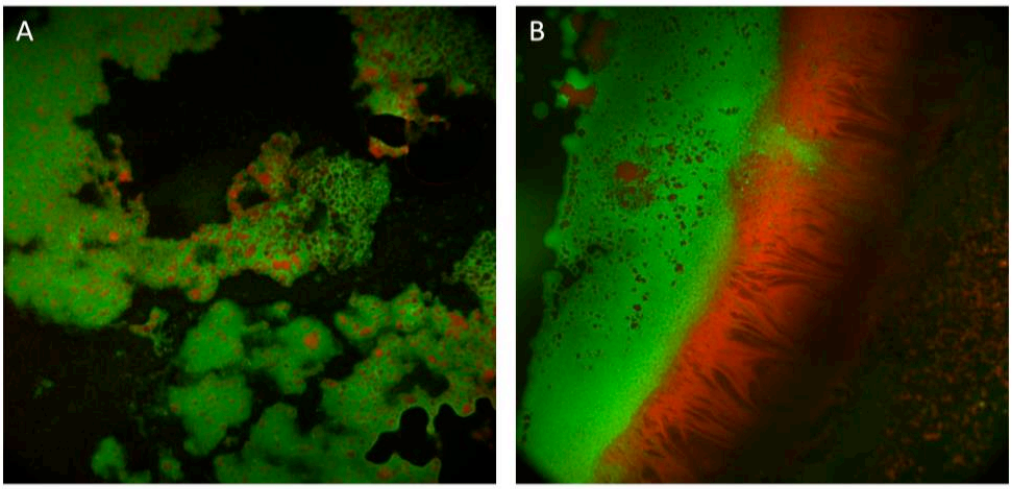

Figure 4-23. Epifluorescence microscopy of PSVPSSI-GFP + ETETOR-DsRedExpress (A) and PSVPSSR-GFP + ETETOR-DsRedExpress (B). Objective of 10x was used and biofilms were grown for 120h.

4.6 ET possesses a stringently regulated QS system

As previously reported by Hosni *et al*. 2011, ET was shown to be able to synthesize AHLs via the EtoI/R QS system. The ETETOI mutant resulted in no AHL production hence it was concluded that ET possessed one AHL QS system. Sequencing of the ET genome and its analysis performed as part of this thesis, revealed that ET possessed a second complete canonical AHL QS system. This QS system was composed of the transcriptional regulator gene which was designated *tolR* and an autoinducer synthase designated *tolI*. As no AHLs from this system could be detected in the supernatant of the ETETOI mutant, it was concluded that this system was either tightly regulated or inactive under the laboratory conditions used (Figure 4-24).

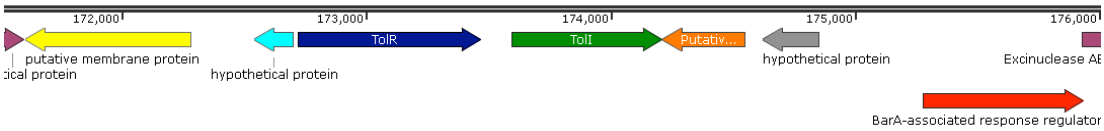

Figure 4-24. Graphical representation of automated predicted coding sequences from Contig 229. *tolR* is represented in blue, *tolI* is represented in green, yellow and orange are loci encoding for putative membrane proteins. In gray a locus encoding a putative hypothetical protein and in red is a potential *barA*-associated response regulator.

The *tolI* synthase was cloned and expressed in heterologous *E. coli* DH5α ™ as well as in the ETETOI mutant. AHLs were detected when *tolI* was expressed in ETETOI (migrating in TLC as OHC6 and OHC8 AHLs; Figure 4-25) indicating that *tolI* encodes a functional LuxI-family protein. AHLs were also detected but in lower amounts when *tolI* was expressed in DH5α ™. The promoters of *tolI* and *tolR* QS genes were then studied in order to try and obtain some insight in the regulation of this QS system. The two promoter regions were cloned upstream a promoterless β-galactosidase gene in the promoter probe vector pMP220. These constructs were then transferred to *E. coli* DH5α ™ and to ET. The *tolR* promoter displayed low activity in both *E. coli* and ET whereas the *tolI* promoter had a relatively higher promoter activity in *E. coli* compared to rather low levels in ET. This indicated that most likely the *tolI* promoter was being repressed in ET and derepressed in *E. coli* since it most probably lacked a repressor(s) present in ET (Figure 4. 26).

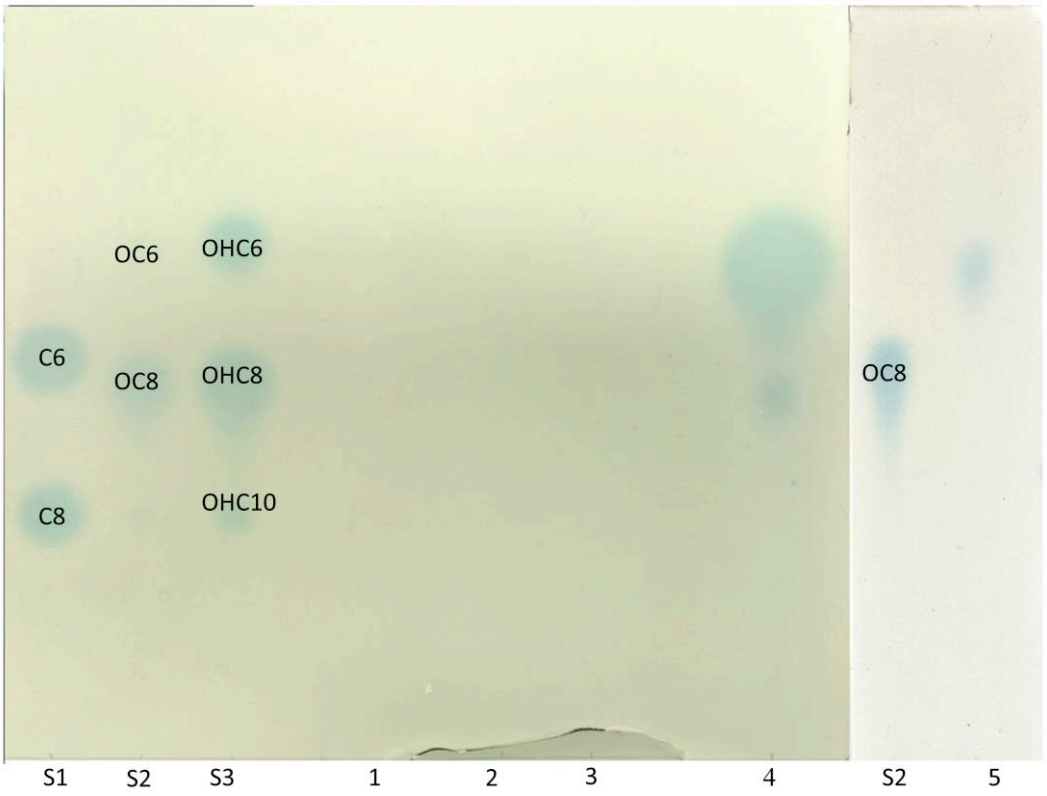

Figure 4-25. TLC analysis of AHL profiles. Standard AHLs (Lanes S1, S2 and S3); KB (Lane 1); DH5α ™ pBBR3TOLI (Lane 2); ETETOI (Lane 3), ETETOI pBBR3TOLI (Lane 4) and DH5α™ pBBR3TOLI (Lane 5). Lanes 1-4 were loaded with an ethyl acetate extract correspondent to 10 mL of culture while Lane 5 is correspondent to 40 mL of culture.

In an attempt to identify the putative repressor(s) acting on the *tolI* promoter, a transposon mutant library of ET was constructed (as described in Materials and Methods) and screened for de-regulation in the *tolI* promoter. For this experiment, the *tolI* promoter region was cloned upstream of a promorterless *xylE* gene encoding for a 2,3- catechol dioxigenase in the promoter probe vector pMP77 (pTOLI77). The activity of the XylE enzyme can be conveniently detected upon spraying the colonies on plate with a 0.1 M catechol solution; the presence of the enzyme converts the colonies to a yellow color. When pTOLI77 was introduced into *E. coli* DH5αTM, cells developed yellow color when sprayed with catechol, while ET pTOLI77 did not confirming previous promoter studies that the *tolI* promoter is active in *E. coli* and not in ET. The pTOLI77 was then introduced by conjugation into a miniTn5 genomic bank of ET

and 50000 colonies were screened for yellow color colony phenotype after catechol spraying. This screen resulted in 35 (Y1-Y35) colonies which turned yellow possibly indicating that in these mutants the *tolI* promoter was active. The positions of insertions in the ET genome of the miniTn5 in 5 mutants were determined by cloning of DNA fragments harboring the transposon in the vector

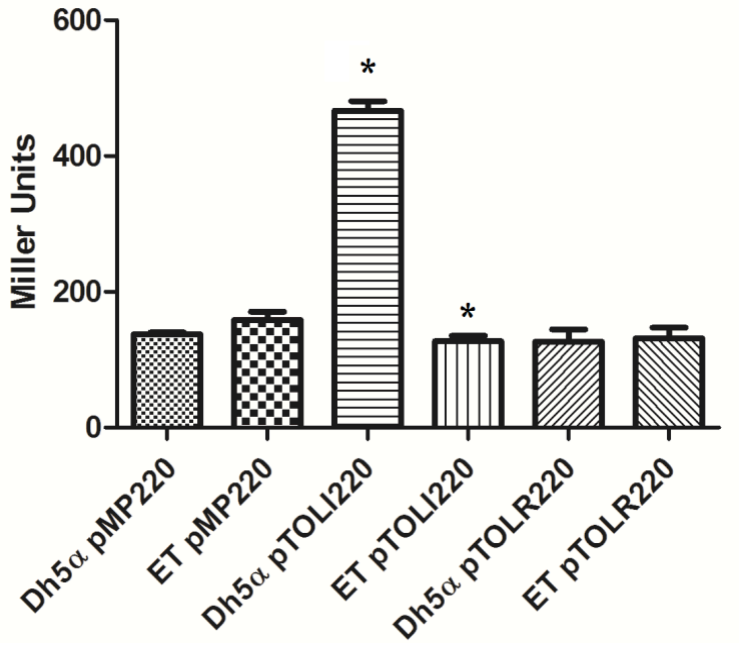

Figure 4-26. Promoter activity measurements of pMP220, pTOLI220 and pTOLR220 harbored in ET and in *E. coli* DH5α^{TM}. Error bars represent the SEM from 3 independent biological experiments and statistical difference was measured by Student's *t* test with a P value < 0.0001.

pBluescript II KS+. The precise positions were then mapped by DNA sequencing. All mapped mutants possessed insertions in a gene encoding a putative membrane protein (NCBI Refseq G200_18815), located adjacently upstream the *tolR* and *tolI* genes (Figure 4-27). The remaining 30 mutants were also shown to possess the transposon in the same locus as determined by Southern blot analysis (Figure 4-28). To determine the orientation of miniTn5 insertions a PCR reaction using a pair of primers annealing at one edge of the miniTn5 (mTn5Downint) and upstream *tolR* gene (TolRpromRv) were used. The presence of amplicons in all mutants (Figure 4-29) suggests that insertions are all oriented in the same orientation. In silico analysis of the amino acid sequence of the

mutated protein was performed using HMMTOP transmembrane topology server (Tusnady and Simon 2001) and it was predicted that this protein possessed 6 transmembrane helices (Figure 4-30).

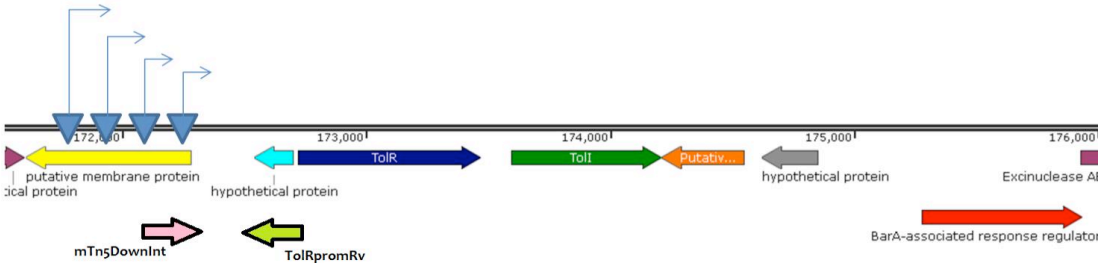

Figure 4-27. Graphical representation of mapped miniTn5 insertions in the ET genome. Blue inverted triangles are some of the insertion points and are demonstrating that all mapped insertions occurred on the same putative membrane protein as blue arrows are showing orientation of miniTn5 insertions. Pink (mTn5DownInt) and light green (TolRpromRv) arrows represent the pair of primers used to detect the orientation of miniTn5 insertions.

The promoter fusion pTOLI220, in which the *tolI* promoter controls the expression of the *lacZ* gene, was then introduced into Y6 mutant of ET (ETG200_18815) which had the transposon insertion mapped. The phenotype of the mutant was confirmed since it displayed high promoter activity when compared to wild type ET (Figure 4-31). In an attempt to complement this de-regulated *tolI* promoter phenotype, the complete wild type of the putative membrane protein (G200_18815) was cloned in pBBR1MCS5 and conjugated into ETG200_18815 mutant. Unfortunately, no convincing complementation of the promoter activity was observed questioning the role of this gene in the observed phenotype (Figure 4-31). As it was observed that all 35 transposon insertions mapped in the same orientation (Figure 4-29) it was concluded that this is very unlikely to be by chance and it could important in causing the observed increased in *tolI* promoter activity. One possible effect of the positioning of the transposon

is the increase of transcription of neighboring genes by promoters present in the transposon. Importantly, the *tolR* gene maps next to the transposon in the correct orientation (Figure 4-27), raising the possibility that the transposon might affect *tolR* expression directly. In order to address this possibility, the *tolR* gene cloned in pBBR1MCS2 under the constitutive expression of the *lac* promoter. This construct was introduced into wild type ET harboring pTOLI220 and β-galactosidase activities were determined (Figure 4-31). Results indicated that over-expression of *tolR* increased significantly *tolI* gene promoter activity indicating that the observed phenotype in the transposon mutants might be due to increased expression of *tolR* and not by the inactivation of the gene encoding for the membrane protein. This possibility needs to be further validated by creation of a knock-out mutant in the gene encoding for the membrane protein and/or RNA quantification studies of *tolR* in the transposon mutants. Multiple attempts were made to generate a knock-out mutant in the membrane protein encoding gene, unfortunately they were unsuccessful; the reason for this is currently unknown.

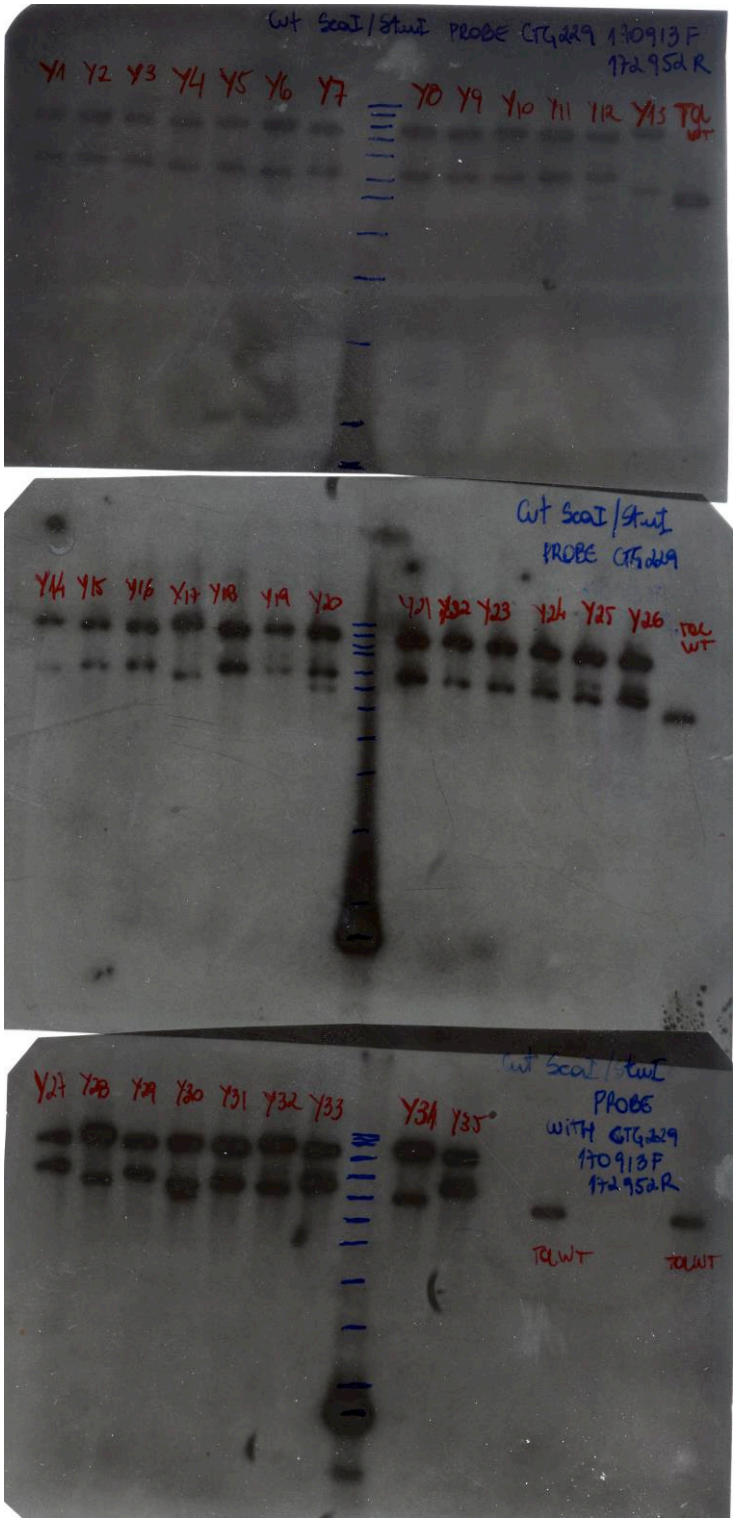

Figure 4-28. Autoradiogram of the Southern blot analysis of genomic from ET miniTn5 mutants. Digestions with ScaI/StuI were hybridized with a probe for a region upstream *tolR* gene.

```
Length:  225
N-terminus:  IN
Number of transmembrane helices: 6
Transmembrane helices: 6-25 32-56 87-109 118-141 162-183 192-216

Total entropy of the model:  17.0022
Entropy of the best path:  17.0045

The best path:

     seq  MLNQFAMLCL ILGICTALMI ARDLIRSPHH LAVMSIVWPI TGLYMPFFGW    50
     pred IiiiiHHHHH HHHHHHHHHH HHHHHooooo oHHHHHHHHH HHHHHHHHHH

     seq  LAWWYLGRNH FHKRAPALRI PQHAGGHLLL WQRVFTSTSL CAAACVLGTS   100
     pred HHHHHHiiii iiiiiiiiii iiiiiiiiii iiiiiiHHHH HHHHHHHHHH

     seq  ATVPLLILLQ HLAIVTPLWL EGVYCLLLSL LLGVLFQFLI IRQTRSLRVI   150
     pred HHHHHHHHHo ooooooooHHH HHHHHHHHHH HHHHHHHHHH Hiiiiiiiii

     seq  PALLLACRSQ TFPLVIYQLG ILFTMSLALK FVLHDQVNPM LLLFWFMLQV   200
     pred iiiiiiiiii iHHHHHHHHH HHHHHHHHHH HHHooooooo oHHHHHHHHH

     seq  AMIAGFLFSW PASTFLLKHG KKAAL  225
     pred HHHHHHHHHH HHHHHHiiii iiiii
```

Figure 4-29. Transmembrane prediction of CTG229 G200_18815. Evidence of 6 transmembrane helices present in this protein.

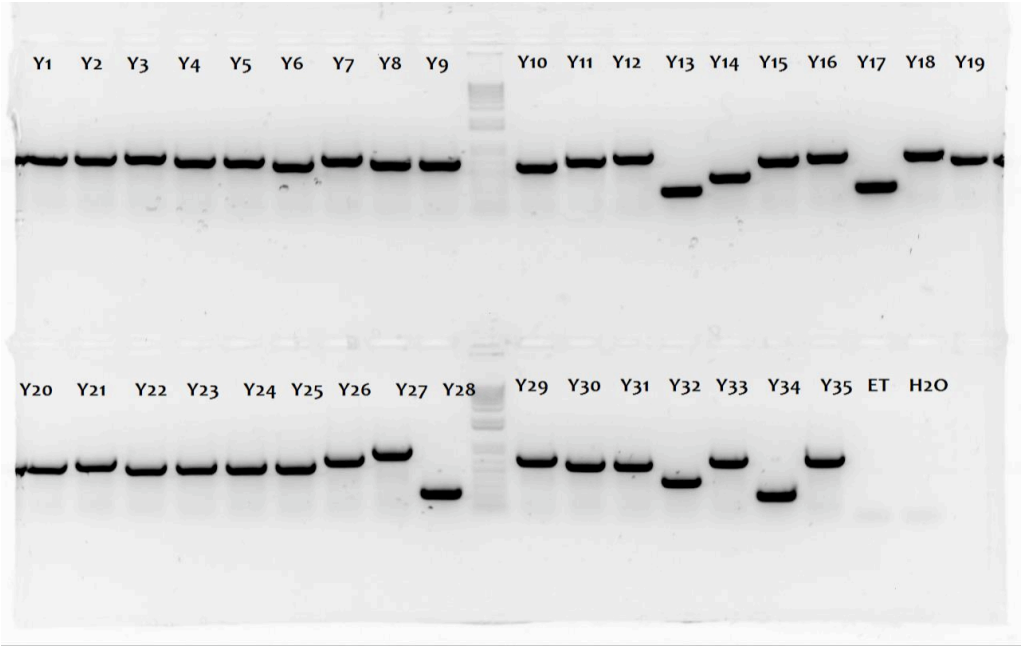

Figure 4-30. PCR on ET miniTn5 mutants. Primers used were mTn5DownInt and promTolRRv. The presence of amplicons in all mutants indicates that all of them possess a miniTn5 insertion in the same orientation. Amplicon size indicates the proximity to *tolR*, where the smaller the amplicon size the closer to *tolR*.

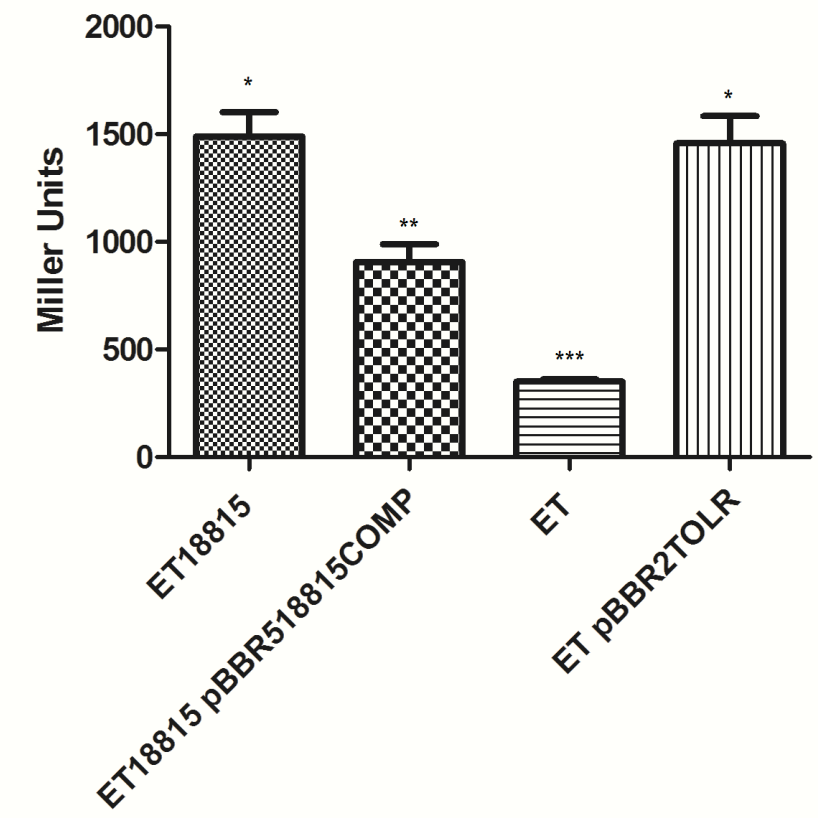

Figure 4-31. Promoter activity measurements of pTOLI220 on ET18815, ET18815 pBBR518815COMP, ET and ET pBBR2TOLR. Error bars represent the SEM from 3 independent biological experiments and statistical difference was measured by Student's t test with a P value < 0.005.

5 DISCUSSION

5.1 PSV and ET localization in the olive knot

The olive knot disease has thus far been poorly studied focusing mainly on the molecular genetics of the causal agent PSV (Surico *et al.* 1985; Scortichini *et al.* 2004; Perez-Martinez *et al.* 2008; Marchi *et al.* 2009; Matas *et al.* 2009; Rodriguez-Moreno *et al.* 2009; Perez-Martinez *et al.* 2010; Ramos *et al.* 2012). To our knowledge the main recent discoveries are the identification of several virulence factors (Surico *et al.* 1985; Iacobellis *et al.* 1994; Rojas *et al.* 2004; Rodriguez-Moreno *et al.* 2008; Matas *et al.* 2009; Rodriguez-Moreno *et al.* 2009; Perez-Martinez *et al.* 2010; Rodriguez-Palenzuela *et al.* 2010; Hosni *et al.* 2011; Matas *et al.* 2012; Ramos *et al.* 2012) and the localization in the intercellular space of the parenchymal tissue as a biofilm structure (Rodriguez-Moreno *et al.* 2009). It was previously reported that harmless ET can colonize the knot in the presence of PSV; sharing of AHL quorum sensing signals between ET and PSV in the tumor microenvironment was demonstrated (Hosni *et al.* 2011). In addition, co-inoculation of PSV with ET resulted in increased tumor size; interestingly this synergism was also observed when the AHL synthase mutant of ET was used indicating that signal sharing was not the only interaction taking place between ET and PSV (Hosni *et al.* 2011). The localization of ET in relation to PSV during the knot development could provide insights on possible mechanisms of interspecies interactions that play a role in the olive knot disease.

Differently from the previous methodology of inoculation of one-year old plants to understand ET and PSV interactions, a laboratory micropropagated olive plantlet was used for experiments carried out as part of this thesis. Enumeration of recovered bacteria from the inoculation site at 28 d.p.i and phenotype of the disease in both single and co-inoculations with ET, ETETOI, PSV and PSVPSSI allowed the following conclusions. Firstly, in contrast to observations in one-year old olive plant from the cultivar Frantoio, the QS system of PSV is not essential for the development of tumor in 3 months old olive plants

from the cultivar Arbequina, as observed in this study. Secondly, although in single and co-inoculations the cell numbers of PSV and PSVPSSI increased over the course of the disease, their growth was reduced in co-inoculations when compared to single inoculations. The growth of ET however increased when co-inoculated with either PSV or PSVPSSI. Similarly, ETETOI also showed improved growth when co-inoculated with PSVPSSI. However, when inoculated in combination with PSV, ETETOI number in the inoculation site diminished although not as drastically as in single inoculations. This suggests that PSV delays the dispersion of ETETOI from the inoculation site, but not as effectively as PSVPSSI. These results suggest that in micropropagated olive plantlets, ET QS is important for its maintenance *in planta* and PSV QS has a negative effect on the co-existence/maintenance of ETETOI in the olive knot.

By using epifluorescence stereoscopic microscopy and confocal scanning laser microscopy it was observed that ET was consistently in the vicinity of PSV possibly meaning that ET requires this close proximity with PSV for its persistence and growth in the olive knot. This closeness is in line with AHL signal sharing between PSV and Et in the olive knot was previously observed to be taking place between PSV and ET in the olive knot (Hosni *et al.* 2011); AHLs of ET can therefore easily diffuse into PSV (Nilsson *et al.* 2001; Egland *et al.* 2004). In addition, close proximity can result in community signaling by cell contact (Pratt and Kolter 1998; Barken *et al.* 2008) and/or facilitated sharing of metabolites (Ramsey *et al.* 2011). PSV cells form biofilm structures in the olive knot (Rodriguez-Moreno *et al.* 2009), thus this close proximity of ET during the knot formation suggests that mixed biofilms are most probably formed and this could be more advantageous for both species to facilitate cell-to-cell contact (Pratt and Kolter 1998; Barken *et al.* 2008; Blango and Mulvey 2009; Atkinson *et al.* 2011; Fazli *et al.* 2014) and diffusion of metabolites and signals in a definite area (Egland *et al.* 2004; Kim *et al.* 2008; Hosni *et al.* 2011; Ramsey *et al.* 2011) possibly resulting in a more stable biofilm.

5.2 Metabolic complementarity between PSV and ET

It is believed that metabolic sharing/complementarity is one of the features that allows the formation of a stable bacterial consortia (Egland *et al.* 2004; Kim *et al.* 2008). For example, the diffused metabolites can be transformed by one species that can then be further utilized by the neighboring species resulting in a mutualistic interaction (Egland *et al.* 2004; Kim *et al.* 2008; Ramsey *et al.* 2011). To evaluate the possibility of metabolic sharing between ET and PSV an *in silico* approach was initially used. The metabolic pathways and single reactions that each of the two organisms was able to individually perform was predicted via analysis of the genome. Interestingly, in some cases the missing gene(s)/enzyme(s) of a specific pathway could be completed by the presence of these loci on the genome of the second species. Possible degradation pathways of several plant related aromatic compounds, some of which are known to be associated with plant defense, were only possible *in silico* when the two genomes were joined. Compounds such as salicylate, shikimate and sucrose are key examples that could only be mineralized by the dual-species community *in silico*. Other compounds such as sorbitol and β-D-glucose-6-phosphate were also predicted to be fully metabolized when both PSV and ET were present.

Phenotypic microarray analysis performed with Biolog plates PM1-20 showed that ET is metabolically more active than PSV and the combined metabolic profile obtained by co-inoculation was more similar to ET. Many compounds presented an improved metabolic activity when PSV and ET were co-inoculated confirming *in silico* prediction as observed for salicylate, sucrose, sorbitol and β-D-glucose-6-phosphate. Possible metabolic complementarity was tested *in vitro* using growth tests in liquid and solid media supplemented with salicylic acid and sucrose. Binary growth studies of PSV and ET in the laboratory conditions that were tested provided no evidence for metabolic sharing/complementarity. It could be that *in vitro* laboratory conditions do not

favor such an interaction which on the other hand might take place *in planta*. Many more compounds and processes need to be further validated in the laboratory as both the Biolog data and *in silico* analysis provide a large amount of information regarding metabolic activities of the dual-species community composed of PSV and ET. Future studies therefore need to focus in this direction using all the possible compounds that the *in silico* and Biolog analysis revealed as potential substrates that could be transformed using metabolic sharing. Pathways tools used for *in silico* analysis are powerful tools for complex systems such as multi-species communities associated with a host; however the dynamics of metabolites under *in planta* conditions during infection are only beginning to be understood and extreme caution is required while interpreting and validating these results.

5.3 Bacterial community in the olive knot

Previous studies to assess the bacterial community in olive knots were performed in the past using culturing methods (Rojas *et al.* 2004; Ouzari *et al.* 2008; Moretti *et al.* 2011). This approach underestimates the bacterial population due to uncultivable bacteria or low represented species. For this reason, a metagenomics approach via the generation of amplicon libraries and sequencing of 16S rRNA provides far more complete information on the bacterial species commonly present in olive knots. Nine naturally generated olive knots from different regions of Italy were sampled [Città della Domenica (PG), Foligno (PG), Martina Franca(TA), Valenzano (BA) and Locorotondo(BA)] from three different cultivars of olive tree (six samples from the olive cultivar Frantoio, two from the cultivar Oliva Rossa and one from the cultivar Clima di Mola). These metagenomics studies proved that apart from PSV there was a dominance of *Pantoea* throughout all nine samples; the presence of *Pantoea agglomerans* on olive knots has been extensively described but its role on the tumor

development remains unclear (Marchi *et al.* 2006; Hosni *et al.* 2011). These results indicate that the enrichment of *Pantoea* in the tumor environment is an important aspect which merits further attention. It was surprising to see the presence of so many different genera in the olive knot; this indicates a community structure present in the olive knot which could have evolved together with PSV. Observations made here in these studies with ET could be applicable to other species and most probably also to multispecies studies involving more than two bacterial species. *Clavibacter, Curtobacterium, Hymenobacter, Kineococcus, Proteus* and *Sphingomonas* were present in almost all samples and reported for the first time in this study. Within these genera there are species being able to tolerate high concentrations of copper (Bagwell *et al.* 2010), facilitating the mineralization of polycyclic aromatic compounds (Manickam *et al.* 2012) or even associated with fungi that degrades decaying matter (Kamei *et al.* 2012) this shows diverse biological roles that could aid the maintenance and progression of the disease. The identification of the microbial core present on the disease and their metabolic potential could be useful to select the best chemical treatment or biological control strain to be used for the disease treatment. Interestingly, α-diversity seems to be directly related to the geographical location from where the sample was collected (Table 4-3). Samples from south of Italy (Clima di Mola and Oliva Rossa 1 and 2) have shown higher diversity when compared to samples from central Italy (Frantoio 1 to 6). This might be due to the difference of average temperature and humidity (Teviotdale and Krueger 2004) or possibly the susceptibility of distinct cultivar of olive trees (Penyalver *et al.* 2006). Even though a core microbiome group of bacterial genera seems to be present in all samples, a large part of the community present in the nine different samples shows considerable variation also in abundance. Importantly however, the phylogenetic variation present among the samples might not necessarily reflect on the genetic pool (Burke *et al.* 2011). It is possible that major roles in community interactions are being played by the genera that are found in all samples (e.g. *Pantoea*) while the other bacteria present in only some or even one of the samples, might be recruited in response to some

specific traits like cultivar or by diverse environmental condition. Based on the results from this thesis, future studies aiming to identify bacterial communities or bacterial metabolic potential present in naturally occurred olive knots should consider associating environmental and/or human influence in selecting the microbial partners of PSV. For example increased presence of copper tolerant bacteria (as observed in some samples of this study) could be product of recent copper treatment or the detection of bacteria known to be associated with fungi could indicate that the plant was suffering secondary infections.

5.4 QS importance for mixed biofilm formation between PSV and ET

The importance of QS in biofilm formation has been extensively described in bacteria associated with humans, whereas the role of plant associated biofilms is largely unknown (Elias and Banin 2012). Multispecies interactions in biofilms is now being studied by several research groups as it is becoming evident that these are most common in nature (Elias and Banin 2012). *In planta* experiments confirm the presence of both PSV and ET in biofilm/aggregates in the tumor tissue and the importance of QS in PSV + ET for community stability and survival of ET. *In vitro* experiments were performed to assess the role of QS in biofilm formation of single and dual-species communities composed of PSV and ET. Biofilm quantification assays indicated that biofilm formation by PSV QS mutants (PSVPSSI and PSVPSSR) was not affected; similarly ETETOR formed biofilms at levels comparable to ET wild type in single inoculations. ETETOI on the other hand was able to produce an increased biofilm in single inoculations. Co-inoculations of ET and PSV with functional quorum sensing systems generated an improved biofilm when compared to its single inoculations. Co-inoculations of PSV and its QS mutant derivatives using ETETOI resulted in the largest biofilms. The addition of AHLs reduced the levels of biofilm in both single and co-inoculation experiments. These results suggest that ET QS

system has a strong negative effect on biofilm formation. Architecturally, biofilm structure of ET and PSV were influenced by QS in both single and co-inoculations. In PSV + ET a completely mixed and densely packed biofilm structure was observed, while co-inoculations involving ETETOI and ETETOR presented low levels of mixing evidencing the importance of QS to the dual-species biofilm formation between PSV and ET. The relevance of the second QS system which is tightly regulated was not assessed in this thesis and needs to be studied to further improve the knowledge about biofilm formation in ET alone and when mixed with PSV.

5.5 Identification of a second QS system in ET

Genome sequencing of ET led to the discovery of a second canonical QS system (*tolR/I*) which was tightly regulated; only by expressing the AHL synthase (designated *tolI*) from a constitutive promoter resulted in AHL production (tentatively designated as OHC6 and OHC8). Measurements of promoter activities from *tolI* promoter region in *E. coli* DH5α ™ and ET indicated that either *E. coli* DH5α™ possessed a transcriptional machinery/activator that is not present in ET or there was the presence of a repressor in ET that was absent in *E. coli* DH5α™. A random mutagenesis approach was performed and a gene putatively involved in the repression (G200_18815) of *tolR*/*tolI* system was discovered just upstream *tolR*. Complementation of ETG200_18815 phenotype was only partial, but it is arguable that fine tuning of expression levels is needed, especially considering the putative repression role and transmembrane nature of the protein which is the target of complementation. The observation that all screened mutants possessed insertions upstream *tolR* with the same orientation allows the possibility that the observed phenotype is due to an artifact generated by the promoters present in the miniTn5 construct which causes the increase of *tolR* transcriptional levels. Overexpression of TolR in expression

vector in fact resulted in the activation of *tolI* promoter region indicating that increasing the amount of TolR is enough to derepress the system. Unfortunately it was not possible to generate a knock-out mutant of this gene encoding a membrane protein thus the phenotype of the mutant could not be validated. It cannot be excluded that the putative repressor involved in regulating the *tolR/I* system cannot be inactivated thus it was not found in the genetic screen. Alternatively more than one repressor protein are operative on the *tolI* promoter hence inactivating one is not sufficient to generate a phenotype. Further studies are needed to elucidate the mechanisms of regulation of the *tolR/I* system and its importance for the environmental role of ET.

5.6 Summarizing discussion

In summary in this thesis it was shown that PSV and ET are localized in close proximity during the knot development and the presence of PSV is essential for the maintenance and growth of ET cells in the olive knot. This is a clear example of harmless and beneficial organisms teaming up in a disease (Venturi and da Silva 2012). The close proximity of ET and PSV in the knot indicates that they are most probably interacting via a variety of mechanisms. It was observed that mixed biofilms of these two bacterial strains develop larger communities compared to single inoculations and that QS plays an important role in *in vitro* mixed-species biofilm formation. By *in silico* analysis and phenotypic microarray potential compounds that could be shared *in planta* were identified; these compounds might be possibly involved in improving the stability of the community via metabolic complementarity. Metagenomic sequencing revealed that some genera are commonly found associated with the olive knot comprising the core of the community, nevertheless high bacterial diversity occurs in the satellite community among different knots and this could to be related to environmental factors and/or cultivar of *Olea europaea*. The discovery a

new QS system in ET that is tightly repressed could prove to be an interesting factor in the interaction between PSV and ET. This study opens new possibilities on the PSV/ET interaction and presents a valid model to study multispecies interactions in a plant bacterial disease.

5.7 Future directions

All the results presented here are advancements in the understanding of the interaction between PSV and ET that could possibly apply to other bacterial inter-species interactions. Most of the studies on bacterial pathogenesis in plants have focused on the pathogen and thus far possible interactions with resident bacteria have been at large ignored. These could however be involved in the establishment and progression of the disease and the olive knot represents an attractive model to study polybacterial interactions in a plant disease. The findings reported here lay foundation for further research on this topic and some of the areas to be studied in future are given below:

I. To answer the question of which metabolites are being shared by PSV and ET during the olive knot development a metatranscriptomics approach could be applied to compare mixed and single inoculations.

II. *In vitro* verification of the *in silico* metabolic complementarity predictions which were tested or not in the Biolog system.

III. Close vicinity on *in vitro* and *in planta* co-inoculations of PSV and ET leads the speculation about cell-to-cell contact importance for this interaction. Analysis of ET's secretion system (T1SS, T2SS, T3SS and

T4SS) influence for *in planta* colonization and *in vitro* biofilm formation when co-inoculated with PSV.

IV. Architectural analysis of biofilms formed by PSV, PSVPSSI, PSVPSSR, ET, ETETOI and ETETOR in single and co-inoculations in continuous flow chambers using confocal microscopy and evaluation of plant metabolites on biofilm formation.

V. Regulation of the *tolR/I* system; identification of the regulatory switch and possible regulation *in planta*.

6 REFERENCES

Alfano, J. R. and Collmer, A. (1997). "The type III (Hrp) secretion pathway of plant pathogenic bacteria: trafficking harpins, Avr proteins, and death." J Bacteriol **179**(18): 5655-5662.

Almeida, C., Azevedo, N. F., Santos, S., Keevil, C. W. and Vieira, M. J. (2011). "Discriminating multi-species populations in biofilms with peptide nucleic acid fluorescence *in situ* hybridization (PNA FISH)." PLoS One **6**(3): e14786.

Anderson, J. M., Rayner, A. D. M., Walton, D. W. H. and Society, B. M. (1984). Invertebrate-microbial interactions: Joint symposium of the british mycological society and the british ecological society, Held at the University of Exeter, September 1982, Cambridge University Press.

Aragon, I. M., Perez-Martinez, I., Moreno-Perez, A., Cerezo, M. and Ramos, C. (2014). "New insights into the role of indole-3-acetic acid in the virulence of *Pseudomonas savastanoi* pv. *savastanoi*." FEMS Microbiol Lett.

Arnold, A. E., Mejia, L. C., Kyllo, D., Rojas, E. I., Maynard, Z., Robbins, N. and Herre, E. A. (2003). "Fungal endophytes limit pathogen damage in a tropical tree." Proc Natl Acad Sci U S A **100**(26): 15649-15654.

Atkinson, S., Goldstone, R. J., Joshua, G. W., Chang, C. Y., Patrick, H. L., Camara, M., Wren, B. W. and Williams, P. (2011). "Biofilm development on *Caenorhabditis elegans* by *Yersinia* is facilitated by quorum sensing-dependent repression of type III secretion." PLoS Pathog **7**(1): e1001250.

Aziz, R. K., Bartels, D., Best, A. A., DeJongh, M., Disz, T., Edwards, R. A., Formsma, K., Gerdes, S., Glass, E. M., Kubal, M., Meyer, F., Olsen, G. J., Olson, R., Osterman, A. L., Overbeek, R. A., McNeil, L. K., Paarmann, D., Paczian, T., Parrello, B., Pusch, G. D., Reich, C., Stevens, R., Vassieva, O., Vonstein, V., Wilke, A. and Zagnitko, O. (2008). "The RAST Server: rapid annotations using subsystems technology." BMC Genomics **9**: 75.

Bagwell, C. E., Hixson, K. K., Milliken, C. E., Lopez-Ferrer, D. and Weitz, K. K. (2010). "Proteomic and physiological responses of *Kineococcus radiotolerans* to copper." PLoS One **5**(8): e12427.

Bais, H. P., Weir, T. L., Perry, L. G., Gilroy, S. and Vivanco, J. M. (2006). "The role of root exudates in rhizosphere interactions with plants and other organisms." Annu Rev Plant Biol **57**: 233-266.

Baratta, B. and Di Marco, L. (1981). "Control of olive knot attacks on the cultivar Nocellara del belice." Informatore Fitopatologico **31**: 115-116.

Bardaji, L., Perez-Martinez, I., Rodriguez-Moreno, L., Rodriguez-Palenzuela, P., Sundin, G. W., Ramos, C. and Murillo, J. (2011). "Sequence and role in virulence of the three plasmid complement of the model tumor-inducing bacterium *Pseudomonas savastanoi* pv. *savastanoi* NCPPB 3335." PLoS One **6**(10): e25705.

Barken, K. B., Pamp, S. J., Yang, L., Gjermansen, M., Bertrand, J. J., Klausen, M., Givskov, M., Whitchurch, C. B., Engel, J. N. and Tolker-Nielsen, T. (2008). "Roles of type IV pili, flagellum-mediated motility and extracellular DNA in the formation of mature multicellular structures in *Pseudomonas aeruginosa* biofilms." Environ Microbiol **10**(9): 2331-2343.

Barnard, A. M., Bowden, S. D., Burr, T., Coulthurst, S. J., Monson, R. E. and Salmond, G. P. (2007). "Quorum sensing, virulence and secondary metabolite production in plant soft-rotting bacteria." Philos Trans R Soc Lond B Biol Sci **362**(1483): 1165-1183.

Baumgartner, L. K., Spear, J. R., Buckley, D. H., Pace, N. R., Reid, R. P., Dupraz, C. and Visscher, P. T. (2009). "Microbial diversity in modern marine stromatolites, Highborne Cay, Bahamas." Environ Microbiol **11**(10): 2710-2719.

Beard, C. B., Cordon-Rosales, C. and Durvasula, R. V. (2002). "Bacterial symbionts of the triatominae and their potential use in control of Chagas disease transmission." Annu Rev Entomol **47**: 123-141.

Better, M., Lewis, B., Corbin, D., Ditta, G. and Helinski, D. R. (1983). "Structural relationships among *Rhizobium meliloti* symbiotic promoters." Cell **35**(2 Pt 1): 479-485.

Bhat, T. K., Singh, B. and Sharma, O. P. (1998). "Microbial degradation of tannins--a current perspective." Biodegradation **9**(5): 343-357.

Blango, M. G. and Mulvey, M. A. (2009). "Bacterial landlines: contact-dependent signaling in bacterial populations." Curr Opin Microbiol **12**(2): 177-181.

Bochner, B. R., Gadzinski, P. and Panomitros, E. (2001). "Phenotype microarrays for high-throughput phenotypic testing and assay of gene function." Genome Res **11**(7): 1246-1255.

Bowman, J. S., Rasmussen, S., Blom, N., Deming, J. W., Rysgaard, S. and Sicheritz-Ponten, T. (2012). "Microbial community structure of Arctic multiyear sea ice and surface seawater by 454 sequencing of the 16S RNA gene." ISME J **6**(1): 11-20.

Bradbury, J. F. (1986). Guide to plant pathogenic bacteria, CAB International.

Broderick, N. A., Raffa, K. F. and Handelsman, J. (2006). "Midgut bacteria required for *Bacillus thuringiensis* insecticidal activity." Proc Natl Acad Sci U S A **103**(41): 15196-15199.

Broderick, N. A., Robinson, C. J., McMahon, M. D., Holt, J., Handelsman, J. and Raffa, K. F. (2009). "Contributions of gut bacteria to *Bacillus thuringiensis*-induced mortality vary across a range of Lepidoptera." BMC Biol **7**: 11.

Brummel, T., Ching, A., Seroude, L., Simon, A. F. and Benzer, S. (2004). "*Drosophila* lifespan enhancement by exogenous bacteria." Proc Natl Acad Sci U S A **101**(35): 12974-12979.

Buchner, P. (1965). Endosymbiosis of animals with plant microorganisms, Interscience Publishers.

Buee, M., Reich, M., Murat, C., Morin, E., Nilsson, R. H., Uroz, S. and Martin, F. (2009). "454 pyrosequencing analyses of forest soils reveal an unexpectedly high fungal diversity." New Phytol **184**(2): 449-456.

Bull, C. T., De Boer, S. H., Denny, T. P., Firrao, G., Fischer-Le Saux, M., Sadler, G. M., Scortichini, M., Stead, D. E. and Takikawa, Y. (2010). "Comprehensive list of names of plant pathogenic bacteria, 1980 - 2007." J Plant Pathol **92**(3): 551 -592.

Burke, C., Kjelleberg, S. and Thomas, T. (2009). "Selective extraction of bacterial DNA from the surfaces of macroalgae." Appl Environ Microbiol **75**(1): 252-256.

Burke, C., Steinberg, P., Rusch, D., Kjelleberg, S. and Thomas, T. (2011). "Bacterial community assembly based on functional genes rather than species." Proc Natl Acad Sci U S A **108**(34): 14288-14293.

Cantarel, B. L., Erickson, A. R., VerBerkmoes, N. C., Erickson, B. K., Carey, P. A., Pan, C., Shah, M., Mongodin, E. F., Jansson, J. K., Fraser-Liggett, C. M. and Hettich, R. L. (2011). "Strategies for metagenomic-guided whole-community proteomics of complex microbial environments." PLoS One **6**(11): e27173.

Caspi, R., Altman, T., Dreher, K., Fulcher, C. A., Subhraveti, P., Keseler, I. M., Kothari, A., Krummenacker, M., Latendresse, M., Mueller, L. A., Ong, Q., Paley, S., Pujar, A., Shearer, A. G., Travers, M., Weerasinghe, D., Zhang, P. and Karp, P. D. (2012). "The MetaCyc database of metabolic pathways and

enzymes and the BioCyc collection of pathway/genome databases." Nucleic Acids Res **40**(Database issue): D742-753.

Chen, L., Xiong, Z., Sun, L., Yang, J. and Jin, Q. (2012). "VFDB 2012 update: toward the genetic diversity and molecular evolution of bacterial virulence factors." Nucleic Acids Res **40**(D1): D641-D645.

Chernysh, S., Kim, S. I., Bekker, G., Pleskach, V. A., Filatova, N. A., Anikin, V. B., Platonov, V. G. and Bulet, P. (2002). "Antiviral and antitumor peptides from insects." Proc Natl Acad Sci U S A **99**(20): 12628-12632.

Chi, F., Shen, S. H., Cheng, H. P., Jing, Y. X., Yanni, Y. G. and Dazzo, F. B. (2005). "Ascending migration of endophytic rhizobia, from roots to leaves, inside rice plants and assessment of benefits to rice growth physiology." Appl Environ Microbiol **71**(11): 7271-7278.

Comai, L. and Kosuge, T. (1980). "Involvement of plasmid deoxyribonucleic acid in indoleacetic acid synthesis in *Pseudomonas savastanoi*." J Bacteriol **143**(2): 950-957.

Comai, L. and Kosuge, T. (1982). "Cloning characterization of *iaaM*, a virulence determinant of *Pseudomonas savastanoi*." J Bacteriol **149**(1): 40-46.

Compant, S., Reiter, B., Sessitsch, A., Nowak, J., Clement, C. and Ait Barka, E. (2005). "Endophytic colonization of *Vitis vinifera* L. by plant growth-promoting bacterium *Burkholderia* sp. strain PsJN." Appl Environ Microbiol **71**(4): 1685-1693.

Corby-Harris, V., Pontaroli, A. C., Shimkets, L. J., Bennetzen, J. L., Habel, K. E. and Promislow, D. E. (2007). "Geographical distribution and diversity of bacteria associated with natural populations of *Drosophila melanogaster*." Appl Environ Microbiol **73**(11): 3470-3479.

Cox, C. R. and Gilmore, M. S. (2007). "Native microbial colonization of *Drosophila melanogaster* and its use as a model of *Enterococcus faecalis* pathogenesis." Infect Immun **75**(4): 1565-1576.

Curtis, T. P., Sloan, W. T. and Scannell, J. W. (2002). "Estimating prokaryotic diversity and its limits." Proc Natl Acad Sci U S A **99**(16): 10494-10499.

Dalton, T., Dowd, S. E., Wolcott, R. D., Sun, Y., Watters, C., Griswold, J. A. and Rumbaugh, K. P. (2011). "An *in vivo* polymicrobial biofilm wound infection model to study interspecies interactions." PLoS One **6**(11): e27317.

Dangl, J. L., Dietrich, R. A. and Richberg, M. H. (1996). "Death don't have no mercy: cell death programs in plant-microbe interactions." Plant Cell **8**(10): 1793-1807.

Danhorn, T. and Fuqua, C. (2007). "Biofilm formation by plant-associated bacteria." Annu Rev Microbiol **61**: 401-422.

Darling, A. E., Mau, B. and Perna, N. T. (2010). "progressiveMauve: multiple genome alignment with gene gain, loss and rearrangement." PLoS One **5**(6): e11147.

De Boer, W., Wagenaar, A.-M., Klein Gunnewiek, P. J. A. and Van Veen, J. A. (2007). "*In vitro* suppression of fungi caused by combinations of apparently non-antagonistic soil bacteria." FEMS Microbiol Ecol **59**(1): 177-185.

Dillon, R. and Charnley, K. (2002). "Mutualism between the desert locust *Schistocerca gregaria* and its gut microbiota." Res Microbiol **153**(8): 503-509.

Dillon, R. J. and Charnley, A. K. (1995). "Chemical barriers to gut infection in the desert locust: *in vivo* production of antimicrobial phenols associated with the bacterium *Pantoea agglomerans*." J Invertebr Pathol **66**(1): 72-75.

Dominguez-Bello, M. G., Costello, E. K., Contreras, M., Magris, M., Hidalgo, G., Fierer, N. and Knight, R. (2010). "Delivery mode shapes the acquisition and structure of the initial microbiota across multiple body habitats in newborns." Proc Natl Acad Sci U S A **107**(26): 11971-11975.

Driver, J. A. and Kuniyuki, A. (1984). "*In vitro* propagation of paradox wallnut rootstcok." HortScience **19**: 507-509.

Duan, K., Dammel, C., Stein, J., Rabin, H. and Surette, M. G. (2003). "Modulation of *Pseudomonas aeruginosa* gene expression by host microflora through interspecies communication." Mol Microbiol **50**(5): 1477-1491.

Egamberdieva, D., Kamilova, F., Validov, S., Gafurova, L., Kucharova, Z. and Lugtenberg, B. (2008). "High incidence of plant growth-stimulating bacteria associated with the rhizosphere of wheat grown on salinated soil in Uzbekistan." Environ Microbiol **10**(1): 1-9.

Egland, P. G., Palmer, R. J., Jr. and Kolenbrander, P. E. (2004). "Interspecies communication in *Streptococcus gordonii-Veillonella atypica* biofilms: signaling in flow conditions requires juxtaposition." Proc Natl Acad Sci U S A **101**(48): 16917-16922.

Elasri, M., Delorme, S., Lemanceau, P., Stewart, G., Laue, B., Glickmann, E., Oger, P. M. and Dessaux, Y. (2001). "Acyl-homoserine lactone production is more common among plant-associated *Pseudomonas* spp. than among soilborne *Pseudomonas* spp." Appl Environ Microbiol **67**(3): 1198-1209.

Elias, S. and Banin, E. (2012). "Multi-species biofilms: living with friendly neighbors." FEMS Microbiol Rev **36**(5): 990-1004

Elsas, J. D., Jansson, J. K. and Trevors, J. T. (2007). Modern Soil Microbiology, CRC Press/Taylor & Francis.

Elvira-Recuenco, M. and van Vuurde, J. W. (2000). "Natural incidence of endophytic bacteria in pea cultivars under field conditions." Can J Microbiol **46**(11): 1036-1041.

Ercolani, G. L. (1978). "*Pseudomonas savastanoi* and other bacteria colonizing the surface of olive leaves in the field." J Gen Microbiol **109**(2): 245-257.

Ercolani, G. L. (1991). "Distribution of epiphytic bacteria on olive leaves and the influence of leaf age and sampling time." Microb Ecol **21**(1): 35-48.

Evidente, A., Surico, G., Iacobellis, N. S. and Randazzo, G. (1985). "α-*N*-acetyl-indole-3-acetyl-ε-L-lysine: A metabolite of indole-3-acetic acid from *Pseudomonas syringae* pv. *savastanoi*." Phytochemistry **25**(1): 125-128.

Fazli, M., Almblad, H., Rybtke, M. L., Givskov, M., Eberl, L. and Tolker-Nielsen, T. (2014). "Regulation of biofilm formation in *Pseudomonas* and *Burkholderia* species." Environ Microbiol.

Ferluga, S. and Venturi, V. (2009). "OryR is a LuxR-family protein involved in interkingdom signaling between pathogenic *Xanthomonas oryzae* pv. *oryzae* and rice." J Bacteriol **191**(3): 890-897.

Figurski, D. H. and Helinski, D. R. (1979). "Replication of an origin-containing derivative of plasmid RK2 dependent on a plasmid function provided in trans." Proc Natl Acad Sci U S A **76**(4): 1648-1652.

Foster, K. R., Shaulsky, G., Strassmann, J. E., Queller, D. C. and Thompson, C. R. (2004). "Pleiotropy as a mechanism to stabilize cooperation." Nature **431**(7009): 693-696.

Galardini, M., Mengoni, A., Biondi, E. G., Semeraro, R., Florio, A., Bazzicalupo, M., Benedetti, A. and Mocali, S. (2014). "DuctApe: a suite for the analysis and correlation of genomic and OmniLog Phenotype Microarray data." Genomics **103**(1): 1-10.

Gans, J., Wolinsky, M. and Dunbar, J. (2005). "Computational improvements reveal great bacterial diversity and high metal toxicity in soil." Science **309**(5739): 1387-1390.

Gao, M., Teplitski, M., Robinson, J. B. and Bauer, W. D. (2003). "Production of substances by *Medicago truncatula* that affect bacterial quorum sensing." Mol Plant Microbe Interact **16**(9): 827-834.

Garbeva, P., Silby, M. W., Raaijmakers, J. M., Levy, S. B. and Boer, W. (2011). "Transcriptional and antagonistic responses of *Pseudomonas fluorescens* Pf0-1 to phylogenetically different bacterial competitors." ISME J **5**(6): 973-985.

Garbeva, P., van Veen, J. A. and van Elsas, J. D. (2004). "Microbial diversity in soil: selection microbial populations by plant and soil type and implications for disease suppressiveness." Annu Rev Phytopathol **42**: 243-270.

Gardan, L., Bollet, C., Abu Ghorrah, M., Grimont, F. and Grimont, P. A. D. (1992). "DNA Relatedness among the pathovar strains of *Pseudomonas syringae* subsp. *savastanoi* Janse (1982) and proposal of *Pseudomonas savastanoi* sp. nov." Int J Syst Bacteriol **42**(4): 606-612.

Gardan, L., Shafik, H., Belouin, S., Broch, R., Grimont, F. and Grimont, P. A. (1999). "DNA relatedness among the pathovars of *Pseudomonas syringae* and description of *Pseudomonas tremae* sp. nov. and *Pseudomonas cannabina* sp. nov. (ex Sutic and Dowson 1959)." Int J Syst Bacteriol **49 Pt 2**: 469-478.

Gilbert, J. A., Field, D., Huang, Y., Edwards, R., Li, W., Gilna, P. and Joint, I. (2008). "Detection of large numbers of novel sequences in the metatranscriptomes of complex marine microbial communities." PLoS One **3**(8): e3042.

Glass, N. L. and Kosuge, T. (1988). "Role of indoleacetic acid-lysine synthetase in regulation of indoleacetic acid pool size and virulence of *Pseudomonas syringae* subsp. *savastanoi*." J Bacteriol **170**(5): 2367-2373.

Griffin, A. S., West, S. A. and Buckling, A. (2004). "Cooperation and competition in pathogenic bacteria." Nature **430**(7003): 1024-1027.

Hall-Stoodley, L., Costerton, J. W. and Stoodley, P. (2004). "Bacterial biofilms: from the natural environment to infectious diseases." Nat Rev Microbiol **2**(2): 95-108.

Hanahan, D., Jessee, J. and Bloom, F. R. (1991). "Plasmid transformation of *Escherichia coli* and other bacteria." Methods Enzymol **204**: 63-113.

Hardoim, P. R., van Overbeek, L. S. and Elsas, J. D. (2008). "Properties of bacterial endophytes and their proposed role in plant growth." Trends Microbiol **16**(10): 463-471.

Harrison, F., Paul, J., Massey, R. C. and Buckling, A. (2008). "Interspecific competition and siderophore-mediated cooperation in *Pseudomonas aeruginosa*." ISME J **2**(1): 49-55.

Hayes, K. S., Bancroft, A. J., Goldrick, M., Portsmouth, C., Roberts, I. S. and Grencis, R. K. (2010). "Exploitation of the intestinal microflora by the parasitic nematode *Trichuris muris*." Science **328**(5984): 1391-1394.

Hoitink, H. and Boehm, M. (1999). "Biocontrol within the context of soil microbial communities: a substrate-dependent phenomenon." Annu Rev Phytopathol **37**: 427-446.

Hosni, T., Moretti, C., Devescovi, G., Suarez-Moreno, Z. R., Fatmi, M. B., Guarnaccia, C., Pongor, S., Onofri, A., Buonaurio, R. and Venturi, V. (2011). "Sharing of quorum-sensing signals and role of interspecies communities in a bacterial plant disease." ISME J **5**(12): 1857-1870.

Huang, W. E., Ferguson, A., Singer, A. C., Lawson, K., Thompson, I. P., Kalin, R. M., Larkin, M. J., Bailey, M. J. and Whiteley, A. S. (2009). "Resolving genetic functions within microbial populations: *in situ* analyses using rRNA and mRNA stable isotope probing coupled with single-cell raman-fluorescence *in situ* hybridization." Appl Environ Microbiol **75**(1): 234-241.

Huang, W. E., Griffiths, R. I., Thompson, I. P., Bailey, M. J. and Whiteley, A. S. (2004). "Raman microscopic analysis of single microbial cells." Anal Chem **76**(15): 4452-4458.

Huang, W. E., Li, M., Jarvis, R. M., Goodacre, R. and Banwart, S. A. (2010). "Shining light on the microbial world the application of Raman microspectroscopy." Adv Appl Microbiol **70**: 153-186.

Huber, B., Riedel, K., Hentzer, M., Heydorn, A., Gotschlich, A., Givskov, M., Molin, S. and Eberl, L. (2001). "The cep quorum-sensing system of Burkholderia cepacia H111 controls biofilm formation and swarming motility." Microbiology **147**(Pt 9): 2517-2528.

Iacobellis, N. S. (2001). Olive knot. In "Encyclopaedia of plant pathology". O. C. Malloy and T. D. Murray. John Wiley & Sons. **Vol. 2**.

Iacobellis, N. S., Sisto, A., Surico, G., Evidente, A. and DiMaio, E. (1994). "Pathogenicity of *Pseudomonas syringae* subsp. *savastanoi* mutants defective in phytohormone production." J Phytopath **140**(3): 238-248.

Idris, R., Trifonova, R., Puschenreiter, M., Wenzel, W. W. and Sessitsch, A. (2004). "Bacterial communities associated with flowering plants of the Ni hyperaccumulator *Thlaspi goesingense*." Appl Environ Microbiol **70**(5): 2667-2677.

Inacio, J., Pereira, P., de Carvalho, M., Fonseca, A., Amaral-Collaco, M. T. and Spencer-Martins, I. (2002). "Estimation and diversity of phylloplane

mycobiota on selected plants in a Mediterranean-type ecosystem in Portugal." Microb Ecol **44**(4): 344-353.

James, E. K., Gyaneshwar, P., Mathan, N., Barraquio, W. L., Reddy, P. M., Iannetta, P. P., Olivares, F. L. and Ladha, J. K. (2002). "Infection and colonization of rice seedlings by the plant growth-promoting bacterium *Herbaspirillum seropedicae* Z67." Mol Plant Microbe Interact **15**(9): 894-906.

Jiao, J. Y., Wang, H. X., Zeng, Y. and Shen, Y. M. (2006). "Enrichment for microbes living in association with plant tissues." J Appl Microbiol **100**(4): 830-837.

Johnston, P. R. and Crickmore, N. (2009). "Gut bacteria are not required for the insecticidal activity of *Bacillus thuringiensis* toward the tobacco hornworm, *Manduca sexta*." Appl Environ Microbiol **75**(15): 5094-5099.

Kadivar, H. and Stapleton, A. E. (2003). "Ultraviolet radiation alters maize phyllosphere bacterial diversity." Microb Ecol **45**(4): 353-361.

Kamei, I., Yoshida, T., Enami, D. and Meguro, S. (2012). "Coexisting *Curtobacterium* bacterium promotes growth of white-rot fungus *Stereum* sp." Curr Microbiol **64**(2): 173-178.

Kane, M., Case, L. K., Kopaskie, K., Kozlova, A., MacDearmid, C., Chervonsky, A. V. and Golovkina, T. V. (2011). "Successful transmission of a retrovirus depends on the commensal microbiota." Science **334**(6053): 245-249.

Karp, P. D., Paley, S. M., Krummenacker, M., Latendresse, M., Dale, J. M., Lee, T. J., Kaipa, P., Gilham, F., Spaulding, A., Popescu, L., Altman, T., Paulsen, I., Keseler, I. M. and Caspi, R. (2010). "Pathway Tools version 13.0: integrated software for pathway/genome informatics and systems biology." Brief Bioinform **11**(1): 40-79.

Kerr, B., Riley, M. A., Feldman, M. W. and Bohannan, B. J. (2002). "Local dispersal promotes biodiversity in a real-life game of rock-paper-scissors." Nature **418**(6894): 171-174.

Kim, H. J., Boedicker, J. Q., Choi, J. W. and Ismagilov, R. F. (2008). "Defined spatial structure stabilizes a synthetic multispecies bacterial community." Proc Natl Acad Sci U S A **105**(47): 18188-18193.

Koch, B., Jensen, L. E. and Nybroe, O. (2001). "A panel of Tn7-based vectors for insertion of the *gfp* marker gene or for delivery of cloned DNA into Gram-negative bacteria at a neutral chromosomal site." J Microbiol Methods **45**(3): 187-195.

Kovach, M. E., Elzer, P. H., Hill, D. S., Robertson, G. T., Farris, M. A., Roop, R. M., 2nd and Peterson, K. M. (1995). "Four new derivatives of the broad-host-range cloning vector pBBR1MCS, carrying different antibiotic-resistance cassettes." Gene **166**(1): 175-176.

Kreft, J. U. (2004). "Biofilms promote altruism." Microbiology **150**(Pt 8): 2751-2760.

Kurtz, S., Phillippy, A., Delcher, A. L., Smoot, M., Shumway, M., Antonescu, C. and Salzberg, S. L. (2004). "Versatile and open software for comparing large genomes." Genome Biol **5**(2): R12.

Kuss, S. K., Best, G. T., Etheredge, C. A., Pruijssers, A. J., Frierson, J. M., Hooper, L. V., Dermody, T. S. and Pfeiffer, J. K. (2011). "Intestinal microbiota promote enteric virus replication and systemic pathogenesis." Science **334**(6053): 249-252.

Kuypers, M. M. and Jorgensen, B. B. (2007). "The future of single-cell environmental microbiology." Environ Microbiol **9**(1): 6-7.

Lacava, P. T., Araujo, W. L. and Azevedo, J. L. (2007). "Evaluation of endophytic colonization of *Citrus sinensis* and *Catharanthus roseus* seedlings by endophytic bacteria." J Microbiol **45**(1): 11-14.

Lambais, M. R., Crowley, D. E., Cury, J. C., Bull, R. C. and Rodrigues, R. R. (2006). "Bacterial diversity in tree canopies of the Atlantic forest." Science **312**(5782): 1917.

Lambertsen, L., Sternberg, C. and Molin, S. (2004). "Mini-Tn7 transposons for site-specific tagging of bacteria with fluorescent proteins." Environ Microbiol **6**(7): 726-732.

Lee, Y. K. and Mazmanian, S. K. (2010). "Has the microbiota played a critical role in the evolution of the adaptive immune system?" Science **330**(6012): 1768-1773.

Lindow, S. E. and Brandl, M. T. (2003). "Microbiology of the phyllosphere." Appl Environ Microbiol **69**(4): 1875-1883.

Lindow, S. E., Hecht-Poinar, E. I. and Elliott, V. J. (2002). Phyllosphere Microbiology, APS Press/American Phytopathological Society.

Loake, G. and Grant, M. (2007). "Salicylic acid in plant defence--the players and protagonists." Curr Opin Plant Biol **10**(5): 466-472.

Lundberg, D. S., Lebeis, S. L., Paredes, S. H., Yourstone, S., Gehring, J., Malfatti, S., Tremblay, J., Engelbrektson, A., Kunin, V., del Rio, T. G., Edgar, R. C., Eickhorst, T., Ley, R. E., Hugenholtz, P., Tringe, S. G. and Dangl, J. L. (2012). "Defining the core *Arabidopsis thaliana* root microbiome." Nature **488**(7409): 86-90.

Luo, Z. Q., Su, S. and Farrand, S. K. (2003). "*In situ* activation of the quorum-sensing transcription factor TraR by cognate and noncognate acyl-homoserine lactone ligands: kinetics and consequences." J Bacteriol **185**(19): 5665-5672.

Lysenko, O. (1985). "Non-sporeforming bacteria pathogenic to insects: incidence and mechanisms." Annu Rev Microbiol **39**: 673-695.

Maldonado-Gonzalez, M. M., Prieto, P., Ramos, C. and Mercado-Blanco, J. (2013). "From the root to the stem: interaction between the biocontrol root endophyte *Pseudomonas fluorescens* PICF7 and the pathogen *Pseudomonas savastanoi* NCPPB 3335 in olive knots." Microb Biotechnol **6**(3): 275-287.

Manickam, N., Bajaj, A., Saini, H. S. and Shanker, R. (2012). "Surfactant mediated enhanced biodegradation of hexachlorocyclohexane (HCH) isomers by *Sphingomonas* sp. NM05." Biodegradation **23**(5): 673-682.

Mansfield, J., Genin, S., Magori, S., Citovsky, V., Sriariyanum, M., Ronald, P., Dow, M., Verdier, V., Beer, S. V., Machado, M. A., Toth, I., Salmond, G. and Foster, G. D. (2012). "Top 10 plant pathogenic bacteria in molecular plant pathology." Mol Plant Pathol **13**(6): 614-629.

Marchi, G., Mori, B., Pollacci, P., Mencuccini, M. and Surico, G. (2009). "Systemic spread of *Pseudomonas savastanoi* pv. *savastanoi* in olive explants." Plant Pathology **58**(1): 152-158.

Marchi, G., Sisto, A., Cimmino, A., Andolfi, A., Cipriani, M. G., Evidente, A. and Surico, G. (2006). "Interaction between *Pseudomonas savastanoi* pv. *savastanoi* and *Pantoea agglomerans* in olive knots." Plant Pathology **55**(5): 614-624.

Mason, K. L., Stepien, T. A., Blum, J. E., Holt, J. F., Labbe, N. H., Rush, J. S., Raffa, K. F. and Handelsman, J. (2011). "From commensal to pathogen: translocation of *Enterococcus faecalis* from the midgut to the hemocoel of *Manduca sexta*." MBio **2**(3): e00065-00011.

Matas, I. M., Lambertsen, L., Rodriguez-Moreno, L. and Ramos, C. (2012). "Identification of novel virulence genes and metabolic pathways required

for full fitness of *Pseudomonas savastanoi* pv. *savastanoi* in olive (*Olea europaea*) knots." New Phytol **196**(4): 1182-1196.

Matas, I. M., Perez-Martinez, I., Quesada, J. M., Rodriguez-Herva, J. J., Penyalver, R. and Ramos, C. (2009). "*Pseudomonas savastanoi pv. savastanoi* contains two *iaaL* paralogs, one of which exhibits a variable number of a trinucleotide (TAC) tandem repeat." Appl Environ Microbiol **75**(4): 1030-1035.

McCully, M. E. (2001). "Niches for bacterial endophytes in crop plants: a plant biologist's view." Funct Plant Biol **28**(9): 983-990.

Mendes, R., Kruijt, M., de Bruijn, I., Dekkers, E., van der Voort, M., Schneider, J. H., Piceno, Y. M., DeSantis, T. Z., Andersen, G. L., Bakker, P. A. and Raaijmakers, J. M. (2011). "Deciphering the rhizosphere microbiome for disease-suppressive bacteria." Science **332**(6033): 1097-1100.

Meyer, F., Paarmann, D., D'Souza, M., Olson, R., Glass, E. M., Kubal, M., Paczian, T., Rodriguez, A., Stevens, R., Wilke, A., Wilkening, J. and Edwards, R. A. (2008). "The metagenomics RAST server - a public resource for the automatic phylogenetic and functional analysis of metagenomes." BMC Bioinformatics **9**: 386.

Miche, L. and Balandreau, J. (2001). "Effects of rice seed surface sterilization with hypochlorite on inoculated *Burkholderia vietnamiensis*." Appl Environ Microbiol **67**(7): 3046-3052.

Miller, M. B. and Bassler, B. L. (2001). "Quorum sensing in bacteria." Annu Rev Microbiol **55**: 165-199.

Mitri, S., Xavier, J. B. and Foster, K. R. (2011). "Social evolution in multispecies biofilms." Proc Natl Acad Sci U S A **108 Suppl 2**: 10839-10846.

Monds, R. D. and O'Toole, G. A. (2009). "The developmental model of microbial biofilms: ten years of a paradigm up for review." Trends Microbiol **17**(2): 73-87.

Monier, J. M. and Lindow, S. E. (2005). "Spatial organization of dual-species bacterial aggregates on leaf surfaces." Appl Environ Microbiol **71**(9): 5484-5493.

Moretti, C., Hosni, T., Vandemeulebroecke, K., Brady, C., De Vos, P., Buonaurio, R. and Cleenwerck, I. (2011). "*Erwinia oleae* sp. nov., isolated from olive knots caused by *Pseudomonas savastanoi* pv. *savastanoi*." Int J Syst Evol Microbiol **61**(Pt 11): 2745-2752.

Nicholson, J. K., Holmes, E., Kinross, J., Burcelin, R., Gibson, G., Jia, W. and Pettersson, S. (2012). "Host-gut microbiota metabolic interactions." Science **336**(6086): 1262-1267.

Nilsson, P., Olofsson, A., Fagerlind, M., Fagerstrom, T., Rice, S., Kjelleberg, S. and Steinberg, P. (2001). "Kinetics of the AHL regulatory system in a model biofilm system: how many bacteria constitute a "quorum"?" J Mol Biol **309**(3): 631-640.

O'Toole, G. A. and Kolter, R. (1998). "Flagellar and twitching motility are necessary for *Pseudomonas aeruginosa* biofilm development." Mol Microbiol **30**(2): 295-304.

O'Toole, G. A., Pratt, L. A., Watnick, P. I., Newman, D. K., Weaver, V. B. and Kolter, R. (1999). "Genetic approaches to study of biofilms." Methods Enzymol **310**: 91-109.

Oehler, D. Z., Robert, F., Walter, M. R., Sugitani, K., Meibom, A., Mostefaoui, S. and Gibson, E. K. (2010). "Diversity in the Archean biosphere: new insights from NanoSIMS." Astrobiology **10**(4): 413-424.

Ouzari, H., Khsairi, A., Raddadi, N., Jaoua, L., Hassen, A., Zarrouk, M., Daffonchio, D. and Boudabous, A. (2008). "Diversity of auxin-producing bacteria associated to *Pseudomonas savastanoi* -induced olive knots." J Basic Microbiol **48**(5): 370-377.

Owen, R. W., Giacosa, A., Hull, W. E., Haubner, R., Wurtele, G., Spiegelhalder, B. and Bartsch, H. (2000). "Olive-oil consumption and health: the possible role of antioxidants." Lancet Oncol **1**: 107-112.

Panagopoulos, C. G. (1993). "Olive knot disease in Greece." EPPO Bulletin **23**(3): 417-422.

Parkinson, N., Bryant, R., Bew, J. and Elphinstone, J. (2011). "Rapid phylogenetic identification of members of the *Pseudomonas syringae* species complex using the *rpoD* locus." Plant Pathol **60**(2): 338-344.

Passos da Silva, D., Devescovi, G., Paszkiewicz, K., Moretti, C., Buonaurio, R., Studholme, D. J. and Venturi, V. (2013). "Draft genome sequence of *Erwinia toletana*, a bacterium associated with olive knots caused by *Pseudomonas savastanoi* pv. *savastanoi*." Genome Announc **1**(3).

Peiffer, J. A., Spor, A., Koren, O., Jin, Z., Tringe, S. G., Dangl, J. L., Buckler, E. S. and Ley, R. E. (2013). "Diversity and heritability of the maize rhizosphere microbiome under field conditions." Proc Natl Acad Sci U S A **110**(16): 6548-6553.

Penyalver, R., Garcia, A., Ferrer, A., Bertolini, E. and Lopez, M. M. (2000). "Detection of *Pseudomonas savastanoi* pv. *savastanoi* in olive plants by enrichment and PCR." Appl Environ Microbiol **66**(6): 2673-2677.

Penyalver, R., Garcia, A., Ferrer, A., Bertolini, E., Quesada, J. M., Salcedo, C. I., Piquer, J., Perez-Panades, J., Carbonell, E. A., Del Rio, C., Caballero, J. M. and Lopez, M. M. (2006). "Factors affecting *Pseudomonas savastanoi* pv.

savastanoi plant inoculations and their use for evaluation of olive cultivar susceptibility." Phytopathology **96**(3): 313-319.

Perez-Martinez, I., Rodriguez-Moreno, L., Lambertsen, L., Matas, I. M., Murillo, J., Tegli, S., Jimenez, A. J. and Ramos, C. (2010). "Fate of a *Pseudomonas savastanoi* pv. *savastanoi* type III secretion system mutant in olive plants (*Olea europaea* L.)." Appl Environ Microbiol **76**(11): 3611-3619.

Perez-Martinez, I., Zhao, Y., Murillo, J., Sundin, G. W. and Ramos, C. (2008). "Global genomic analysis of *Pseudomonas savastanoi* pv. *savastanoi* plasmids." J Bacteriol **190**(2): 625-635.

Powell, G. K. and Morris, R. O. (1986). "Nucleotide sequence and expression of a *Pseudomonas savastanoi* cytokinin biosynthetic gene: homology with *Agrobacterium tumefaciens tmr* and *tzs* loci." Nucleic Acids Res **14**(6): 2555-2565.

Pratt, L. A. and Kolter, R. (1998). "Genetic analysis of *Escherichia coli* biofilm formation: roles of flagella, motility, chemotaxis and type I pili." Mol Microbiol **30**(2): 285-293.

Quesada, J. M., Garcia, A., Bertolini, E., Lopez, M. M. and Penyalver, R. (2007). "Recovery of *Pseudomonas savastanoi* pv. *savastanoi* from symptomless shoots of naturally infected olive trees." Int Microbiol **10**(2): 77-84.

Quesada, J. M., Penyalver, R., Pérez-Panadés, J., Salcedo, C. I., Carbonell, E. A. and López, M. M. (2010). "Dissemination of *Pseudomonas savastanoi* pv. *savastanoi* populations and subsequent appearance of olive knot disease." Plant Pathology **59**(2): 262-269.

Raaijmakers, J. M., Paulitz, T. C., Steinberg, C., Alabouvette, C. and Moënne-Loccoz, Y. (2009). "The rhizosphere: a playground and battlefield for soilborne pathogens and beneficial microorganisms." Plant & Soil **321**(1/2): 341-361.

Ramos, C., Matas, I. M., Bardaji, L., Aragon, I. M. and Murillo, J. (2012). "*Pseudomonas savastanoi* pv. *savastanoi*: some like it knot." Mol Plant Pathol **13**(9): 998-1009.

Ramsey, M. M., Rumbaugh, K. P. and Whiteley, M. (2011). "Metabolite cross-feeding enhances virulence in a model polymicrobial infection." PLoS Pathog **7**(3): e1002012.

Raymond, B., Johnston, P. R., Nielsen-LeRoux, C., Lereclus, D. and Crickmore, N. (2010). "*Bacillus thuringiensis*: an impotent pathogen?" Trends Microbiol **18**(5): 189-194.

Raymond, B., Johnston, P. R., Wright, D. J., Ellis, R. J., Crickmore, N. and Bonsall, M. B. (2009). "A mid-gut microbiota is not required for the pathogenicity of *Bacillus thuringiensis* to diamondback moth larvae." Environ Microbiol **11**(10): 2556-2563.

Reeve, W. G., Tiwari, R. P., Worsley, P. S., Dilworth, M. J., Glenn, A. R. and Howieson, J. G. (1999). "Constructs for insertional mutagenesis, transcriptional signal localization and gene regulation studies in root nodule and other bacteria." Microbiology **145 (Pt 6)**: 1307-1316.

Ren, C., Webster, P., Finkel, S. E. and Tower, J. (2007). "Increased internal and external bacterial load during *Drosophila* aging without life-span trade-off." Cell Metab **6**(2): 144-152.

Rodriguez-Moreno, L., Barcelo-Munoz, A. and Ramos, C. (2008). "*In vitro* analysis of the interaction of *Pseudomonas savastanoi* pv. *savastanoi* and *nerii* with micropropagated olive plants." Phytopathology **98**(7): 815-822.

Rodriguez-Moreno, L., Jimenez, A. J. and Ramos, C. (2009). "Endopathogenic lifestyle of *Pseudomonas savastanoi* pv. *savastanoi* in olive knots." Microb Biotechnol **2**(4): 476-488.

Rodriguez-Palenzuela, P., Matas, I. M., Murillo, J., Lopez-Solanilla, E., Bardaji, L., Perez-Martinez, I., Rodriguez-Moskera, M. E., Penyalver, R., Lopez, M. M., Quesada, J. M., Biehl, B. S., Perna, N. T., Glasner, J. D., Cabot, E. L., Neeno-Eckwall, E. and Ramos, C. (2010). "Annotation and overview of the *Pseudomonas savastanoi* pv. *savastanoi* NCPPB 3335 draft genome reveals the virulence gene complement of a tumour-inducing pathogen of woody hosts." Environ Microbiol **12**(6): 1604-1620.

Roesch, L. F., Fulthorpe, R. R., Riva, A., Casella, G., Hadwin, A. K., Kent, A. D., Daroub, S. H., Camargo, F. A., Farmerie, W. G. and Triplett, E. W. (2007). "Pyrosequencing enumerates and contrasts soil microbial diversity." ISME J **1**(4): 283-290.

Rojas, A. M., de Los Rios, J. E., Fischer-Le Saux, M., Jimenez, P., Reche, P., Bonneau, S., Sutra, L., Mathieu-Daude, F. and McClelland, M. (2004). "*Erwinia toletana* sp. nov., associated with *Pseudomonas savastanoi*-induced tree knots." Int J Syst Evol Microbiol **54**(Pt 6): 2217-2222.

Rosenblueth, M. and Martinez-Romero, E. (2006). "Bacterial endophytes and their interactions with hosts." Mol Plant Microbe Interact **19**(8): 827-837.

Roussos, P. A., Pontikis, C. A. and Tsantili, E. (2002). "Root promoting compounds detected in olive knot extract in high quantities as a response to infection by the bacterium *Pseudomonas savastanoi* pv. *savastanoi*." Plant Science **163**(3): 533-541.

Ryu, J. H., Kim, S. H., Lee, H. Y., Bai, J. Y., Nam, Y. D., Bae, J. W., Lee, D. G., Shin, S. C., Ha, E. M. and Lee, W. J. (2008). "Innate immune homeostasis by the homeobox gene caudal and commensal-gut mutualism in *Drosophila*." Science **319**(5864): 777-782.

Saad, A. T. and Hanna, L. (2002). "Two new hosts of *Pseudomonas savastanoi* and variability in strains isolated from different hosts." Phytopathology **92**: S71.

Sambrook, J. F. and Russell, D. W. (2001). Molecular cloning : a laboratory manual / Joseph Sambrook, David W. Russell. Cold Spring Harbor, N.Y, Cold Spring Harbor Laboratory.

Sarkar, S. F. and Guttman, D. S. (2004). "Evolution of the core genome of *Pseudomonas syringae*, a highly clonal, endemic plant pathogen." Appl Environ Microbiol **70**(4): 1999-2012.

Savastano, L. (1886). "Les maladies de l'olivier, et la tuberculose en particulier." Comptes Rendu des Séances de l'Académie d'Agriculture de France CIII: 103-114.

Sboner, A., Mu, X. J., Greenbaum, D., Auerbach, R. K. and Gerstein, M. B. (2011). "The real cost of sequencing: higher than you think!" Genome Biol **12**(8): 125.

Schloss, P. D., Gevers, D. and Westcott, S. L. (2011). "Reducing the effects of PCR amplification and sequencing artifacts on 16S rRNA-based studies." PLoS One **6**(12): e27310.

Schneider, C. A., Rasband, W. S. and Eliceiri, K. W. (2012). "NIH Image to ImageJ: 25 years of image analysis." Nat Methods **9**(7): 671-675.

Schroth, M. N., Osgood, J. W. and Miller, T. D. (1973). "Quantitative assessment of the effect of the olive knot disease on olive yield and quality." Phytopathology **63**: 1064-1065.

Scortichini, M., Rossi, M. P. and Salerno, M. (2004). "Relationship of genetic structure of *Pseudomonas savastanoi* pv. *savastanoi* populations from Italian olive trees and patterns of host genetic diversity." Plant Pathology **53**(4): 491-497.

Sessitsch, A., Hardoim, P., Doring, J., Weilharter, A., Krause, A., Woyke, T., Mitter, B., Hauberg-Lotte, L., Friedrich, F., Rahalkar, M., Hurek, T., Sarkar, A., Bodrossy, L., van Overbeek, L., Brar, D., van Elsas, J. D. and Reinhold-

Hurek, B. (2012). "Functional characteristics of an endophyte community colonizing rice roots as revealed by metagenomic analysis." Mol Plant Microbe Interact **25**(1): 28-36.

Sharon, G., Segal, D., Ringo, J. M., Hefetz, A., Zilber-Rosenberg, I. and Rosenberg, E. (2010). "Commensal bacteria play a role in mating preference of *Drosophila melanogaster*." Proc Natl Acad Sci U S A **107**(46): 20051-20056.

Shaw, P. D., Ping, G., Daly, S. L., Cha, C., Cronan, J. E., Jr., Rinehart, K. L. and Farrand, S. K. (1997). "Detecting and characterizing *N*-acyl-homoserine lactone signal molecules by thin-layer chromatography." Proc Natl Acad Sci U S A **94**(12): 6036-6041.

Sibley, C. D., Duan, K., Fischer, C., Parkins, M. D., Storey, D. G., Rabin, H. R. and Surette, M. G. (2008a). "Discerning the complexity of community interactions using a *Drosophila* model of polymicrobial infections." PLoS Pathog **4**(10): e1000184.

Sibley, C. D., Parkins, M. D., Rabin, H. R., Duan, K., Norgaard, J. C. and Surette, M. G. (2008b). "A polymicrobial perspective of pulmonary infections exposes an enigmatic pathogen in cystic fibrosis patients." Proc Natl Acad Sci U S A **105**(39): 15070-15075.

Sisto, A., Cipriani, M. G. and Morea, M. (2004). "Knot formation caused by *Pseudomonas syringae* subsp. *savastanoi* on olive plants Is *hrp*-dependent." Phytopathology **94**(5): 484-489.

Smith, E. R. and Rorer, J. B. (1904). ""The olive tubercule"." Science **19**(480): 416-417.

Sogin, M. L., Morrison, H. G., Huber, J. A., Mark Welch, D., Huse, S. M., Neal, P. R., Arrieta, J. M. and Herndl, G. J. (2006). "Microbial diversity in the deep sea and the underexplored "rare biosphere"." Proc Natl Acad Sci U S A **103**(32): 12115-12120.

Spaink, H. P., Okker, R. J., Wijffelman, C. A., Pees, E. and Lugtenberg, B. J. (1987). "Promoters in the nodulation region of the *Rhizobium leguminosarum* Sym plasmid pRL1JI." Plant Mol Biol **9**(1): 27-39.

Starkey, M., Hickman, J. H., Ma, L., Zhang, N., De Long, S., Hinz, A., Palacios, S., Manoil, C., Kirisits, M. J., Starner, T. D., Wozniak, D. J., Harwood, C. S. and Parsek, M. R. (2009). "*Pseudomonas aeruginosa* rugose small-colony variants have adaptations that likely promote persistence in the cystic fibrosis lung." J Bacteriol **191**(11): 3492-3503.

Steinhaus, E. A. (1960). "The importance of environmental factors in the insect-microbe ecosystem." Bacteriol Rev **24**(4): 365-373.

Steinhaus, E. A. (1963). Insect pathology: an advanced treatise, Academic Press.

Stoodley, P., Sauer, K., Davies, D. G. and Costerton, J. W. (2002). "Biofilms as complex differentiated communities." Annu Rev Microbiol **56**: 187-209.

Storelli, G., Defaye, A., Erkosar, B., Hols, P., Royet, J. and Leulier, F. (2011). "*Lactobacillus plantarum* promotes *Drosophila* systemic growth by modulating hormonal signals through TOR-dependent nutrient sensing." Cell Metab **14**(3): 403-414.

Studholme, D. J., Ibanez, S. G., MacLean, D., Dangl, J. L., Chang, J. H. and Rathjen, J. P. (2009). "A draft genome sequence and functional screen reveals the repertoire of type III secreted proteins of *Pseudomonas syringae* pathovar *tabaci* 11528." BMC Genomics **10**: 395.

Surico, G. (1993). "Scanning electron microscopy of olive and leaves colonized by *Pseudomonas syringae* subsp. *savastanoi*." J Phytopathol **138**(1): 31-40.

Surico, G. and Iacobellis, N. S. (1992). Phytohormones and olive knot disease. Molecular signals in plant-microbe communications. D. P. S. Verma, CRC Press**:** 209 - 227.

Surico, G., Iacobellis, N. S. and Sisto, A. (1985). "Studies on the role of indole-3-acetic acid and cytokinins in the formation of knots on olive and oleander plants by *Pseudomonas syringae* pv. *savastanoi*." Physiol Plant Pathol **26**(3): 309-320.

Tanada, Y. and Kaya, H. K. (1993). Insect Pathology, Academic Press.

Teplitski, M., Chen, H., Rajamani, S., Gao, M., Merighi, M., Sayre, R. T., Robinson, J. B., Rolfe, B. G. and Bauer, W. D. (2004). "*Chlamydomonas reinhardtii* secretes compounds that mimic bacterial signals and interfere with quorum sensing regulation in bacteria." Plant Physiol **134**(1): 137-146.

Teplitski, M., Robinson, J. B. and Bauer, W. D. (2000). "Plants secrete substances that mimic bacterial *N*-acyl homoserine lactone signal activities and affect population density-dependent behaviors in associated bacteria." Mol Plant Microbe Interact **13**(6): 637-648.

Teviotdale, B. L. and Krueger, W. H. (2004). "Effects of timing of copper sprays, defoliation, rainfall, and inoculum concentration on incidence of olive knot disease." Plant Disease **88**(2): 131-135.

Thomas, T., Gilbert, J. and Meyer, F. (2012). "Metagenomics - a guide from sampling to data analysis." Microb Inform Exp **2**(1): 3.

Tlaskalova-Hogenova, H., Stepankova, R., Hudcovic, T., Tuckova, L., Cukrowska, B., Lodinova-Zadnikova, R., Kozakova, H., Rossmann, P., Bartova, J., Sokol, D., Funda, D. P., Borovska, D., Rehakova, Z., Sinkora, J., Hofman, J., Drastich, P. and Kokesova, A. (2004). "Commensal bacteria (normal microflora), mucosal immunity and chronic inflammatory and autoimmune diseases." Immunol Lett **93**(2-3): 97-108.

Torsvik, V., Ovreas, L. and Thingstad, T. F. (2002). "Prokaryotic diversity--magnitude, dynamics, and controlling factors." Science **296**(5570): 1064-1066.

Turnbaugh, P. J., Ley, R. E., Hamady, M., Fraser-Liggett, C. M., Knight, R. and Gordon, J. I. (2007). "The human microbiome project." Nature **449**(7164): 804-810.

Tusnady, G. E. and Simon, I. (2001). "The HMMTOP transmembrane topology prediction server." Bioinformatics **17**(9): 849-850.

Valinsky, L., Manulis, S., Nizan, R., Ezra, D. and Barash, I. (1998). "A pathogenicity gene isolated from the pPATH plasmid of *Erwinia herbicola* pv. *gypsophilae* determines host specificity." Mol Plant Microbe Interact **11**(8): 753-762.

Valm, A. M., Mark Welch, J. L., Rieken, C. W., Hasegawa, Y., Sogin, M. L., Oldenbourg, R., Dewhirst, F. E. and Borisy, G. G. (2011). "Systems-level analysis of microbial community organization through combinatorial labeling and spectral imaging." Proc Natl Acad Sci U S A **108**(10): 4152-4157.

Varvaro, L. and Surico, G. (1978). "Comportamento di diverse cultivars do olivo (*Olea europea* L.) alla inoculazione articiale con *Pseudomonas savastanoi* (E.F. Smith) Stevens." Phytopathology Mediterranea **17**: 174-178.

Venturi, V. and da Silva, D. P. (2012). "Incoming pathogens team up with harmless 'resident' bacteria." Trends Microbiol **20**(4): 160-164.

Wagner, M., Amann, R., Lemmer, H. and Schleifer, K. H. (1993). "Probing activated sludge with oligonucleotides specific for proteobacteria: inadequacy of culture-dependent methods for describing microbial community structure." Appl Environ Microbiol **59**(5): 1520-1525.

Weller, D. M., Raaijmakers, J. M., Gardener, B. B. and Thomashow, L. S. (2002). "Microbial populations responsible for specific soil suppressiveness to plant pathogens." Annu Rev Phytopathol **40**: 309-348.

Wilmes, P. and Bond, P. L. (2006). "Metaproteomics: studying functional gene expression in microbial ecosystems." Trends Microbiol **14**(2): 92-97.

Wong, C. N., Ng, P. and Douglas, A. E. (2011). "Low-diversity bacterial community in the gut of the fruitfly *Drosophila melanogaster*." Environ Microbiol **13**(7): 1889-1900.

Xavier, J. B., Kim, W. and Foster, K. R. (2011). "A molecular mechanism that stabilizes cooperative secretions in *Pseudomonas aeruginosa*." Mol Microbiol **79**(1): 166-179.

Xie, C., Mace, J., Dinno, M. A., Li, Y. Q., Tang, W., Newton, R. J. and Gemperline, P. J. (2005). "Identification of single bacterial cells in aqueous solution using confocal laser tweezers Raman spectroscopy." Anal Chem **77**(14): 4390-4397.

Yang, C. H., Crowley, D. E., Borneman, J. and Keen, N. T. (2001). "Microbial phyllosphere populations are more complex than previously realized." Proc Natl Acad Sci U S A **98**(7): 3889-3894.

Yooseph, S., Sutton, G., Rusch, D. B., Halpern, A. L., Williamson, S. J., Remington, K., Eisen, J. A., Heidelberg, K. B., Manning, G., Li, W., Jaroszewski, L., Cieplak, P., Miller, C. S., Li, H., Mashiyama, S. T., Joachimiak, M. P., van Belle, C., Chandonia, J. M., Soergel, D. A., Zhai, Y., Natarajan, K., Lee, S., Raphael, B. J., Bafna, V., Friedman, R., Brenner, S. E., Godzik, A., Eisenberg, D., Dixon, J. E., Taylor, S. S., Strausberg, R. L., Frazier, M. and Venter, J. C. (2007). "The Sorcerer II Global Ocean Sampling expedition: expanding the universe of protein families." PLoS Biol **5**(3): e16.

Young, J. (2004). "Olive knot and its pathogens." Australas Plant Pathol **33**(1): 33-39.

Young, J. M. (2010). "Taxonomy of *Pseudomonas syringae*." J Plant Pathol **92**(4 sup): S5-S14.

Zerbino, D. R. and Birney, E. (2008). "Velvet: algorithms for *de novo* short read assembly using de Bruijn graphs." Genome Res **18**(5): 821-829.

Zinniel, D. K., Lambrecht, P., Harris, N. B., Feng, Z., Kuczmarski, D., Higley, P., Ishimaru, C. A., Arunakumari, A., Barletta, R. G. and Vidaver, A. K. (2002). "Isolation and characterization of endophytic colonizing bacteria from agronomic crops and prairie plants." Appl Environ Microbiol **68**(5): 2198-2208.

7 APPENDIX

7.1 Media and solutions

LB-Luria Broth (Sambrook and Russell, 2001) **(g/L)**

Tryptone	10
Yeast Extract	5
NaCl	10
Agar	15
pH	6.7

KING's B (King *et al.*, 1954) **(g/L)**

Proteose peptone No. 3	20
$MgSO_4$	1.5
Glycerol	10
KH_2PO_4	1.2
Agar	15
pH	7

M9C (Sambrook and Russell, 2001) **(g/L)**

Na_2HPO_4	6
KH_2PO_4	3
NaCl	0.5
NH_4Cl	1
Casaminoacids	2

Autoclaved and added:

$MgSO_4$ 1 M	2 mL
$CaCl_2$ 1M	0.1 mL

Carbon source at desired concentration

Antibiotic usage

Antibiotic	Solvent	Final concentration (µg/mL)		
		PSV	ET	*E. coli*
Ampicilin	Water	100	100	100
Kanamycin	Water	100	100	100
Gentamycin	Water	40	40	10
Chloramphenicol	Ethanol	200	200	100
Tetracycline	Ethanol 50%	40	40	15
Nitrofuratoin	DMF	50	50	

Southern Solutions

Depurination solution

HCl 11 N	11 mL
Water	898 mL

Denaturation buffer (g/L)

NaCl	87.66
NaOH	20

Saline solution citrate (SSC 20 X) (g/L)

Tri-sodium citrate	88.23
NaCl	175.32

Denhart's solution 100 X (g/L)

Bovine Serum Albumin	2
Ficoll 400	2
Polyvinyl pyrrolidone	2

Hybridization solution

20x SSC	100 mL
100x Denhardt's	20 mL
SDS 10%	20 mL
H_2O	360 mL

7.2 Biolog inoculation procedure

Bacterial growth and inoculum

ET and PSV were plated in solid King's B medium and incubated at room temperature for 48 hours. Cells were removed from the plate using a sterile swab and transferred into a sterile capped tube containing 20 mL of 1x IF-0a (Biolog) plus M9 medium as additive solution. Cell suspension was stirred with the swab (avoiding vortexing) until the obtainment of a uniform suspension; the turbidity was adjusted in order to achieve 81% T (transmittance).

Preparation of PM additive solutions

For the inoculum of PM plates it is necessary to prepare an inoculation fluid that is different for different plates. For example PM 1 and 2 contain C sources, therefore the PM solution has to be C free. The same thing for PM 3, 6 , 7, 8 (N sources), PM 5 (nutrient stimulation), PM 4 (P and S sources), PM 9, 10 (osmolites and pH) and PM 11 to 20 (chemicals and toxic sources).The IF-0a, IF-10b and Dye mix A solutions are commercially available whereas the PM additive has to be customized by preparing a minimum medium suitable for the bacteria. In this case, M9 minimal medium was used, modified to avoid the presence of C for plates 1, 2, 4, 5, 9-20, to avoid the presence of N for plates 3, 6, 7, 8 and to avoid also the presence of P and S in plate number 4. In general it is necessary to prepare several solutions, as follows:

IF solution (IF-0a or IF-10b) + Dye mix (A, D, G, or H) + PM additive + Cell suspension. Usually IF-0a is used for plates PM1-10 and IF-10b for plates PM 11-20. In this work Dye mix A was selected as dye solution as it worked well with gram negative strains (Biolog, personal communication) and previously used for

Pseudomonas spp. (Starkey *et al.* 2009). Moreover some preliminary tube tests confirmed its suitability for both strains.

Table 7-1 preparation of solutions for PM inoculation.

Reagents for PSV and ET	PM1,2 C source	PM3,6, 7,8 N source	PM4 P,S source	PM5 nutrients		PM9-10 osmolites	PM10-20
IF-0a (1.2X) (mL)	19.528	38.816	6.065	3.648	9.704	19.408	-
IF-10b (1.2X) (mL)	-	-	-	-	-	-	97.04
M9 salts (10X) C-(mL)	2.4	-	-	0.45	1.2	2.4	12
M9 salts (10X) N-(mL)	-	4.8	-	-	-	-	-
M9 salts (10X) P-(mL)	-	-	0.75	-	-	-	-
$CaCl_2$ 100 mM(µL)	24	48	7.5	4.5	12	24	120
$MgSO_4$ $7H_2O$ 1 M (µL)	48	96	15	-	24	48	240
Succinate (20%) (µL)	-	240	37.5	22.5	60	120	1200
Dye mix A (100X) (µL)	240	480	75	45	120	240	1200
Cell suspension (81% T) (mL)	1.76	3.52	0.55	0.33	0.88	1.76	8.8
Total Volume (mL)	24	48	7,5	4,5	12	24	120

PM data analysis.

After inoculation, all 60 PM microtiter plates were incubated at 30°C in an OmniLog reader, and changes of color in the wells were monitored automatically every 15 min. Readings were recorded during 96 h, and data were analyzed using DuctApe Software version 0.16.2 (Galardini *et al.* 2014) using the default settings. The "dphenome" module of the software has been used to assess the metabolic activity of the three tests, and to obtain the "Ring Graphs" showed in result session. Metabolic activity from all three tests has been analyzed with the DuctApe software.

7.3 ß-galactosidase activity measurement.

1. Pellet 1 mL of overnight grown culture, and resuspend in the same volume of pre-chilled Z buffer.
2. Resuspend 100 µL of cells in 900 µL of Z buffer and determine the OD600.
3. Permeabilize 100 µL of cells by adding 20 µL of SDS 0.05%, 20 µL of chloroform and 500 µL of Z buffer. Vortex vigorously for 20 seconds. Incubate at 30°C for 20 min.
4. Add 100 µL of 0.4% ONPG (Ortho-nitrophenyl-β-D-galactopyranoside), and allow the reaction to take place, note the time (*t*).
5. Stop the reaction after sufficient yellow color has developed by adding 250 µL 1 M Na2CO3.
6. Spin each sample for 10 min. at maximum speed to remove debris and chloroform and record the optical density of the supernatant at 420 nm.

Calculate the Miller units of activity:

Miller Units= $(OD_{420} \times 1000)/ (OD_{600} \times t)$

Where *t* is the time in min of ONPG reaction

Z Buffer:

Na2HPO4	0.06 M
NaH2PO4	0.04 M
KCl	0.01 M
MgSO4	0.001 M
ß-mercaptoethanol	0.05 M

7.4 Preparation of *E. coli* competent cells

Based on methodology from Hanahan (Hanahan *et al.* 1991).

1. Take the frozen stock of cell type and streak out on LB medium plate.
2. Incubate overnight at 37°C.
3. Pick a colony off of the fresh streak plate and inoculate 10 mL of LB.
4. Grow overnight.
5. Inoculate 1 mL of the overnight culture into 100 mL of prewarmed LB medium and grow at 37°C in a shaker until the OD_{600} reaches 0.6.
6. Transfer the cells to pre-chilled falcon tubes and pellet the cells at 4000 rpm at 4°C for 10-15 min. Drain thoroughly by inverting and tapping on paper towels to remove all traces of medium.
7. Resuspend cells by pipetting in 1/3 the original culture volume in $CaCl_2$ 0.1 M, and incubate on ice for at least 3 hours.
8. Pellet the cells by centrifugation at 4000 g. Resuspend cells by pipetting in 8 mL of RF2. Incubate on ice for 15 min.
9. Pipet 100 µL of cells into sterile prechilled tubes.
10. Flash freeze cells in dry ice or liquid nitrogen and transfer to -80°C.

RF2 Solution

MOPS	10 mM
RbCl	10 mM
CaCl2·2H2O	75 mM
Glycerol	15% wt/vol

Sterilize by filtration through 22 µm

7.5 VFDB guided analysis of virulence factors from ET

Table 7-2. Virulence factors from ET according to VFDB database.

Contig	Start	End	Orientation	Feature
174	1728669	1728238	-	Flagellar biosynthesis protein FlgN
174	1728983	1728675	-	Negative regulator of flagellin synthesis FlgM
174	1729736	1729077	-	Flagellar basal-body P-ring formation protein FlgA
174	1729894	1730307	+	Flagellar basal-body rod protein FlgB
174	1730311	1730715	+	Flagellar basal-body rod protein FlgC
174	1730728	1731399	+	Flagellar basal-body rod modification protein FlgD
174	1731415	1732173	+	Flagellar basal-body rod protein FlgF
174	1732191	1732973	+	Flagellar basal-body rod protein FlgG
174	1733140	1733748	+	Flagellar L-ring protein FlgH
174	1733758	1734867	+	Flagellar P-ring protein FlgI
174	1734867	1735820	+	Flagellar protein FlgJ [peptidoglycan hydrolase] (EC 3.2.1.-)
174	1735948	1737606	+	Flagellar hook-associated protein FlgK

174	1737633	1738595	+	Flagellar hook-associated protein FlgL
13	15277	14477	-	Cystine ABC transporter, periplasmic cystine-binding protein FliY
13	16817	16413	-	Flagellar biosynthesis protein FliZ
13	23505	22696	-	Flagellar biosynthesis protein FliC
13	31363	32811	+	Flagellar hook-associated protein FliD
13	32831	33241	+	Flagellar biosynthesis protein FliS
13	33241	33603	+	Flagellar biosynthesis protein FliT
13	41348	41037	-	Flagellar hook-basal body complex protein FliE
13	41593	43323	+	Flagellar M-ring protein FliF
13	43320	44312	+	Flagellar motor switch protein FliG
13	44305	45006	+	Flagellar assembly protein FliH
13	45006	46367	+	Flagellum-specific ATP synthase FliI
13	46401	46847	+	Flagellar protein FliJ
13	46844	48142	+	Flagellar hook-length control protein FliK
13	48274	48762	+	Flagellar biosynthesis protein FliL
13	48767	49774	+	Flagellar motor switch protein FliM
13	49767	50174	+	Flagellar motor switch protein FliN

13	50241	50570	+	Flagellar biosynthesis protein FliQ
13	50567	51307	+	Flagellar biosynthesis protein FliP
13	51326	51595	+	Flagellar biosynthesis protein FliQ
13	51595	52380	+	Flagellar biosynthesis protein FliR
174	993231	992224	-	Flagellar regulatory protein FleQ
5	86995	84908	-	Flagellar biosynthesis protein FlhA
5	88028	86988	-	Flagellar biosynthesis protein FlhB
5	88968	88324	-	Chemotaxis response - phosphatase CheZ
5	89367	88978	-	Chemotaxis regulator - transmits chemoreceptor signals to flagelllar motor components CheY
5	90458	89409	-	Chemotaxis response regulator protein-glutamate methylesterase CheB (EC 3.1.1.61)
5	91333	90458	-	Chemotaxis protein methyltransferase CheR (EC 2.1.1.80)
5	92974	91397	-	Methyl-accepting chemotaxis protein IV (dipeptide chemoreceptor protein)
5	94702	93023	-	Methyl-accepting chemotaxis protein I (serine chemoreceptor protein)
5	95286	94813	-	Methyl-accepting chemotaxis protein I (serine chemoreceptor protein)
5	98835	98338	-	Positive regulator of CheA protein activity (CheW)
5	100848	98860	-	Signal transduction histidine kinase CheA (EC 2.7.3.-)
5	101890	100859	-	Flagellar motor rotation protein MotB

5	102774	101887	-	Flagellar motor rotation protein MotA
5	103491	102913	-	Flagellar transcriptional activator FlhC
5	103841	103491	-	Flagellar transcriptional activator FlhD
174	827995	826643	-	Flagellum-specific ATP synthase FliI
174	214213	214665	+	Type IV pilin PilA
174	214665	216068	+	Type IV fimbrial assembly, ATPase PilB
174	216046	217260	+	Type IV fimbrial assembly protein PilC
8	57858	58685	+	Type IV pilus biogenesis protein PilM
8	58685	59230	+	Type IV pilus biogenesis protein PilN
8	59223	59717	+	hypothetical protein
8	59707	60105	+	hypothetical protein
8	60065	61294	+	Type IV pilus biogenesis protein PilQ
8	268233	268967	+	Type IV pilus biogenesis protein PilF
90	17608	18669	+	Twitching motility protein PilT
112	129965	129333	-	Type III secretion bridge between inner and outermembrane lipoprotein (YscJ,HrcJ,EscJ, PscJ)
112	130644	130393	-	Type III secretion cytoplasmic protein (YscF)
112	137265	136747	-	Type III secretion chaperone protein for YopD (SycD); Chaperone protein SicA (Salmonella invasin chaperone)

112	138451	137333	-	type III secretion protein
112	139222	138470	-	Type III secretion inner membrane protein (YscT,HrcT,SpaR,EscT,EpaR1,homologous to flagellar export components)
112	139489	139232	-	Type III secretion inner membrane protein (YscS,homologous to flagellar export components); Surface presentation of antigens protein SpaQ
112	140160	139489	-	Type III secretion inner membrane protein (YscR,SpaR,HrcR,EscR,homologous to flagellar export components)
112	141094	140150	-	type III secretion apparatus SpaO
112	144050	143652	-	type III secretion apparatus InvB
112	146131	144065	-	Type III secretion inner membrane channel protein (LcrD,HrcV,EscV,SsaV)
112	147297	146164	-	Type III secretion outermembrane contact sensing protein (YopN,Yop4b,LcrE); Invasion protein InvE
112	148931	147294	-	Type III secretion outermembrane pore forming protein (YscC,MxiD,HrcC, InvG)
112	149698	148928	-	Type III secretion thermoregulatory protein (LcrF,VirF,transcription regulation of virulence plasmid)
174	799896	800270	+	type III secretion protein
174	800278	801054	+	Type III secretion bridge between inner and outermembrane lipoprotein (YscJ,HrcJ,EscJ, PscJ)
174	801061	801651	+	type III secretion protein HrpD
174	802588	804690	+	Type III secretion outermembrane pore forming protein (YscC,MxiD,HrcC, InvG)
174	822754	821669	-	Type III secretion inner membrane protein (YscU,SpaS,EscU,HrcU,SsaU, homologous to flagellar export components)
174	823563	822751	-	Type III secretion inner membrane protein (YscT,HrcT,SpaR,EscT,EpaR1,homologous to flagellar

				export components)
174	823817	823563	-	Type III secretion inner membrane protein (YscS,homologous to flagellar export components)
174	824478	823825	-	Type III secretion inner membrane protein (YscR,SpaR,HrcR,EscR,homologous to flagellar export components)
174	825524	824484	-	type III secretion protein HrcQb
174	826210	825524	-	HrpP
174	826659	826207	-	type III secretion protein
174	828861	827995	-	type III secretion protein
174	830984	828861	-	Type III secretion inner membrane channel protein (LcrD,HrcV,EscV,SsaV)
174	832123	830984	-	type III secretion protein
174	833139	834617	+	HrpX
8	119161	117653	-	Type III secretion translocator of effector proteins (HrpF, NolX)
3	30592	29822	-	Iron(III) dicitrate transport ATP-binding protein FecE (TC 3.A.1.14.1)
3	31542	30592	-	Iron(III) dicitrate transport system permease protein FecD (TC 3.A.1.14.1)
3	32543	31539	-	Iron(III) dicitrate transport system permease protein FecC (TC 3.A.1.14.1)
3	33442	32540	-	Iron(III) dicitrate transport system, periplasmic iron-binding protein FecB (TC 3.A.1.14.1)
3	35861	33501	-	Iron(III) dicitrate transport protein FecA
3	36948	35974	-	Iron(III) dicitrate transmembrane sensor protein FecR
3	**39724**	**37568**	**-**	**Ferrichrome-iron receptor**

3	44967	42835	-	Ferrichrome-iron receptor
3	48848	46656	-	Ferrichrome-iron receptor
3	49086	50396	+	Enterobactin esterase
3	51234	50416	-	Ferric enterobactin transport ATP-binding protein FepC (TC 3.A.1.14.2)
3	52268	51231	-	Ferric enterobactin transport system permease protein FepG (TC 3.A.1.14.2) @ ABC-type Fe3+-siderophore transport system, permease 2 component
3	53274	52279	-	Ferric enterobactin transport system permease protein FepD (TC 3.A.1.14.2)
3	54248	53271	-	Ferric enterobactin-binding periplasmic protein FepB (TC 3.A.1.14.2)
229	175278	175937	+	BarA-associated response regulator UvrY (= GacA = SirA)
90	163229	160497	-	BarA sensory histidine kinase (= VarS = GacS)
113	274798	275463	+	N-3-oxohexanoyl-L-homoserine lactone quorum-sensing transcriptional activator
113	276094	275441	-	N-3-oxohexanoyl-L-homoserine lactone synthase
229	172720	173469	+	N-3-oxohexanoyl-L-homoserine lactone quorum-sensing transcriptional activator @ N-3-oxooctanoyl-L-homoserine lactone quorum-sensing transcriptional activator
229	173596	174210	+	COG3916: N-acyl-L-homoserine lactone synthetase
113	237959	237678	-	HigA protein (antitoxin to HigB)
113	238250	237969	-	HigB toxin protein
174	1204987	1204703	-	HigA protein (antitoxin to HigB)
174	1687923	1684984	-	Putative insecticidal toxin complex

174	1692269	1687923	-	Putative toxin subunit
174	1699406	1692303	-	Unknown, probable insecticidal toxin
62	2615	2229	-	VapC toxin protein
62	2854	2627	-	VapB protein (antitoxin to VapC)
174	2078599	2078751	+	HigB toxin protein
174	2078751	2079053	+	HigA protein (antitoxin to HigB)

7.6 Phenotypic microarray of PSV, ET and PSV + ET via Biolog

Table 7-3 Metabolic activity in each well analyzed by DuctApe software. The table is organized in a scale going from 0 (No metabolic activity) to 9 (Maximum metabolic activity). Chemicals highlighted in yellow represents the ones where improvement in metabolic activity was detected when ET and PSV were co-inoculated.

Plate id	Well id	Chemical	Category	Activity ET	Activity PSV	Activity PSV + ET
PM01	A01	Negative Control	carbon	1	2	4
PM01	A02	L-Arabinose	carbon	8	2	8
PM01	A03	N-Acetyl-D-Glucosamine	carbon	9	0	8
PM01	A04	D-Saccharic acid	carbon	9	7	6
PM01	A05	Succinic acid	carbon	8	2	6
PM01	A06	D-Galactose	carbon	9	1	8
PM01	A07	L-Aspartic acid	carbon	7	3	6
PM01	A08	L-Proline	carbon	5	1	6
PM01	A09	D-Alanine	carbon	6	2	6
PM01	A10	D-Trehalose	carbon	9	2	8
PM01	A11	D-Mannose	carbon	9	7	8
PM01	A12	Dulcitol	carbon	1	2	3
PM01	B01	D-Serine	carbon	1	2	3
PM01	B02	D-Sorbitol	carbon	1	0	3
PM01	B03	Glycerol	carbon	9	7	8
PM01	B04	L-Fucose	carbon	1	0	4
PM01	B05	D-Glucuronic acid	carbon	8	1	6

PM01	B06	D-Gluconic acid	carbon	9	3	8
PM01	B07	DL-a-Glycerol Phosphate	carbon	7	1	8
PM01	B08	D-Xylose	carbon	8	3	8
PM01	B09	L-Lactic acid	carbon	1	0	5
PM01	B10	Formic acid	carbon	3	2	6
PM01	B11	D-Mannitol	carbon	9	7	8
PM01	B12	L-Glutamic acid	carbon	8	5	6
PM01	C01	D-Glucose-6-Phosphate	carbon	4	0	6
PM01	C02	D-Galactonic acid-g-Lactone	carbon	1	5	5
PM01	C03	DL-Malic acid	carbon	8	5	6
PM01	C04	D-Ribose	carbon	8	1	8
PM01	C05	Tween 20	carbon	1	3	3
PM01	C06	L-Rhamnose	carbon	1	0	3
PM01	C07	D-Fructose	carbon	9	1	8
PM01	C08	Acetic acid	carbon	3	0	6
PM01	C09	a-D-Glucose	carbon	9	7	8
PM01	C10	Maltose	carbon	8	0	7
PM01	C11	D-Melibiose	carbon	8	2	8
PM01	C12	Thymidine	carbon	4	2	6
PM01	D01	L-Asparagine	carbon	4	5	6
PM01	D02	D-Aspartic acid	carbon	1	0	2
PM01	D03	D-Glucosaminic acid	carbon	4	5	5
PM01	D04	1,2-Propanediol	carbon	1	1	2
PM01	D05	Tween 40	carbon	1	3	4
PM01	D06	a-Ketoglutaric acid	carbon	1	1	4
PM01	D07	a-Ketobutyric acid	carbon	1	1	2
PM01	D08	a-Methyl-D-Galactoside	carbon	8	1	8
PM01	D09	a-D-Lactose	carbon	8	0	7
PM01	D10	Lactulose	carbon	8	0	7

PM01	D11	Sucrose	carbon	1	7	8
PM01	D12	Uridine	carbon	4	2	8
PM01	E01	L-Glutamine	carbon	4	7	6
PM01	E02	m-Tartaric acid	carbon	1	1	1
PM01	E03	D-Glucose-1-Phosphate	carbon	8	0	7
PM01	E04	D-Fructose-6-Phosphate	carbon	4	0	5
PM01	E05	Tween 80	carbon	1	3	3
PM01	E06	a-Hydroxyglutaric acid-g-Lactone	carbon	1	0	2
PM01	E07	a-Hydroxybutyric acid	carbon	1	1	1
PM01	E08	b-Methyl-D-Glucoside	carbon	9	0	7
PM01	E09	Adonitol	carbon	1	0	3
PM01	E10	Maltotriose	carbon	8	2	8
PM01	E11	2`-Deoxyadenosine	carbon	7	2	6
PM01	E12	Adenosine	carbon	7	4	6
PM01	F01	Gly-Asp	carbon	1	2	2
PM01	F02	Citric acid	carbon	7	3	6
PM01	F03	m-Inositol	carbon	8	7	8
PM01	F04	D-Threonine	carbon	1	1	2
PM01	F05	Fumaric acid	carbon	8	5	6
PM01	F06	Bromosuccinic acid	carbon	8	1	6
PM01	F07	Propionic acid	carbon	1	0	1
PM01	F08	Mucic acid	carbon	8	0	6
PM01	F09	Glycolic acid	carbon	1	0	1
PM01	F10	Glyoxylic acid	carbon	1	2	2
PM01	F11	D-Cellobiose	carbon	8	2	7
PM01	F12	Inosine	carbon	7	2	6
PM01	G01	Gly-Glu	carbon	1	2	2
PM01	G02	Tricarballylic acid	carbon	1	0	1
PM01	G03	L-Serine	carbon	8	5	6

PM01	G04	L-Threonine	carbon	1	1	2
PM01	G05	L-Alanine	carbon	5	3	5
PM01	G06	Ala-Gly	carbon	1	3	5
PM01	G07	Acetoacetic acid	carbon	1	0	1
PM01	G08	N-Acetyl-D-Mannosamine	carbon	8	0	8
PM01	G09	Mono-Methylsuccinate	carbon	5	3	6
PM01	G10	Methylpyruvate	carbon	7	2	6
PM01	G11	D-Malic acid	carbon	3	2	3
PM01	G12	L-Malic acid	carbon	8	5	6
PM01	H01	Gly-Pro	carbon	1	2	1
PM01	H02	p-Hydroxyphenyl Acetic acid	carbon	1	2	2
PM01	H03	m-Hydroxyphenyl Acetic acid	carbon	1	0	1
PM01	H04	Tyramine	carbon	1	0	1
PM01	H05	D-Psicose	carbon	1	2	1
PM01	H06	L-Lyxose	carbon	4	3	1
PM01	H07	Glucuronamide	carbon	7	0	6
PM01	H08	Pyruvic acid	carbon	7	5	6
PM01	H09	L-Galactonic acid-g-Lactone	carbon	1	2	1
PM01	H10	D-Galacturonic acid	carbon	9	2	7
PM01	H11	Phenylethylamine	carbon	1	2	1
PM01	H12	2-Aminoethanol	carbon	2	2	1
PM02	A01	Negative Control	carbon	3	0	3
PM02	A02	Chondroitin Sulfate C	carbon	3	0	1
PM02	A03	a-Cyclodextrin	carbon	3	1	1
PM02	A04	b-Cyclodextrin	carbon	3	0	1
PM02	A05	g-Cyclodextrin	carbon	3	1	3
PM02	A06	Dextrin	carbon	7	0	6
PM02	A07	Gelatin	carbon	3	0	3
PM02	A08	Glycogen	carbon	3	1	3

PM02	A09	Inulin	carbon	3	0	1
PM02	A10	Laminarin	carbon	3	0	3
PM02	A11	Mannan	carbon	3	0	3
PM02	A12	Pectin	carbon	3	2	3
PM02	B01	N-Acetyl-D-Galactosamine	carbon	3	0	1
PM02	B02	N-Acetyl-Neuraminic acid	carbon	8	1	8
PM02	B03	b-D-Allose	carbon	1	0	1
PM02	B04	Amygdalin	carbon	3	0	2
PM02	B05	D-Arabinose	carbon	4	0	3
PM02	B06	D-Arabitol	carbon	9	7	8
PM02	B07	L-Arabitol	carbon	1	0	3
PM02	B08	Arbutin	carbon	8	1	8
PM02	B09	2-Deoxy-D-Ribose	carbon	3	0	6
PM02	B10	i-Erythritol	carbon	1	0	1
PM02	B11	D-Fucose	carbon	3	0	2
PM02	B12	3-O-b-D-Galactopyranosyl-D-Arabinose	carbon	3	2	8
PM02	C01	Gentiobiose	carbon	8	0	8
PM02	C02	L-Glucose	carbon	1	0	1
PM02	C03	D-Lactitol	carbon	1	0	1
PM02	C04	D-Melezitose	carbon	1	0	1
PM02	C05	Maltitol	carbon	1	0	1
PM02	C06	a-Methyl-D-Glucoside	carbon	1	0	1
PM02	C07	b-Methyl-D-Galactoside	carbon	8	1	7
PM02	C08	3-Methylglucose	carbon	1	0	1
PM02	C09	b-Methyl-D-Glucuronic acid	carbon	8	0	6
PM02	C10	a-Methyl-D-Mannoside	carbon	1	0	1
PM02	C11	b-Methyl-D-Xyloside	carbon	1	0	1
PM02	C12	Palatinose	carbon	1	1	1
PM02	D01	D-Raffinose	carbon	3	0	3

PM02	D02	Salicin	carbon	7	0	6
PM02	D03	Sedoheptulosan	carbon	1	1	1
PM02	D04	L-Sorbose	carbon	1	0	1
PM02	D05	Stachyose	carbon	1	0	1
PM02	D06	D-Tagatose	carbon	1	1	1
PM02	D07	Turanose	carbon	1	1	1
PM02	D08	Xylitol	carbon	1	1	1
PM02	D09	N-Acetyl-D-Glucosaminitol	carbon	1	0	1
PM02	D10	g-Amino-N-Butyric acid	carbon	1	7	6
PM02	D11	d-Amino Valeric acid	carbon	1	0	1
PM02	D12	Butyric acid	carbon	1	2	1
PM02	E01	Capric acid	carbon	1	1	1
PM02	E02	Caproic acid	carbon	1	1	1
PM02	E03	Citraconic acid	carbon	1	1	1
PM02	E04	Citramalic acid	carbon	1	1	1
PM02	E05	D-Glucosamine	carbon	1	1	7
PM02	E06	2-Hydroxybenzoic acid	carbon	1	1	1
PM02	E07	4-Hydroxybenzoic acid	carbon	1	0	1
PM02	E08	b-Hydroxybutyric acid	carbon	1	1	1
PM02	E09	g-Hydroxybutyric acid	carbon	1	0	1
PM02	E10	a-Keto-Valeric acid	carbon	1	0	1
PM02	E11	Itaconic acid	carbon	1	0	1
PM02	E12	5-Keto-D-Gluconic acid	carbon	3	2	4
PM02	F01	D-Lactic acid Methyl Ester	carbon	1	0	1
PM02	F02	Malonic acid	carbon	1	0	2
PM02	F03	Melibionic acid	carbon	1	0	1
PM02	F04	Oxalic acid	carbon	1	1	1
PM02	F05	Oxalomalic acid	carbon	1	0	1
PM02	F06	Quinic acid	carbon	3	1	3

PM02	F07	D-Ribono-1,4-Lactone	carbon	1	0	1
PM02	F08	Sebacic acid	carbon	1	0	1
PM02	F09	Sorbic acid	carbon	3	1	1
PM02	F10	Succinamic acid	carbon	1	3	3
PM02	F11	D-Tartaric acid	carbon	1	1	1
PM02	F12	L-Tartaric acid	carbon	1	2	1
PM02	G01	Acetamide	carbon	1	2	1
PM02	G02	L-Alaninamide	carbon	1	0	1
PM02	G03	N-Acetyl-L-Glutamic acid	carbon	1	1	1
PM02	G04	L-Arginine	carbon	1	1	2
PM02	G05	Glycine	carbon	1	1	0
PM02	G06	L-Histidine	carbon	4	3	4
PM02	G07	L-Homoserine	carbon	1	0	0
PM02	G08	Hydroxy-L-Proline	carbon	1	0	1
PM02	G09	L-Isoleucine	carbon	1	3	2
PM02	G10	L-Leucine	carbon	1	1	2
PM02	G11	L-Lysine	carbon	1	2	1
PM02	G12	L-Methionine	carbon	1	2	1
PM02	H01	L-Ornithine	carbon	1	1	1
PM02	H02	L-Phenylalanine	carbon	1	2	1
PM02	H03	L-Pyroglutamic acid	carbon	1	3	2
PM02	H04	L-Valine	carbon	1	2	1
PM02	H05	D,L-Carnitine	carbon	1	1	1
PM02	H06	sec-Butylamine	carbon	1	0	0
PM02	H07	D,L-Octopamine	carbon	1	0	1
PM02	H08	Putrescine	carbon	1	2	1
PM02	H09	Dihydroxyacetone	carbon	3	6	8
PM02	H10	2,3-Butanediol	carbon	1	1	1
PM02	H11	2,3-Butanedione	carbon	1	3	1

PM02	H12	3-Hydroxy-2-buta	carbon	1	2	1
PM03	A01	Negative Control	nitrogen	1	2	3
PM03	A02	Ammonia	nitrogen	3	1	4
PM03	A03	Nitrite	nitrogen	5	1	4
PM03	A04	Nitrate	nitrogen	5	3	3
PM03	A05	Urea	nitrogen	7	1	4
PM03	A06	Biuret	nitrogen	2	1	3
PM03	A07	L-Alanine	nitrogen	7	1	3
PM03	A08	L-Arginine	nitrogen	5	1	4
PM03	A09	L-Asparagine	nitrogen	5	3	3
PM03	A10	L-Aspartic acid	nitrogen	5	3	5
PM03	A11	L-Cysteine	nitrogen	4	3	6
PM03	A12	L-Glutamic acid	nitrogen	5	3	3
PM03	B01	L-Glutamine	nitrogen	3	3	3
PM03	B02	Glycine	nitrogen	3	1	4
PM03	B03	L-Histidine	nitrogen	5	3	4
PM03	B04	L-Isoleucine	nitrogen	4	3	4
PM03	B05	L-Leucine	nitrogen	4	3	5
PM03	B06	L-Lysine	nitrogen	4	1	3
PM03	B07	L-Methionine	nitrogen	4	1	4
PM03	B08	L-Phenylalanine	nitrogen	4	1	4
PM03	B09	L-Proline	nitrogen	7	5	3
PM03	B10	L-Serine	nitrogen	5	3	4
PM03	B11	L-Threonine	nitrogen	4	1	4
PM03	B12	L-Tryptophan	nitrogen	4	3	6
PM03	C01	L-Tyrosine	nitrogen	4	5	4
PM03	C02	L-Valine	nitrogen	4	1	4
PM03	C03	D-Alanine	nitrogen	7	1	4
PM03	C04	D-Asparagine	nitrogen	5	3	4

PM03	C05	D-Aspartic acid	nitrogen	4	1	4
PM03	C06	D-Glutamic acid	nitrogen	4	1	4
PM03	C07	D-Lysine	nitrogen	2	1	1
PM03	C08	D-Serine	nitrogen	4	1	2
PM03	C09	D-Valine	nitrogen	2	3	2
PM03	C10	L-Citrulline	nitrogen	4	1	4
PM03	C11	L-Homoserine	nitrogen	2	0	2
PM03	C12	L-Ornithine	nitrogen	5	3	4
PM03	D01	N-Acetyl-L-Glutamic acid	nitrogen	1	1	2
PM03	D02	N-Phthaloyl-L-Glutamic acid	nitrogen	1	1	2
PM03	D03	L-Pyroglutamic acid	nitrogen	2	5	5
PM03	D04	Hydroxylamine	nitrogen	1	0	1
PM03	D05	Methylamine	nitrogen	0	1	2
PM03	D06	N-Amylamine	nitrogen	5	1	4
PM03	D07	N-Butylamine	nitrogen	4	1	4
PM03	D08	Ethylamine	nitrogen	2	1	2
PM03	D09	Ethanolamine	nitrogen	5	3	4
PM03	D10	Ethylenediamine	nitrogen	1	3	1
PM03	D11	Putrescine	nitrogen	2	3	4
PM03	D12	Agmatine	nitrogen	5	3	4
PM03	E01	Histamine	nitrogen	5	1	4
PM03	E02	b-Phenylethylamine	nitrogen	2	1	4
PM03	E03	Tyramine	nitrogen	4	1	2
PM03	E04	Acetamide	nitrogen	3	1	2
PM03	E05	Formamide	nitrogen	3	1	2
PM03	E06	Glucuronamide	nitrogen	7	3	5
PM03	E07	DL-Lactamide	nitrogen	5	1	4
PM03	E08	D-Glucosamine	nitrogen	8	7	6
PM03	E09	D-Galactosamine	nitrogen	4	1	2

PM03	E10	D-Mannosamine	nitrogen	3	3	4
PM03	E11	N-Acetyl-D-Glucosamine	nitrogen	8	7	7
PM03	E12	N-Acetyl-D-Galactosamine	nitrogen	1	1	1
PM03	F01	N-Acetyl-D-Mannosamine	nitrogen	8	5	6
PM03	F02	Adenine	nitrogen	2	1	4
PM03	F03	Adenosine	nitrogen	7	3	5
PM03	F04	Cytidine	nitrogen	8	5	7
PM03	F05	Cytosine	nitrogen	5	1	4
PM03	F06	Guanine	nitrogen	5	1	4
PM03	F07	Guanosine	nitrogen	7	3	5
PM03	F08	Thymine	nitrogen	2	3	2
PM03	F09	Thymidine	nitrogen	4	1	2
PM03	F10	Uracil	nitrogen	2	3	2
PM03	F11	Uridine	nitrogen	3	5	4
PM03	F12	Inosine	nitrogen	7	5	5
PM03	G01	Xanthine	nitrogen	7	3	4
PM03	G02	Xanthosine	nitrogen	4	3	4
PM03	G03	Uric acid	nitrogen	5	3	4
PM03	G04	Alloxan	nitrogen	4	1	2
PM03	G05	Allantoin	nitrogen	5	1	4
PM03	G06	Parabanic acid	nitrogen	5	1	4
PM03	G07	DL-a-Amino-N-Butyric acid	nitrogen	2	1	2
PM03	G08	g-Amino-N-Butyric acid	nitrogen	5	5	5
PM03	G09	e-Amino-N-Caproic acid	nitrogen	2	1	2
PM03	G10	DL-a-Amino-Caprylic acid	nitrogen	1	2	1
PM03	G11	d-Amino-N-Valeric acid	nitrogen	2	3	2
PM03	G12	a-Amino-N-Valeric acid	nitrogen	4	3	4
PM03	H01	Ala-Asp	nitrogen	7	2	4
PM03	H02	Ala-Gln	nitrogen	5	3	3

PM03	H03	Ala-Glu	nitrogen	7	3	3
PM03	H04	Ala-Gly	nitrogen	7	3	3
PM03	H05	Ala-His	nitrogen	7	3	4
PM03	H06	Ala-Leu	nitrogen	7	3	4
PM03	H07	Ala-Thr	nitrogen	7	3	4
PM03	H08	Gly-Asn	nitrogen	5	3	3
PM03	H09	Gly-Gln	nitrogen	7	3	3
PM03	H10	Gly-Glu	nitrogen	5	3	4
PM03	H11	Gly-Met	nitrogen	5	3	4
PM03	H12	Met-Ala	nitrogen	5	4	3
PM04	A01	Negative Control	phosphate & sulphur	1	0	3
PM04	A02	Phosphate	phosphate & sulphur	3	0	3
PM04	A03	Pyrophosphate	phosphate & sulphur	4	1	4
PM04	A04	Trimetaphosphate	phosphate & sulphur	2	1	3
PM04	A05	Tripolyphosphate	phosphate & sulphur	4	1	4
PM04	A06	Triethyl Phosphate	phosphate & sulphur	1	0	1
PM04	A07	Hypophosphite	phosphate & sulphur	1	0	1
PM04	A08	Adenosine 2`-Monophosphate	phosphate & sulphur	2	1	4
PM04	A09	Adenosine 3`-Monophosphate	phosphate & sulphur	6	0	3
PM04	A10	Adenosine 5`-Monophosphate	phosphate & sulphur	4	2	5
PM04	A11	Adenosine 2`,3`-Cyclic Monophosphate	phosphate & sulphur	4	1	3
PM04	A12	Adenosine 3`,5`-Cyclic Monophosphate	phosphate & sulphur	3	2	3
PM04	B01	Thiophosphate	phosphate & sulphur	2	0	1
PM04	B02	Dithiophosphate	phosphate & sulphur	2	0	2
PM04	B03	DL-a-Glycerol Phosphate	phosphate & sulphur	3	0	4
PM04	B04	b-Glycerol Phosphate	phosphate & sulphur	1	0	2
PM04	B05	Carbamyl Phosphate	phosphate & sulphur	1	1	4
PM04	B06	D-2-Phospho-Glyceric acid	phosphate & sulphur	1	0	2
PM04	B07	D-3-Phospho-Glyceric acid	phosphate & sulphur	3	1	4

PM04	B08	Guanosine 2`-Monophosphate	phosphate & sulphur	2	1	2
PM04	B09	Guanosine 3`-Monophosphate	phosphate & sulphur	3	0	2
PM04	B10	Guanosine 5`-Monophosphate	phosphate & sulphur	2	0	2
PM04	B11	Guanosine 2`,3`-Cyclic Monophosphate	phosphate & sulphur	3	0	1
PM04	B12	Guanosine 3`,5`-Cyclic Monophosphate	phosphate & sulphur	1	1	3
PM04	C01	Phosphoenol Pyruvate	phosphate & sulphur	2	1	2
PM04	C02	Phospho-Glycolic acid	phosphate & sulphur	1	1	2
PM04	C03	D-Glucose-1-Phosphate	phosphate & sulphur	2	0	4
PM04	C04	D-Glucose-6-Phosphate	phosphate & sulphur	1	0	2
PM04	C05	2-Deoxy-D-Glucose 6-Phosphate	phosphate & sulphur	1	0	2
PM04	C06	D-Glucosamine-6-Phosphate	phosphate & sulphur	1	1	2
PM04	C07	6-Phospho-Gluconic acid	phosphate & sulphur	1	0	2
PM04	C08	Cytidine 2`-Monophosphate	phosphate & sulphur	4	1	4
PM04	C09	Cytidine 3`-Monophosphate	phosphate & sulphur	4	0	5
PM04	C10	Cytidine 5`-Monophosphate	phosphate & sulphur	1	0	4
PM04	C11	Cytidine 2`,3`-Cyclic Monophosphate	phosphate & sulphur	1	1	5
PM04	C12	Cytidine 3`,5`-Cyclic Monophosphate	phosphate & sulphur	1	2	4
PM04	D01	D-Mannose-1-Phosphate	phosphate & sulphur	4	1	4
PM04	D02	D-Mannose-6-Phosphate	phosphate & sulphur	2	1	4
PM04	D03	Cysteamine-S-Phosphate	phosphate & sulphur	0	0	2
PM04	D04	Phospho-L-Arginine	phosphate & sulphur	1	0	2
PM04	D05	O-Phospho-D-Serine	phosphate & sulphur	2	0	2
PM04	D06	O-Phospho-L-Serine	phosphate & sulphur	2	0	4
PM04	D07	O-Phospho-L-Threonine	phosphate & sulphur	3	1	4
PM04	D08	Uridine 2`-Monophosphate	phosphate & sulphur	1	1	2
PM04	D09	Uridine 3`-Monophosphate	phosphate & sulphur	2	1	4
PM04	D10	Uridine 5`-Monophosphate	phosphate & sulphur	2	3	5
PM04	D11	Uridine 2`,3`-Cyclic Monophosphate	phosphate & sulphur	6	1	5
PM04	D12	Uridine 3`,5`-Cyclic Monophosphate	phosphate & sulphur	1	3	1

PM04	E01	O-Phospho-D-Tyrosine	phosphate & sulphur	4	1	4
PM04	E02	O-Phospho-L-Tyrosine	phosphate & sulphur	4	1	4
PM04	E03	Phosphocreatine	phosphate & sulphur	2	0	2
PM04	E04	Phosphoryl Choline	phosphate & sulphur	2	0	2
PM04	E05	O-Phosphoryl-Ethanolamine	phosphate & sulphur	2	0	2
PM04	E06	Phosphono Acetic acid	phosphate & sulphur	2	1	2
PM04	E07	2-Aminoethyl Phosphonic acid	phosphate & sulphur	2	1	4
PM04	E08	Methylene Diphosphonic acid	phosphate & sulphur	2	1	2
PM04	E09	Thymidine 3`-Monophosphate	phosphate & sulphur	2	1	4
PM04	E10	Thymidine 5`-Monophosphate	phosphate & sulphur	3	1	5
PM04	E11	Inositol Hexaphosphate	phosphate & sulphur	3	3	5
PM04	E12	Thymidine 3`,5`-Cyclic Monophosphate	phosphate & sulphur	2	3	4
PM04	F01	Negative Control	phosphate & sulphur	3	1	3
PM04	F02	Sulfate	phosphate & sulphur	5	1	5
PM04	F03	Thiosulfate	phosphate & sulphur	5	1	5
PM04	F04	Tetrathionate	phosphate & sulphur	5	1	5
PM04	F05	Thiophosphate	phosphate & sulphur	5	1	4
PM04	F06	Dithiophosphate	phosphate & sulphur	5	1	5
PM04	F07	L-Cysteine	phosphate & sulphur	7	0	5
PM04	F08	D-Cysteine	phosphate & sulphur	5	0	5
PM04	F09	Cys-Gly	phosphate & sulphur	5	1	4
PM04	F10	L-Cysteic acid	phosphate & sulphur	5	1	5
PM04	F11	Cysteamine	phosphate & sulphur	3	1	4
PM04	F12	L-Cysteine Sulfinic acid	phosphate & sulphur	3	3	4
PM04	G01	N-Acetyl-L-Cysteine	phosphate & sulphur	5	1	4
PM04	G02	S-Methyl-L-Cysteine	phosphate & sulphur	3	1	4
PM04	G03	Cystathionine	phosphate & sulphur	5	1	5
PM04	G04	Lanthionine	phosphate & sulphur	5	1	5
PM04	G05	Glutathione	phosphate & sulphur	5	1	4

PM04	G06	DL-Ethionine	phosphate & sulphur	3	1	2
PM04	G07	L-Methionine	phosphate & sulphur	5	1	5
PM04	G08	D-Methionine	phosphate & sulphur	7	0	5
PM04	G09	Gly-Met	phosphate & sulphur	5	1	5
PM04	G10	N-Acetyl-D,L-Methionine	phosphate & sulphur	5	1	5
PM04	G11	L-Methionine Sulfoxide	phosphate & sulphur	5	3	5
PM04	G12	L-Methionine Sulfone	phosphate & sulphur	3	3	1
PM04	H01	L-Djenkolic acid	phosphate & sulphur	5	2	5
PM04	H02	Thiourea	phosphate & sulphur	3	1	4
PM04	H03	1-Thio-b-D-Glucose	phosphate & sulphur	3	1	2
PM04	H04	DL-Lipoamide	phosphate & sulphur	5	1	4
PM04	H05	Taurocholic acid	phosphate & sulphur	1	3	4
PM04	H06	Taurine	phosphate & sulphur	5	1	4
PM04	H07	Hypotaurine	phosphate & sulphur	5	1	4
PM04	H08	p-Aminobenzene Sulfonic acid	phosphate & sulphur	3	3	2
PM04	H09	Butane Sulfonic acid	phosphate & sulphur	5	1	5
PM04	H10	2-Hydroxyethane Sulfonic acid	phosphate & sulphur	5	5	5
PM04	H11	Methane Sulfonic acid	phosphate & sulphur	3	5	4
PM04	H12	Tetramethylene Sulfone	phosphate & sulphur	3	6	4
PM05	A01	Negative Control	nutrient stimulation	5	3	4
PM05	A02	Positive Control	nutrient stimulation	5	1	3
PM05	A03	L-Alanine	nutrient stimulation	5	3	4
PM05	A04	L-Arginine	nutrient stimulation	5	3	4
PM05	A05	L-Asparagine	nutrient stimulation	5	3	4
PM05	A06	L-Aspartic acid	nutrient stimulation	5	1	4
PM05	A07	L-Cysteine	nutrient stimulation	5	3	4
PM05	A08	L-Glutamic acid	nutrient stimulation	5	3	4
PM05	A09	Adenosine 3`,5`-Cyclic Monophosphate	nutrient stimulation	5	3	4
PM05	A10	Adenine	nutrient stimulation	3	3	4

PM05	A11	Adenosine	nutrient stimulation	5	3	4
PM05	A12	2`-Deoxyadenosine	nutrient stimulation	3	3	3
PM05	B01	L-Glutamine	nutrient stimulation	5	3	4
PM05	B02	Glycine	nutrient stimulation	5	3	4
PM05	B03	L-Histidine	nutrient stimulation	5	3	4
PM05	B04	L-Isoleucine	nutrient stimulation	5	3	4
PM05	B05	L-Leucine	nutrient stimulation	5	3	4
PM05	B06	L-Lysine	nutrient stimulation	5	3	4
PM05	B07	L-Methionine	nutrient stimulation	5	3	4
PM05	B08	L-Phenylalanine	nutrient stimulation	5	3	4
PM05	B09	Guanosine 3`,5`-Cyclic Monophosphate	nutrient stimulation	5	3	4
PM05	B10	Guanine	nutrient stimulation	5	3	4
PM05	B11	Guanosine	nutrient stimulation	5	3	4
PM05	B12	2`-Deoxyguanosine	nutrient stimulation	5	3	4
PM05	C01	L-Proline	nutrient stimulation	5	3	4
PM05	C02	L-Serine	nutrient stimulation	5	3	3
PM05	C03	L-Threonine	nutrient stimulation	5	3	4
PM05	C04	L-Tryptophan	nutrient stimulation	5	3	4
PM05	C05	L-Tyrosine	nutrient stimulation	5	3	4
PM05	C06	L-Valine	nutrient stimulation	5	3	4
PM05	C07	L-Isoleucine + L-Valine	nutrient stimulation	5	3	4
PM05	C08	Hydroxy-L-Proline	nutrient stimulation	5	3	4
PM05	C09	(5) 4-Amino-Imidazole-4(5)-Carboxamide	nutrient stimulation	5	3	4
PM05	C10	Hypoxanthine	nutrient stimulation	5	3	3
PM05	C11	Inosine	nutrient stimulation	5	3	4
PM05	C12	2`-Deoxyinosine	nutrient stimulation	1	3	3
PM05	D01	L-Ornithine	nutrient stimulation	5	3	4
PM05	D02	L-Citrulline	nutrient stimulation	5	3	4
PM05	D03	Chorismic acid	nutrient stimulation	5	3	4

PM05	D04	(-)Shikimic acid	nutrient stimulation	5	3	4
PM05	D05	L-Homoserine Lactone	nutrient stimulation	5	3	4
PM05	D06	D-Alanine	nutrient stimulation	5	3	4
PM05	D07	D-Aspartic acid	nutrient stimulation	5	3	4
PM05	D08	D-Glutamic acid	nutrient stimulation	5	3	4
PM05	D09	DL-Diamino-a,e-Pimelic acid	nutrient stimulation	5	3	4
PM05	D10	Cytosine	nutrient stimulation	5	3	4
PM05	D11	Cytidine	nutrient stimulation	5	3	3
PM05	D12	2`-Deoxycytidine	nutrient stimulation	5	3	3
PM05	E01	Putrescine	nutrient stimulation	5	3	4
PM05	E02	Spermidine	nutrient stimulation	5	3	4
PM05	E03	Spermine	nutrient stimulation	5	3	4
PM05	E04	Pyridoxine	nutrient stimulation	5	3	4
PM05	E05	Pyridoxal	nutrient stimulation	5	3	4
PM05	E06	Pyridoxamine	nutrient stimulation	5	3	4
PM05	E07	b-Alanine	nutrient stimulation	5	3	4
PM05	E08	D-Pantothenic acid	nutrient stimulation	5	3	4
PM05	E09	Orotic acid	nutrient stimulation	5	3	4
PM05	E10	Uracil	nutrient stimulation	5	3	4
PM05	E11	Uridine	nutrient stimulation	7	3	4
PM05	E12	2`-Deoxyuridine	nutrient stimulation	5	3	3
PM05	F01	Quinolinic acid	nutrient stimulation	5	3	4
PM05	F02	Nicotinic acid	nutrient stimulation	5	3	4
PM05	F03	Nicotinamide	nutrient stimulation	5	3	4
PM05	F04	b-Nicotinamide Adenine Dinucleotide	nutrient stimulation	5	3	4
PM05	F05	d-Amino-levulinic acid	nutrient stimulation	5	3	4
PM05	F06	Hematin	nutrient stimulation	5	3	4
PM05	F07	Deferoxamine	nutrient stimulation	5	3	4
PM05	F08	a-D-Glucose	nutrient stimulation	5	3	4

PM05	F09	N-Acetyl-D-Glucosamine	nutrient stimulation	7	3	4
PM05	F10	Thymine	nutrient stimulation	5	3	4
PM05	F11	Glutathione	nutrient stimulation	5	3	3
PM05	F12	Thymidine	nutrient stimulation	5	3	3
PM05	G01	Oxaloacetic acid	nutrient stimulation	5	3	4
PM05	G02	D-Biotin	nutrient stimulation	5	3	4
PM05	G03	Cyanocobalamin	nutrient stimulation	5	3	4
PM05	G04	p-Amino-Benzoic acid	nutrient stimulation	5	3	4
PM05	G05	Folic acid	nutrient stimulation	5	3	4
PM05	G06	Inosine + Thiamine	nutrient stimulation	5	3	4
PM05	G07	Thiamine	nutrient stimulation	5	3	4
PM05	G08	Thiamine Pyrophosphate	nutrient stimulation	5	3	4
PM05	G09	Riboflavin	nutrient stimulation	5	3	4
PM05	G10	Pyrrolo-Quinoline Qui	nutrient stimulation	5	3	4
PM05	G11	Menadione	nutrient stimulation	5	3	4
PM05	G12	m-Inositol	nutrient stimulation	5	3	3
PM05	H01	Butyric acid	nutrient stimulation	5	3	3
PM05	H02	a-Hydroxybutyric acid	nutrient stimulation	5	3	4
PM05	H03	a-Ketobutyric acid	nutrient stimulation	5	3	4
PM05	H04	Caprylic acid	nutrient stimulation	5	3	2
PM05	H05	DL-Thioctic acid	nutrient stimulation	5	3	4
PM05	H06	DL-Mevalonic acid Lactone	nutrient stimulation	5	3	2
PM05	H07	DL-Carnitine	nutrient stimulation	5	3	4
PM05	H08	Choline	nutrient stimulation	5	3	4
PM05	H09	Tween 20	nutrient stimulation	5	3	4
PM05	H10	Tween 40	nutrient stimulation	5	3	4
PM05	H11	Tween 60	nutrient stimulation	5	5	4
PM05	H12	Tween 80	nutrient stimulation	7	3	4
PM06	A01	Negative Control	nitrogen peptides	3	1	3

PM06	A02	L-Glutamine	nitrogen peptides	5	3	4
PM06	A03	Ala-Ala	nitrogen peptides	7	1	4
PM06	A04	Ala-Arg	nitrogen peptides	7	1	4
PM06	A05	Ala-Asn	nitrogen peptides	5	1	3
PM06	A06	Ala-Glu	nitrogen peptides	7	3	3
PM06	A07	Ala-Gly	nitrogen peptides	7	1	3
PM06	A08	Ala-His	nitrogen peptides	7	3	4
PM06	A09	Ala-Leu	nitrogen peptides	7	3	5
PM06	A10	Ala-Lys	nitrogen peptides	3	1	4
PM06	A11	Ala-Phe	nitrogen peptides	7	3	4
PM06	A12	Ala-Pro	nitrogen peptides	7	2	3
PM06	B01	Ala-Ser	nitrogen peptides	7	3	3
PM06	B02	Ala-Thr	nitrogen peptides	5	1	4
PM06	B03	Ala-Trp	nitrogen peptides	7	3	4
PM06	B04	Ala-Tyr	nitrogen peptides	7	5	5
PM06	B05	Arg-Ala	nitrogen peptides	7	1	4
PM06	B06	Arg-Arg	nitrogen peptides	7	3	4
PM06	B07	Arg-Asp	nitrogen peptides	5	1	4
PM06	B08	Arg-Gln	nitrogen peptides	7	3	4
PM06	B09	Arg-Glu	nitrogen peptides	7	3	3
PM06	B10	Arg-Ile	nitrogen peptides	5	5	5
PM06	B11	Arg-Leu	nitrogen peptides	5	5	5
PM06	B12	Arg-Lys	nitrogen peptides	5	3	3
PM06	C01	Arg-Met	nitrogen peptides	5	3	4
PM06	C02	Arg-Phe	nitrogen peptides	5	1	4
PM06	C03	Arg-Ser	nitrogen peptides	5	1	4
PM06	C04	Arg-Trp	nitrogen peptides	5	3	4
PM06	C05	Arg-Tyr	nitrogen peptides	7	5	5
PM06	C06	Arg-Val	nitrogen peptides	5	1	4

PM06	C07	Asn-Glu	nitrogen peptides	5	3	4
PM06	C08	Asn-Val	nitrogen peptides	5	3	4
PM06	C09	Asp-Asp	nitrogen peptides	5	1	4
PM06	C10	Asp-Glu	nitrogen peptides	5	3	4
PM06	C11	Asp-Leu	nitrogen peptides	7	5	5
PM06	C12	Asp-Lys	nitrogen peptides	7	3	4
PM06	D01	Asp-Phe	nitrogen peptides	7	3	4
PM06	D02	Asp-Trp	nitrogen peptides	5	3	4
PM06	D03	Asp-Val	nitrogen peptides	5	1	4
PM06	D04	Cys-Gly	nitrogen peptides	7	1	4
PM06	D05	Gln-Gln	nitrogen peptides	5	1	4
PM06	D06	Gln-Gly	nitrogen peptides	7	1	4
PM06	D07	Glu-Asp	nitrogen peptides	4	1	4
PM06	D08	Glu-Glu	nitrogen peptides	4	1	4
PM06	D09	Glu-Gly	nitrogen peptides	4	3	4
PM06	D10	Glu-Ser	nitrogen peptides	7	3	3
PM06	D11	Glu-Trp	nitrogen peptides	4	3	4
PM06	D12	Glu-Tyr	nitrogen peptides	5	5	5
PM06	E01	Glu-Val	nitrogen peptides	4	3	3
PM06	E02	Gly-Ala	nitrogen peptides	5	1	4
PM06	E03	Gly-Arg	nitrogen peptides	5	3	4
PM06	E04	Gly-Cys	nitrogen peptides	4	1	4
PM06	E05	Gly-Gly	nitrogen peptides	5	1	4
PM06	E06	Gly-His	nitrogen peptides	7	3	4
PM06	E07	Gly-Leu	nitrogen peptides	5	3	4
PM06	E08	Gly-Lys	nitrogen peptides	5	3	4
PM06	E09	Gly-Met	nitrogen peptides	5	3	4
PM06	E10	Gly-Phe	nitrogen peptides	7	2	4
PM06	E11	Gly-Pro	nitrogen peptides	4	3	4

PM06	E12	Gly-Ser	nitrogen peptides	7	3	3
PM06	F01	Gly-Thr	nitrogen peptides	4	3	4
PM06	F02	Gly-Trp	nitrogen peptides	4	3	4
PM06	F03	Gly-Tyr	nitrogen peptides	4	5	5
PM06	F04	Gly-Val	nitrogen peptides	5	1	4
PM06	F05	His-Asp	nitrogen peptides	5	1	4
PM06	F06	His-Gly	nitrogen peptides	5	3	4
PM06	F07	His-Leu	nitrogen peptides	7	5	5
PM06	F08	His-Lys	nitrogen peptides	5	5	4
PM06	F09	His-Met	nitrogen peptides	7	3	4
PM06	F10	His-Pro	nitrogen peptides	5	3	4
PM06	F11	His-Ser	nitrogen peptides	7	3	4
PM06	F12	His-Trp	nitrogen peptides	7	3	5
PM06	G01	His-Tyr	nitrogen peptides	7	5	4
PM06	G02	His-Val	nitrogen peptides	5	3	4
PM06	G03	Ile-Ala	nitrogen peptides	7	5	4
PM06	G04	Ile-Arg	nitrogen peptides	7	5	4
PM06	G05	Ile-Gln	nitrogen peptides	7	5	4
PM06	G06	Ile-Gly	nitrogen peptides	5	3	4
PM06	G07	Ile-His	nitrogen peptides	7	5	5
PM06	G08	Ile-Ile	nitrogen peptides	5	5	4
PM06	G09	Ile-Met	nitrogen peptides	4	3	4
PM06	G10	Ile-Phe	nitrogen peptides	5	5	4
PM06	G11	Ile-Pro	nitrogen peptides	4	3	4
PM06	G12	Ile-Ser	nitrogen peptides	7	6	4
PM06	H01	Ile-Trp	nitrogen peptides	2	3	4
PM06	H02	Ile-Tyr	nitrogen peptides	3	5	4
PM06	H03	Ile-Val	nitrogen peptides	4	3	4
PM06	H04	Leu-Ala	nitrogen peptides	7	3	4

PM06	H05	Leu-Arg	nitrogen peptides	7	5	5
PM06	H06	Leu-Asp	nitrogen peptides	4	5	4
PM06	H07	Leu-Glu	nitrogen peptides	7	3	5
PM06	H08	Leu-Gly	nitrogen peptides	5	6	4
PM06	H09	Leu-Ile	nitrogen peptides	3	5	5
PM06	H10	Leu-Leu	nitrogen peptides	4	3	4
PM06	H11	Leu-Met	nitrogen peptides	3	3	4
PM06	H12	Leu-Phe	nitrogen peptides	5	3	3
PM07	A01	Negative Control	nitrogen peptides	1	0	3
PM07	A02	L-Glutamine	nitrogen peptides	3	3	4
PM07	A03	Leu-Ser	nitrogen peptides	5	3	5
PM07	A04	Leu-Trp	nitrogen peptides	4	3	5
PM07	A05	Leu-Val	nitrogen peptides	4	1	4
PM07	A06	Lys-Ala	nitrogen peptides	2	1	2
PM07	A07	Lys-Arg	nitrogen peptides	7	1	5
PM07	A08	Lys-Glu	nitrogen peptides	4	1	4
PM07	A09	Lys-Ile	nitrogen peptides	1	3	4
PM07	A10	Lys-Leu	nitrogen peptides	1	3	4
PM07	A11	Lys-Lys	nitrogen peptides	4	2	3
PM07	A12	Lys-Phe	nitrogen peptides	3	2	3
PM07	B01	Lys-Pro	nitrogen peptides	2	1	4
PM07	B02	Lys-Ser	nitrogen peptides	2	1	2
PM07	B03	Lys-Thr	nitrogen peptides	2	1	2
PM07	B04	Lys-Trp	nitrogen peptides	4	1	5
PM07	B05	Lys-Tyr	nitrogen peptides	1	5	4
PM07	B06	Lys-Val	nitrogen peptides	0	1	2
PM07	B07	Met-Arg	nitrogen peptides	5	1	4
PM07	B08	Met-Asp	nitrogen peptides	4	1	3
PM07	B09	Met-Gln	nitrogen peptides	5	1	3

PM07	B10	Met-Glu	nitrogen peptides	7	3	3
PM07	B11	Met-Gly	nitrogen peptides	4	1	4
PM07	B12	Met-His	nitrogen peptides	5	2	3
PM07	C01	Met-Ile	nitrogen peptides	4	3	3
PM07	C02	Met-Leu	nitrogen peptides	4	1	4
PM07	C03	Met-Lys	nitrogen peptides	4	1	3
PM07	C04	Met-Met	nitrogen peptides	4	1	4
PM07	C05	Met-Phe	nitrogen peptides	4	1	4
PM07	C06	Met-Pro	nitrogen peptides	4	1	4
PM07	C07	Met-Trp	nitrogen peptides	4	1	4
PM07	C08	Met-Val	nitrogen peptides	4	1	3
PM07	C09	Phe-Ala	nitrogen peptides	5	1	4
PM07	C10	Phe-Gly	nitrogen peptides	4	1	4
PM07	C11	Phe-Ile	nitrogen peptides	4	5	3
PM07	C12	Phe-Phe	nitrogen peptides	4	1	4
PM07	D01	Phe-Pro	nitrogen peptides	2	1	4
PM07	D02	Phe-Ser	nitrogen peptides	4	1	4
PM07	D03	Phe-Trp	nitrogen peptides	2	1	2
PM07	D04	Pro-Ala	nitrogen peptides	5	1	4
PM07	D05	Pro-Asp	nitrogen peptides	2	1	4
PM07	D06	Pro-Gln	nitrogen peptides	5	5	5
PM07	D07	Pro-Gly	nitrogen peptides	2	1	5
PM07	D08	Pro-Hyp	nitrogen peptides	2	1	1
PM07	D09	Pro-Leu	nitrogen peptides	7	5	5
PM07	D10	Pro-Phe	nitrogen peptides	4	1	5
PM07	D11	Pro-Pro	nitrogen peptides	2	1	2
PM07	D12	Pro-Tyr	nitrogen peptides	4	3	4
PM07	E01	Ser-Ala	nitrogen peptides	5	3	4
PM07	E02	Ser-Gly	nitrogen peptides	4	2	4

PM07	E03	Ser-His	nitrogen peptides	5	3	4
PM07	E04	Ser-Leu	nitrogen peptides	7	3	5
PM07	E05	Ser-Met	nitrogen peptides	5	1	3
PM07	E06	Ser-Phe	nitrogen peptides	4	3	4
PM07	E07	Ser-Pro	nitrogen peptides	4	1	5
PM07	E08	Ser-Ser	nitrogen peptides	5	3	4
PM07	E09	Ser-Tyr	nitrogen peptides	5	3	5
PM07	E10	Ser-Val	nitrogen peptides	5	3	4
PM07	E11	Thr-Ala	nitrogen peptides	5	1	4
PM07	E12	Thr-Arg	nitrogen peptides	5	3	3
PM07	F01	Thr-Glu	nitrogen peptides	4	3	3
PM07	F02	Thr-Gly	nitrogen peptides	4	1	2
PM07	F03	Thr-Leu	nitrogen peptides	4	5	5
PM07	F04	Thr-Met	nitrogen peptides	4	1	2
PM07	F05	Thr-Pro	nitrogen peptides	4	1	5
PM07	F06	Trp-Ala	nitrogen peptides	7	1	4
PM07	F07	Trp-Arg	nitrogen peptides	5	3	4
PM07	F08	Trp-Asp	nitrogen peptides	4	3	4
PM07	F09	Trp-Glu	nitrogen peptides	4	3	5
PM07	F10	Trp-Gly	nitrogen peptides	5	3	4
PM07	F11	Trp-Leu	nitrogen peptides	5	3	5
PM07	F12	Trp-Lys	nitrogen peptides	5	3	4
PM07	G01	Trp-Phe	nitrogen peptides	2	1	3
PM07	G02	Trp-Ser	nitrogen peptides	4	3	4
PM07	G03	Trp-Trp	nitrogen peptides	2	2	3
PM07	G04	Trp-Tyr	nitrogen peptides	2	3	4
PM07	G05	Tyr-Ala	nitrogen peptides	5	5	5
PM07	G06	Tyr-Gln	nitrogen peptides	5	5	4
PM07	G07	Tyr-Glu	nitrogen peptides	4	5	5

PM07	G08	Tyr-Gly	nitrogen peptides	4	5	5
PM07	G09	Tyr-His	nitrogen peptides	7	5	4
PM07	G10	Tyr-Leu	nitrogen peptides	5	5	5
PM07	G11	Tyr-Lys	nitrogen peptides	4	5	5
PM07	G12	Tyr-Phe	nitrogen peptides	4	3	4
PM07	H01	Tyr-Trp	nitrogen peptides	1	3	2
PM07	H02	Tyr-Tyr	nitrogen peptides	2	5	4
PM07	H03	Val-Arg	nitrogen peptides	5	3	2
PM07	H04	Val-Asn	nitrogen peptides	5	3	3
PM07	H05	Val-Asp	nitrogen peptides	4	1	4
PM07	H06	Val-Gly	nitrogen peptides	4	3	2
PM07	H07	Val-His	nitrogen peptides	5	3	4
PM07	H08	Val-Ile	nitrogen peptides	4	3	2
PM07	H09	Val-Leu	nitrogen peptides	4	3	4
PM07	H10	Val-Tyr	nitrogen peptides	4	3	4
PM07	H11	Val-Val	nitrogen peptides	5	3	2
PM07	H12	g-Glu-Gly	nitrogen peptides	3	2	2
PM08	A01	Negative Control	nitrogen peptides	3	0	3
PM08	A02	L-Glutamine	nitrogen peptides	5	3	3
PM08	A03	Ala-Asp	nitrogen peptides	5	1	4
PM08	A04	Ala-Gln	nitrogen peptides	5	1	3
PM08	A05	Ala-Ile	nitrogen peptides	7	3	4
PM08	A06	Ala-Met	nitrogen peptides	5	1	3
PM08	A07	Ala-Val	nitrogen peptides	7	1	4
PM08	A08	Asp-Ala	nitrogen peptides	7	1	3
PM08	A09	Asp-Gln	nitrogen peptides	5	1	3
PM08	A10	Asp-Gly	nitrogen peptides	7	2	4
PM08	A11	Glu-Ala	nitrogen peptides	7	2	3
PM08	A12	Gly-Asn	nitrogen peptides	7	2	3

PM08	B01	Gly-Asp	nitrogen peptides	5	0	4
PM08	B02	Gly-Ile	nitrogen peptides	5	3	4
PM08	B03	His-Ala	nitrogen peptides	5	1	4
PM08	B04	His-Glu	nitrogen peptides	5	1	5
PM08	B05	His-His	nitrogen peptides	7	3	4
PM08	B06	Ile-Asn	nitrogen peptides	5	3	4
PM08	B07	Ile-Leu	nitrogen peptides	7	5	5
PM08	B08	Leu-Asn	nitrogen peptides	7	3	5
PM08	B09	Leu-His	nitrogen peptides	7	5	5
PM08	B10	Leu-Pro	nitrogen peptides	7	1	5
PM08	B11	Leu-Tyr	nitrogen peptides	5	5	5
PM08	B12	Lys-Asp	nitrogen peptides	5	2	4
PM08	C01	Lys-Gly	nitrogen peptides	4	1	2
PM08	C02	Lys-Met	nitrogen peptides	1	1	2
PM08	C03	Met-Thr	nitrogen peptides	4	1	2
PM08	C04	Met-Tyr	nitrogen peptides	4	5	5
PM08	C05	Phe-Asp	nitrogen peptides	5	1	4
PM08	C06	Phe-Glu	nitrogen peptides	5	1	4
PM08	C07	Gln-Glu	nitrogen peptides	5	0	3
PM08	C08	Phe-Met	nitrogen peptides	4	1	4
PM08	C09	Phe-Tyr	nitrogen peptides	4	3	3
PM08	C10	Phe-Val	nitrogen peptides	5	1	4
PM08	C11	Pro-Arg	nitrogen peptides	7	3	4
PM08	C12	Pro-Asn	nitrogen peptides	7	4	3
PM08	D01	Pro-Glu	nitrogen peptides	4	1	4
PM08	D02	Pro-Ile	nitrogen peptides	4	1	4
PM08	D03	Pro-Lys	nitrogen peptides	4	1	2
PM08	D04	Pro-Ser	nitrogen peptides	5	1	4
PM08	D05	Pro-Trp	nitrogen peptides	2	1	2

PM08	D06	Pro-Val	nitrogen peptides	5	1	4
PM08	D07	Ser-Asn	nitrogen peptides	5	1	3
PM08	D08	Ser-Asp	nitrogen peptides	5	1	4
PM08	D09	Ser-Gln	nitrogen peptides	5	3	3
PM08	D10	Ser-Glu	nitrogen peptides	5	2	4
PM08	D11	Thr-Asp	nitrogen peptides	5	2	3
PM08	D12	Thr-Gln	nitrogen peptides	5	2	3
PM08	E01	Thr-Phe	nitrogen peptides	4	1	3
PM08	E02	Thr-Ser	nitrogen peptides	5	1	4
PM08	E03	Trp-Val	nitrogen peptides	4	1	4
PM08	E04	Tyr-Ile	nitrogen peptides	4	5	4
PM08	E05	Tyr-Val	nitrogen peptides	4	3	4
PM08	E06	Val-Ala	nitrogen peptides	5	1	4
PM08	E07	Val-Gln	nitrogen peptides	5	3	4
PM08	E08	Val-Glu	nitrogen peptides	4	3	3
PM08	E09	Val-Lys	nitrogen peptides	1	1	2
PM08	E10	Val-Met	nitrogen peptides	5	3	2
PM08	E11	Val-Phe	nitrogen peptides	5	1	4
PM08	E12	Val-Pro	nitrogen peptides	4	2	4
PM08	F01	Val-Ser	nitrogen peptides	5	1	3
PM08	F02	b-Ala-Ala	nitrogen peptides	2	1	2
PM08	F03	b-Ala-Gly	nitrogen peptides	1	1	2
PM08	F04	b-Ala-His	nitrogen peptides	4	1	2
PM08	F05	Met-b-Ala	nitrogen peptides	2	1	2
PM08	F06	b-Ala-Phe	nitrogen peptides	1	1	2
PM08	F07	D-Ala-D-Ala	nitrogen peptides	2	1	2
PM08	F08	D-Ala-Gly	nitrogen peptides	2	1	2
PM08	F09	D-Ala-Leu	nitrogen peptides	2	2	5
PM08	F10	D-Leu-D-Leu	nitrogen peptides	1	2	2

PM08	F11	D-Leu-Gly	nitrogen peptides	1	1	2
PM08	F12	D-Leu-Tyr	nitrogen peptides	1	1	1
PM08	G01	g-Glu-Gly	nitrogen peptides	1	1	2
PM08	G02	g-D-Glu-Gly	nitrogen peptides	4	1	2
PM08	G03	Gly-D-Ala	nitrogen peptides	1	1	2
PM08	G04	Gly-D-Asp	nitrogen peptides	5	1	2
PM08	G05	Gly-D-Ser	nitrogen peptides	1	1	2
PM08	G06	Gly-D-Thr	nitrogen peptides	1	1	2
PM08	G07	Gly-D-Val	nitrogen peptides	1	1	2
PM08	G08	Leu-b-Ala	nitrogen peptides	3	3	4
PM08	G09	Leu-D-Leu	nitrogen peptides	1	1	2
PM08	G10	Phe-b-Ala	nitrogen peptides	1	1	2
PM08	G11	Ala-Ala-Ala	nitrogen peptides	7	3	4
PM08	G12	D-Ala-Gly-Gly	nitrogen peptides	3	2	1
PM08	H01	Gly-Gly-Ala	nitrogen peptides	5	3	3
PM08	H02	Gly-Gly-D-Leu	nitrogen peptides	1	2	2
PM08	H03	Gly-Gly-Gly	nitrogen peptides	3	1	4
PM08	H04	Gly-Gly-Ile	nitrogen peptides	4	3	4
PM08	H05	Gly-Gly-Leu	nitrogen peptides	5	3	5
PM08	H06	Gly-Gly-Phe	nitrogen peptides	5	3	4
PM08	H07	Val-Tyr-Val	nitrogen peptides	4	1	2
PM08	H08	Gly-Phe-Phe	nitrogen peptides	4	2	3
PM08	H09	Leu-Gly-Gly	nitrogen peptides	5	3	4
PM08	H10	Leu-Leu-Leu	nitrogen peptides	3	3	2
PM08	H11	Phe-Gly-Gly	nitrogen peptides	5	2	4
PM08	H12	Tyr-Gly-Gly	nitrogen peptides	3	3	1
PM09	A01	1% NaCl	osmolites & ph	9	0	8
PM09	A02	2% NaCl	osmolites & ph	9	1	8
PM09	A03	3% NaCl	osmolites & ph	9	0	8

PM09	A04	4% NaCl	osmolites & ph	8	0	8
PM09	A05	5% NaCl	osmolites & ph	8	0	6
PM09	A06	5.5% NaCl	osmolites & ph	7	0	6
PM09	A07	6% NaCl	osmolites & ph	7	2	5
PM09	A08	6.5% NaCl	osmolites & ph	4	0	5
PM09	A09	7% NaCl	osmolites & ph	1	2	3
PM09	A10	8% NaCl	osmolites & ph	1	2	3
PM09	A11	9% NaCl	osmolites & ph	1	2	1
PM09	A12	10% NaCl	osmolites & ph	1	1	3
PM09	B01	6% NaCl	osmolites & ph	7	0	6
PM09	B02	6% NaCl + Betaine	osmolites & ph	7	0	5
PM09	B03	6% NaCl + NN Dimethyl Glycine	osmolites & ph	7	0	5
PM09	B04	6% NaCl + Sarcosine	osmolites & ph	7	1	6
PM09	B05	6% NaCl + Dimethyl Sulphonyl Propionate	osmolites & ph	7	0	6
PM09	B06	6% NaCl + MOPS	osmolites & ph	5	1	5
PM09	B07	6% NaCl + Ectoine	osmolites & ph	8	0	5
PM09	B08	6% NaCl + Choline	osmolites & ph	7	0	4
PM09	B09	6% NaCl + Phosphorylcholine	osmolites & ph	7	2	6
PM09	B10	6% NaCl + Creatine	osmolites & ph	7	2	5
PM09	B11	6% NaCl + Creatinine	osmolites & ph	7	2	5
PM09	B12	6% NaCl + L-Carnitine	osmolites & ph	8	2	3
PM09	C01	6% NaCl + KCl	osmolites & ph	7	0	4
PM09	C02	6% NaCl + L-Proline	osmolites & ph	7	0	5
PM09	C03	6% NaCl + N-Acetyl-L-Glutamine	osmolites & ph	7	0	5
PM09	C04	6% NaCl + b-Glutamic acid	osmolites & ph	7	2	5
PM09	C05	6% NaCl + g-Amino-N-Butyric acid	osmolites & ph	7	0	6
PM09	C06	6% NaCl + Glutathione	osmolites & ph	8	1	5
PM09	C07	6% NaCl + Glycerol	osmolites & ph	7	0	5
PM09	C08	6% NaCl + Trehalose	osmolites & ph	7	1	5

PM09	C09	6% NaCl + Trimethylamine-N-Oxide	osmolites & ph	7	0	5
PM09	C10	6% NaCl + Trimethylamine	osmolites & ph	7	0	5
PM09	C11	6% NaCl + Octopine	osmolites & ph	7	1	5
PM09	C12	6% NaCl + Trigonelline	osmolites & ph	8	2	1
PM09	D01	3% Potassium Chloride	osmolites & ph	9	0	8
PM09	D02	4% Potassium chloride	osmolites & ph	8	0	6
PM09	D03	5% Potassium Chloride	osmolites & ph	8	0	7
PM09	D04	6% Potassium chloride	osmolites & ph	8	1	7
PM09	D05	2% Sodium Sulfate	osmolites & ph	9	0	7
PM09	D06	3% Sodium Sulfate	osmolites & ph	9	0	7
PM09	D07	4% Sodium Sulfate	osmolites & ph	9	0	8
PM09	D08	5% Sodium Sulfate	osmolites & ph	9	0	8
PM09	D09	5% Ethylene Glycol	osmolites & ph	8	1	7
PM09	D10	10% Ethylene Glycol	osmolites & ph	8	5	7
PM09	D11	15% Ethylene Glycol	osmolites & ph	8	1	7
PM09	D12	20% Ethylene Glycol	osmolites & ph	8	2	6
PM09	E01	1% Sodium Formate	osmolites & ph	9	7	8
PM09	E02	2% Sodium Formate	osmolites & ph	9	1	8
PM09	E03	3% Sodium Formate	osmolites & ph	8	0	7
PM09	E04	4% Sodium Formate	osmolites & ph	8	1	7
PM09	E05	5% Sodium Formate	osmolites & ph	7	0	5
PM09	E06	6% Sodium Formate	osmolites & ph	7	2	5
PM09	E07	2% Urea	osmolites & ph	8	1	8
PM09	E08	3% Urea	osmolites & ph	4	0	5
PM09	E09	4% Urea	osmolites & ph	1	0	5
PM09	E10	5% Urea	osmolites & ph	1	2	1
PM09	E11	6% Urea	osmolites & ph	1	2	1
PM09	E12	7% Urea	osmolites & ph	3	2	1
PM09	F01	1% Sodium Lactate	osmolites & ph	9	1	7

PM09	F02	2% Sodium Lactate	osmolites & ph	8	1	7
PM09	F03	3% Sodium Lactate	osmolites & ph	9	0	7
PM09	F04	4% Sodium Lactate	osmolites & ph	9	0	7
PM09	F05	5% Sodium Lactate	osmolites & ph	9	0	7
PM09	F06	6% Sodium Lactate	osmolites & ph	8	0	7
PM09	F07	7% Sodium Lactate	osmolites & ph	8	0	7
PM09	F08	8% Sodium Lactate	osmolites & ph	8	0	7
PM09	F09	9% Sodium Lactate	osmolites & ph	8	0	7
PM09	F10	10% Sodium Lactate	osmolites & ph	8	2	7
PM09	F11	11% Sodium Lactate	osmolites & ph	8	2	7
PM09	F12	12% Sodium Lactate	osmolites & ph	9	3	8
PM09	G01	20mM Sodium Phosphate pH 7	osmolites & ph	9	1	7
PM09	G02	50mM Sodium Phosphate pH 7	osmolites & ph	9	2	7
PM09	G03	100mM Sodium Phosphate pH 7	osmolites & ph	9	0	7
PM09	G04	200mM Sodium Phosphate pH 7	osmolites & ph	9	0	7
PM09	G05	20mM Sodium Benzoate pH 5.2	osmolites & ph	8	1	5
PM09	G06	50mM Sodium Benzoate pH 5.2	osmolites & ph	4	0	2
PM09	G07	100mM Sodium Benzoate pH 5.2	osmolites & ph	1	1	2
PM09	G08	200mM Sodium Benzoate pH 5.2	osmolites & ph	1	0	1
PM09	G09	10mM Ammonium Sulfate pH 8	osmolites & ph	9	7	7
PM09	G10	20mM Ammonium Sulfate pH 8	osmolites & ph	9	7	7
PM09	G11	50mM Ammonium Sulfate pH 8	osmolites & ph	8	3	7
PM09	G12	100mM Ammonium Sulfate pH 8	osmolites & ph	9	7	8
PM09	H01	10mM Sodium Nitrate	osmolites & ph	9	2	6
PM09	H02	20mM Sodium Nitrate	osmolites & ph	9	1	6
PM09	H03	40mM Sodium Nitrate	osmolites & ph	8	1	6
PM09	H04	60mM Sodium Nitrate	osmolites & ph	9	2	6
PM09	H05	80mM Sodium Nitrate	osmolites & ph	9	2	6
PM09	H06	100mM Sodium Nitrate	osmolites & ph	9	2	7

PM09	H07	10mM Sodium Nitrite	osmolites & ph	8	1	6
PM09	H08	20mM Sodium Nitrite	osmolites & ph	9	2	6
PM09	H09	40mM Sodium Nitrite	osmolites & ph	7	2	5
PM09	H10	60mM Sodium Nitrite	osmolites & ph	7	2	4
PM09	H11	80mM Sodium Nitrite	osmolites & ph	5	2	2
PM09	H12	100mM Sodium Nitrite	osmolites & ph	7	2	2
PM10	A01	pH 3.5	osmolites & ph	7	3	6
PM10	A02	pH 4	osmolites & ph	7	7	6
PM10	A03	pH 4.5	osmolites & ph	8	1	8
PM10	A04	pH 5	osmolites & ph	8	1	8
PM10	A05	pH 5.5	osmolites & ph	8	1	8
PM10	A06	pH 6	osmolites & ph	8	1	8
PM10	A07	pH 7	osmolites & ph	9	1	8
PM10	A08	pH 8	osmolites & ph	9	1	8
PM10	A09	pH 8.5	osmolites & ph	8	1	8
PM10	A10	pH 9	osmolites & ph	8	2	8
PM10	A11	pH 9.5	osmolites & ph	8	2	8
PM10	A12	pH 10	osmolites & ph	7	2	8
PM10	B01	pH 4.5	osmolites & ph	8	1	6
PM10	B02	pH 4.5 + L-Alanine	osmolites & ph	8	7	7
PM10	B03	pH 4.5 + L-Arginine	osmolites & ph	8	0	7
PM10	B04	pH 4.5 + L-Asparagine	osmolites & ph	8	7	8
PM10	B05	pH 4.5 + L-Aspartic acid	osmolites & ph	9	7	8
PM10	B06	pH 4.5 + L-Glutamic acid	osmolites & ph	9	7	8
PM10	B07	pH 4.5 + L-Glutamine	osmolites & ph	8	7	8
PM10	B08	pH 4.5 + Glycine	osmolites & ph	9	1	8
PM10	B09	pH 4.5 + L-Histidine	osmolites & ph	8	3	8
PM10	B10	pH 4.5 + L-Isoleucine	osmolites & ph	8	3	6
PM10	B11	pH 4.5 + L-Leucine	osmolites & ph	8	7	8

PM10	B12	pH 4.5 + L-Lysine	osmolites & ph	9	3	8
PM10	C01	pH 4.5 + L-Methionine	osmolites & ph	8	7	6
PM10	C02	pH 4.5 + L-Phenylalanine	osmolites & ph	8	3	6
PM10	C03	pH 4.5 + L-Proline	osmolites & ph	8	5	8
PM10	C04	pH 4.5 + L-Serine	osmolites & ph	8	3	8
PM10	C05	pH 4.5 + L-Threonine	osmolites & ph	8	5	8
PM10	C06	pH 4.5 + L-Tryptophan	osmolites & ph	8	1	6
PM10	C07	pH 4.5 + L-Citrulline	osmolites & ph	9	1	8
PM10	C08	pH 4.5 + L-Valine	osmolites & ph	9	3	6
PM10	C09	pH 4.5 + Hydroxy-L-Proline	osmolites & ph	8	5	8
PM10	C10	pH 4.5 + L-Ornithine	osmolites & ph	9	5	8
PM10	C11	pH 4.5 + L-Homoarginine	osmolites & ph	8	7	6
PM10	C12	pH 4.5 + L-Homoserine	osmolites & ph	8	2	6
PM10	D01	pH 4.5 + Anthranilic acid	osmolites & ph	3	2	1
PM10	D02	pH 4.5 + L-Norleucine	osmolites & ph	7	0	5
PM10	D03	pH 4.5 + L-Norvaline	osmolites & ph	8	0	7
PM10	D04	pH 4.5 + a-Amino-N-Butyric acid	osmolites & ph	7	0	5
PM10	D05	pH 4.5 + p-Aminobenzoate	osmolites & ph	3	1	1
PM10	D06	pH 4.5 + L-Cysteic acid	osmolites & ph	9	3	8
PM10	D07	pH 4.5 + D-Lysine	osmolites & ph	6	0	3
PM10	D08	pH 4.5 + 5-Hydroxy-L-Lysine	osmolites & ph	8	0	8
PM10	D09	pH 4.5 + 5-Hydroxy-L-Tryptophan	osmolites & ph	8	5	8
PM10	D10	pH 4.5 + DL-Diamino-a,e-Pimelic acid	osmolites & ph	8	3	8
PM10	D11	pH 4.5 + Trimethylamine-N-Oxide	osmolites & ph	8	1	8
PM10	D12	pH 4.5 + Urea	osmolites & ph	9	2	8
PM10	E01	pH 9.5	osmolites & ph	7	2	6
PM10	E02	pH 9.5 + L-Alanine	osmolites & ph	8	0	6
PM10	E03	pH 9.5 + L-Arginine	osmolites & ph	8	0	5
PM10	E04	pH 9.5 + L-Asparagine	osmolites & ph	7	1	5

PM10	E05	pH 9.5 + L-Aspartic acid	osmolites & ph	8	0	6
PM10	E06	pH 9.5 + L-Glutamic acid	osmolites & ph	8	1	6
PM10	E07	pH 9.5 + L-Glutamine	osmolites & ph	7	0	8
PM10	E08	pH 9.5 + Glycine	osmolites & ph	5	1	6
PM10	E09	pH 9.5 + L-Histidine	osmolites & ph	3	2	1
PM10	E10	pH 9.5 + L-Isoleucine	osmolites & ph	5	2	4
PM10	E11	pH 9.5 + L-Leucine	osmolites & ph	7	2	2
PM10	E12	pH 9.5 + L-Lysine	osmolites & ph	8	2	6
PM10	F01	pH 9.5 + L-Methionine	osmolites & ph	4	2	3
PM10	F02	pH 9.5 + L-Phenylalanine	osmolites & ph	1	1	1
PM10	F03	pH 9.5 + L-Proline	osmolites & ph	8	3	6
PM10	F04	pH 9.5 + L-Serine	osmolites & ph	8	0	7
PM10	F05	pH 9.5 + L-Threonine	osmolites & ph	7	0	5
PM10	F06	pH 9.5 + L-Tryptophan	osmolites & ph	1	2	3
PM10	F07	pH 9.5 + L-Tyrosine	osmolites & ph	7	9	9
PM10	F08	pH 9.5 + L-Valine	osmolites & ph	3	2	1
PM10	F09	pH 9.5 + Hydroxy-L-Proline	osmolites & ph	7	2	6
PM10	F10	pH 9.5 + L-Ornithine	osmolites & ph	7	2	5
PM10	F11	pH 9.5 + L-Homoarginine	osmolites & ph	7	2	6
PM10	F12	pH 9.5 + L-Homoserine	osmolites & ph	5	2	5
PM10	G01	pH 9.5 + Anthranilic acid	osmolites & ph	3	2	2
PM10	G02	pH 9.5 + L-Norleucine	osmolites & ph	1	2	1
PM10	G03	pH 9.5 + L-Norvaline	osmolites & ph	8	2	6
PM10	G04	pH 9.5 + Agmatine	osmolites & ph	1	2	1
PM10	G05	pH 9.5 + Cadaverine	osmolites & ph	3	2	1
PM10	G06	pH 9.5 + Putrescine	osmolites & ph	5	2	4
PM10	G07	pH 9.5 + Histamine	osmolites & ph	1	2	1
PM10	G08	pH 9.5 + b-Phenylethylamine	osmolites & ph	3	2	2
PM10	G09	pH 9.5 + Tyramine	osmolites & ph	3	6	3

PM10	G10	pH 9.5 + Creatine	osmolites & ph	8	2	6
PM10	G11	pH 9.5 + Trimethylamine-N-Oxide	osmolites & ph	7	2	6
PM10	G12	pH 9.5 + Urea	osmolites & ph	8	2	5
PM10	H01	X-Caprylate	osmolites & ph	8	2	8
PM10	H02	X-a-D-Glucoside	osmolites & ph	8	1	7
PM10	H03	X-b-D-Glucoside	osmolites & ph	9	1	8
PM10	H04	X-a-D-Galactoside	osmolites & ph	9	6	8
PM10	H05	X-b-D-Galactoside	osmolites & ph	9	3	8
PM10	H06	X-a-D-Glucuronide	osmolites & ph	8	2	7
PM10	H07	X-b-D-Glucuronide	osmolites & ph	9	8	8
PM10	H08	X-b-D-Glucosaminide	osmolites & ph	9	8	7
PM10	H09	X-b-D-Galactosaminide	osmolites & ph	8	2	8
PM10	H10	X-a-D-Mannoside	osmolites & ph	9	8	8
PM10	H11	X-PO4	osmolites & ph	8	2	8
PM10	H12	X-SO4	osmolites & ph	8	2	8
PM11	A01	Amikacin	chemicals	9	8	8
PM11	A02	Amikacin	chemicals	9	8	8
PM11	A03	Amikacin	chemicals	9	1	8
PM11	A04	Amikacin	chemicals	9	0	8
PM11	A05	Chlortetracycline	chemicals	9	7	8
PM11	A06	Chlortetracycline	chemicals	9	7	8
PM11	A07	Chlortetracycline	chemicals	9	2	8
PM11	A08	Chlortetracycline	chemicals	8	2	8
PM11	A09	Lincomycin	chemicals	9	7	8
PM11	A10	Lincomycin	chemicals	9	7	8
PM11	A11	Lincomycin	chemicals	5	5	5
PM11	A12	Lincomycin	chemicals	6	2	3
PM11	B01	Amoxicillin	chemicals	9	8	8
PM11	B02	Amoxicillin	chemicals	9	7	7

PM11	B03	Amoxicillin	chemicals	9	3	7
PM11	B04	Amoxicillin	chemicals	9	0	8
PM11	B05	Cloxacillin	chemicals	9	7	7
PM11	B06	Cloxacillin	chemicals	9	5	8
PM11	B07	Cloxacillin	chemicals	9	5	8
PM11	B08	Cloxacillin	chemicals	9	0	8
PM11	B09	Lomefloxacin	chemicals	9	5	8
PM11	B10	Lomefloxacin	chemicals	9	5	8
PM11	B11	Lomefloxacin	chemicals	9	5	8
PM11	B12	Lomefloxacin	chemicals	9	2	8
PM11	C01	Bleomycin	chemicals	9	8	8
PM11	C02	Bleomycin	chemicals	9	5	7
PM11	C03	Bleomycin	chemicals	9	5	7
PM11	C04	Bleomycin	chemicals	8	5	7
PM11	C05	Colistin	chemicals	9	5	7
PM11	C06	Colistin	chemicals	9	5	8
PM11	C07	Colistin	chemicals	9	2	7
PM11	C08	Colistin	chemicals	1	0	1
PM11	C09	Minocycline	chemicals	9	0	8
PM11	C10	Minocycline	chemicals	9	2	8
PM11	C11	Minocycline	chemicals	9	2	6
PM11	C12	Minocycline	chemicals	1	2	1
PM11	D01	Capreomycin	chemicals	9	8	8
PM11	D02	Capreomycin	chemicals	9	3	7
PM11	D03	Capreomycin	chemicals	9	2	7
PM11	D04	Capreomycin	chemicals	9	7	7
PM11	D05	Demeclocycline	chemicals	9	0	7
PM11	D06	Demeclocycline	chemicals	9	0	7
PM11	D07	Demeclocycline	chemicals	9	0	8

PM11	D08	Demeclocycline	chemicals	1	0	4
PM11	D09	Nafcillin	chemicals	9	2	7
PM11	D10	Nafcillin	chemicals	9	2	8
PM11	D11	Nafcillin	chemicals	9	2	8
PM11	D12	Nafcillin	chemicals	9	2	8
PM11	E01	Cefazolin	chemicals	9	8	8
PM11	E02	Cefazolin	chemicals	9	5	7
PM11	E03	Cefazolin	chemicals	9	5	7
PM11	E04	Cefazolin	chemicals	9	5	7
PM11	E05	Enoxacin	chemicals	9	5	7
PM11	E06	Enoxacin	chemicals	9	3	7
PM11	E07	Enoxacin	chemicals	9	0	7
PM11	E08	Enoxacin	chemicals	9	0	7
PM11	E09	Nalidixic acid	chemicals	9	5	7
PM11	E10	Nalidixic acid	chemicals	9	5	8
PM11	E11	Nalidixic acid	chemicals	9	5	7
PM11	E12	Nalidixic acid	chemicals	9	8	8
PM11	F01	Chloramphenicol	chemicals	9	8	7
PM11	F02	Chloramphenicol	chemicals	9	7	7
PM11	F03	Chloramphenicol	chemicals	9	7	7
PM11	F04	Chloramphenicol	chemicals	7	0	4
PM11	F05	Erythromycin	chemicals	9	5	7
PM11	F06	Erythromycin	chemicals	9	3	7
PM11	F07	Erythromycin	chemicals	9	2	7
PM11	F08	Erythromycin	chemicals	7	2	1
PM11	F09	Neomycin	chemicals	9	5	7
PM11	F10	Neomycin	chemicals	9	2	7
PM11	F11	Neomycin	chemicals	9	2	7
PM11	F12	Neomycin	chemicals	9	2	8

PM11	G01	Ceftriaxone	chemicals	9	8	8
PM11	G02	Ceftriaxone	chemicals	9	8	7
PM11	G03	Ceftriaxone	chemicals	9	5	7
PM11	G04	Ceftriaxone	chemicals	9	5	7
PM11	G05	Gentamicin	chemicals	9	5	7
PM11	G06	Gentamicin	chemicals	9	5	7
PM11	G07	Gentamicin	chemicals	9	3	7
PM11	G08	Gentamicin	chemicals	9	2	7
PM11	G09	Potassium tellurite	chemicals	9	5	7
PM11	G10	Potassium tellurite	chemicals	9	5	7
PM11	G11	Potassium tellurite	chemicals	9	5	8
PM11	G12	Potassium tellurite	chemicals	9	5	8
PM11	H01	Cephalothin	chemicals	9	8	7
PM11	H02	Cephalothin	chemicals	9	8	7
PM11	H03	Cephalothin	chemicals	9	5	7
PM11	H04	Cephalothin	chemicals	9	8	7
PM11	H05	Kanamycin	chemicals	9	8	7
PM11	H06	Kanamycin	chemicals	9	8	7
PM11	H07	Kanamycin	chemicals	9	2	7
PM11	H08	Kanamycin	chemicals	9	2	7
PM11	H09	Ofloxacin	chemicals	9	6	7
PM11	H10	Ofloxacin	chemicals	9	7	7
PM11	H11	Ofloxacin	chemicals	9	8	7
PM11	H12	Ofloxacin	chemicals	9	8	8
PM12	A01	Penicillin G	chemicals	9	8	8
PM12	A02	Penicillin G	chemicals	9	8	8
PM12	A03	Penicillin G	chemicals	9	8	8
PM12	A04	Penicillin G	chemicals	9	0	8
PM12	A05	Tetracycline	chemicals	9	5	8

PM12	A06	Tetracycline	chemicals	9	5	8
PM12	A07	Tetracycline	chemicals	9	3	8
PM12	A08	Tetracycline	chemicals	9	2	8
PM12	A09	Carbenicillin	chemicals	9	5	8
PM12	A10	Carbenicillin	chemicals	9	5	8
PM12	A11	Carbenicillin	chemicals	9	2	8
PM12	A12	Carbenicillin	chemicals	9	2	8
PM12	B01	Oxacillin	chemicals	9	8	8
PM12	B02	Oxacillin	chemicals	9	8	7
PM12	B03	Oxacillin	chemicals	9	8	7
PM12	B04	Oxacillin	chemicals	8	0	8
PM12	B05	Penimepicycline	chemicals	9	8	7
PM12	B06	Penimepicycline	chemicals	9	3	7
PM12	B07	Penimepicycline	chemicals	9	3	8
PM12	B08	Penimepicycline	chemicals	9	2	8
PM12	B09	Polymyxin B	chemicals	9	5	8
PM12	B10	Polymyxin B	chemicals	9	5	7
PM12	B11	Polymyxin B	chemicals	9	5	8
PM12	B12	Polymyxin B	chemicals	9	2	8
PM12	C01	Paromomycin	chemicals	9	5	7
PM12	C02	Paromomycin	chemicals	9	8	7
PM12	C03	Paromomycin	chemicals	9	8	7
PM12	C04	Paromomycin	chemicals	9	0	7
PM12	C05	Vancomycin	chemicals	9	8	7
PM12	C06	Vancomycin	chemicals	9	3	7
PM12	C07	Vancomycin	chemicals	9	1	7
PM12	C08	Vancomycin	chemicals	9	0	7
PM12	C09	DL-Serine hydroxamate	chemicals	9	8	8
PM12	C10	DL-Serine hydroxamate	chemicals	9	3	7

PM12	C11	DL-Serine hydroxamate	chemicals	8	2	8
PM12	C12	DL-Serine hydroxamate	chemicals	9	2	7
PM12	D01	Sisomicin	chemicals	9	5	7
PM12	D02	Sisomicin	chemicals	9	3	7
PM12	D03	Sisomicin	chemicals	9	7	7
PM12	D04	Sisomicin	chemicals	9	7	7
PM12	D05	Sulfamethazine	chemicals	9	7	7
PM12	D06	Sulfamethazine	chemicals	9	7	7
PM12	D07	Sulfamethazine	chemicals	9	5	7
PM12	D08	Sulfamethazine	chemicals	9	5	7
PM12	D09	Novobiocin	chemicals	9	3	7
PM12	D10	Novobiocin	chemicals	9	3	7
PM12	D11	Novobiocin	chemicals	9	2	8
PM12	D12	Novobiocin	chemicals	8	6	6
PM12	E01	2,4-Diamino-6,7-diisopropylpteridine	chemicals	9	8	7
PM12	E02	2,4-Diamino-6,7-diisopropylpteridine	chemicals	9	7	7
PM12	E03	2,4-Diamino-6,7-diisopropylpteridine	chemicals	9	7	7
PM12	E04	2,4-Diamino-6,7-diisopropylpteridine	chemicals	9	5	7
PM12	E05	Sulfadiazine	chemicals	9	7	7
PM12	E06	Sulfadiazine	chemicals	9	5	7
PM12	E07	Sulfadiazine	chemicals	9	7	7
PM12	E08	Sulfadiazine	chemicals	8	5	7
PM12	E09	Benzethonium Chloride	chemicals	9	7	7
PM12	E10	Benzethonium Chloride	chemicals	9	8	7
PM12	E11	Benzethonium Chloride	chemicals	6	2	1
PM12	E12	Benzethonium Chloride	chemicals	3	2	1
PM12	F01	Tobramycin	chemicals	9	3	7
PM12	F02	Tobramycin	chemicals	9	8	7
PM12	F03	Tobramycin	chemicals	9	7	7

PM12	F04	Tobramycin	chemicals	9	7	7
PM12	F05	Sulfathiazole	chemicals	9	5	7
PM12	F06	Sulfathiazole	chemicals	9	7	7
PM12	F07	Sulfathiazole	chemicals	9	3	7
PM12	F08	Sulfathiazole	chemicals	9	2	7
PM12	F09	5-Fluoroorotic acid	chemicals	9	8	7
PM12	F10	5-Fluoroorotic acid	chemicals	9	7	7
PM12	F11	5-Fluoroorotic acid	chemicals	9	2	7
PM12	F12	5-Fluoroorotic acid	chemicals	9	8	8
PM12	G01	Spectinomycin	chemicals	9	8	7
PM12	G02	Spectinomycin	chemicals	9	8	7
PM12	G03	Spectinomycin	chemicals	9	8	7
PM12	G04	Spectinomycin	chemicals	9	2	7
PM12	G05	Sulfamethoxazole	chemicals	9	5	7
PM12	G06	Sulfamethoxazole	chemicals	9	5	7
PM12	G07	Sulfamethoxazole	chemicals	9	5	7
PM12	G08	Sulfamethoxazole	chemicals	9	5	7
PM12	G09	L-Aspartic-b-hydroxamate	chemicals	9	5	7
PM12	G10	L-Aspartic-b-hydroxamate	chemicals	9	5	7
PM12	G11	L-Aspartic-b-hydroxamate	chemicals	8	5	7
PM12	G12	L-Aspartic-b-hydroxamate	chemicals	8	2	7
PM12	H01	Spiramycin	chemicals	9	2	7
PM12	H02	Spiramycin	chemicals	9	8	7
PM12	H03	Spiramycin	chemicals	8	5	5
PM12	H04	Spiramycin	chemicals	8	2	1
PM12	H05	Rifampicin	chemicals	9	8	7
PM12	H06	Rifampicin	chemicals	9	8	7
PM12	H07	Rifampicin	chemicals	9	2	7
PM12	H08	Rifampicin	chemicals	9	2	8

PM12	H09	Dodecyltrimethyl ammonium bromide	chemicals	9	8	7
PM12	H10	Dodecyltrimethyl ammonium bromide	chemicals	9	5	7
PM12	H11	Dodecyltrimethyl ammonium bromide	chemicals	6	3	5
PM12	H12	Dodecyltrimethyl ammonium bromide	chemicals	3	2	1
PM13	A01	Ampicillin, Sodium salt	chemicals	9	8	8
PM13	A02	Ampicillin, Sodium salt	chemicals	9	8	8
PM13	A03	Ampicillin, Sodium salt	chemicals	9	7	8
PM13	A04	Ampicillin, Sodium salt	chemicals	9	5	8
PM13	A05	Dequalinium chloride	chemicals	9	8	8
PM13	A06	Dequalinium chloride	chemicals	9	1	8
PM13	A07	Dequalinium chloride	chemicals	9	8	8
PM13	A08	Dequalinium chloride	chemicals	9	2	8
PM13	A09	Nickel chloride	chemicals	9	5	8
PM13	A10	Nickel chloride	chemicals	9	7	8
PM13	A11	Nickel chloride	chemicals	9	8	8
PM13	A12	Nickel chloride	chemicals	9	3	8
PM13	B01	Azlocillin	chemicals	9	8	8
PM13	B02	Azlocillin	chemicals	9	8	7
PM13	B03	Azlocillin	chemicals	9	1	7
PM13	B04	Azlocillin	chemicals	9	2	8
PM13	B05	2,2`-Dipyridyl	chemicals	6	0	2
PM13	B06	2,2`-Dipyridyl	chemicals	1	2	2
PM13	B07	2,2`-Dipyridyl	chemicals	1	0	2
PM13	B08	2,2`-Dipyridyl	chemicals	1	2	1
PM13	B09	Oxolinic acid	chemicals	9	5	8
PM13	B10	Oxolinic acid	chemicals	9	5	8
PM13	B11	Oxolinic acid	chemicals	9	5	8
PM13	B12	Oxolinic acid	chemicals	9	3	8
PM13	C01	6-Mercaptopurine monohydrate	chemicals	9	8	7

PM13	C02	6-Mercaptopurine monohydrate	chemicals	8	8	7
PM13	C03	6-Mercaptopurine monohydrate	chemicals	8	3	7
PM13	C04	6-Mercaptopurine monohydrate	chemicals	8	7	5
PM13	C05	Doxycycline	chemicals	9	8	8
PM13	C06	Doxycycline	chemicals	9	2	8
PM13	C07	Doxycycline	chemicals	8	2	5
PM13	C08	Doxycycline	chemicals	7	0	2
PM13	C09	Potassium chromate	chemicals	9	3	8
PM13	C10	Potassium chromate	chemicals	9	2	8
PM13	C11	Potassium chromate	chemicals	8	2	8
PM13	C12	Potassium chromate	chemicals	9	2	8
PM13	D01	Cefuroxime	chemicals	9	8	8
PM13	D02	Cefuroxime	chemicals	9	5	7
PM13	D03	Cefuroxime	chemicals	9	5	7
PM13	D04	Cefuroxime	chemicals	9	3	7
PM13	D05	5-Fluorouracil	chemicals	9	1	7
PM13	D06	5-Fluorouracil	chemicals	8	1	7
PM13	D07	5-Fluorouracil	chemicals	8	0	7
PM13	D08	5-Fluorouracil	chemicals	6	1	6
PM13	D09	Rolitetracycline	chemicals	9	5	7
PM13	D10	Rolitetracycline	chemicals	9	7	8
PM13	D11	Rolitetracycline	chemicals	9	2	8
PM13	D12	Rolitetracycline	chemicals	9	2	8
PM13	E01	Cytosine-1-beta-D-arabinofuranoside	chemicals	9	8	8
PM13	E02	Cytosine-1-beta-D-arabinofuranoside	chemicals	9	8	7
PM13	E03	Cytosine-1-beta-D-arabinofuranoside	chemicals	9	7	7
PM13	E04	Cytosine-1-beta-D-arabinofuranoside	chemicals	8	3	8
PM13	E05	Geneticin disulfate (G418)	chemicals	9	3	7
PM13	E06	Geneticin disulfate (G418)	chemicals	9	3	8

PM13	E07	Geneticin disulfate (G418)	chemicals	9	2	8
PM13	E08	Geneticin disulfate (G418)	chemicals	9	2	8
PM13	E09	Ruthenium red	chemicals	9	3	8
PM13	E10	Ruthenium red	chemicals	9	3	8
PM13	E11	Ruthenium red	chemicals	9	2	8
PM13	E12	Ruthenium red	chemicals	9	6	8
PM13	F01	Cesium chloride	chemicals	9	8	8
PM13	F02	Cesium chloride	chemicals	8	7	7
PM13	F03	Cesium chloride	chemicals	9	7	7
PM13	F04	Cesium chloride	chemicals	9	3	8
PM13	F05	Glycine HCl	chemicals	9	5	7
PM13	F06	Glycine HCl	chemicals	9	3	7
PM13	F07	Glycine HCl	chemicals	9	3	7
PM13	F08	Glycine HCl	chemicals	9	2	7
PM13	F09	Thallium (I) acetate	chemicals	9	5	8
PM13	F10	Thallium (I) acetate	chemicals	8	5	7
PM13	F11	Thallium (I) acetate	chemicals	8	5	6
PM13	F12	Thallium (I) acetate	chemicals	3	2	2
PM13	G01	Cobalt (II) chloride	chemicals	9	8	8
PM13	G02	Cobalt (II) chloride	chemicals	9	5	7
PM13	G03	Cobalt (II) chloride	chemicals	9	5	8
PM13	G04	Cobalt (II) chloride	chemicals	9	8	8
PM13	G05	Manganese chloride	chemicals	9	8	7
PM13	G06	Manganese chloride	chemicals	9	6	8
PM13	G07	Manganese chloride	chemicals	9	8	8
PM13	G08	Manganese chloride	chemicals	9	9	8
PM13	G09	Trifluoperazine	chemicals	8	8	7
PM13	G10	Trifluoperazine	chemicals	8	7	8
PM13	G11	Trifluoperazine	chemicals	6	5	8

PM13	G12	Trifluoperazine	chemicals	8	5	8
PM13	H01	Cupric chloride	chemicals	9	8	8
PM13	H02	Cupric chloride	chemicals	9	8	8
PM13	H03	Cupric chloride	chemicals	9	3	8
PM13	H04	Cupric chloride	chemicals	8	7	8
PM13	H05	Moxalactam	chemicals	9	8	8
PM13	H06	Moxalactam	chemicals	9	8	7
PM13	H07	Moxalactam	chemicals	9	5	8
PM13	H08	Moxalactam	chemicals	9	5	8
PM13	H09	Tylosin	chemicals	9	8	8
PM13	H10	Tylosin	chemicals	9	8	8
PM13	H11	Tylosin	chemicals	7	2	8
PM13	H12	Tylosin	chemicals	5	7	6
PM14	A01	Acriflavine	chemicals	9	8	8
PM14	A02	Acriflavine	chemicals	9	8	8
PM14	A03	Acriflavine	chemicals	9	8	8
PM14	A04	Acriflavine	chemicals	9	6	8
PM14	A05	Furaltadone	chemicals	9	5	8
PM14	A06	Furaltadone	chemicals	9	5	8
PM14	A07	Furaltadone	chemicals	9	5	8
PM14	A08	Furaltadone	chemicals	9	5	8
PM14	A09	Sanguinarine chloride	chemicals	9	7	8
PM14	A10	Sanguinarine chloride	chemicals	9	7	8
PM14	A11	Sanguinarine chloride	chemicals	9	5	8
PM14	A12	Sanguinarine chloride	chemicals	9	3	8
PM14	B01	9-Aminoacridine	chemicals	9	8	8
PM14	B02	9-Aminoacridine	chemicals	8	3	7
PM14	B03	9-Aminoacridine	chemicals	7	0	3
PM14	B04	9-Aminoacridine	chemicals	3	0	1

PM14	B05	Fusaric acid	chemicals	9	8	7
PM14	B06	Fusaric acid	chemicals	9	8	8
PM14	B07	Fusaric acid	chemicals	9	5	8
PM14	B08	Fusaric acid	chemicals	9	5	7
PM14	B09	Sodium Arsenate	chemicals	9	8	8
PM14	B10	Sodium Arsenate	chemicals	9	5	8
PM14	B11	Sodium Arsenate	chemicals	9	5	8
PM14	B12	Sodium Arsenate	chemicals	7	5	5
PM14	C01	Boric acid	chemicals	9	8	7
PM14	C02	Boric acid	chemicals	8	3	7
PM14	C03	Boric acid	chemicals	7	1	5
PM14	C04	Boric acid	chemicals	3	2	1
PM14	C05	1-Hydroxypyridine-2-thione (pyrithione)	chemicals	9	7	7
PM14	C06	1-Hydroxypyridine-2-thione (pyrithione)	chemicals	9	5	7
PM14	C07	1-Hydroxypyridine-2-thione (pyrithione)	chemicals	9	5	7
PM14	C08	1-Hydroxypyridine-2-thione (pyrithione)	chemicals	9	0	7
PM14	C09	Sodium Cyanate	chemicals	9	8	8
PM14	C10	Sodium Cyanate	chemicals	9	7	8
PM14	C11	Sodium Cyanate	chemicals	8	8	8
PM14	C12	Sodium Cyanate	chemicals	8	2	4
PM14	D01	Cadmium chloride	chemicals	9	2	7
PM14	D02	Cadmium chloride	chemicals	8	7	6
PM14	D03	Cadmium chloride	chemicals	8	5	6
PM14	D04	Cadmium chloride	chemicals	5	3	4
PM14	D05	Iodoacetic acid	chemicals	9	7	7
PM14	D06	Iodoacetic acid	chemicals	9	1	7
PM14	D07	Iodoacetic acid	chemicals	9	0	7
PM14	D08	Iodoacetic acid	chemicals	9	7	7
PM14	D09	Sodium Dichromate	chemicals	9	5	7

PM14	D10	Sodium Dichromate	chemicals	9	7	7
PM14	D11	Sodium Dichromate	chemicals	9	2	8
PM14	D12	Sodium Dichromate	chemicals	9	8	8
PM14	E01	Cefoxitin	chemicals	9	8	8
PM14	E02	Cefoxitin	chemicals	9	5	7
PM14	E03	Cefoxitin	chemicals	9	8	7
PM14	E04	Cefoxitin	chemicals	9	3	7
PM14	E05	Nitrofurantoin	chemicals	9	7	7
PM14	E06	Nitrofurantoin	chemicals	9	5	7
PM14	E07	Nitrofurantoin	chemicals	9	7	7
PM14	E08	Nitrofurantoin	chemicals	9	5	7
PM14	E09	Sodium metaborate	chemicals	9	7	7
PM14	E10	Sodium metaborate	chemicals	9	7	7
PM14	E11	Sodium metaborate	chemicals	7	2	4
PM14	E12	Sodium metaborate	chemicals	3	3	3
PM14	F01	Chloramphenicol	chemicals	9	8	7
PM14	F02	Chloramphenicol	chemicals	9	3	7
PM14	F03	Chloramphenicol	chemicals	9	7	7
PM14	F04	Chloramphenicol	chemicals	9	1	7
PM14	F05	Piperacillin	chemicals	9	8	7
PM14	F06	Piperacillin	chemicals	9	5	7
PM14	F07	Piperacillin	chemicals	9	8	7
PM14	F08	Piperacillin	chemicals	9	5	7
PM14	F09	Sodium metavanadate	chemicals	1	1	1
PM14	F10	Sodium metavanadate	chemicals	1	1	2
PM14	F11	Sodium metavanadate	chemicals	1	3	2
PM14	F12	Sodium metavanadate	chemicals	1	3	2
PM14	G01	Chelerythrine chloride	chemicals	9	8	7
PM14	G02	Chelerythrine chloride	chemicals	9	8	7

PM14	G03	Chelerythrine chloride	chemicals	8	8	7
PM14	G04	Chelerythrine chloride	chemicals	8	2	7
PM14	G05	Carbenicillin	chemicals	9	8	7
PM14	G06	Carbenicillin	chemicals	9	8	7
PM14	G07	Carbenicillin	chemicals	9	8	7
PM14	G08	Carbenicillin	chemicals	9	8	7
PM14	G09	Sodium Nitrite	chemicals	9	8	7
PM14	G10	Sodium Nitrite	chemicals	9	2	8
PM14	G11	Sodium Nitrite	chemicals	7	3	6
PM14	G12	Sodium Nitrite	chemicals	1	2	1
PM14	H01	Ethylene Glycol-bis(b-Aminoethyl ether)-NNN`N`-Tetraacetic Acid	chemicals	9	8	7
PM14	H02	Ethylene Glycol-bis(b-Aminoethyl ether)-NNN`N`-Tetraacetic Acid	chemicals	9	8	7
PM14	H03	Ethylene Glycol-bis(b-Aminoethyl ether)-NNN`N`-Tetraacetic Acid	chemicals	9	7	7
PM14	H04	Ethylene Glycol-bis(b-Aminoethyl ether)-NNN`N`-Tetraacetic Acid	chemicals	9	2	7
PM14	H05	Promethazine	chemicals	9	8	7
PM14	H06	Promethazine	chemicals	6	8	7
PM14	H07	Promethazine	chemicals	5	2	4
PM14	H08	Promethazine	chemicals	1	2	1
PM14	H09	Sodium orthovanadate	chemicals	1	2	2
PM14	H10	Sodium orthovanadate	chemicals	1	2	1
PM14	H11	Sodium orthovanadate	chemicals	1	2	1
PM14	H12	Sodium orthovanadate	chemicals	1	2	1
PM15	A01	Procaine	chemicals	9	8	8
PM15	A02	Procaine	chemicals	9	1	6
PM15	A03	Procaine	chemicals	1	1	1
PM15	A04	Procaine	chemicals	1	0	1
PM15	A05	Guanidine hydrochloride	chemicals	9	8	8
PM15	A06	Guanidine hydrochloride	chemicals	9	7	8
PM15	A07	Guanidine hydrochloride	chemicals	4	3	3

PM15	A08	Guanidine hydrochloride	chemicals	1	0	1
PM15	A09	Cefmetazole	chemicals	9	5	8
PM15	A10	Cefmetazole	chemicals	9	5	8
PM15	A11	Cefmetazole	chemicals	9	8	8
PM15	A12	Cefmetazole	chemicals	9	5	8
PM15	B01	D-Cycloserine	chemicals	9	8	8
PM15	B02	D-Cycloserine	chemicals	9	5	7
PM15	B03	D-Cycloserine	chemicals	9	7	8
PM15	B04	D-Cycloserine	chemicals	9	5	8
PM15	B05	EDTA	chemicals	9	8	7
PM15	B06	EDTA	chemicals	9	3	8
PM15	B07	EDTA	chemicals	9	1	8
PM15	B08	EDTA	chemicals	8	1	1
PM15	B09	5,7-Dichloro-8-hydroxyquinaldine	chemicals	9	5	8
PM15	B10	5,7-Dichloro-8-hydroxyquinaldine	chemicals	9	5	7
PM15	B11	5,7-Dichloro-8-hydroxyquinaldine	chemicals	9	5	8
PM15	B12	5,7-Dichloro-8-hydroxyquinaldine	chemicals	9	3	8
PM15	C01	5,7-Dichloro-8-hydroxyquinoline	chemicals	9	8	7
PM15	C02	5,7-Dichloro-8-hydroxyquinoline	chemicals	9	5	7
PM15	C03	5,7-Dichloro-8-hydroxyquinoline	chemicals	9	7	7
PM15	C04	5,7-Dichloro-8-hydroxyquinoline	chemicals	9	7	7
PM15	C05	Fusidic acid, sodium salt	chemicals	9	3	7
PM15	C06	Fusidic acid, sodium salt	chemicals	9	8	7
PM15	C07	Fusidic acid, sodium salt	chemicals	8	5	7
PM15	C08	Fusidic acid, sodium salt	chemicals	6	2	3
PM15	C09	1,10-Phenanthroline Monohydrate	chemicals	9	5	7
PM15	C10	1,10-Phenanthroline Monohydrate	chemicals	9	5	7
PM15	C11	1,10-Phenanthroline Monohydrate	chemicals	9	3	8
PM15	C12	1,10-Phenanthroline Monohydrate	chemicals	8	2	5

PM15	D01	Phleomycin	chemicals	9	8	8
PM15	D02	Phleomycin	chemicals	8	5	7
PM15	D03	Phleomycin	chemicals	7	5	1
PM15	D04	Phleomycin	chemicals	1	3	1
PM15	D05	Domiphen bromide	chemicals	9	7	7
PM15	D06	Domiphen bromide	chemicals	9	7	7
PM15	D07	Domiphen bromide	chemicals	8	1	7
PM15	D08	Domiphen bromide	chemicals	1	1	1
PM15	D09	Nordihydroguaiaretic acid	chemicals	9	7	7
PM15	D10	Nordihydroguaiaretic acid	chemicals	9	7	8
PM15	D11	Nordihydroguaiaretic acid	chemicals	9	7	8
PM15	D12	Nordihydroguaiaretic acid	chemicals	9	6	8
PM15	E01	Alexidine	chemicals	9	8	7
PM15	E02	Alexidine	chemicals	9	3	7
PM15	E03	Alexidine	chemicals	8	1	7
PM15	E04	Alexidine	chemicals	1	1	1
PM15	E05	5-Nitro-2-furaldehyde semicarbazone (Nitrofurazone)	chemicals	9	7	7
PM15	E06	5-Nitro-2-furaldehyde semicarbazone (Nitrofurazone)	chemicals	9	7	7
PM15	E07	5-Nitro-2-furaldehyde semicarbazone (Nitrofurazone)	chemicals	9	7	7
PM15	E08	5-Nitro-2-furaldehyde semicarbazone (Nitrofurazone)	chemicals	8	3	2
PM15	E09	Methyl viologen	chemicals	9	5	8
PM15	E10	Methyl viologen	chemicals	8	5	7
PM15	E11	Methyl viologen	chemicals	6	2	1
PM15	E12	Methyl viologen	chemicals	1	2	1
PM15	F01	3,4-Dimethoxybenzyl alcohol	chemicals	9	8	7
PM15	F02	3,4-Dimethoxybenzyl alcohol	chemicals	8	7	7
PM15	F03	3,4-Dimethoxybenzyl alcohol	chemicals	1	1	1
PM15	F04	3,4-Dimethoxybenzyl alcohol	chemicals	1	1	1
PM15	F05	Oleandomycin, phosphate salt	chemicals	9	7	7

PM15	F06	Oleandomycin, phosphate salt	chemicals	9	3	7
PM15	F07	Oleandomycin, phosphate salt	chemicals	8	5	7
PM15	F08	Oleandomycin, phosphate salt	chemicals	8	3	7
PM15	F09	Puromycin	chemicals	9	7	8
PM15	F10	Puromycin	chemicals	9	7	7
PM15	F11	Puromycin	chemicals	9	3	8
PM15	F12	Puromycin	chemicals	9	5	8
PM15	G01	Carbonyl-cyanide m-chlorophenylhydrazone (CCCP)	chemicals	8	8	7
PM15	G02	Carbonyl-cyanide m-chlorophenylhydrazone (CCCP)	chemicals	8	8	7
PM15	G03	Carbonyl-cyanide m-chlorophenylhydrazone (CCCP)	chemicals	8	6	8
PM15	G04	Carbonyl-cyanide m-chlorophenylhydrazone (CCCP)	chemicals	8	6	6
PM15	G05	Sodium Azide	chemicals	9	8	7
PM15	G06	Sodium Azide	chemicals	1	2	1
PM15	G07	Sodium Azide	chemicals	1	1	1
PM15	G08	Sodium Azide	chemicals	1	1	2
PM15	G09	Menadione, sodium bisulfite	chemicals	9	5	8
PM15	G10	Menadione, sodium bisulfite	chemicals	9	7	8
PM15	G11	Menadione, sodium bisulfite	chemicals	8	6	8
PM15	G12	Menadione, sodium bisulfite	chemicals	7	6	6
PM15	H01	2-Nitroimidazole	chemicals	9	8	7
PM15	H02	2-Nitroimidazole	chemicals	9	8	7
PM15	H03	2-Nitroimidazole	chemicals	9	1	7
PM15	H04	2-Nitroimidazole	chemicals	8	2	2
PM15	H05	Hydroxyurea	chemicals	9	8	7
PM15	H06	Hydroxyurea	chemicals	9	7	7
PM15	H07	Hydroxyurea	chemicals	5	2	4
PM15	H08	Hydroxyurea	chemicals	1	2	1
PM15	H09	Zinc chloride	chemicals	9	5	8
PM15	H10	Zinc chloride	chemicals	9	8	7

PM15	H11	Zinc chloride	chemicals	9	8	8
PM15	H12	Zinc chloride	chemicals	9	6	8
PM16	A01	Cefotaxime	chemicals	9	8	8
PM16	A02	Cefotaxime	chemicals	9	8	8
PM16	A03	Cefotaxime	chemicals	9	7	7
PM16	A04	Cefotaxime	chemicals	9	8	8
PM16	A05	Phosphomycin	chemicals	9	8	8
PM16	A06	Phosphomycin	chemicals	9	8	7
PM16	A07	Phosphomycin	chemicals	9	8	8
PM16	A08	Phosphomycin	chemicals	9	5	7
PM16	A09	5-Chloro-7-iodo-8-hydroxy-quinoline	chemicals	9	5	7
PM16	A10	5-Chloro-7-iodo-8-hydroxy-quinoline	chemicals	9	5	8
PM16	A11	5-Chloro-7-iodo-8-hydroxy-quinoline	chemicals	9	5	8
PM16	A12	5-Chloro-7-iodo-8-hydroxy-quinoline	chemicals	9	3	8
PM16	B01	Norfloxacin	chemicals	8	8	8
PM16	B02	Norfloxacin	chemicals	9	7	7
PM16	B03	Norfloxacin	chemicals	9	7	7
PM16	B04	Norfloxacin	chemicals	9	3	7
PM16	B05	Sulfanilamide	chemicals	9	7	7
PM16	B06	Sulfanilamide	chemicals	9	5	7
PM16	B07	Sulfanilamide	chemicals	9	7	7
PM16	B08	Sulfanilamide	chemicals	8	1	6
PM16	B09	Trimethoprim	chemicals	9	7	8
PM16	B10	Trimethoprim	chemicals	9	8	8
PM16	B11	Trimethoprim	chemicals	9	8	8
PM16	B12	Trimethoprim	chemicals	9	5	8
PM16	C01	Dichlofluanid	chemicals	9	8	7
PM16	C02	Dichlofluanid	chemicals	8	8	7
PM16	C03	Dichlofluanid	chemicals	8	3	7

PM16	C04	Dichlofluanid	chemicals	6	1	4
PM16	C05	Protamine sulfate	chemicals	9	3	7
PM16	C06	Protamine sulfate	chemicals	9	0	1
PM16	C07	Protamine sulfate	chemicals	8	0	1
PM16	C08	Protamine sulfate	chemicals	6	0	1
PM16	C09	Cetylpyridinium chloride	chemicals	9	8	8
PM16	C10	Cetylpyridinium chloride	chemicals	9	8	8
PM16	C11	Cetylpyridinium chloride	chemicals	9	8	8
PM16	C12	Cetylpyridinium chloride	chemicals	9	2	8
PM16	D01	Chlorodinitrobenzene	chemicals	9	8	7
PM16	D02	Chlorodinitrobenzene	chemicals	9	8	7
PM16	D03	Chlorodinitrobenzene	chemicals	9	3	7
PM16	D04	Chlorodinitrobenzene	chemicals	3	3	3
PM16	D05	Diamide	chemicals	9	3	7
PM16	D06	Diamide	chemicals	9	5	7
PM16	D07	Diamide	chemicals	9	5	7
PM16	D08	Diamide	chemicals	4	3	7
PM16	D09	Cinoxacin	chemicals	9	8	7
PM16	D10	Cinoxacin	chemicals	9	5	8
PM16	D11	Cinoxacin	chemicals	9	8	7
PM16	D12	Cinoxacin	chemicals	9	8	8
PM16	E01	Streptomycin	chemicals	9	8	8
PM16	E02	Streptomycin	chemicals	9	7	7
PM16	E03	Streptomycin	chemicals	9	7	7
PM16	E04	Streptomycin	chemicals	9	5	7
PM16	E05	5-Azacytidine	chemicals	9	7	7
PM16	E06	5-Azacytidine	chemicals	8	7	7
PM16	E07	5-Azacytidine	chemicals	8	5	7
PM16	E08	5-Azacytidine	chemicals	7	5	7

PM16	E09	Rifamycin SV	chemicals	9	5	8
PM16	E10	Rifamycin SV	chemicals	9	8	8
PM16	E11	Rifamycin SV	chemicals	9	2	8
PM16	E12	Rifamycin SV	chemicals	9	9	9
PM16	F01	Potassium tellurite	chemicals	9	8	7
PM16	F02	Potassium tellurite	chemicals	8	8	7
PM16	F03	Potassium tellurite	chemicals	8	7	7
PM16	F04	Potassium tellurite	chemicals	3	3	5
PM16	F05	Sodium Selenite	chemicals	3	3	1
PM16	F06	Sodium Selenite	chemicals	2	2	1
PM16	F07	Sodium Selenite	chemicals	1	1	1
PM16	F08	Sodium Selenite	chemicals	1	2	1
PM16	F09	Aluminum sulfate	chemicals	9	8	7
PM16	F10	Aluminum sulfate	chemicals	9	7	7
PM16	F11	Aluminum sulfate	chemicals	9	5	7
PM16	F12	Aluminum sulfate	chemicals	9	8	8
PM16	G01	Chromium (III) chloride	chemicals	9	8	7
PM16	G02	Chromium (III) chloride	chemicals	9	8	7
PM16	G03	Chromium (III) chloride	chemicals	9	7	7
PM16	G04	Chromium (III) chloride	chemicals	9	8	7
PM16	G05	Ferric chloride	chemicals	9	8	7
PM16	G06	Ferric chloride	chemicals	9	5	7
PM16	G07	Ferric chloride	chemicals	9	8	7
PM16	G08	Ferric chloride	chemicals	9	8	8
PM16	G09	L-Glutamic acid g-monohydroxamate	chemicals	9	5	8
PM16	G10	L-Glutamic acid g-monohydroxamate	chemicals	9	5	7
PM16	G11	L-Glutamic acid g-monohydroxamate	chemicals	9	7	8
PM16	G12	L-Glutamic acid g-monohydroxamate	chemicals	9	8	8
PM16	H01	Glycine hydroxamate	chemicals	9	8	7

PM16	H02	Glycine hydroxamate	chemicals	6	2	1
PM16	H03	Glycine hydroxamate	chemicals	1	2	1
PM16	H04	Glycine hydroxamate	chemicals	1	2	1
PM16	H05	4-Chloro-3,5-dimethyl-phenol	chemicals	9	8	7
PM16	H06	4-Chloro-3,5-dimethyl-phenol	chemicals	9	8	7
PM16	H07	4-Chloro-3,5-dimethyl-phenol	chemicals	9	8	3
PM16	H08	4-Chloro-3,5-dimethyl-phenol	chemicals	6	2	4
PM16	H09	Sorbic acid	chemicals	9	8	7
PM16	H10	Sorbic acid	chemicals	9	8	8
PM16	H11	Sorbic acid	chemicals	9	8	8
PM16	H12	Sorbic acid	chemicals	9	8	8
PM17	A01	D-Serine	chemicals	9	8	8
PM17	A02	D-Serine	chemicals	9	1	6
PM17	A03	D-Serine	chemicals	1	1	1
PM17	A04	D-Serine	chemicals	1	0	2
PM17	A05	b-Chloro-L-alanine	chemicals	9	8	8
PM17	A06	b-Chloro-L-alanine	chemicals	9	8	8
PM17	A07	b-Chloro-L-alanine	chemicals	9	8	8
PM17	A08	b-Chloro-L-alanine	chemicals	9	8	8
PM17	A09	Thiosalicylate	chemicals	9	8	8
PM17	A10	Thiosalicylate	chemicals	9	8	8
PM17	A11	Thiosalicylate	chemicals	9	8	8
PM17	A12	Thiosalicylate	chemicals	9	8	8
PM17	B01	Salicylate, sodium	chemicals	9	8	8
PM17	B02	Salicylate, sodium	chemicals	8	5	7
PM17	B03	Salicylate, sodium	chemicals	7	1	5
PM17	B04	Salicylate, sodium	chemicals	1	1	2
PM17	B05	Hygromycin B	chemicals	9	8	7
PM17	B06	Hygromycin B	chemicals	9	8	7

PM17	B07	Hygromycin B	chemicals	9	1	8
PM17	B08	Hygromycin B	chemicals	9	8	7
PM17	B09	Ethionamide	chemicals	9	7	7
PM17	B10	Ethionamide	chemicals	9	3	6
PM17	B11	Ethionamide	chemicals	7	2	3
PM17	B12	Ethionamide	chemicals	7	3	3
PM17	C01	4-Aminopyridine	chemicals	9	8	8
PM17	C02	4-Aminopyridine	chemicals	9	7	7
PM17	C03	4-Aminopyridine	chemicals	8	3	5
PM17	C04	4-Aminopyridine	chemicals	6	3	1
PM17	C05	Sulfachloropyridazine	chemicals	9	7	7
PM17	C06	Sulfachloropyridazine	chemicals	9	8	7
PM17	C07	Sulfachloropyridazine	chemicals	9	8	7
PM17	C08	Sulfachloropyridazine	chemicals	9	7	7
PM17	C09	Sulfamonomethoxine	chemicals	9	7	7
PM17	C10	Sulfamonomethoxine	chemicals	9	8	7
PM17	C11	Sulfamonomethoxine	chemicals	9	5	7
PM17	C12	Sulfamonomethoxine	chemicals	9	5	7
PM17	D01	Oxycarboxin	chemicals	9	8	7
PM17	D02	Oxycarboxin	chemicals	9	8	7
PM17	D03	Oxycarboxin	chemicals	8	5	7
PM17	D04	Oxycarboxin	chemicals	1	3	1
PM17	D05	3-Amino-1,2,4-triazole	chemicals	8	8	7
PM17	D06	3-Amino-1,2,4-triazole	chemicals	8	8	7
PM17	D07	3-Amino-1,2,4-triazole	chemicals	8	7	6
PM17	D08	3-Amino-1,2,4-triazole	chemicals	5	1	5
PM17	D09	Chlorpromazine	chemicals	9	8	7
PM17	D10	Chlorpromazine	chemicals	8	7	8
PM17	D11	Chlorpromazine	chemicals	8	3	8

PM17	D12	Chlorpromazine	chemicals	8	3	7
PM17	E01	Niaproof	chemicals	9	8	8
PM17	E02	Niaproof	chemicals	7	5	6
PM17	E03	Niaproof	chemicals	3	3	4
PM17	E04	Niaproof	chemicals	3	3	2
PM17	E05	Compound 48/80	chemicals	9	7	7
PM17	E06	Compound 48/80	chemicals	8	7	7
PM17	E07	Compound 48/80	chemicals	8	3	6
PM17	E08	Compound 48/80	chemicals	5	2	2
PM17	E09	Sodium Tungstate	chemicals	9	8	7
PM17	E10	Sodium Tungstate	chemicals	9	8	7
PM17	E11	Sodium Tungstate	chemicals	9	7	7
PM17	E12	Sodium Tungstate	chemicals	9	5	5
PM17	F01	Lithium chloride	chemicals	9	8	7
PM17	F02	Lithium chloride	chemicals	8	3	3
PM17	F03	Lithium chloride	chemicals	3	1	1
PM17	F04	Lithium chloride	chemicals	5	4	6
PM17	F05	DL-Methionine hydroxamate	chemicals	9	8	7
PM17	F06	DL-Methionine hydroxamate	chemicals	8	8	7
PM17	F07	DL-Methionine hydroxamate	chemicals	1	1	1
PM17	F08	DL-Methionine hydroxamate	chemicals	1	3	3
PM17	F09	Tannic acid	chemicals	9	8	8
PM17	F10	Tannic acid	chemicals	9	8	8
PM17	F11	Tannic acid	chemicals	9	6	6
PM17	F12	Tannic acid	chemicals	9	9	9
PM17	G01	Chlorambucil	chemicals	9	8	7
PM17	G02	Chlorambucil	chemicals	9	8	7
PM17	G03	Chlorambucil	chemicals	9	8	7
PM17	G04	Chlorambucil	chemicals	9	8	7

PM17	G05	Cefamandole nafate	chemicals	9	8	7
PM17	G06	Cefamandole nafate	chemicals	9	8	7
PM17	G07	Cefamandole nafate	chemicals	9	8	7
PM17	G08	Cefamandole nafate	chemicals	9	5	7
PM17	G09	Cefoperazone	chemicals	9	8	7
PM17	G10	Cefoperazone	chemicals	9	8	7
PM17	G11	Cefoperazone	chemicals	9	5	7
PM17	G12	Cefoperazone	chemicals	9	8	7
PM17	H01	Cefsulodin	chemicals	9	8	7
PM17	H02	Cefsulodin	chemicals	9	8	7
PM17	H03	Cefsulodin	chemicals	9	8	7
PM17	H04	Cefsulodin	chemicals	9	8	7
PM17	H05	Caffeine	chemicals	9	8	7
PM17	H06	Caffeine	chemicals	9	3	7
PM17	H07	Caffeine	chemicals	8	8	7
PM17	H08	Caffeine	chemicals	3	2	1
PM17	H09	Oxophenylarsine	chemicals	9	5	8
PM17	H10	Oxophenylarsine	chemicals	9	8	7
PM17	H11	Oxophenylarsine	chemicals	9	3	7
PM17	H12	Oxophenylarsine	chemicals	9	8	7
PM18	A01	Ketoprofen	chemicals	9	8	8
PM18	A02	Ketoprofen	chemicals	9	8	8
PM18	A03	Ketoprofen	chemicals	9	8	8
PM18	A04	Ketoprofen	chemicals	8	5	6
PM18	A05	Sodium pyrophosphate	chemicals	9	5	8
PM18	A06	Sodium pyrophosphate	chemicals	9	5	8
PM18	A07	Sodium pyrophosphate	chemicals	9	3	8
PM18	A08	Sodium pyrophosphate	chemicals	8	5	7
PM18	A09	Thiamphenicol	chemicals	9	8	8

PM18	A10	Thiamphenicol	chemicals	9	8	8
PM18	A11	Thiamphenicol	chemicals	9	2	8
PM18	A12	Thiamphenicol	chemicals	8	5	6
PM18	B01	Trifluorothymidine	chemicals	8	8	8
PM18	B02	Trifluorothymidine	chemicals	9	8	7
PM18	B03	Trifluorothymidine	chemicals	9	8	7
PM18	B04	Trifluorothymidine	chemicals	9	8	7
PM18	B05	Pipemidic Acid	chemicals	9	8	7
PM18	B06	Pipemidic Acid	chemicals	9	5	7
PM18	B07	Pipemidic Acid	chemicals	9	8	8
PM18	B08	Pipemidic Acid	chemicals	9	0	7
PM18	B09	Azathioprine	chemicals	9	5	8
PM18	B10	Azathioprine	chemicals	9	5	7
PM18	B11	Azathioprine	chemicals	9	7	8
PM18	B12	Azathioprine	chemicals	9	8	8
PM18	C01	Poly-L-lysine	chemicals	9	8	8
PM18	C02	Poly-L-lysine	chemicals	8	8	7
PM18	C03	Poly-L-lysine	chemicals	8	8	7
PM18	C04	Poly-L-lysine	chemicals	9	2	8
PM18	C05	Sulfisoxazole	chemicals	9	7	7
PM18	C06	Sulfisoxazole	chemicals	9	5	7
PM18	C07	Sulfisoxazole	chemicals	8	5	7
PM18	C08	Sulfisoxazole	chemicals	7	2	4
PM18	C09	Pentachlorophenol	chemicals	9	8	7
PM18	C10	Pentachlorophenol	chemicals	9	5	7
PM18	C11	Pentachlorophenol	chemicals	9	7	7
PM18	C12	Pentachlorophenol	chemicals	8	5	6
PM18	D01	Sodium Arsenite	chemicals	1	2	1
PM18	D02	Sodium Arsenite	chemicals	1	0	1

PM18	D03	Sodium Arsenite	chemicals	1	1	1
PM18	D04	Sodium Arsenite	chemicals	1	0	1
PM18	D05	Sodium Bromate	chemicals	8	5	7
PM18	D06	Sodium Bromate	chemicals	7	3	7
PM18	D07	Sodium Bromate	chemicals	1	2	4
PM18	D08	Sodium Bromate	chemicals	2	0	1
PM18	D09	Lidocaine	chemicals	9	7	6
PM18	D10	Lidocaine	chemicals	8	5	5
PM18	D11	Lidocaine	chemicals	3	2	3
PM18	D12	Lidocaine	chemicals	3	2	3
PM18	E01	Sodium metasilicate	chemicals	9	8	8
PM18	E02	Sodium metasilicate	chemicals	9	8	7
PM18	E03	Sodium metasilicate	chemicals	6	7	7
PM18	E04	Sodium metasilicate	chemicals	5	2	3
PM18	E05	Sodium periodate	chemicals	9	2	7
PM18	E06	Sodium periodate	chemicals	6	0	7
PM18	E07	Sodium periodate	chemicals	1	0	6
PM18	E08	Sodium periodate	chemicals	1	0	1
PM18	E09	Antimony (III) chloride	chemicals	9	5	7
PM18	E10	Antimony (III) chloride	chemicals	9	5	7
PM18	E11	Antimony (III) chloride	chemicals	1	8	7
PM18	E12	Antimony (III) chloride	chemicals	1	2	3
PM18	F01	Semicarbazide hydrochloride	chemicals	9	8	7
PM18	F02	Semicarbazide hydrochloride	chemicals	9	8	7
PM18	F03	Semicarbazide hydrochloride	chemicals	8	7	6
PM18	F04	Semicarbazide hydrochloride	chemicals	1	0	1
PM18	F05	Tinidazole	chemicals	9	8	7
PM18	F06	Tinidazole	chemicals	9	5	7
PM18	F07	Tinidazole	chemicals	9	7	7

PM18	F08	Tinidazole	chemicals	8	5	7
PM18	F09	Aztreonam	chemicals	9	5	7
PM18	F10	Aztreonam	chemicals	9	8	7
PM18	F11	Aztreonam	chemicals	9	8	8
PM18	F12	Aztreonam	chemicals	9	8	8
PM18	G01	Triclosan	chemicals	9	8	7
PM18	G02	Triclosan	chemicals	9	8	7
PM18	G03	Triclosan	chemicals	9	8	7
PM18	G04	Triclosan	chemicals	9	8	7
PM18	G05	3,5- Diamino-1,2,4-triazole (Guanazole)	chemicals	9	8	7
PM18	G06	3,5- Diamino-1,2,4-triazole (Guanazole)	chemicals	9	8	7
PM18	G07	3,5- Diamino-1,2,4-triazole (Guanazole)	chemicals	9	2	7
PM18	G08	3,5- Diamino-1,2,4-triazole (Guanazole)	chemicals	9	7	7
PM18	G09	Myricetin	chemicals	9	8	7
PM18	G10	Myricetin	chemicals	9	8	8
PM18	G11	Myricetin	chemicals	9	8	8
PM18	G12	Myricetin	chemicals	9	9	8
PM18	H01	5-Fluoro-5'-deoxyuridine	chemicals	9	8	7
PM18	H02	5-Fluoro-5'-deoxyuridine	chemicals	9	8	7
PM18	H03	5-Fluoro-5'-deoxyuridine	chemicals	8	8	7
PM18	H04	5-Fluoro-5'-deoxyuridine	chemicals	8	7	7
PM18	H05	2- Phenylphenol	chemicals	9	8	7
PM18	H06	2- Phenylphenol	chemicals	9	8	7
PM18	H07	2- Phenylphenol	chemicals	9	8	8
PM18	H08	2- Phenylphenol	chemicals	9	6	3
PM18	H09	Plumbagin	chemicals	9	8	7
PM18	H10	Plumbagin	chemicals	9	8	8
PM18	H11	Plumbagin	chemicals	9	8	8
PM18	H12	Plumbagin	chemicals	9	7	6

PM19	A01	Josamycin	chemicals	9	8	8
PM19	A02	Josamycin	chemicals	9	8	8
PM19	A03	Josamycin	chemicals	8	1	8
PM19	A04	Josamycin	chemicals	7	1	8
PM19	A05	Gallic acid	chemicals	9	6	6
PM19	A06	Gallic acid	chemicals	8	9	8
PM19	A07	Gallic acid	chemicals	9	9	9
PM19	A08	Gallic acid	chemicals	9	9	9
PM19	A09	Coumarin	chemicals	9	5	8
PM19	A10	Coumarin	chemicals	9	5	8
PM19	A11	Coumarin	chemicals	9	3	8
PM19	A12	Coumarin	chemicals	3	3	3
PM19	B01	Methyltrioctylammonium chloride	chemicals	9	8	7
PM19	B02	Methyltrioctylammonium chloride	chemicals	9	8	7
PM19	B03	Methyltrioctylammonium chloride	chemicals	8	1	7
PM19	B04	Methyltrioctylammonium chloride	chemicals	3	0	7
PM19	B05	Harmane	chemicals	9	5	7
PM19	B06	Harmane	chemicals	9	5	7
PM19	B07	Harmane	chemicals	8	3	8
PM19	B08	Harmane	chemicals	3	2	3
PM19	B09	2,4-Dintrophenol	chemicals	9	5	8
PM19	B10	2,4-Dintrophenol	chemicals	9	5	8
PM19	B11	2,4-Dintrophenol	chemicals	9	6	8
PM19	B12	2,4-Dintrophenol	chemicals	5	6	6
PM19	C01	Chlorhexidine diacetate	chemicals	9	8	7
PM19	C02	Chlorhexidine diacetate	chemicals	9	8	7
PM19	C03	Chlorhexidine diacetate	chemicals	9	5	7
PM19	C04	Chlorhexidine diacetate	chemicals	9	3	7
PM19	C05	7-Hydroxycoumarin	chemicals	9	3	7

PM19	C06	7-Hydroxycoumarin	chemicals	9	1	7
PM19	C07	7-Hydroxycoumarin	chemicals	7	2	6
PM19	C08	7-Hydroxycoumarin	chemicals	1	2	3
PM19	C09	trans-Cinnamic acid	chemicals	9	7	7
PM19	C10	trans-Cinnamic acid	chemicals	9	5	7
PM19	C11	trans-Cinnamic acid	chemicals	9	5	8
PM19	C12	trans-Cinnamic acid	chemicals	9	5	8
PM19	D01	Tetraethylthiuram disulfide	chemicals	9	8	7
PM19	D02	Tetraethylthiuram disulfide	chemicals	9	5	7
PM19	D03	Tetraethylthiuram disulfide	chemicals	9	3	7
PM19	D04	Tetraethylthiuram disulfide	chemicals	9	1	6
PM19	D05	INT	chemicals	9	6	8
PM19	D06	INT	chemicals	9	9	9
PM19	D07	INT	chemicals	6	9	9
PM19	D08	INT	chemicals	9	9	9
PM19	D09	Phenyl-methylsulfonyl-fluoride (PMSF)	chemicals	9	5	7
PM19	D10	Phenyl-methylsulfonyl-fluoride (PMSF)	chemicals	9	5	7
PM19	D11	Phenyl-methylsulfonyl-fluoride (PMSF)	chemicals	9	5	8
PM19	D12	Phenyl-methylsulfonyl-fluoride (PMSF)	chemicals	9	8	8
PM19	E01	FCCP	chemicals	9	8	7
PM19	E02	FCCP	Chemicals	8	8	7
PM19	E03	FCCP	Chemicals	9	6	8
PM19	E04	FCCP	Chemicals	8	6	6
PM19	E05	DL-Thioctic acid	Chemicals	9	7	7
PM19	E06	DL-Thioctic acid	Chemicals	9	3	8
PM19	E07	DL-Thioctic acid	Chemicals	9	7	8
PM19	E08	DL-Thioctic acid	Chemicals	7	5	6
PM19	E09	2-Hydroxy-1,4-Naphthoquinone	Chemicals	9	5	8
PM19	E10	2-Hydroxy-1,4-Naphthoquinone	Chemicals	9	9	9

PM19	E11	2-Hydroxy-1,4-Naphthoquinone	Chemicals	9	9	9
PM19	E12	2-Hydroxy-1,4-Naphthoquinone	chemicals	9	9	9
PM19	F01	Phenethicilllin	chemicals	9	8	8
PM19	F02	Phenethicilllin	chemicals	9	7	7
PM19	F03	Phenethicilllin	chemicals	8	8	7
PM19	F04	Phenethicilllin	chemicals	8	8	7
PM19	F05	Blasticidin S	chemicals	9	7	7
PM19	F06	Blasticidin S	chemicals	9	1	7
PM19	F07	Blasticidin S	chemicals	8	7	7
PM19	F08	Blasticidin S	chemicals	8	2	6
PM19	F09	Sodium Caprylate	chemicals	9	8	8
PM19	F10	Sodium Caprylate	chemicals	8	5	8
PM19	F11	Sodium Caprylate	chemicals	3	2	3
PM19	F12	Sodium Caprylate	chemicals	3	2	3
PM19	G01	Lauryl sulfobetaine	chemicals	3	7	6
PM19	G02	Lauryl sulfobetaine	chemicals	3	5	4
PM19	G03	Lauryl sulfobetaine	chemicals	3	5	3
PM19	G04	Lauryl sulfobetaine	chemicals	3	3	2
PM19	G05	Dihydrostreptomycin	chemicals	9	8	7
PM19	G06	Dihydrostreptomycin	chemicals	9	8	7
PM19	G07	Dihydrostreptomycin	chemicals	9	8	8
PM19	G08	Dihydrostreptomycin	chemicals	9	8	8
PM19	G09	Hydroxylamine	chemicals	9	8	8
PM19	G10	Hydroxylamine	chemicals	9	8	8
PM19	G11	Hydroxylamine	chemicals	9	2	8
PM19	G12	Hydroxylamine	chemicals	9	8	8
PM19	H01	Hexammine cobalt (III) chloride	chemicals	9	8	8
PM19	H02	Hexammine cobalt (III) chloride	chemicals	9	8	8
PM19	H03	Hexammine cobalt (III) chloride	chemicals	9	8	7

PM19	H04	Hexammine cobalt (III) chloride	chemicals	9	2	6
PM19	H05	a-Monothioglycerol	chemicals	9	8	8
PM19	H06	a-Monothioglycerol	chemicals	9	8	7
PM19	H07	a-Monothioglycerol	chemicals	8	5	6
PM19	H08	a-Monothioglycerol	chemicals	3	6	6
PM19	H09	Polymyxin B	chemicals	9	8	8
PM19	H10	Polymyxin B	chemicals	9	8	8
PM19	H11	Polymyxin B	chemicals	1	2	6
PM19	H12	Polymyxin B	chemicals	3	2	2
PM20	A01	Amitriptyline	chemicals	9	5	8
PM20	A02	Amitriptyline	chemicals	8	5	8
PM20	A03	Amitriptyline	chemicals	7	1	6
PM20	A04	Amitriptyline	chemicals	3	0	4
PM20	A05	Apramycin	chemicals	9	5	8
PM20	A06	Apramycin	chemicals	9	3	8
PM20	A07	Apramycin	chemicals	9	2	8
PM20	A08	Apramycin	chemicals	9	0	8
PM20	A09	Benserazide	chemicals	9	6	8
PM20	A10	Benserazide	chemicals	9	6	6
PM20	A11	Benserazide	chemicals	8	6	6
PM20	A12	Benserazide	chemicals	9	9	9
PM20	B01	Orphenadrine	chemicals	8	5	8
PM20	B02	Orphenadrine	chemicals	6	3	7
PM20	B03	Orphenadrine	chemicals	1	0	2
PM20	B04	Orphenadrine	chemicals	3	0	2
PM20	B05	DL-Propanolol	chemicals	9	5	8
PM20	B06	DL-Propanolol	chemicals	8	5	8
PM20	B07	DL-Propanolol	chemicals	3	3	2
PM20	B08	DL-Propanolol	chemicals	3	0	2

PM20	B09	Tetrazolium violet	chemicals	9	5	8
PM20	B10	Tetrazolium violet	chemicals	9	2	8
PM20	B11	Tetrazolium violet	chemicals	3	2	3
PM20	B12	Tetrazolium violet	chemicals	5	6	3
PM20	C01	Thioridazine	chemicals	9	3	8
PM20	C02	Thioridazine	chemicals	8	3	8
PM20	C03	Thioridazine	chemicals	9	3	8
PM20	C04	Thioridazine	chemicals	9	5	8
PM20	C05	Atropine	chemicals	9	3	8
PM20	C06	Atropine	chemicals	9	1	5
PM20	C07	Atropine	chemicals	7	1	2
PM20	C08	Atropine	chemicals	3	0	2
PM20	C09	Ornidazole	chemicals	9	5	8
PM20	C10	Ornidazole	chemicals	9	5	8
PM20	C11	Ornidazole	chemicals	8	5	8
PM20	C12	Ornidazole	chemicals	8	2	4
PM20	D01	Proflavine	chemicals	9	5	8
PM20	D02	Proflavine	chemicals	9	3	8
PM20	D03	Proflavine	chemicals	9	2	8
PM20	D04	Proflavine	chemicals	8	3	6
PM20	D05	Ciprofloxacin	chemicals	9	5	8
PM20	D06	Ciprofloxacin	chemicals	9	3	8
PM20	D07	Ciprofloxacin	chemicals	9	3	8
PM20	D08	Ciprofloxacin	chemicals	9	1	8
PM20	D09	18-Crown-6 ether	chemicals	9	5	7
PM20	D10	18-Crown-6 ether	chemicals	9	5	8
PM20	D11	18-Crown-6 ether	chemicals	9	5	8
PM20	D12	18-Crown-6 ether	chemicals	8	5	8
PM20	E01	Crystal violet	chemicals	9	3	8

PM20	E02	Crystal violet	chemicals	9	6	8
PM20	E03	Crystal violet	chemicals	9	6	8
PM20	E04	Crystal violet	chemicals	9	9	9
PM20	E05	Dodine (n-Dodecylguanidine)	chemicals	9	7	7
PM20	E06	Dodine (n-Dodecylguanidine)	chemicals	9	5	7
PM20	E07	Dodine (n-Dodecylguanidine)	chemicals	9	3	7
PM20	E08	Dodine (n-Dodecylguanidine)	chemicals	8	1	7
PM20	E09	Hexachlorophene	chemicals	9	5	8
PM20	E10	Hexachlorophene	chemicals	9	5	8
PM20	E11	Hexachlorophene	chemicals	9	5	8
PM20	E12	Hexachlorophene	chemicals	9	6	6
PM20	F01	4-Hydroxycoumarin	chemicals	9	5	8
PM20	F02	4-Hydroxycoumarin	chemicals	9	5	7
PM20	F03	4-Hydroxycoumarin	chemicals	9	5	7
PM20	F04	4-Hydroxycoumarin	chemicals	9	5	7
PM20	F05	Oxytetracycline	chemicals	9	1	7
PM20	F06	Oxytetracycline	chemicals	9	0	7
PM20	F07	Oxytetracycline	chemicals	9	1	7
PM20	F08	Oxytetracycline	chemicals	9	2	8
PM20	F09	Pridinol	chemicals	9	5	7
PM20	F10	Pridinol	chemicals	9	5	7
PM20	F11	Pridinol	chemicals	9	2	8
PM20	F12	Pridinol	chemicals	9	3	8
PM20	G01	Captan	chemicals	9	8	8
PM20	G02	Captan	chemicals	8	8	7
PM20	G03	Captan	chemicals	7	1	7
PM20	G04	Captan	chemicals	5	3	7
PM20	G05	3,5-Dinitrobenzoic acid	chemicals	9	5	7
PM20	G06	3,5-Dinitrobenzoic acid	chemicals	9	5	7

PM20	G07	3,5-Dinitrobenzoic acid	chemicals	8	5	7
PM20	G08	3,5-Dinitrobenzoic acid	chemicals	6	3	8
PM20	G09	8-Hydroxyquinoline	chemicals	9	5	7
PM20	G10	8-Hydroxyquinoline	chemicals	9	6	7
PM20	G11	8-Hydroxyquinoline	chemicals	9	2	8
PM20	G12	8-Hydroxyquinoline	chemicals	3	2	2
PM20	H01	Patulin	chemicals	9	8	8
PM20	H02	Patulin	chemicals	9	8	8
PM20	H03	Patulin	chemicals	9	1	7
PM20	H04	Patulin	chemicals	9	2	8
PM20	H05	Tolylfluanid	chemicals	9	5	7
PM20	H06	Tolylfluanid	chemicals	9	5	7
PM20	H07	Tolylfluanid	chemicals	9	5	7
PM20	H08	Tolylfluanid	chemicals	9	5	8
PM20	H09	Troleandomycin	chemicals	9	3	8
PM20	H10	Troleandomycin	chemicals	9	2	8
PM20	H11	Troleandomycin	chemicals	9	2	8
PM20	H12	Troleandomycin	chemicals	7	2	5